

Advanced oxidation of micropollutants in water by photolytic and photocatalytic processes

Dissertation

zur Erlangung des akademischen Grades eines

Doktors der Naturwissenschaften

– Dr. rer. nat. –

vorgelegt von

Alaa Salma

geboren in Tartous, Syrien

Fakultät für Chemie

der

Universität Duisburg-Essen

2017

Die vorliegende Arbeit wurde im Zeitraum von Januar 2011 bis Dezember 2016 im Arbeitskreis von Prof. Dr. Torsten C. Schmidt in der Fakultät für Chemie im Bereich Instrumentelle Analytische Chemie der Universität Duisburg-Essen durchgeführt.

Tag der Disputation: 16.11. 2017

Gutachter:	Prof. Dr. Torsten C. Schmidt
	Prof. Dr. Kristof Demeestere
Vorsitzender:	Prof. Dr. Christian Mayer

Summary

Photochemical processes and related technologies have been often used in the 20th century for the disinfection of drinking water and wastewater (secondary and tertiary sewage effluents). Recently, direct ultraviolet (UV) photolysis, photocatalysis and advanced oxidation procedures have been widely reported as emerging methods for the removal of organic micropollutants from water. Nowadays, based on the progress made in analytical techniques' sensitivity, micropollutants such as pharmaceuticals can be determined down to ng L⁻¹ scale in the aquatic environment. There is growing interest in the removal of these contaminants from water, particularly driven by the overall public concern about potential toxic effects they might induce in humans and ecosystems.

In this work, the beta-blocker nebivolol has been detected for the first time in effluent samples of 12 wastewater treatment plants (WWTPs) in Germany. The photolytic degradation of nebivolol has been investigated under three different UV sources, namely, UV-C (main emission band at 254 nm), UV-B (main emission band at 312 nm) and UV-A (main emission band at 365 nm) in different matrices: pure water, pure water in the presence of a hydroxyl radical scavenger and in wastewater. During the photodegradation study, no elimination of nebivolol was observed under UV-A radiation. In contrast, nebivolol degradation under UV-B and UV-C radiation followed pseudo first order reaction kinetics, with the highest removal rate under UV-C radiation in pure water ($k = 7.8 \times 10^{-4} \text{ s}^{-1}$). Also the degradation mechanism of nebivolol under the UV-B and UV-C radiation has been studied. Three transformation products (TPs) were identified after UV-B and UV-C photolytic degradation using high resolution mass spectrometry. The TPs are formed by the substitution of the fluorine atom from the benzopyran ring with a hydroxyl group. The biologically active part of nebivolol is still preserved in the identified TPs even after two hours of irradiation. The matrices' pH plays an important role for the elimination mechanism of the micropollutants in the environment. With regard to photolysis, the different species might have various photolytic degradation pathways, transformation products and kinetics of mechanism-based degradation. In order to demonstrate this, the influence of different pH values (3, 5, 7 and 9) on the reaction kinetics and on the degradation mechanism of ciprofloxacin by direct ultraviolet photolysis (UV-C irradiation) and photocatalysis (TiO₂/UV-C) has been investigated. During the photolytic and photocatalytic degradation of ciprofloxacin, pseudo-first order kinetics were found with the highest removal rates at pH 9 ($k_{\text{UV and TiO}_2/\text{UV}} = 4.0 \times 10^{-4} \text{ s}^{-1}$). 18 transformation products have been identified at different pH values (3, 5, 7 and 9). Four

transformation products have been detected for the first time, two of the newly proposed structures were supported by the results obtained using deuterated ciprofloxacin.

Photolysis was studied for five further common micropollutants. A corrosion inhibitor (1*H*-benzotriazole) and four pharmaceuticals from different compound classes were included in the study: a β -blocker (metoprolol), an antibiotic (sulfamethoxazole), an anti-inflammatory drug (diclofenac) and an anti-epileptic agent (carbamazepine). The photodegradation was affected by the WWTP effluent matrix. Organic and inorganic substances in wastewater or natural water environments played a dual role of sensitizer and quencher in the photodegradation. In this study, photodegradation rate constants of metoprolol and carbamazepine increased in presence of WWTP effluent matrix, probably due to the presence of photosensitizer compounds. In contrast, diclofenac and sulfamethoxazole showed decreased photodegradation rate constants, due to physical or chemical quenching of the photochemical degradation intermediates by competitors. The matrix also posed non-negligible influences on benzotriazole photodegradation process. Overall, direct photolysis was demonstrated to be relevant for micropollutant abatement from the aquatic environment. However, to promote the photolysis application on a broader scale, it is essential to further understand how this process is affected by the UV sources, micropollutant structures and matrix composition.

Zusammenfassung

Photochemische Prozesse und verwandte Technologien wurden im 20. Jahrhundert häufig für die Desinfektion von Trinkwasser als auch Abwasser (sekundäre und tertiäre Kläranlagenabwässer) eingesetzt. Aktuell werden die direkte UV-Photolyse, Photokatalyse und erweiterte Oxidationsverfahren zur Entfernung von organischen Mikroschadstoffen in Wasser angewendet. Basierend auf den Entwicklungen neuester Analysetechniken und die damit einhergehende höhere Empfindlichkeit können heutzutage Mikroschadstoffe wie beispielsweise Arzneimittelwirkstoffen bereits in dem unteren ng L^{-1} Bereich in aquatischen Umweltproben nachgewiesen werden. Zudem gibt es ein steigendes Interesse an der Entfernung von solchen Kontaminanten aus den Gewässern in der Öffentlichkeit, unter anderem aufgrund von potentiell toxischen Effekten auf den Menschen und die Umwelt. In dieser Arbeit wurde zum ersten Mal der beta-Blocker Nebivolol in Ablaufproben von 12 deutschen Kläranlagen detektiert. Der photolytische Abbau von Nebivolol wurde mit drei verschiedenen UV-Quellen in Reinstwasser, Reinstwasser in Anwesenheit eines Hydroxylradikalfängers und in Abwasser untersucht. Die eingesetzten UV-Quellen waren UV-C (Emission bei 254 nm), UV-B (Hauptemission bei 312 nm) und UV-A (Hauptemission bei 365 nm). Während der photolytischen Untersuchungen konnte keine Elimination von Nebivolol mittels UV-A-Bestrahlung festgestellt werden. Im Gegensatz dazu konnte bei dem Einsatz von UV-B- und UV-C-Strahlern ein Abbau nach pseudo-erster Ordnung mit der höchsten Eliminationsrate bei UV-C in Reinstwasser erreicht werden ($k = 7.8 \times 10^{-4} \text{ s}^{-1}$). Auch der Abbaumechanismus von Nebivolol bei dem Einsatz von UV-B- und UV-C-Strahlern wurden in dieser Arbeit untersucht. Dabei konnten drei Transformationsprodukte (TPs) nach UV-B- und UV-C-Bestrahlung mittels hochauflösender Massenspektrometrie identifiziert werden. Die TPs werden bei der Substitution von Fluor-Atomen des Benzopyran-Ringsystems mit einer Hydroxylgruppe gebildet. Der biologisch aktive Teil von Nebivolol ist auch nach Bestrahlung von zwei Stunden noch in den TPs vorhanden. Der pH-Wert der Matrix spielt bei dem Eliminationsmechanismus in der Umwelt eine wichtige Rolle. Im Hinblick auf die Photolyse, können die verschiedenen Spezies unterschiedliche Reaktionsmechanismen und -kinetiken haben, die zu verschiedenen Abbauebenen und Transformationsprodukten führen. Um dies zu demonstrieren, wurde der Einfluss von verschiedenen pH-Werten (3, 5, 7 und 9) auf die Reaktionskinetik und den Abbaumechanismus von Ciprofloxacin während der UV-Photolyse (UV-C) und Photokatalyse ($\text{TiO}_2/\text{UV-C}$) untersucht. Während des photolytischen und photokatalytischen

Abbaus von Ciprofloxacin, konnte eine Kinetik pseudo-erster Ordnung mit der höchsten Eliminationsrate bei pH 9 ($k_{\text{UV and TiO}_2/\text{UV}} = 4.0 \times 10^{-4} \text{ s}^{-1}$) festgestellt werden. Insgesamt sind 18 Transformationsprodukte bei den verschiedenen pH-Werten (3, 5, 7 und 9) identifiziert worden. Vier dieser Transformationsprodukte wurden das erste Mal detektiert, zwei der neu vorgeschlagenen Strukturen werden unterstützt durch Untersuchungsergebnisse mit deuteriertem Ciprofloxacin. Der Einsatz der Photolyse wurden für weitere fünf bekannte Mikroschadstoffe untersucht, ein Korrosionsschutzmittel (1*H*-Benzotriazol) und vier Arzneimittelwirkstoffe verschiedener Substanzklassen. Diese waren zum einen ein β -Blocker (Metoprolol), ein Antibiotikum (Sulfamethoxazol), ein Entzündungshemmer (Diclofenac) sowie ein anti-Epileptikum (Carbamazepin). Der photolytische Abbau war von der Abwassermatrix beeinflusst. Einige organische und/oder anorganische Substanzen, welche in Abwasser oder natürlichen Gewässern vorkommen, wirkten sich verstärkend oder auch als Quencher auf den photolytischen Abbau aus. In dieser Arbeit konnte einen Anstieg der photolytischen Abbauraten von Metoprolol und Carbamazepin in Anwesenheit der Abwassermatrix, wahrscheinlich auf Grund der Anwesenheit von Photosensibilisatoren, gezeigt werden. Im Gegensatz dazu konnte für Diclofenac und Sulfamethoxazol eine Reduktion der photolytischen Abbauraten gezeigt werden. Dies kann auf physikalisches oder chemisches Quenchen der photochemischen Zwischenprodukte von Kompetitoren zurückgeführt werden. Auch auf den photolytischen Abbau von Benzotriazol hat die Matrix einen nicht zu vernachlässigenden Einfluss. Durch diese Arbeit konnte die Relevanz der direkten Photolyse zur Elimination von Mikroschadstoffen in der aquatischen Umwelt gezeigt werden. Um die Anwendung der Photolyse in einem größeren Maßstab einzusetzen, ist es essentiell, den Einfluss der UV-Quellen, der für den Abbau relevanten Strukturelemente der Mikroschadstoffe sowie der Matrixzusammensetzung auf den Prozess besser zu verstehen.

Table of Content

1.	Introduction	1
1.1	Preface	1
1.2	Pharmaceuticals in the environment: Sources and effects	2
1.2.1	β -Blockers in the environment	5
1.2.2	Fluoroquinolone antibiotics in the environment	7
1.3	Analysis of pharmaceuticals in water and wastewater	10
1.4	Elimination of pharmaceuticals from water and wastewater	15
1.5	Advanced oxidation processes: photolysis and semiconductor photocatalysis	16
1.6	Transformation products of the pharmaceuticals oxidation.....	20
1.7	Scope of the thesis.....	21
1.8	Reference.....	22
2	Photolytic degradation of the β-blocker nebivolol in aqueous solution	34
2.1	Abstract.....	34
2.2	Keywords	34
2.3	Introduction	35
2.4	Experimental section.....	36
2.4.1	Reagents and materials.....	36
2.4.2	Photodegradation investigations	37
2.4.2.1	Experimental set-up.....	37
2.4.2.2	Ferrioxalate actinometry	37
2.4.2.3	Kinetic experiments.....	37
2.4.3	Analytical Methods	38
2.4.3.1	Ion chromatography for fluoride determination	38
2.4.3.2	LC-MS/MS analysis	38
2.4.3.3	LC-HRMS analysis for structure elucidation.....	39
2.5	Results and discussion.....	40
2.5.1	NEB occurrence in wastewater	40
2.5.2	Degradation kinetics of NEB in photodegradation	41
2.5.3	Influence of the of OH-radical in NEB degradation	42
2.5.4	Influence of the wastewater matrix on the degradation of NEB	43
2.5.5	Characterization of the transformation products of NEB formed during photolytic degradation.....	44

2.5.6	Proposed mechanisms for the photolytic degradation of NEB	47
2.6	Conclusions	49
2.7	Acknowledgment	50
2.8	References	50
3	pH effects on photolysis and photocatalysis of ciprofloxacin.....	55
3.1	Abstract.....	55
3.2	Keywords	55
3.3	Introduction	56
3.4	Material and methods	58
3.4.1	Materials.....	58
3.4.2	Immobilization of TiO ₂ on glass plates	58
3.4.3	Degradation experiments.....	58
3.4.4	CIP-d8 degradation and samples enrichment using solid phase extraction (SPE).....	59
3.4.5	LC-MS/MS analysis	59
3.5	Results and discussion.....	61
3.5.1	Influence of pH on the degradation of CIP.....	61
3.5.2	Characterization of the transformation products of CIP resulted during photolytic and photocatalytic degradation	63
3.5.3	Elucidation of transformation products for different ciprofloxacin species.....	65
3.5.4	Proposed mechanisms for the photolytic and photocatalytic degradation of CIP	66
3.6	Conclusions	72
3.7	Acknowledgment	74
3.8	References	74
4	Evaluation of UV irradiation effects on the photolytic degradation of micropollutants in water	81
4.1	Abstract.....	81
4.2	Keywords	81
4.3	Introduction	82
4.4	Experimental section.....	83
4.4.1	Reagents and materials.....	83
4.4.2	Sample preparation.....	84
4.4.3	HPLC-MS/MS analysis.....	84
4.4.4	Ferrioxalate actinometry	86

4.4.5	Photodegradation experiments	86
4.4.6	Kinetic experiments.....	87
4.5	Results and discussions	88
4.5.1	Occurrence of the micropollutants in the wastewater treatment plant effluent	88
4.5.2	Photolysis of the micropollutants	89
4.6	Acknowledgement	92
4.7	References	92
5	General conclusions and outlook	100
5.1	References	102
6	Appendix	104
6.1	Supplementary material of chapter 2.....	104
6.2	Supplementary material of chapter 3.....	115
6.3	List of abbreviations.....	145
6.4	List of figures	149
6.5	List of tables.....	151
6.6	List of supplementary figures and tables	152
6.7	List of publications	154
6.8	Lebenslauf.....	156
6.9	Erklärung.....	158
6.10	Acknowledgements.....	159

1. Introduction

1.1 Preface

Life on earth without water would be non-existent. Water is certainly the most valuable natural resource that exists on our planet and it is essential for all species in our life. Nearly 71% of the earth's surface is covered with water, the oceans hold about 96.5% of the water resources. Only 2.5% exists as freshwater in the form of icecaps and glaciers in the polar regions (about 99%) and ~ 0.3% as freshwater in rivers, lakes and groundwater. In spite of the lack of freshwater on the earth, we continuously pollute it with various chemicals like pesticides, biocides, industrial chemicals, personal care products and pharmaceuticals.

The occurrence of pharmaceuticals in the water sources has been widely discussed and published in the literature in the last decade, making them an emerging concern for the public due to their potential to reach drinking water. Pharmaceuticals are stable compounds, with pharmacological effects. Unfortunately, this stability means that they also persist after they have been excreted from the human body, thus reaching the wastewater treatment plants. Because they are not (fully) eliminated there, they might create an environmental problem. During the last several decades, in particular over the past two decades, the production and consumption of pharmaceuticals has amplified due to the population growth. Several thousand compounds, belonging to a variety of therapeutic classes, are used as medicine and annually hundreds of tons are being consumed.

Pharmaceuticals have been detected in urban and livestock agricultural wastewater and surface water. Therefore, a classification of their environmental hazard and an environmental risk assessment was carried out by many countries [1, 2]. Environmental risks of some pharmaceuticals have been detected, for others, gaps of knowledge still exist.

Estrogens and diclofenac have been identified as pharmaceuticals affecting the wildlife [3, 4]. Other pharmaceuticals, including antibiotics, antiparasitics, antidepressants and anticancer medications give reason for concern [5-8].

The present chapter provides a short overview of organic trace pollutants in the environment, focusing on sources and effects of β -blockers and fluoroquinolones in the aquatic environment. The analysis methodologies and the identification of the pharmaceuticals and their transformation products in water and wastewater are of particular interest since the main focus of present work is to investigate the photolytic and semiconductor photocatalytic degradation of the β -blocker nebivolol and the fluoroquinolone antibiotic ciprofloxacin in water.

1.2 Pharmaceuticals in the environment: Sources and effects

The global use of pharmaceuticals in human and veterinary medical therapy, aquaculture and agricultural products has frequently led to the release of a wide spectrum of pharmaceuticals in the environment. The occurrence of pharmaceuticals in the aquatic environment and their effects have been extensively investigated and several studies have been published in the last decade [9]. The progress in their detection, even at trace levels, is attributable to the advances in the analytical techniques and instrumentation [9] (see abaixo). Many studies have confirmed the presence of pharmaceuticals at very low concentrations, in the range of ng L^{-1} to $\mu\text{g L}^{-1}$, in wastewater [10], surface water [11, 12], groundwater [13-15] and even drinking water [16]. Pharmaceuticals and their metabolites enter the aquatic environment through different routes, which are presented in Figure 1.1. Firstly, they can be emitted during their production and transport. The emissions of pharmaceuticals during manufacturing in the EU, US and Canada to the aquatic environment rarely occurs, due to the strong regulations existing in these countries. Nevertheless, these do not prevent the occurrence of some local incidents during manufacturing, transport or storage, which might lead to the release of different pharmaceuticals in the environment.

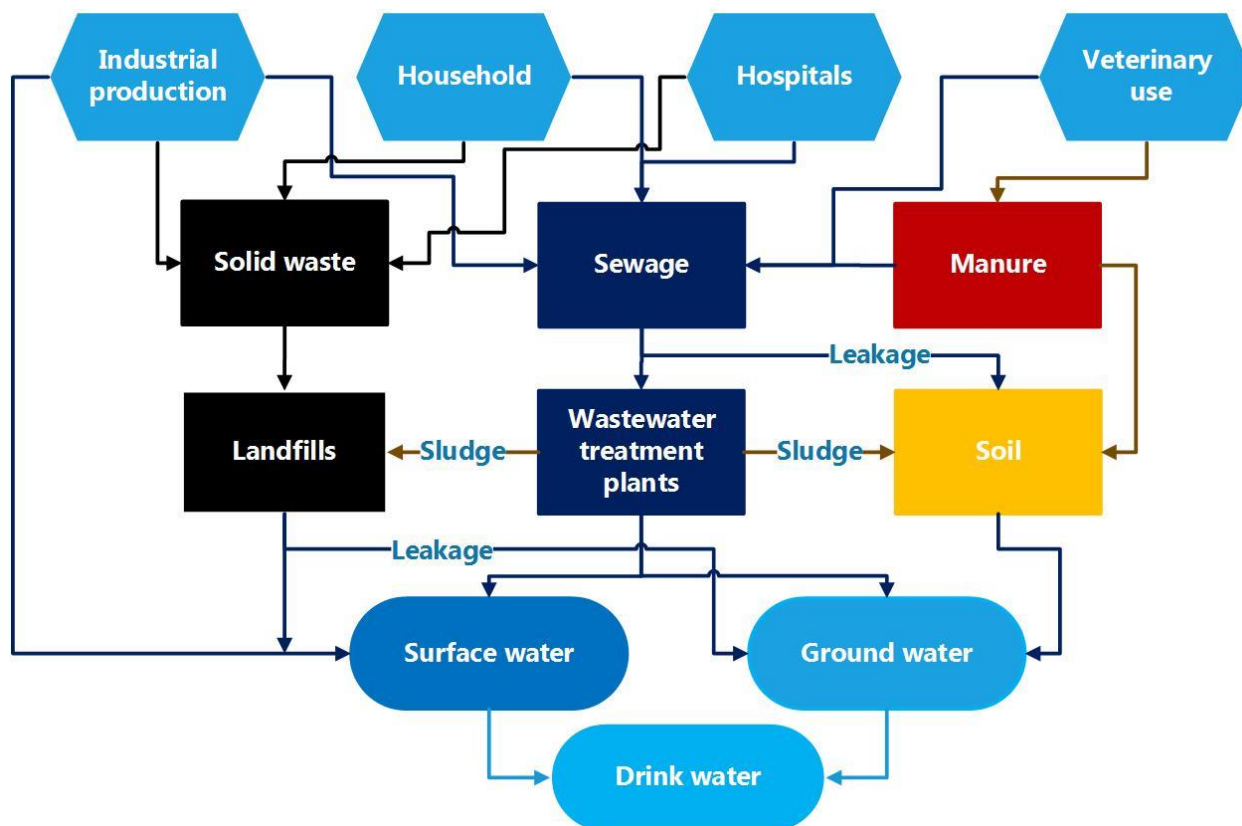


Figure 1.1 Fate and transport of pharmaceuticals in the environment.

The major pharmaceutical emission sources into the environment stem from human consumption and veterinarian applications (see the paragraph 1.2.1 and 1.2.2). After administration, most of the drugs are excreted through the urine and faeces and end up in municipal wastewater and the wastewater treatment plants (WWTPs). Escher, et al. [17] estimated that 62% of pharmaceuticals load in the WWTPs originates from household use, while the other 38% originates from hospitals.

Some pharmaceuticals are largely metabolized before they are excreted, while others are poorly metabolised and excreted mainly intact. For example diclofenac is excreted around 15% as parent compound [18], while in the case of atenolol the excretion rate for the active pharmaceutical ingredient is more than 90% [19]. Most of these drugs and their metabolites are not eliminated from municipal wastewater and via the WWTPs effluent they may end up in the aquatic environment. Drugs administered in livestock and their metabolites are excreted with manure. Farmers use manure and sometimes the WWTP sludge to fertilize their fields, thus the pharmaceutical and veterinary residues may end up in the soil and from there further in the surface and ground water. Application of veterinary drugs in aquaculture, leads to direct emission into surface and ground water.

Expired pharmaceuticals may be disposed of either via the household drains or via the household solid waste. If they are disposed of via the household drains, they end up intact into the WWTPs, if their disposal occurs with the household waste, outdated drugs might end up on landfill sites, and further may reach the ground water through the landfill leachate [20].

The estimated annual worldwide consumption of active pharmaceuticals is around a few hundred thousand tons. In Germany more than 2,300 pharmaceutical products, with an estimated annual consumption of more than 30,000 tons, are sold in human medicine [21]. According to information from the Federal Environment Agency [22], about half of human pharmaceuticals are classified as potential pollutants because they are toxic and not readily degradable. In 2012 the consumption of around 1,200 pharmaceuticals with possible pollution relevance was 8,120 tons [23]. Approximately 600 active pharmaceuticals are approved in animal medicine [24]. Many of these substances are used also in human medicine. Antibiotics make up the bulk of the veterinary medicines sold. As biologically active substances, human and veterinary pharmaceuticals have in principle (eco) toxicological potential [25].

Many studies have shown that pharmaceuticals have adverse effects on wildlife even at very low concentrations. Kidd, et al. [4] found in a controlled study on the fathead minnow (type of fish living in the downstream of some wastewater outfalls), that the chronic exposure to low concentrations (5 - 6 ng L⁻¹) of the 17 α -Ethinylestradiol led to feminization of males

through the production of vitellogenin mRNA and protein. This has impacts on gonadal development, as evidenced by intersex in males and altered oogenesis in females, and, ultimately, a near extinction of this species from the lake. Oaks, et al. [3] reported that diclofenac, administered either by direct oral exposure or through diclofenac-treated livestock, has caused renal failure and visceral gout in the case of vultures. Diclofenac was the reason behind the catastrophic decrease in the numbers of vultures in India.

Therefore, under the water framework directive (WFD) of the European commission, environmental quality standards (EQS) have been established for 33 substances, the so called 'priority substances', and eight other pollutants were listed in the Annex X of the WFD [26]. When the directive on environmental quality standards was amended in 2013, a watch list mechanism was established, requiring a temporary monitoring of other substances for which evidence suggested a possible risk to or via the environment. The purpose of this watch mechanism was to identify other priority substances. In addition, the 2013 directive identified three other substances (the natural hormone 17 β -Estradiol (E2), the anti-inflammatory drug diclofenac and the synthetic hormone 17 α -Ethinylestradiol (EE2), used in contraceptives) for inclusion in the first watch list to facilitate the determination of appropriate measures to address the risk posed by these substances [27]. In 2015 the watch list was expanded to include other pharmaceuticals which were classified as emerging pollutants [28]. In the future, the substances included in the watch list might be placed on the list of priority substances (Annex X), and further measures should be taken for monitoring and controlling their emissions. For example the EQS proposed a maximum level of 0.1 $\mu\text{g L}^{-1}$ for diclofenac, 0.5 $\mu\text{g L}^{-1}$ for carbamazepine and 0.15 $\mu\text{g L}^{-1}$ for sulfamethoxazole in surface waters [29]. However, these pharmaceuticals were detected up to several $\mu\text{g L}^{-1}$ in the wastewater treatment plant effluents [24, 30].

The increase of pharmaceuticals' consumption makes them an emerging concern for the public due to their potential to reach drinking water. At very low concentrations pharmaceuticals are unlikely to pose any direct perceptible risks to human health, but they might have an indirect effect when a resistance to pathogens is developed [31, 32]. Pharmaceuticals are synthetic chemicals designed to have pharmacological effects on the organism. Thus, it is to be expected that they will be critical against bacteria, fungi, higher organisms, but sometimes they also might have negative impacts on human health [33].

Antibiotics have an impact on cell functions, which might change the genetic expression of virulence factors or transfer of antibiotic resistance [34].

A number of preliminary reports [10, 35] proposed that even low concentrations of human and veterinary pharmaceuticals can have adverse effects on a variety of organisms [17], and consequently might cause a threat to wildlife [31].

1.2.1 β -Blockers in the environment

β -Blockers are β -adrenergic receptor antagonist drugs. They belong to the group of cardiovascular pharmaceuticals and are generally used for treatment of hypertension and cardiac dysfunction. The most commonly used β -blockers are atenolol, propranolol and metoprolol (see Figure 1.2. for their structures); thus they are widely consumed in the world. According to sales data from IMS Health AG, in Germany alone consumption exceeds 200 tons yearly of β -Blockers; e.g. more than 157 tons of metoprolol were consumed in Germany in 2012. Metoprolol was classified on the first place among the top 25 medicines prescribed in USA in 2013, and accounts for more than 80% of total β -blocker consumption in Europe according to sales data from IMS Health [36, 37]. In 2004 more than 35 and 18 tons of propranolol and atenolol respectively, were consumed in France [38]. Due to their massive use, β -blockers have been detected in aquatic environments [39, 40] and have shown effects on fishes [41]. Haider and Baqri [42] found that aqueous solutions of propranolol and other β -blockers have an effect on the oocyte maturation of catfish. Huggett, et al. [43] observed growth dysfunctions on the invertebrates in the presence of 0.5 mg L^{-1} of propranolol.

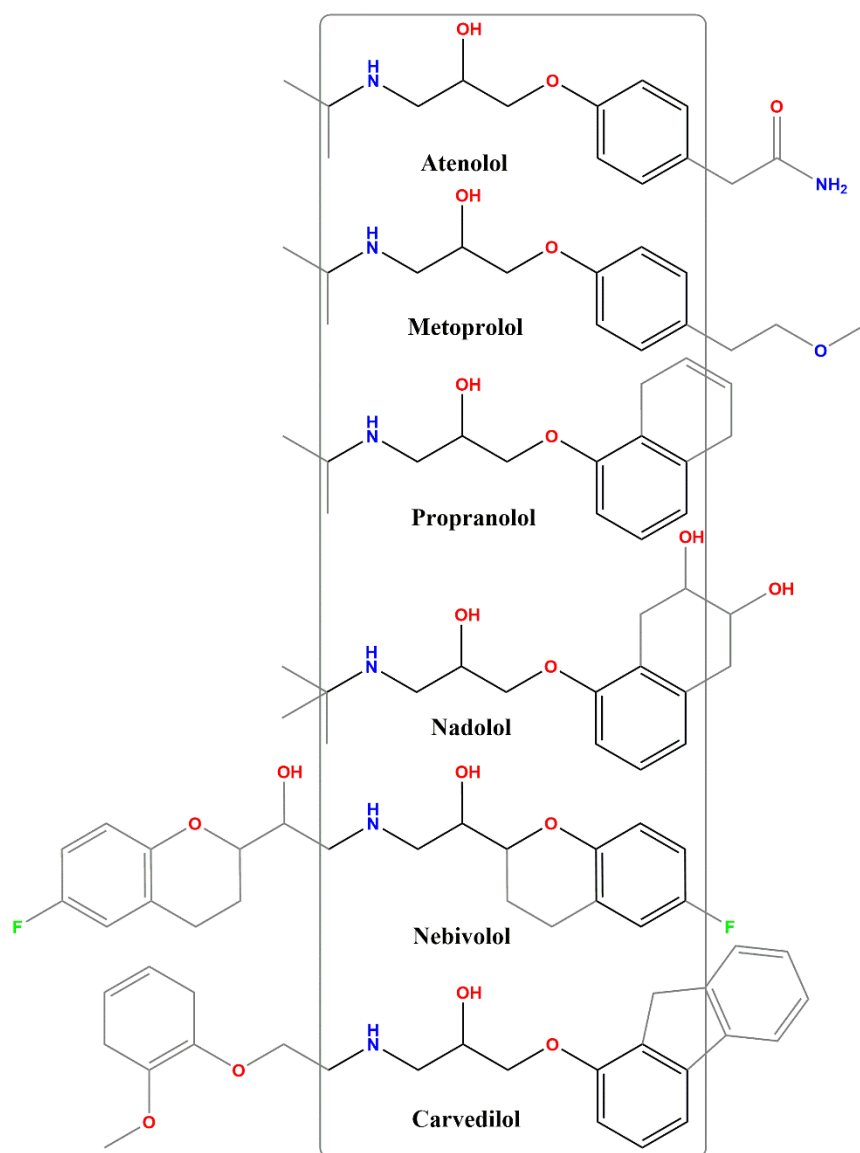


Figure 1.2 Chemical structure of β -blockers. The active moieties responsible for the biological activity are highlighted with bold line, based on [44].

β -blockers have been frequently identified in aquatic environments (Table 1.1) because of their low sorption affinity on the activated sludge [45]. The average removal reported in conventional wastewater treatments plants ranges from 58% to 80% for atenolol, 20 - 40% for metoprolol, and 20 - 60% for propranolol [46-48]. Maszkowska, et al. [39] indicated in their study a high hydrolytic stability of nadolol, metoprolol and propranolol with estimated half-lives of more than one year.

Their high hydrolytic stability, as well as their high mobility in natural soils/sediments causes these drugs to be bioavailable and to accumulate in the water ecosystems [49].

Table 1.1 β -blockers concentrations in different aqueous matrices. The aqueous matrices were categorized: +++ for $c_{\max} > 1000 \text{ ng L}^{-1}$; ++ for $c_{\max} 100\text{-}1000 \text{ ng L}^{-1}$; + for $c_{\max} < 100 \text{ ng L}^{-1}$; n.d. if no data were available.

β -blockers	Hospital wastewaters	WWTPs effluent	Surface water	Ground water	References
Acebutolol	n.d.	+++	++	n.d.	[48, 50-52]
Atenolol	+++	+++	++	+	[13, 36, 48, 50, 52-61]
Sotalol	+++	++	++	++	[36, 48, 50, 52, 55, 57, 58] [62]
Metoprolol	+++	+++	+++	+	[36, 38, 43, 48, 50-52, 54-60, 62-66]
Propranolol	+	+++	++	+	[36, 38, 43, 48, 51, 52, 54-60, 63-65, 67, 68]
Betaxolol	++	++	+	n.d.	[48, 51, 55, 58, 63, 64]
Bisoprolol	n.d.	+++	+++	+	[38, 48, 62-64]
Oxprenolol	n.d.	+	+	n.d.	[48, 51]
Pindolol	++	+	n.d.	n.d.	[55, 58]
Timolol	+	+	+	n.d.	[48, 55, 58, 64]
Carazolol	+	+	++	n.d.	[55, 58, 64]
Nadolol	+	++	+	n.d.	[43, 48, 58, 64]
Celiprolol	n.d.	++	n.d.	n.d.	[52, 64]
Nebivolol	n.d.	n.d.	n.d.	n.d.	

Atenolol was detected in the highest ranges concentrations in wastewater (Table 1.1), in some cases ranging up to mg L^{-1} [38]. As a result of the incomplete removal during conventional wastewater treatment, these compounds were also found in surface waters in the ng L^{-1} to mg L^{-1} range [57].

1.2.2 Fluoroquinolone antibiotics in the environment

Quinolones are a potent group of antibiotics, with effects on both bacteria type gram-negative and gram-positive. Quinolones and derivatives are applied for the therapeutic treatment of both humans and animals. Nalidixic acid, the first compound of this type, was developed in the 1960s. The second generation of more effective quinolones, named fluoroquinolones (FQs), were developed between 1980s and 1990s, including norfloxacin, enoxacin, ciprofloxacin and ofloxacin. The fluoroquinolones represent the third largest group of antibiotics, accounting for 17% of the global market [69]. In Figure 1.3. the skeleton of 4-quinolone is displayed, while Table 1.2 presents all types of fluoroquinolones. The

modification on the 4-quinolone skeleton aims to create new and more effective FQ compounds, with better pharmacological properties and less side effects.

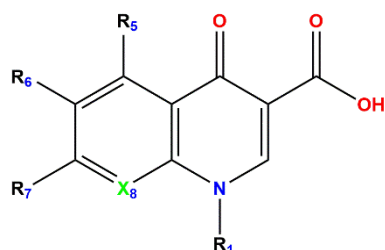

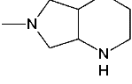
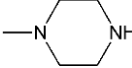
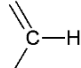
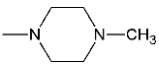
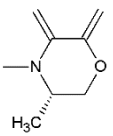
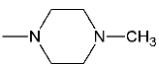
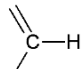

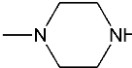
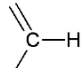
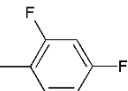
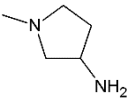
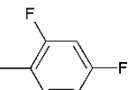
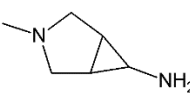


Figure 1.3 4-quinolone skeleton of fluoroquinolones.

Table 1.2 Structural formulae of fluoroquinolones.

FQs Name	Abbreviation	M / g mol ⁻¹	R ₁	R ₅	R ₆	R ₇	X ₈
Ciprofloxacin	CIP	331.35		H	F		
Danofloxacin	DAN	357.37		H	F		
Difloxacin	DIF	399.39		H	F		
Enoxacin	ENO	320.31	-CH ₂ -CH ₃	H	F		=N-
Enrofloxacin	ENR	359.46		H	F		
Fleroxacin	FLE	369.34	-CH ₂ -CH ₂ - F	H	F		
Flumequine	FLU	261.25	H	H	F	H	
Levofloxacin	LEV	361.37	H	H	F		
Lomefloxacin	LOM	351.35	-CH ₂ -CH ₃	H	F		
Marbofloxacin	MAR	362.36	H	H	F		

Moxifloxacin	MOX	401.43		H	F		-O-CH ₃
Norfloxacin	NOR	319.33	-CH ₂ -CH ₃	H	F		
Ofloxacin	OFL	361.37	H	H	F		
Pefloxacin	PEF	333.36	-CH ₂ -CH ₃	H	F		
Sarafloxacin	SAR	385.36		H	F		
Tosufloxacin	TOS	404.34		H	F		=N-
Trovafloxacin	TRO	416.35		H	F		=N-

FQs are widely used in hospitals, households, and in veterinary applications. In Germany alone approximately 571 tons of antibiotics were consumed yearly, among which FQs represented a large fraction [37]. Both human and veterinary FQs are expected to enter the environment in active form through excretion via urine (~80%) and the faeces (20%) [70]. Approximately 70% of the consumed FQs are excreted unchanged, and are only partially eliminated from water and in WWTPs [71]. Due to their high consumption, FQs can reach water bodies through different routes. The first and main route is the point source WWTP effluent but a second relevant route are the veterinary applications of FQs in livestock and in aquaculture.

Interest is growing in the fate of the FQs in the WWTPs since residues of these have been detected in the natural environment of many countries. The total FQs load determined in Chinese WWTP effluents, with a size from 100,000 to 2,400,000 population equivalent (PE), were in the range of 216 to 1,228 g d⁻¹, while values ranging from 190 to 326 g d⁻¹ were determined in WWTPs in the EU. On the other hand the total load of FQs in hospital wastewater was determined to be in the range of 0.3 to 29 g d⁻¹ in Norwegian, Swiss and Chinese hospitals. The concentrations observed for CIP, NOR, OFL and other FQs in the WWTPs influent were up to 30 times lower in comparison to the hospital wastewaters. Verlicchi, et al. [58] reported that 5%, 15% and 67%, respectively, of NOR, CIP and OFL load entering the WWTP originated from hospital use. This indicates that the contribution of

hospital loads to the overall FQ load is situation specific, and that both sources are of importance, with hospital wastewaters as a point source and urban wastewater as a more disperse source of FQ pollution (Table 1.3).

Table 1.3 FQs concentrations in different aqueous matrices. The aqueous matrices were categorized: +++ for $c_{\max} > 1,000 \text{ ng L}^{-1}$; ++ for $c_{\max} 100 - 1,000 \text{ ng L}^{-1}$; + for $c_{\max} < 100 \text{ ng L}^{-1}$. n.d. if no data were available.

FQs	Hospital wastewaters	WWTPs effluent	Surface water	Ground water	References
CIP	+++	++	++	+	[14, 30, 51, 66, 68, 71-75]
DAN	n.d.	+	++	+	[14, 75]
DIF	n.d.	+	+	n.d.	[75-77]
ENO	++	++	+	n.d.	[51, 68, 71, 76, 78]
ENR	+	+	+	+	[14, 30, 75-77, 79]
FLE	+	+	+	n.d.	[75, 76, 79]
FLU	n.d.	+	n.d.	n.d.	[73]
LEV	+	+	n.d.	n.d.	[71, 75]
LOM	+	++	+	n.d.	[51, 74-77, 79]
MAR	+	n.d.	n.d.	n.d.	[75]
MOX	n.d.	+	+	n.d.	[75, 76, 78, 79]
NOR	+++	++	+	+	[14, 51, 71-77, 79]
OFL	+++	++	++	+	[14, 51, 68, 71, 73-77, 79-81]
PEF	+	+	n.d.	n.d.	[75]
SAR	n.d.	+	+	n.d.	[75-77]
TOS	n.d.	+	+	n.d.	[77]
TRO	+	n.d.	n.d.	n.d.	[71]

1.3 Analysis of pharmaceuticals in water and wastewater

The evolution and improvement in the detection of a broader range of compounds made possible the determination of several pharmaceuticals in the concentration of ng L^{-1} to $\mu\text{g L}^{-1}$ in various environmental matrices (e.g. surface water, groundwater, wastewater and drinking water). This is principally attributable to the technological progress in the sensitivity and accuracy of detection equipment and analytical methods. Today liquid chromatography-mass spectrometry (LC-MS) with various MS detectors is the dominant analytical technique for pharmaceutical analysis in water and wastewater [82]. The selection of the analytical methods

is basically dependent on the physical and chemical properties of the target compound (see Figure 1.4). Pharmaceutical compounds contain in their structure many functional groups such as -SH, -OH, -NH and -COOH, and have the tendency to form intermolecular hydrogen bonds [83]. These intermolecular hydrogen bonds affect the inherent volatility of the compounds, their tendency to interact with column packing materials and their thermal stability.

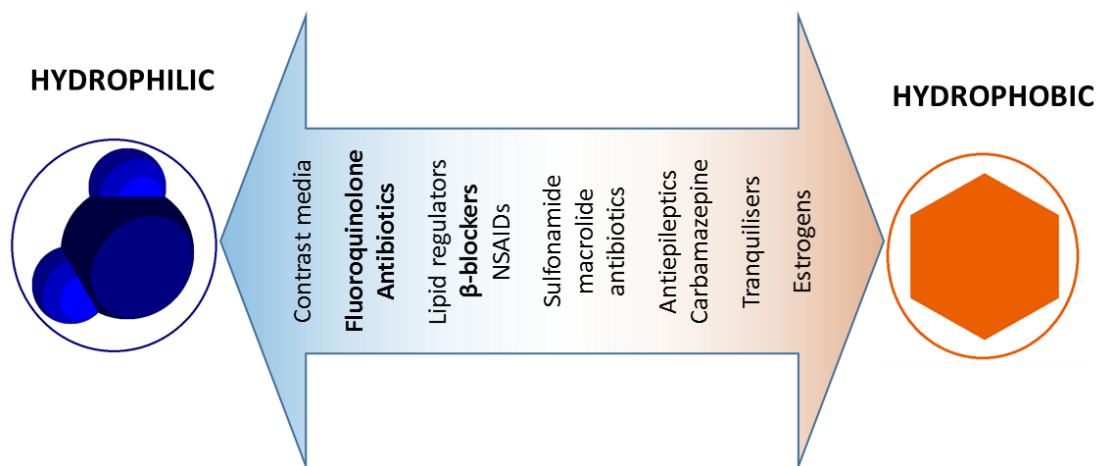


Figure 1.4 Level of hydrophilicity and hydrophobicity of pharmaceutical compounds, based on [84].

Despite the advantages offered by LC-UV in the analysis of polar compounds (e.g., β -blockers, fluoroquinolone antibiotics), the method is unable to provide sufficient information about the compounds' structure. It is very difficult from the LC-UV data alone to say with certainty that a particular peak is pure and contains only a single compound. Using a unit resolution mass spectrometer as a mass-specific detector for LC, provides the masses of all compounds present in the peak, which could be helpful to identify them, and an excellent method to verify the purity of the investigated sample. In LC-MS various detectors are employed, including Ion trap (IT), single quadrupole (SQ), triple quadrupole (TQ), and quadrupole ion trap (QIT). The instruments are used for target analysis, i.e. quantitative or qualitative analysis of known compounds with reference standards. However for non-target analysis many different compounds could potentially lead to the same unit mass in the unit resolution mass spectrometer. To derive a unique sum formula for unknown compounds, a high resolution mass spectrometer (HRMS), such as orbitrap, time-of-flight (TOF), quadrupole time-of-flight (QTOF), and sometimes fourier transform ion cyclotron resonance (FT-ICR) mass spectrometers, connected to LC are required. Another growing trend is the combination of screening for large multi analyte list followed by target quantification. Therefore an instrument with high mass resolution and mass accuracy is needed. Hence, we

have to characterize two important terms: The mass resolution, which is the ability to separate ions of different m/z and it is manifested in the sharpness of the peaks seen in the mass spectrum [85]. Mass resolution can be calculated by using (Eq 1):

$$R = m/\Delta m \quad \text{Eq. 1}$$

Where m is the mass of an ion peak and Δm is the distance to another peak overlapping such that there is a 10% valley between the two peaks (Figure 1.5).

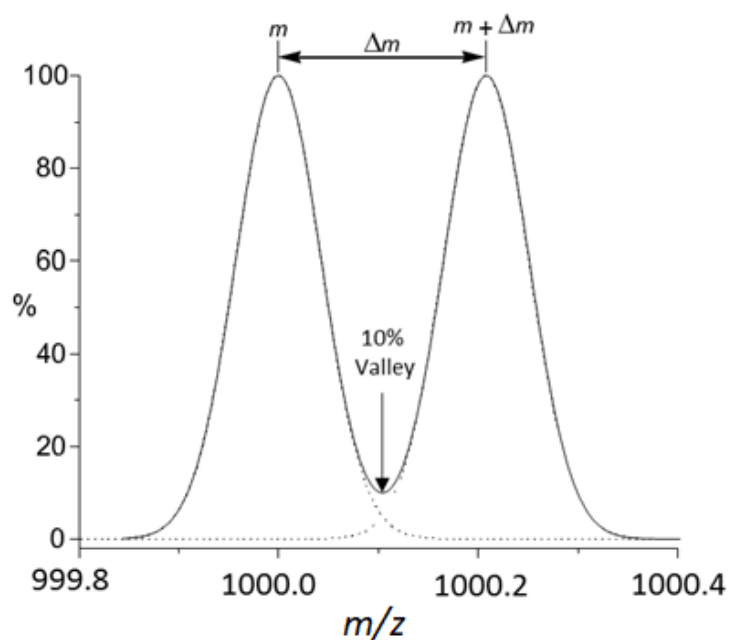


Figure 1.5 Example for the calculation of mass resolution, $m = 1000$ and $\Delta m = 0.208$, so the 10 % valley definition gives a resolution of $1000 / 0.208 = 4,800$.

And the mass accuracy, which is usually reported in parts per million (ppm) (Eq 2), of a spectrometer represents the difference between the calculated mass of an ion and its observed mass, expressed relative to the observed mass (Eq 3) [86].

$$\text{Mass accuracy (ppm)} = 10^6 \times \Delta m/m \quad \text{Eq. 2}$$

$$\Delta m = m_{\text{calculated}} - m_{\text{observed}} \quad \text{Eq. 3}$$

The suspect screening and/or non-target screening can be achieved by tandem-in-time instruments, generally, time-of-flight (TOF). These are capable of up to 60,000, but their sensitivity and the linear dynamic range are still lower than for the other technologies.

Orbitrap technology is increasingly applied due to the combination of high resolving power (up to 280,000), high mass accuracy (<2 ppm), and a sensitivity down to the femtogram range. Fourier transform ion cyclotron resonance (FT-ICR) mass analyzers have been rarely used in polar organic trace analytics due to their high costs and to the fact that the FT-ICR does not support the fast chromatography analysis. Hybrid instruments such as quadrupole TOF (QTOF), linear ion trap or quadrupole orbitrap (LTQ Orbitrap or Q Exactive™) have

particularly shown excellent detection and identification capabilities for low molecular weight compounds in various matrices based on high resolution accurate mass measurements of precursor and product ions.

These instruments are able to record a complete mass spectrum of each pulse of ions introduced, so the sensitivity they achieve is extremely high. This advantage makes these instruments suitable for the suspect screening analysis to confirm the suspected compounds, such as known or predicted transformation products or compounds, for which no reference standards are available (see Figure 1.6).

In contrast to suspect screening, non-target (unknown) screening in a strict sense starts without any a priori information on the compounds to be detected.

The information about the compounds is derived solely from the chromatograms and mass spectra. Therefore, high resolving power with high mass accuracy are recommended. For this type of experiment, an identification by HRMS(/MS) alone is not sufficient and many procedures are recommended for the evaluation steps. The workflows are often focused on one specific evaluation step; the following key features have emerged: (i) first step is a manual or automatic peak search by exact mass filtering from the chromatographic run, which leads to a list of detected ions; (ii) second step is an assignment of an elemental formula to the exact mass of interest; and (iii) the third step is searching in database of plausible structures for the determined elemental formula [87].

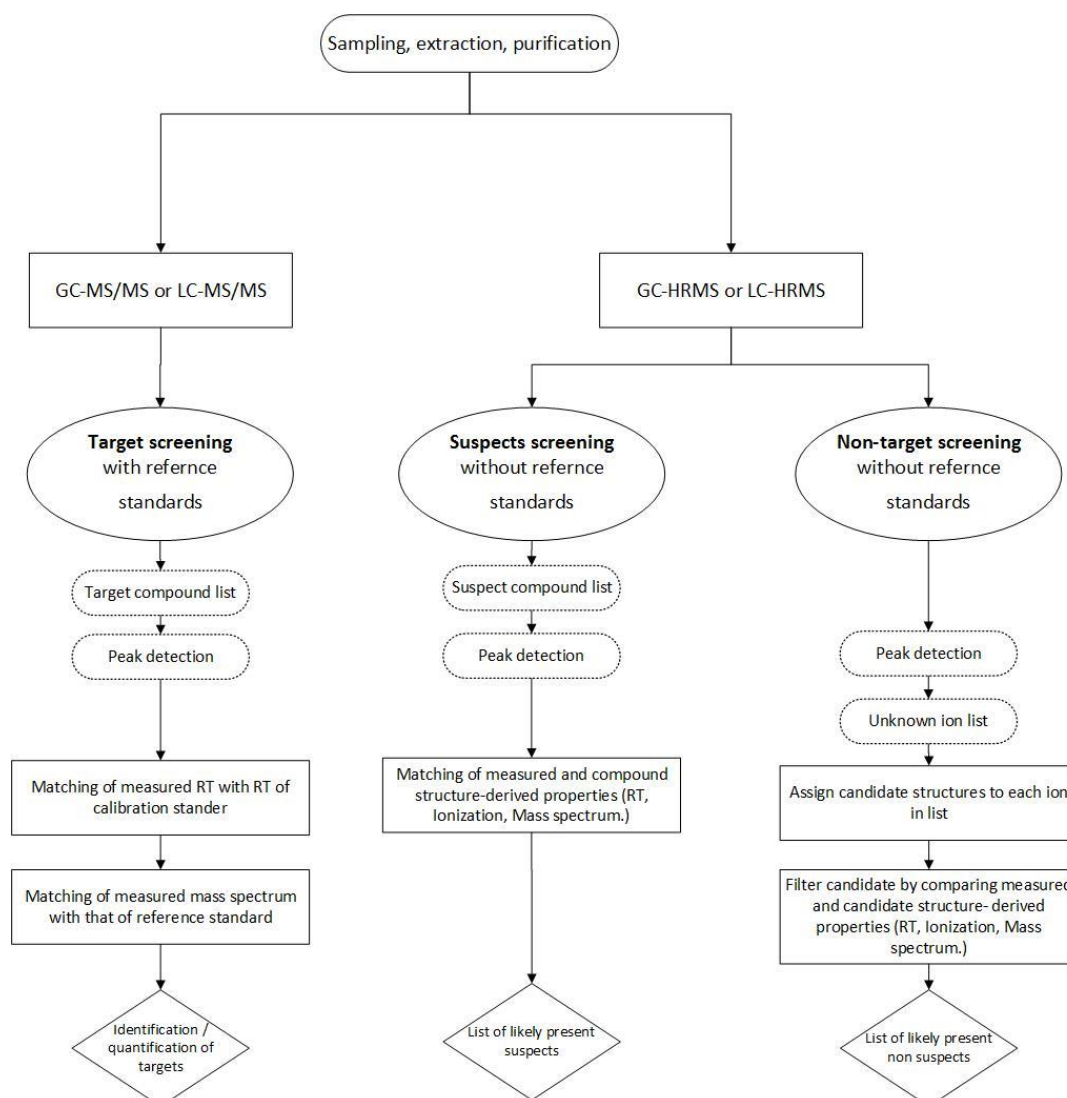


Figure 1.6 Comparison of systematic workflows of environmental samples analysis (i) quantitative target analysis with reference standards, (ii) suspect screening without reference standards, and (iii) non-target screening of unknowns in environmental samples. Reproduced from Krauss, et al. [82].

The most widely applied ionization technique is electrospray ionization (ESI), followed by atmospheric pressure chemical ionization (APCI) [88, 89]. A large number of polar molecules can be ionized in both techniques. Furthermore, the soft ESI generates little fragmentation and provides molecular ions in positive or negative mode, thus the molecular weight can easily be determined [90]. The APCI is usable for molecules showing a low tendency to (de)protonate, so the molecules often induce a stronger fragmentation in APCI [91]. A further ionization technique, called atmospheric pressure photon ionization (APPI), is more selective for individual substance groups and more dependent on the ionization conditions such as flow rate, type and quantity of the non-polar dopant (e.g. toluene, acetone) responsible for the charge or proton transfer [92]. Therefore, APPI is suitable for the determination of non-polar substance groups such as polycyclic aromatic hydrocarbons. Accordingly, the APPI is typically suitable for GC-MS analyses [93].

1.4 Elimination of pharmaceuticals from water and wastewater

In the last two decades, nutrient removal from the water bodies has become increasingly important worldwide. Eutrophication caused by extreme nitrogen and phosphorus in wastewater discharges has disrupted the aquatic life in receiving water bodies, with a subsequent decline in water quality.

Wastewater treatment plants in affected areas and watersheds have to provide additional nutrient removal prior to discharge. Biological nutrient removal is incorporated as part of the secondary treatment or as tertiary treatment. Most of the domestic wastewater treatment plants use biological nitrification–denitrification together with biological oxygen demand (BOD) removal, and/or chemical precipitation for removal of phosphorus. Wastewater treatment plants are essentially divided into two basic stages: primary and secondary treatment (Figure 1.7). Primary treatment in most municipal wastewater treatment plants consists of preliminary and primary stages. These typically consist of screens to remove the large floating objects, grit chambers to settle cinders, sand, and small stones, comminutors, and primary clarifiers to settle smaller particles and suspended solids. The secondary treatment consists of a biological process followed by a secondary clarifier. If the secondary effluent meets the regulatory standards for BOD and the total soluble solids (TSS), then it is discharged to receiving waters following disinfection. The solids and sludge collected from the various units undergo further processing and treatment before disposal. Various options are available for sludge processing.

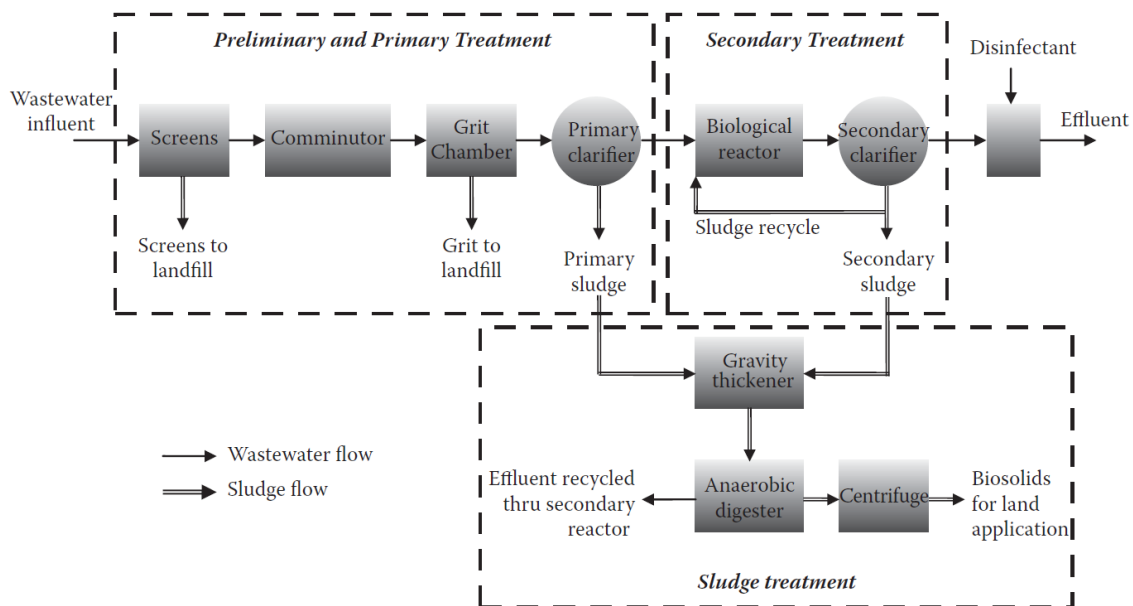


Figure 1.7 Flow diagram of a conventional wastewater treatment plant (figure taken from Riffat [94]).

Pharmaceuticals' elimination during water and wastewater treatment occurs by several mechanisms, where typically one mechanism dominates, depending on the pharmaceutical specifications and the water and wastewater conditions.

In general two elimination processes are important in wastewater treatment: adsorption to suspended solids (sewage sludge) and biodegradation. Adsorption is dependent on both, hydrophobic and electrostatic interactions of the pharmaceutical with particulates and microorganisms. For example, acidic pharmaceuticals, having pK_a values ranging from 4.9 to 4.1, such as ibuprofen, ketoprofen, diclofenac and indomethacin, occur as anions at neutral pH, and have little tendency towards adsorption onto the sludge [95]. However, basic pharmaceuticals and zwitterions can adsorb to sludge to a significant extent, as has been shown for fluoroquinolone antibiotics [96]. When a pharmaceutical compound is present mainly in the dissolved phase, biodegradation is suggested to be the most important elimination process in wastewater treatment. This can occur either in aerobic (and anaerobic) zones in activated sludge treatment, or anaerobically in sewage sludge digestion. In general, biological decomposition of pharmaceuticals increases with an increased hydraulic retention time and with the age of the sludge applied in activated sludge treatment. For example, diclofenac has been shown to be significantly better biodegraded only when the sludge retention time was at least 8 days [97]. In addition to biological reactions, many chemical reactions could be observed such as oxidation-reduction (redox), hydrolysis and acid-base reactions.

Primary and secondary treatment alone in WWTPs has been unable to meet many communities' demands on the water supply. The increasing need to reuse water calls for better wastewater treatment. These challenges are being met through better methods of removing pollutants in treatment plants, such as advanced oxidation processes or through prevention of pollution.

1.5 Advanced oxidation processes: photolysis and semiconductor photocatalysis

The concept of "advanced oxidation processes" (AOPs) was established by Glaze, et al. [98]. AOPs depend mainly on the formation of reactive and short-lived oxygen including intermediates such as hydroxyl radicals ($\cdot\text{OH}$) and they exploit the high reactivity of these species [99]. The underlying oxidative reaction mechanisms essentially imitates the natural photo-initiated processes that take place in sunlit surface waters or in the Earth's atmosphere. The hydroxyl radical is a powerful oxidant (Table 1.4), with a short life and high reactivity, and is considered as a non-selective reagent.

Table 1.4 The redox potential of a number of chemical systems used for water treatment.

Oxidant agent	Redox potential (eV)
$\cdot\text{OH}$	2.80
$\cdot\text{O}$	2.42
O_3	2.07
H_2O_2 (acidic)	1.78
Cl_2	1.36

The photochemical processes are usually classified under this broad definition of AOPs. Most of these processes use a combination of UV with strong oxidants, e.g. O_3 and H_2O_2 , or catalysts, e.g. photocatalyst, and irradiation, e.g. ultrasound (US) systems (Table 1.5).

Table 1.5 List of typical photochemical systems

Photochemical systems
UV
UV / H_2O_2
UV / O_3
UV / H_2O_2 / O_3
UV / H_2O_2 / Fe^{+2}
UV / TiO_2
UV / H_2O_2 / TiO_2
UV / US

The essential photochemical mechanism, termed photooxidation, is induced via the electron excited by the influence of the UV/VIS radiation. Three class of photooxidation reactions are distinguished in:

Photoionization: occurs when a molecule (M) absorbs electromagnetic radiation, followed by the ejection of an electron from the electronically excited molecule (M^*) into the surrounding medium and finally leads to the formation of a radical cation ($\text{M}^{+\cdot}$) (Eq. 4). An excited electron from the excited molecule (M^*) might be quenched by oxygen and yield reactive oxygen species (Eq. 5), which initiate the photochemistry with the molecules (M) (Eq. 6).



Photooxidation: initiated by transient or reactive species which are formed from an electronically excited precursor molecule X^* (Eq. 7). X is an auxiliary oxidant (a-Ox) such as H_2O_2 or O_3 .

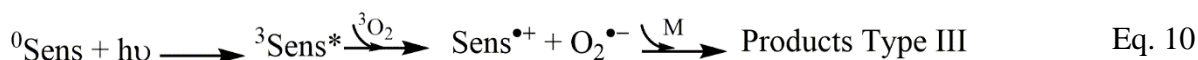
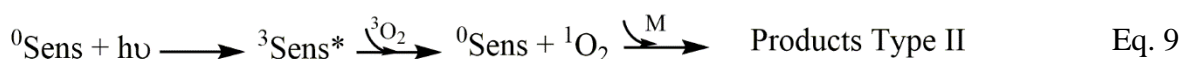
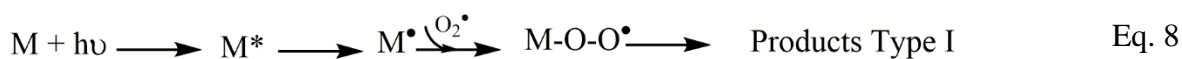


Photooxygenation reactions: which occur via the reactive oxygen species, and have been classified into three different types depending on the oxygen-containing products.

Type I: formed by the reaction of radical ions with the ground state of molecular oxygen (3O_2) via intermediary peroxy radicals (M-O-O \cdot) (Eq. 8).

Type II: obtained by sensitized photooxidations via singlet molecular oxygen (1O_2), which has an electrophilic character, typical biradical (Eq. 9).

Type III: produced by reaction of superoxide radical anions ($O_2^{\bullet-}$) with a suitable molecule M (Eq. 10).



Photocatalysis is one of the AOPs recently used to remove residual micropollutants from the aquatic environment. Titanium dioxide (TiO_2) has been intensively used as a semiconductor photocatalyst to remove the micropollutants from water [100]. The photochemistry of semiconductors like TiO_2 plays an important role in the research concerning heterogeneous photocatalysis and solar synthetic chemistry [101]. The band gap energy E_{bg} of TiO_2 is about 3.2 eV [102]. This energy is equivalent to the wavelength λ of 385.5 nm. Therefore, TiO_2 is able to absorb parts of solar electromagnetic radiation in the UV-A (320 to 400 nm) radiation range. The mechanism of photocatalysis with TiO_2 occurs via absorption of electromagnetic radiation of energy greater than the band gap E_{bg} , leading to the excitation of an electron e^-

from the valence band (VB) to the conduction band (CB). This leaves behind a positive hole h^+ in the valence band. The excited electrons migrate to the reductive side of the TiO_2 surface, while the positive holes migrate to the oxidative surface (see Figure 1.8).

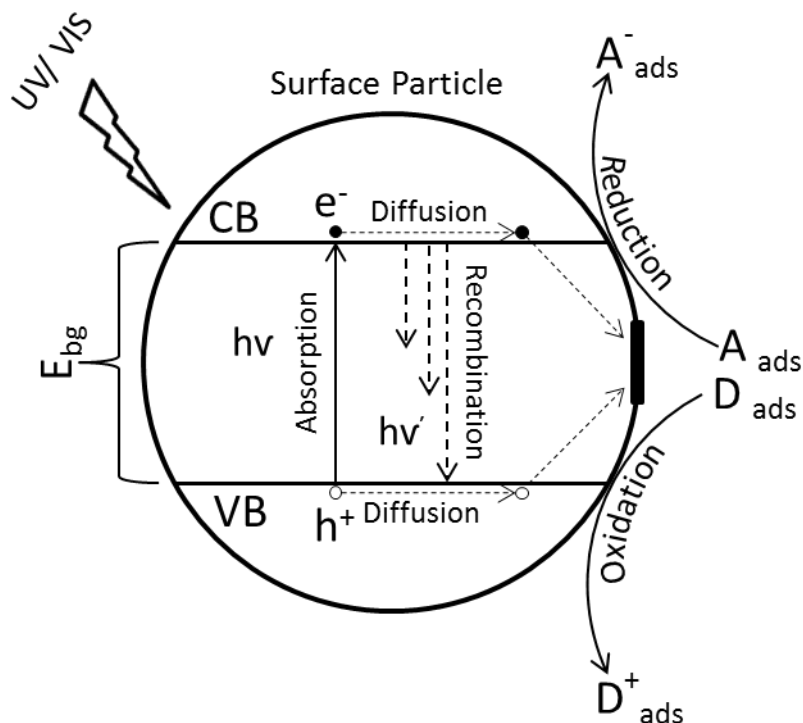
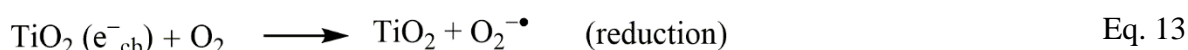
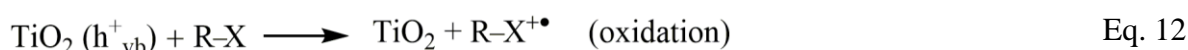
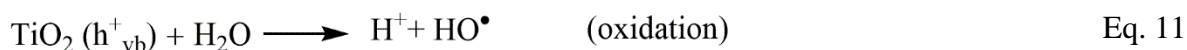
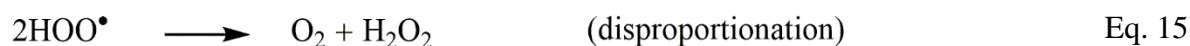
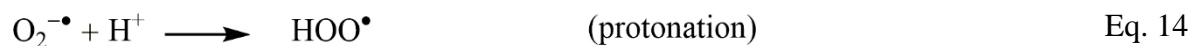


Figure 1.8 Schematic illustration of the photophysical and photochemical processes of the semiconductor particle TiO_2 , modified according to [102].

The formation of an electron-hole pair (h^+_{vb} - e^-_{cb}) is followed by the oxidation of adsorbed water molecules by electron transfer to h^+_{vb} with formation of hydroxyl radicals and H^+ (Eq 11). Otherwise, adsorbed substrate molecules (R-X) may be oxidized directly by electron transfer at the h^+_{vb} side of the TiO_2 particle with formation of radical cations of the substrate (Eq. 12). At the reductive side of TiO_2 particles adsorbed oxygen molecules are acting as electron acceptors to form superoxide radical anions according to Eq. 13, which yield hydroperoxyl radicals after protonation (Eq. 14). Hydrogen peroxide and molecular oxygen are then formed by disproportionation of intermediary hydroperoxyl radicals (Eq 15).





The application of photocatalysis for wastewater treatment has a significant advantage: the UV irradiation of TiO_2 generates $\cdot\text{OH}$ without the use of potentially hazardous short wave radiation or the addition of chemicals. However, there is an associated disadvantage, during photocatalysis with TiO_2 most electrons and holes recombine before they reach the surface of the solid particle [103].

1.6 Transformation products of the pharmaceuticals oxidation

Transformation products (TPs) are assumed to be more abundant in the aquatic environment than their parent compounds, and probably most of the TPs formed during the degradation of the parent compounds have not even been identified yet [104]. Therefore, the aquatic ecosystems are exposed to a changing and unknown cocktail of chemicals. At very low concentrations individual pharmaceuticals are unlikely to pose any direct perceptible risk to human health. On the other hand pharmaceuticals and their TPs can interact with each other resulting in additive or potentially even synergistic mixtures that could have indirect effects on humans, like developing resistance to pathogens [31, 32]. TPs might pose a higher risk than the parent compounds (i) when they form in a high yield; (ii) when they are more mobile than the parent compound; or (iii) if they have a higher toxicity [17]. TPs occurring in the environment can be classified into three categories: (a) Metabolites of the pharmaceuticals formed through initial metabolic reactions in the target organisms (oxidation or conjugation processes inside the livestock and human). (b) TPs formed during environmental reaction systems such as microbial degradation, redox reactions, hydrolysis, or photolysis [105]. (c) TPs formed during advanced water treatment processes (Oxidation processes such as advanced oxidation processes like chlorination, ozonation, UV and UV/ H_2O_2). TPs could be measured and characterized as mentioned in chapter 1.3 using HRMS(/MS) in a suspect screening without reference standards or using a non-target screening workflow.

1.7 Scope of the thesis

The aim of this thesis was to study the photodegradation of several micropollutants in water by UV irradiation. The photolysis of the micropollutants depends on the integrative effects of the photon flux (UV sources), the structure of the micropollutant and the water-matrix composition [106]. Therefore, the systematic investigation of the photodegradation of the micropollutants requires the study of the effects that these three interrelated components have. Figure 1.9 visualize the contribution of the different chapters' to the overall goal of the thesis

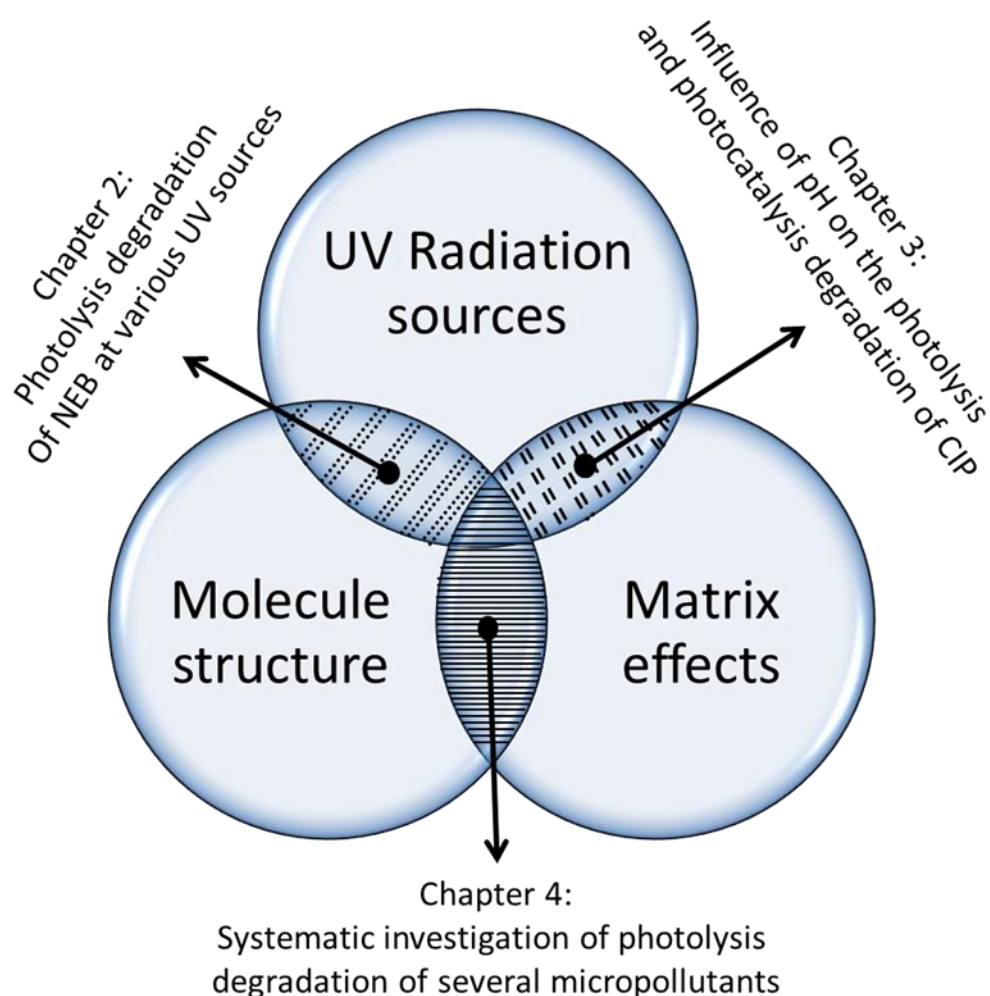


Figure 1.9 Visualization of the different chapters' contribution to the overall goal of the thesis.

The photochemical reactions are initiated by the absorption of a photon. Thus the energy of an absorbed photon is transferred to electrons in the micropollutant and briefly changes their configuration (i.e., promotes the molecule from a ground state to an excited state). The absorption of direct radiation by the micropollutant is a necessary, yet insufficient, condition to lead to photodegradation. Often excited state micropollutants are not kinetically stable in the presence of O_2 or H_2O and can spontaneously decompose (oxidize or hydrolyze).

Sometimes micropollutants decompose to produce high energy, unstable fragments that can react with other micropollutants around them. The two processes are collectively referred to as direct photolysis or indirect photolysis, and both mechanisms contribute to the removal of micropollutants. Therefore, the efficiency of different UV sources, namely, UV-C (254 nm), UV-B (312 nm) and UV-A (365 nm) in the degradation of NEB was investigated, as well as their influence on its reaction kinetic and the photodegradation mechanism (see Chapter 2).

Changes in the matrix's pH might lead to a modification of the molecule's structure, which could enhance or hamper the photodegradation rates. With regard to photolysis, the absorbance spectrum of the reactant dictates the choice of effective UV radiation sources: emission spectrum of the lamp used must match the absorbance spectrum of the molecule to a maximal extent. In addition, the lamps must have sufficient power for successful photolysis degradation. Thus, in Chapter 3 the influence of the pH on the reaction kinetics and the degradation mechanism of ciprofloxacin by direct ultraviolet photolysis (UV) and photocatalysis UV/TiO₂ was investigated.

Diclofenac, metoprolol, carbamazepine, sulfamethoxazole and 1*H*-benzotriazole concentrations have been monitored in the effluent of a wastewater treatment plant over a period of 4 months. This monitoring showed that traditional treatment alone in WWTPs was unable to abate the emerging micropollutants and thus underlined the need to have better methods of removing micropollutants in treatment plants. Therefore, the removal rates, reaction kinetics, and the UV dose required to reduce by 90% the concentration of the above mentioned micropollutants from water by direct UV photolysis, using three different UV sources, namely UV-C, UV-B and UV-A, have been investigated (see Chapter 4).

1.8 Reference

- [1] T. aus der Beek, F.A. Weber, A. Bergmann, S. Hickmann, I. Ebert, A. Hein, A. Kuster, Pharmaceuticals in the environment-Global occurrences and perspectives, *Environ. Toxicol. Chem.*, 35 (2016) 823-835.
- [2] M.J. Bernot, J.C. Becker, J. Doll, T.E. Lauer, A national reconnaissance of trace organic compounds (TOCs) in United States lotic ecosystems, *Sci. Total. Environ.*, 572 (2016) 422-433.
- [3] J.L. Oaks, M. Gilbert, M.Z. Virani, R.T. Watson, C.U. Meteyer, B.A. Rideout, H.L. Shivaprasad, S. Ahmed, M.J. Iqbal Chaudhry, M. Arshad, S. Mahmood, A. Ali, A. Ahmed

Khan, Diclofenac residues as the cause of vulture population decline in Pakistan, *Nature*, 427 (2004) 630-633.

[4] K.A. Kidd, P.J. Blanchfield, K.H. Mills, V.P. Palace, R.E. Evans, J.M. Lazorchak, R.W. Flick, Collapse of a fish population after exposure to a synthetic estrogen, *Proc. Natl. Acad. Sci. USA.*, 104 (2007) 8897-8901.

[5] R. Triebkorn, H. Casper, V. Scheil, J. Schwaiger, Ultrastructural effects of pharmaceuticals (carbamazepine, clofibrac acid, metoprolol, diclofenac) in rainbow trout (*Oncorhynchus mykiss*) and common carp (*Cyprinus carpio*), *Anal. Bioanal. Chem.*, 387 (2007) 1405-1416.

[6] I. Ebert, J. Bachmann, U. Kühnen, A. Küster, C. Kussatz, D. Maletzki, C. Schlüter, Toxicity of the fluoroquinolone antibiotics enrofloxacin and ciprofloxacin to photoautotrophic aquatic organisms, *Environ. Toxicol. Chem.*, 30 (2011) 2786-2792.

[7] H.R. Foster, G.A. Burton, N. Basu, E.E. Werner, Chronic exposure to fluoxetine (Prozac) causes developmental delays in *Rana pipiens* larvae, *Environ. Toxicol. Chem.*, 29 (2010) 2845-2850.

[8] T. Brodin, J. Fick, M. Jonsson, J. Klaminder, Dilute concentrations of a psychiatric drug alter behavior of fish from natural populations, *Science*, 339 (2013) 814-815.

[9] S.D. Richardson, S.Y. Kimura, Water analysis: Emerging contaminants and current issues, *Anal. Chem.*, 88 (2016) 546-582.

[10] B. Petrie, R. Barden, B. Kasprzyk-Hordern, A review on emerging contaminants in wastewaters and the environment: Current knowledge, understudied areas and recommendations for future monitoring, *Water Res.*, 72 (2015) 3-27.

[11] R. Moreno-González, S. Rodríguez-Mozaz, M. Gros, D. Barceló, V.M. León, Seasonal distribution of pharmaceuticals in marine water and sediment from a mediterranean coastal lagoon (SE Spain), *Environ. Res.*, 138 (2015) 326-344.

[12] V. Acuña, D. von Schiller, M.J. García-Galán, S. Rodríguez-Mozaz, L. Corominas, M. Petrovic, M. Poch, D. Barceló, S. Sabater, Occurrence and in-stream attenuation of wastewater-derived pharmaceuticals in Iberian rivers, *Sci. Total. Environ.*, 503-504 (2015) 133-141.

- [13] C. Postigo, D. Barceló, Synthetic organic compounds and their transformation products in groundwater: Occurrence, fate and mitigation, *Sci. Total. Environ.*, 503-504 (2015) 32-47.
- [14] R. López-Serna, A. Jurado, E. Vázquez-Suñé, J. Carrera, M. Petrović, D. Barceló, Occurrence of 95 pharmaceuticals and transformation products in urban groundwaters underlying the metropolis of Barcelona, Spain, *Environ. Pollut.*, 174 (2013) 305-315.
- [15] D.J. Lapworth, N. Baran, M.E. Stuart, R.S. Ward, Emerging organic contaminants in groundwater: A review of sources, fate and occurrence, *Environ. Pollut.*, 163 (2012) 287-303.
- [16] C. Postigo, S.D. Richardson, Transformation of pharmaceuticals during oxidation/disinfection processes in drinking water treatment, *J. Hazard. Mater.*, 279 (2014) 461-475.
- [17] B.I. Escher, R. Baumgartner, M. Koller, K. Treyer, J. Lienert, C.S. McArdell, Environmental toxicology and risk assessment of pharmaceuticals from hospital wastewater, *Water Res.*, 45 (2011) 75-92.
- [18] S. Shen, M.R. Marchick, M.R. Davis, G.A. Doss, L.R. Pohl, Metabolic activation of diclofenac by human cytochrome P450 3A4: role of 5-hydroxydiclofenac, *Chem. Res. Toxicol.*, 12 (1999) 214-222.
- [19] J.P. Bound, N. Voulvoulis, Household disposal of pharmaceuticals as a pathway for aquatic contamination in the United Kingdom, *Environ. Health. Perspect.*, 113 (2005) 1705-1711.
- [20] T. Eggen, M. Moeder, A. Arukwe, Municipal landfill leachates: a significant source for new and emerging pollutants, *Sci. Total. Environ.*, 408 (2010) 5147-5157.
- [21] U. Schwabe, D. Paffrath, *Arzneiverordnungs-Report 2016: Aktuelle Daten, Kosten, Trends und Kommentare*, Springer, Berlin, 2016, pp. 3-27.
- [22] I. Ebert, R. Amato, A. Hein, S. Konradi, *Pharmaceuticals in the environment - avoidance, reduction and monitoring*, Federal environment agency (UBA), Dessau-Roßlau Germany, 2015, pp. 2-24.
- [23] Federal association of the pharmaceutical industry (BPI), *Pharma-Data 2012*, German association for pharmaceutical industry (e.V.), Berlin, 2012, pp. 88.

- [24] F. Vietoris, M. Eberle, T. Jung, M. Lehmann, V. Mertsch, V. Mohaupt, A. Quadflieg, M. Rehfeld-Klein, K. Röske, M. Sengl, T.A. Ternes, R. Wolter, Mikroschadstoffe in Gewässern, Bund/Länder-Arbeitsgemeinschaft Wasser (LAWA), Stuttgart, 2016, pp. 135.
- [25] K. Kümmerer, The presence of pharmaceuticals in the environment due to human use-present knowledge and future challenges, *J. Environ. Manage.*, 90 (2009) 2354-2366.
- [26] Council Directive (EC), Directive 2000/60/EC of the european parliament and of the council of 23 October 2000 establishing a framework for community action in the field of water policy, *OJ. EU. L 327*, 43 (2000) 73.
- [27] Council Directive (EC), Directive 2013/39/EU of the european parliament and of the council *OJ. EU. L 226*, 56 (2013) 44.
- [28] Council Commission (EC), Commission implementing decision (EU) 2015/495 *OJ. EU. L 78*, 58 (2015) 40.
- [29] J.C. Amiard, C.A. Triquet, Chapter 3 - Quality standard setting and environmental monitoring, *Aquatic Ecotoxicology*, Academic Press, 2015, pp. 51-76.
- [30] W.J. Sim, J.W. Lee, E.S. Lee, S.K. Shin, S.R. Hwang, J.E. Oh, Occurrence and distribution of pharmaceuticals in wastewater from households, livestock farms, hospitals and pharmaceutical manufactures, *Chemosphere*, 82 (2011) 179-186.
- [31] W. Xiong, X. Ding, Y. Zhang, Y. Sun, Ecotoxicological effects of a veterinary food additive, copper sulphate, on antioxidant enzymes and mRNA expression in earthworms, *Environ. Toxicol. Pharmacol.*, 37 (2014) 134-140.
- [32] M.S. Diniz, R. Salgado, V.J. Pereira, G. Carvalho, A. Oehmen, M.A. Reis, J.P. Noronha, Ecotoxicity of ketoprofen, diclofenac, atenolol and their photolysis byproducts in zebrafish (*Danio rerio*), *Sci. Total. Environ.*, 505 (2015) 282-289.
- [33] D. Taylor, The pharmaceutical industry and the future of drug development, *Pharmaceuticals in the Environment*, The Royal Society of Chemistry, 2016, pp. 1-33.
- [34] S. Becattini, Y. Taur, E.G. Pamer, Antibiotic-induced changes in the intestinal microbiota and disease, *Trends Mol. Med.*, 22 (2016) 458-478.

- [35] M. Gros, M. Petrović, A. Ginebreda, D. Barceló, Removal of pharmaceuticals during wastewater treatment and environmental risk assessment using hazard indexes, *Environ. Int.*, 36 (2010) 15-26.
- [36] A.C. Alder, C. Schaffner, M. Majewsky, J. Klasmeier, K. Fenner, Fate of beta-blocker human pharmaceuticals in surface water: Comparison of measured and simulated concentrations in the Glatt Valley Watershed, Switzerland, *Water Res.*, 44 (2010) 936-948.
- [37] A. Bergmann, R. Fohrmann, F.A. Weber, Zusammenstellung von Monitoringdaten zu Umweltkonzentrationen von Arzneimitteln, Umweltbundesamt, Germany, 2011, pp. 108.
- [38] C. Miège, M. Favier, C. Brosse, J.P. Canler, M. Coquery, Occurrence of betablockers in effluents of wastewater treatment plants from the Lyon area (France) and risk assessment for the downstream rivers, *Talanta*, 70 (2006) 739-744.
- [39] J. Maszkowska, S. Stolte, J. Kumirska, P. Lukaszewicz, K. Mioduszevska, A. Puckowski, M. Caban, M. Wagil, P. Stepnowski, A. Białk-Bielińska, Beta-blockers in the environment: Part I. Mobility and hydrolysis study, *Sci. Total. Environ.*, 493 (2014) 1112-1121.
- [40] K. Nödler, O. Hillebrand, K. Idzik, M. Strathmann, F. Schiperski, J. Zirlewagen, T. Licha, Occurrence and fate of the angiotensin II receptor antagonist transformation product valsartan acid in the water cycle - A comparative study with selected beta-blockers and the persistent anthropogenic wastewater indicators carbamazepine and acesulfame, *Water Res.*, 47 (2013) 6650-6659.
- [41] S.F. Owen, E. Giltrow, D.B. Huggett, T.H. Hutchinson, J. Saye, M.J. Winter, J.P. Sumpter, Comparative physiology, pharmacology and toxicology of beta-blockers: Mammals versus fish, *Aquat. Toxicol.*, 82 (2007) 145-162.
- [42] S. Haider, S.S. Baqri, Beta-adrenoceptor antagonists reinstate meiotic maturation in *Clarias batrachus* oocytes, *Comp. Biochem. Physiol., A: Mol. Integr. Physiol.*, 126 (2000) 517-525.
- [43] D.B. Huggett, I.A. Khan, C.M. Foran, D. Schlenk, Determination of beta-adrenergic receptor blocking pharmaceuticals in United States wastewater effluent, *Environ. Pollut.*, 121 (2003) 199-205.

- [44] T. Münzel, T. Gori, Nebivolol: the somewhat-different beta-adrenergic receptor blocker, *J. Am. Coll. Cardiol.*, 54 (2009) 1491-1499.
- [45] M. Barbieri, T. Licha, K. Nödler, J. Carrera, C. Ayora, X. Sanchez-Vila, Fate of beta-blockers in aquifer material under nitrate reducing conditions: Batch experiments, *Chemosphere*, 89 (2012) 1272-1277.
- [46] A.Y. Lin, T.H. Yu, S.K. Lateef, Removal of pharmaceuticals in secondary wastewater treatment processes in Taiwan, *J. Hazard. Mater.*, 167 (2009) 1163-1169.
- [47] J. Radjenovic', M. Petrovic', D. Barceló, Fate and distribution of pharmaceuticals in wastewater and sewage sludge of the conventional activated sludge (CAS) and advanced membrane bioreactor (MBR) treatment, *Water Res.*, 43 (2009) 831-841.
- [48] V. Gabet-Giraud, C. Miège, R. Jacquet, M. Coquery, Impact of wastewater treatment plants on receiving surface waters and a tentative risk evaluation: The case of estrogens and beta blockers, *Environ. Sci. Pollut. Res. Int.*, 21 (2014) 1708-1722.
- [49] J. Maszkowska, S. Stolte, J. Kumirska, P. Lukaszewicz, K. Mioduszevska, A. Puckowski, M. Caban, M. Wagil, P. Stepnowski, A. Białk-Bielińska, Beta-blockers in the environment: Part II. Ecotoxicity study, *Sci. Total. Environ.*, 493 (2014) 1122-1126.
- [50] N.M. Vieno, H. Härkki, T. Tuhkanen, L. Kronberg, Occurrence of pharmaceuticals in river water and their elimination in a pilot-scale drinking water treatment plant, *Environ. Sci. Technol.*, 41 (2007) 5077-5084.
- [51] R. Andreozzi, M. Raffaele, P. Nicklas, Pharmaceuticals in STP effluents and their solar photodegradation in aquatic environment, *Chemosphere*, 50 (2003) 1319-1330.
- [52] T. Deblonde, C. Cossu-Leguille, P. Hartemann, Emerging pollutants in wastewater: a review of the literature, *Int. J. Hyg. Environ. Health.*, 214 (2011) 442-448.
- [53] D. Calamari, E. Zuccato, S. Castiglioni, R. Bagnati, R. Fanelli, Strategic survey of therapeutic drugs in the rivers Po and Lambro in northern Italy, *Environ. Sci. Technol.*, 37 (2003) 1241-1248.
- [54] B. Kasprzyk-Hordern, R.M. Dinsdale, A.J. Guwy, Multi-residue method for the determination of basic/neutral pharmaceuticals and illicit drugs in surface water by solid-

phase extraction and ultra performance liquid chromatography-positive electrospray ionisation tandem mass spectrometry, *J. Chromatogr. A*, 1161 (2007) 132-145.

[55] M. Gros, T.M. Pizzolato, M. Petrović, M.J. de Alda, D. Barceló, Trace level determination of beta-blockers in waste waters by highly selective molecularly imprinted polymers extraction followed by liquid chromatography-quadrupole-linear ion trap mass spectrometry, *J. Chromatogr. A*, 1189 (2008) 374-384.

[56] D. Bendz, N.A. Paxéus, T.R. Ginn, F.J. Loge, Occurrence and fate of pharmaceutically active compounds in the environment, a case study: Höje River in Sweden, *J. Hazard. Mater.*, 122 (2005) 195-204.

[57] M. Maurer, B.I. Escher, P. Richle, C. Schaffner, A.C. Alder, Elimination of beta-blockers in sewage treatment plants, *Water Res.*, 41 (2007) 1614-1622.

[58] P. Verlicchi, M. Al Aukidy, A. Galletti, M. Petrovic, D. Barceló, Hospital effluent: investigation of the concentrations and distribution of pharmaceuticals and environmental risk assessment, *Sci. Total. Environ.*, 430 (2012) 109-118.

[59] M.L. Wilde, K. Kümmerer, A.F. Martins, Multivariate optimization of analytical methodology and a first attempt to an environmental risk assessment of beta-blockers in hospital wastewater, *J. Braz. Chem. Soc.*, 23 (2012) 1732-1740.

[60] K.H. Langford, K.V. Thomas, Determination of pharmaceutical compounds in hospital effluents and their contribution to wastewater treatment works, *Environ. Int.*, 35 (2009) 766-770.

[61] R. Meffe, I. de Bustamante, Emerging organic contaminants in surface water and groundwater: A first overview of the situation in Italy, *Sci. Total. Environ.*, 481 (2014) 280-295.

[62] F. Sacher, F.T. Lange, H.J. Brauch, I. Blankenhorn, Pharmaceuticals in groundwaters analytical methods and results of a monitoring program in Baden-Württemberg, Germany, *J. Chromatogr. A*, 938 (2001) 199-210.

[63] T.A. Ternes, Analytical methods for the determination of pharmaceuticals in aqueous environmental samples, *Trends Anal. Chem.*, 20 (2001) 419-434.

- [64] T.A. Ternes, Occurrence of drugs in German sewage treatment plants and rivers, *Water Res.*, 32 (1998) 3245-3260.
- [65] Q. Sui, X. Cao, S. Lu, W. Zhao, Z. Qiu, G. Yu, Occurrence, sources and fate of pharmaceuticals and personal care products in the groundwater: A review, *Emcon.*, 1 (2015) 14-24.
- [66] K.V. Thomas, C. Dye, M. Schlabach, K.H. Langford, Source to sink tracking of selected human pharmaceuticals from two Oslo city hospitals and a wastewater treatment works, *J. Environ. Manage.*, 9 (2007) 1410-1418.
- [67] M.J. Hilton, K.V. Thomas, Determination of selected human pharmaceutical compounds in effluent and surface water samples by high-performance liquid chromatography-electrospray tandem mass spectrometry, *J. Chromatogr. A*, 1015 (2003) 129-141.
- [68] A.Y. Lin, Y.T. Tsai, Occurrence of pharmaceuticals in Taiwan's surface waters: Impact of waste streams from hospitals and pharmaceutical production facilities, *Sci. Total. Environ.*, 407 (2009) 3793-3802.
- [69] B. Hamad, The antibiotics market, *Nat. Rev. Drug. Discov.*, 9 (2010) 675-676.
- [70] R. Lindberg, P.-Å. Jarnheimer, B. Olsen, M. Johansson, M. Tysklind, Determination of antibiotic substances in hospital sewage water using solid phase extraction and liquid chromatography/mass spectrometry and group analogue internal standards, *Chemosphere*, 57 (2004) 1479-1488.
- [71] K. Kümmerer, A. Henninger, Promoting resistance by the emission of antibiotics from hospitals and households into effluent, *Clin. Microbiol. Infect.*, 9 (2003) 1203-1214.
- [72] H.A. Duong, N.H. Pham, H.T. Nguyen, T.T. Hoang, H.V. Pham, V.C. Pham, M. Berg, W. Giger, A.C. Alder, Occurrence, fate and antibiotic resistance of fluoroquinolone antibacterials in hospital wastewaters in Hanoi, Vietnam, *Chemosphere*, 72 (2008) 968-973.
- [73] S. Zorita, L. Mårtensson, L. Mathiasson, Occurrence and removal of pharmaceuticals in a municipal sewage treatment system in the south of Sweden, *Sci. Total. Environ.*, 407 (2009) 2760-2770.

- [74] X. Chang, M.T. Meyer, X. Liu, Q. Zhao, H. Chen, J.A. Chen, Z. Qiu, L. Yang, J. Cao, W. Shu, Determination of antibiotics in sewage from hospitals, nursery and slaughter house, wastewater treatment plant and source water in Chongqing region of Three Gorge Reservoir in China, *Environ. Pollut.*, 158 (2010) 1444-1450.
- [75] X. Van Doorslaer, J. Dewulf, H. Van Langenhove, K. Demeestere, Fluoroquinolone antibiotics: An emerging class of environmental micropollutants, *Sci. Total. Environ.*, 500-501 (2014) 250-269.
- [76] K. He, A.D. Soares, H. Adejumo, M. McDiarmid, K. Squibb, L. Blaney, Detection of a wide variety of human and veterinary fluoroquinolone antibiotics in municipal wastewater and wastewater-impacted surface water, *J. Pharm. Biomed. Anal.*, 106 (2015) 136-143.
- [77] H. Nakata, K. Kannan, P.D. Jones, J.P. Giesy, Determination of fluoroquinolone antibiotics in wastewater effluents by liquid chromatography-mass spectrometry and fluorescence detection, *Chemosphere*, 58 (2005) 759-766.
- [78] N. Dorival-García, A. Zafra-Gómez, S. Cantarero, A. Navalón, J.L. Vílchez, Simultaneous determination of 13 quinolone antibiotic derivatives in wastewater samples using solid-phase extraction and ultra performance liquid chromatography-tandem mass spectrometry, *J. Microc.*, 106 (2013) 323-333.
- [79] A. Jia, Y. Wan, Y. Xiao, J. Hu, Occurrence and fate of quinolone and fluoroquinolone antibiotics in a municipal sewage treatment plant, *Water Res.*, 46 (2012) 387-394.
- [80] G. Teijon, L. Candela, K. Tamoh, A. Molina-Díaz, A.R. Fernandez-Alba, Occurrence of emerging contaminants, priority substances (2008/105/CE) and heavy metals in treated wastewater and groundwater at Depurbaix facility (Barcelona, Spain), *Sci. Total. Environ.*, 408 (2010) 3584-3595.
- [81] Y. Cabeza, L. Candela, D. Ronen, G. Teijon, Monitoring the occurrence of emerging contaminants in treated wastewater and groundwater between 2008 and 2010. The Baix Llobregat (Barcelona, Spain), *J. Hazard. Mater.*, 239-240 (2012) 32-39.
- [82] M. Krauss, H. Singer, J. Hollender, LC-high resolution MS in environmental analysis: from target screening to the identification of unknowns, *Anal. Bioanal. Chem.*, 397 (2010) 943-951.

- [83] C. Christou, H.G. Gika, N. Raikos, G. Theodoridis, GC-MS analysis of organic acids in human urine in clinical settings: a study of derivatization and other analytical parameters, *J. Chromatogr. B* 964 (2014) 195-201.
- [84] D. Fatta, A. Achilleos, A. Nikolaou, S. Meriç, Analytical methods for tracing pharmaceutical residues in water and wastewater, *Trends Anal. Chem.*, 26 (2007) 515-533.
- [85] M. Balogh, Debating resolution and mass accuracy in mass spectrometry, *Spectroscopy*, 19 (2004) 34-34.
- [86] A.G. Brenton, A.R. Godfrey, Accurate mass measurement: Terminology and treatment of data, *J. Am. Soc. Mass Spectrom.*, 21 (2010) 1821-1835.
- [87] P. Gago-Ferrero, E.L. Schymanski, J. Hollender, N.S. Thomaidis, Chapter 13 - Nontarget analysis of environmental samples based on liquid chromatography coupled to high resolution mass spectrometry (LC-HRMS), P.E. Sandra Pérez, B. Damià (Eds.) *Comprehensive. Analyti. Chem.*, Elsevier, 2016, pp. 381-403.
- [88] T. Kuuranne, M. Vahermo, A. Leinonen, R. Kostianen, Electrospray and atmospheric pressure chemical ionization tandem mass spectrometric behavior of eight anabolic steroid glucuronides, *J. Am. Soc. Mass Spectrom.*, 11 (2000) 722-730.
- [89] H. Keski-Hynnila, M. Kurkela, E. Elovaara, L. Antonio, J. Magdalou, L. Luukkanen, J. Taskinen, R. Kostianen, Comparison of electrospray, atmospheric pressure chemical ionization, and atmospheric pressure photoionization in the identification of apomorphine, dobutamine, and entacapone phase II metabolites in biological samples, *Anal. Chem.*, 74 (2002) 3449-3457.
- [90] C.S. Ho, C.W. Lam, M.H. Chan, R.C. Cheung, L.K. Law, L.C. Lit, K.F. Ng, M.W. Suen, H.L. Tai, Electrospray ionisation mass spectrometry: Principles and clinical applications, *Clin. Biochem. Rev.*, 24 (2003) 3-12.
- [91] Y. Tanaka, K. Otsuka, S. Terabe, Evaluation of an atmospheric pressure chemical ionization interface for capillary electrophoresis-mass spectrometry, *J. Pharm. Biomed. Anal.*, 30 (2003) 1889-1895.

- [92] M. Tubaro, E. Marotta, R. Seraglia, P. Traldi, Atmospheric pressure photoionization mechanisms. 2. The case of benzene and toluene, *Rapid Commun. Mass Spectrom*, 17 (2003) 2423-2429.
- [93] D.X. Li, L. Gan, A. Bronja, O.J. Schmitz, Gas chromatography coupled to atmospheric pressure ionization mass spectrometry (GC-API-MS): Review, *Anal. Chim. Acta*, 891 (2015) 43-61.
- [94] R. Riffat, *Fundamentals of wastewater treatment and engineering*, Taylor & Francis Group, LLC, 2013, pp. 31.
- [95] J.L. Tambosi, L.Y. Yamanaka, H.J. José, R.d.F.P.M. Moreira, H.F. Schröder, Recent research data on the removal of pharmaceuticals from sewage treatment plants (STP), *Química Nova*, 33 (2010) 411-420.
- [96] T. Urase, T. Kikuta, Separate estimation of adsorption and degradation of pharmaceutical substances and estrogens in the activated sludge process, *Water Res*, 39 (2005) 1289-1300.
- [97] N. Kreuzinger, M. Clara, B. Strenn, H. Kroiss, Relevance of the sludge retention time (SRT) as design criteria for wastewater treatment plants for the removal of endocrine disruptors and pharmaceuticals from wastewater, *Water Sci. Technol.*, 50 (2004) 149-156.
- [98] W.H. Glaze, J.-W. Kang, D.H. Chapin, The chemistry of water treatment processes involving ozone, hydrogen peroxide and ultraviolet radiation, *Ozone: Sci. Eng.*, 9 (1987) 335-352.
- [99] C. von Sonntag, Advanced oxidation processes: Mechanistic aspects, *Water Sci. Technol.*, 58 (2008) 1015-1021.
- [100] A. Fujishima, X. Zhang, Titanium dioxide photocatalysis: Present situation and future approaches, *C. R. Chim.*, 9 (2006) 750-760.
- [101] A. Fujishima, X. Zhang, D. Tryk, Heterogeneous photocatalysis: From water photolysis to applications in environmental cleanup, *Int. J. Hydrogen Energy*, 32 (2007) 2664-2672.
- [102] M.R. Hoffmann, S.T. Martin, W. Choi, D.W. Bahnemann, Environmental applications of semiconductor photocatalysis, *Chem. Rev.*, 95 (1995) 69-96.

- [103] L. Sun, J.R. Bolton, Determination of the quantum yield for the photochemical generation of hydroxyl radicals in TiO₂ suspensions, *J. Phys. Chem.*, 100 (1996) 4127-4134.
- [104] T. Haddad, E. Baginska, K. Kümmerer, Transformation products of antibiotic and cytostatic drugs in the aquatic cycle that result from effluent treatment and abiotic/biotic reactions in the environment: An increasing challenge calling for higher emphasis on measures at the beginning of the pipe, *Water Res.*, 72 (2015) 75-126.
- [105] D. Fatta-Kassinos, M.I. Vasquez, K. Kümmerer, Transformation products of pharmaceuticals in surface waters and wastewater formed during photolysis and advanced oxidation processes - degradation, elucidation of byproducts and assessment of their biological potency, *Chemosphere*, 85 (2011) 693-709.
- [106] S.R. Batchu, V.R. Panditi, K.E. O'Shea, P.R. Gardinali, Photodegradation of antibiotics under simulated solar radiation: Implications for their environmental fate, *Sci. Total. Environ.*, 470-471 (2014) 299-310.

2 Photolytic degradation of the β -blocker nebivolol in aqueous solution

redrafted from: Alaa Salma , Holger Lutze, Torsten C. Schmidt, Jochen Tuerk, Water Research, 2017, 116, 211-219.

2.1 Abstract

Nebivolol (NEB) is one of the top-sold prescription drugs belonging to the third generation of beta-blockers. However, so far, occurrence data in the environment are lacking. Within this study NEB has been found for the first time in effluent samples of wastewater treatment plants in Germany with an average concentration of 13 ng L^{-1} .

Its photodegradation behavior in the environment and in technical processes is largely unknown. To fill this gap, three different UV treatment procedures (UV-C at 254 nm, UV-B at 312 nm and UV-A at 365 nm) were investigated in three different matrices: pure water, pure water in presence of the hydroxyl radical ($\cdot\text{OH}$) scavenger tert.-butanol and real wastewater. No elimination was observed during UV-A treatment. In contrast, NEB degradation during UV-B and UV-C treatment followed pseudo first order reaction kinetics, with highest removal rate during UV-C treatment in pure water ($k = 7.8 \times 10^{-4} \text{ s}^{-1}$). The rate constant for UV-C irradiation decreased to $2.9 \times 10^{-4} \text{ s}^{-1}$ in the presence of the $\cdot\text{OH}$ scavenger and in the presence of the wastewater matrix. The rate constant for the UV-B lamp was $4.4 \times 10^{-4} \text{ s}^{-1}$. Three transformation products were identified after UV-B and UV-C photolytic degradation using high resolution mass spectrometry. The main photoreaction is the substitution of the fluorine atoms of NEB by hydroxyl groups. A photolytic cleavage of the C-F bond can be excluded, as the high bond dissociation energy of aromatic C-F bonds (525 kJ mol^{-1}), exceeds the energy of electromagnetic radiation applied in the present study ($\geq 254 \text{ nm}$, i.e., max. $471 \text{ kJ Einstein}^{-1}$). The quantum yields for NEB degradation for the UV-C lamp achieved in pure water, the $\cdot\text{OH}$ scavenged system and wastewater matrix were $\Phi_{\text{deg}} = 0.53$, 0.19 and 0.22, respectively. For UV-B Φ_{deg} was 0.023 ± 0.003 , noticeable differences in quantum yield were not found. The photooxidation involves reactive oxygen species such as superoxide and singlet oxygen. These oxidative species may be formed upon reaction of photo-excited NEB with oxygen.

2.2 Keywords

Nebivolol, UV, wastewater treatment, photolysis, transformation products

2.3 Introduction

Due to the large-scale production and consumption of pharmaceuticals, these compounds and their human and wastewater treatment plant derived metabolites are discharged substantially into aquatic environments through sewage. The progress made in analytical chemistry [1] nowadays allows the measurement of pharmaceuticals at very low concentrations in the range of ng L^{-1} to $\mu\text{g L}^{-1}$ in wastewater [2], surface water [3, 4], groundwater [5-7], and even drinking water [8]. Therefore micropollutants are discussed due to possible effects on the ecosystem and their potential to reach drinking water [9]. At very low concentrations, pharmaceuticals are unlikely to pose any direct perceptible risk to human health, but there could be indirect effects such as increasing resistance of pathogens against antibiotics [10, 11] or chronic effects in water organisms [12, 13]. They could possibly affect also aquatic ecosystems. β -blockers are a class of drugs used in various indications such as cardiac arrhythmias, hypertension and cardio protection after a heart attack. Thus, they are consumed widely in the world. Due to their massive use, β -blockers have been detected in aquatic environments [14, 15]. Haider and Baqri [16] found that aqueous solutions of propranolol and other β -blockers have an effect on the oocyte maturation of catfish. Triebkorn, et al. [17] observed that the exposure of rainbow trout to $1 \mu\text{g L}^{-1}$ of metoprolol showed ultrastructural changes in the liver and kidney, as well as in gills at concentration above $20 \mu\text{g L}^{-1}$.

Huggett, et al. [18] studied growth dysfunctions on the invertebrates in the presence of 0.5 mg L^{-1} propranolol. In another study, Huggett, et al. [19] found that exposure to 0.5 mg L^{-1} of propranolol reduced growth rates of Japanese medaka. Propranolol has been detected in WWTP effluents at concentrations from 30 to 373 ng L^{-1} [18, 20, 21] and in surface waters [22, 23] at levels of ng L^{-1} . On the other hand metoprolol has been detected at concentrations up to 590 ng L^{-1} in environmental samples (rivers, lakes, etc.) [22, 24] and up to 122 ng L^{-1} in groundwater [6].

NEB belongs to the third generation of β 1 blockers and is used for the treatment of hypertension. Unlike non-selective drugs, which block both β 1 and β 2-receptors, nebivolol, being a β 1-selective drug, blocks primarily the cardiac and other β 1-adrenoceptors [25], and is used as a drug to treat high blood pressure [26]. Comparison between the safety of NEB and other beta-blockers shows that nebivolol has better pharmacological properties and less side effects [27], e.g. 5 mg daily administration of NEB is as efficacious as any other β -adrenoceptor antagonist against hypertension, with no appreciable difference between peak and trough level of drugs. A daily administration of only 5 mg NEB achieves a higher blood

pressure normalisation rate than a 200 mg daily administration of metoprolol, 100 mg atenolol or 80 mg propranolol, respectively. NEB was listed as one of the top-sold prescription pharmaceuticals in the USA with more than 6.4 million prescriptions from April 2014 to March 2015 [28]. Compared to other beta blockers, NEB has been reported to have a higher selective β_1 -blocking activity, 320 times higher than that of propranolol and carvedilol [26], and it also has better pharmacological properties and less side effects [27]. Considering these advantages, the probability that the consumption of NEB in the future will increase is high. Consequently, the chance that NEB and its degradation products end up in the environment will also increase. Van Nuijs, et al. [29] reported the occurrence of up to 10 ng L^{-1} NEB in the influent of wastewater treatment plants but otherwise no data on occurrence of NEB and its potential effects on the aquatic environment are available. In nature, several drug compounds are degraded photolytically. However, the photodegradation behavior of NEB in the environment and in technical processes is so far largely unknown. Thus, the main goal of this study was to investigate the photolytic degradation of NEB and its transformation products. Therefore, the efficiency of different UV sources, namely, UV-C (254 nm), UV-B (312 nm) and UV-A (365 nm) for the degradation of NEB were investigated, as well as their influence on its degradation rate. Finally a photodegradation mechanism was proposed. Liquid chromatography – high resolution mass spectrometry (LC-HRMS) analysis was used to identify the intermediates at a specific degradation time. In addition, the photolytic reactions were also performed in NEB-containing wastewater for studying the effect of the wastewater matrix on the degradation process.

2.4 Experimental section

2.4.1 Reagents and materials

Following chemicals were used as received: NEB (98%) was obtained from Chemos GmbH (Regenstauf, Germany). Its chemical and physical characteristics are summarized in Suppl. 6.1. The structure of NEB is a racemate of d-nebivolol and l-nebivolol with the stereochemical designations of [S3R]-nebivolol and [R3S]-nebivolol. NEB is soluble in N,N-dimethylformamide, methanol, dimethylsulfoxide; sparingly soluble in polypropylene glycol, polyethylene glycol and ethanol; and very slightly soluble in dichloromethane, hexane and methyl-benzene [30, 31]. HPLC and UPLC/MS grade water and methanol were purchased from Th. Geyer (Renningen, Germany). Potassium ferric oxalate trihydrate ($\text{K}_3\text{Fe}(\text{C}_2\text{O}_4)_3 \cdot 3\text{H}_2\text{O}$) was received from Gentaur (Aachen, Germany). Sulfuric acid (H_2SO_4 97%) was purchased from Merck (Darmstadt, Germany). Sodium acetate (CH_3COONa),

Acetylacetone ($C_5H_8O_2 \geq 99\%$), 4-Chlorobenzoic acid (pCBA 99%) and 1,10-phenanthroline monohydrate were supplied by Sigma-Aldrich (Steinheim, Germany). Ferrous sulfate ($FeSO_4 \cdot 7H_2O$) and tertiary butanol (*tert*-BuOH $\geq 99.7\%$) were obtained from Fluka (Steinheim, Germany). Ammonium acetate ($NH_4C_2H_3O_2 >99\%$) and acetic acid ($CH_3COOH \geq 99\%$) were provided by Biosolve (CE Valkenswaard, Holand).

2.4.2 Photodegradation investigations

2.4.2.1 Experimental set-up

All experiments were carried out in a small recirculating photoreactor (for further information see the supplementary material Suppl. 6.2). Three types of 15 W UV lamps were used during the experiments: (1) a UV-A lamp mainly emitting in the wavelength range 315 to 400 nm, main emission band at 365 nm (Vilber Lourmat, Eberhardzell, Germany), (2) a UV-B lamp mainly emitting in the wavelength range 280 to 360 nm, main emission band at 312 nm (Vilber Lourmat, Eberhardzell, Germany) and (3) a low pressure UV lamp (New NEC Light Ing., Shiga, Japan) that mainly emits in the UV-C range (254 nm). The emission spectra are shown in Suppl. 6.3 of the supplementary material. An open rectangular cuboid pyrex glass reactor 48 x 4 x 3 (L x W x D) cm was used to irradiate the reaction solution. One reservoir was connected to the reactor and for every degradation experiment 500 mL of NEB solution ($25 \mu\text{mol L}^{-1}$) was circulated using a peristaltic pump (Multifix constant MC 1000 FEC, Alfred Schwinherr KG, Schwäbisch-Gmünd, Germany). The reactor was fed with a continuous laminar flow (100 mL min^{-1} , length of the reactor 48 cm). The optical pathlength of the solution in the reactor was below 5 mm. A distance of 5 cm between the lamp and the reaction solution surface was maintained for all experiments.

2.4.2.2 Ferrioxalate actinometry

Ferrioxalate actinometry was conducted according to Bolton and Linden [32] to determine the fluence rate of the UV lamps. UV-A gave polychromatic radiation with the highest E_{avg} (1.95 mW cm^{-2}), followed by UV-B, also with polychromatic radiation (1.67 mW cm^{-2}) and UV-C produced monochromatic radiation (0.64 mW cm^{-2}). Detailed information about the experimental procedure, as well as the calculated values of the light intensity (I) (Einstein/s) and energy flux (E_{avg}) (W m^{-2}) of the UV lamps can be found in the Ferrioxalate actinometry section in appendix 6.2.

2.4.2.3 Kinetic experiments

The degradation kinetics of NEB solutions were evaluated in triplicate experiments at neutral pH and room temperature ($20 \text{ }^\circ\text{C}$). Matrix influence on the degradation kinetics of NEB was

investigated in the effluent of the wastewater treatment plant Duisburg-Hochfeld, Germany (pH 7.2, dissolved organic carbon (DOC) 6.5 mg L⁻¹, specific UV absorbance at 254 nm (SUVA₂₅₄) 1.3 m⁻¹, 220,000 population equivalent). The wastewater was spiked with 25 μmol L⁻¹ of NEB. The formation of [•]OH during the photodegradation process was evaluated based on a *tert*-BuOH assay. In sufficient excess of *tert*-BuOH, [•]OH will quantitatively react with *tert*-BuOH to form formaldehyde with a yield of 50% per [•]OH-attack [33]. Formaldehyde was determined using Hantzsch reaction [34]. Before the start of each new experiment, the whole experimental set-up was cleaned two times with pure water. The UV sources were equilibrated for 15 minutes before each experiment. 1 mL samples were collected in HPLC vials during the experiments at interval times of 0, 5, 10, 15, 20, 30, 45, 60, 90 and 120 minutes. NEB elimination was measured by LC-MS/MS (see section 2.4.2).

2.4.3 Analytical Methods

2.4.3.1 Ion chromatography for fluoride determination

A Metrohm compact ion chromatograph equipped with a 881 Compact IC pro1 conductivity detector (Metrohm AG, Herisau, Switzerland) was employed to measure fluoride. The separation was performed on a Metrosep A Supp 7 - 250/4.0 column (Metrohm AG, Herisau, Switzerland) with a 9.0 mM sodium carbonate (Na₂CO₃) eluent at a flow rate of 0.7 mL min⁻¹. Under these conditions the retention time of fluoride was 6.72 min. The eluents and standards were purchased from Merck KGaA (Darmstadt, Germany).

2.4.3.2 LC-MS/MS analysis

A QTRAP 6500 (AB SCIEX Deutschland GmbH, Darmstadt, Germany) connected to a 1100 series HPLC (Agilent Technologies, Waldbronn, Germany) was used to quantify the NEB concentration during the photodegradation process and in real wastewater samples. The chromatographic separation was performed on a 50 x 2 mm Chromolith[®] Fast Gradient RP 18e HPLC column (Merck KGaA, Darmstadt, Germany) at 40 °C. The mobile phase consisted of 0.1 % formic acid in water (v/v) (mobile phase A) and 0.1 % formic acid in acetonitrile (v/v) (mobile phase B). The gradient program started with 1.0% B organic phase, and it was raised to 99% B within 2.5 minutes, then kept constant for 30 seconds and afterwards again reduced to 1.0% B for 30 seconds, followed by a reequilibration of 4.5 min. The flow rate was 500 μL min⁻¹. To achieve a fast gradient the mixing point was installed directly in front of the injection point of the HTS PAL Autosampler. NEB was quantified after positive electrospray ionisation (ESI⁺) in multiple reaction monitoring (MRM) mode. The optimized MS operating conditions were as follows: the curtain gas was set at 40 psi, the

nebulizer source gas 1 at 55 psi, and the turbo ion source gas 2 at 60 psi. The optimal declustering potential was 100 V, and entrance potential 10 V. The NEB fragmentation was induced by collisionally activated dissociation with nitrogen gas. The collision gas pressure was set at 2.0 psi. A collision energy of 39 eV and a collision cell exit potential of 4.0 V were utilized. The precursor, quantifier, and qualifier ions of the HPLC–MS/MS quantification measurements were set at m/z 406, 151, and 103, respectively. A dwell time of 50 ms was employed. Data evaluation was done with Analyst™ 1.6.2 (AB Sciex Deutschland GmbH, Darmstadt, Germany). The calibration was weighted 1/x with a linear regression.

2.4.3.3 LC-HRMS analysis for structure elucidation

The transformation products (TPs) formed during the degradation of NEB were investigated using an Exactive Orbitrap mass spectrometer (Thermo Fisher Scientific, Bremen, Germany). The TPs separation was carried out on an U-HPLC system (Thermo Scientific Accela™) consisting of a degasser, a quaternary pump, a thermostated Autosampler and a column oven. The chromatographic separation was performed on a 150 x 2 mm Synergi 4u Polar-RP 80A HPLC column (Phenomenex, Aschaffenburg, Germany) at 40 °C. The binary mobile phase consisted of 0.1% formic acid in water (v/v) (mobile phase A) and 0.1% formic acid in acetonitrile (v/v) (mobile phase B). The gradient program started with 5% B, and it was raised to 100% B within 10 minutes, then kept constant for 4 minutes and finally decreased again to 5% B within 30 seconds. Finally, the column was re-equilibrated to the initial conditions and stabilized for 5 minutes. The flow rate was set to 200 $\mu\text{L min}^{-1}$. Electrospray ionization (ESI) in positive and negative ionization mode was used. ESI was operated under the following specific conditions: ionization voltage -3.5 kV for negative mode and +4.0 kV for positive mode; sheath gas 35 psi; auxiliary gas 30 psi; sweep gas 0.03 arbitrary units and capillary temperature 350°C; capillary voltage 25 V and tube lens voltage 120 V. Accurate mass was calibrated using a standard solution mixture of caffeine, sodium dodecyl sulfate, sodium taurocholate, the tetrapeptide Met-Arg-Phe-Ala acetate salt and ultramark (Sigma Aldrich, Steinheim, Germany) according to the guidelines of the manufacturer. Nitrogen (>99.98%) was employed as a sheath, auxiliary and sweep gas. The samples were measured using a full-scan experiment at a resolution of 50,000 (at m/z 400). Centroid mass spectra were acquired in the mass range of m/z 50–750. Instrument control and data acquisition (such as chemical formulas, retention time, fragment ions, products and the experimental m/z for product ions, and the error between the theoretical and experimental m/z for product ions) were performed with Xcalibur 2.1.0 software (Thermo Fisher Scientific, Bremen, Germany).

2.5 Results and discussion

2.5.1 NEB occurrence in wastewater

Coutu, et al. [35] applied a procedure to list common pharmaceuticals used in Switzerland according to their hazardous risk for the aquatic ecosystem and the human health. In this list NEB is on place 22 and 31 from 58 of the priorities for environment and human health, respectively. Indeed, NEB was measured in influent samples of wastewater treatment plants (WWTP) in Belgium in a concentration range of 1 - 10 ng L⁻¹ but this was the sole published data. In our study NEB was found in effluent samples of 12 WWTPs in Germany (Figure 2.1). The calculated limit of detection (LOD) for a signal-to noise ratio (S/N) of 3 was 1.4 ng L⁻¹, while the calculated limit of quantification (LOQ) for a S/N of ten was 4.6 ng L⁻¹. The linear range for NEB analysis was 2.5 ng L⁻¹ to 25 µg L⁻¹ with a good linearity ($r > 0.999$) and good accuracy for each calibration point between 80 and 120 %.

Median concentrations of NEB in WWTPs influent and effluent were respectively 21 and 13 ng L⁻¹, with maximum concentrations of 58 and 31 ng L⁻¹. The average elimination rate during conventional biological wastewater treatment was 38 %. However, residual concentrations of NEB are still substantial and care has to be taken on the fate of NEB in the environment.

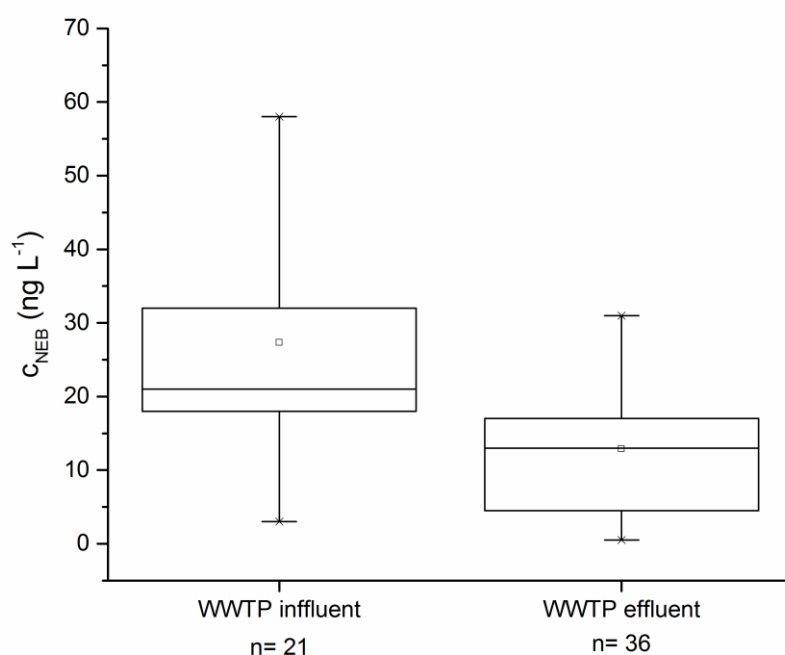


Figure 2.1 NEB concentrations in influents and effluents of 12 German WWTPs presented as box-and-whisker plots (median, 25 % quartile, 75 % quartile, maximum and minimum).

2.5.2 Degradation kinetics of NEB in photodegradation

Figure 2.2 shows that no significant degradation of NEB by UV-A takes place whereas NEB is degraded by UV-B and UV-C up to > 90% within 2 hours. This can be explained by the fact that NEB does not absorb within the UV-A spectrum as can be seen in Suppl. 6.3 that compares the UV-Vis absorption spectrum of NEB and the emission spectra of the three used UV sources. NEB absorbs UV radiation in the range from 243 nm to 302 nm with a maximum at 281 nm.

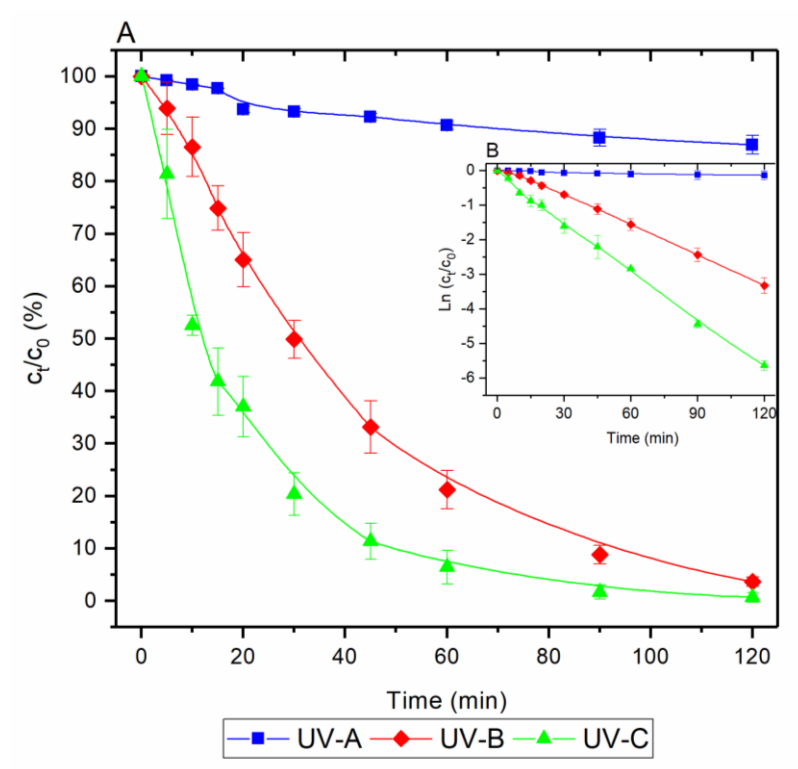


Figure 2.2 Elimination of NEB (A), inset: reaction kinetic plot (B) for the three UV sources (Experimental conditions c_0 (NEB) = $25 \mu\text{mol L}^{-1}$, volume = 500 mL, flow rate = 100 mL min^{-1} , pH = 7, T = $20 \pm 2^\circ\text{C}$).

The degradation of NEB follows pseudo first-order kinetics with the highest rate for UV-C ($k = 7.8 \times 10^{-4} \text{ s}^{-1}$) followed by UV-B ($k = 4.7 \times 10^{-4} \text{ s}^{-1}$). Table 2.1 summarizes the investigated first order rate constants, quantum yields (Φ) and half life times ($t_{1/2}$).

Table 2.1 Pseudo-first order rate constants (time-based and fluence-based), half life time and quantum yields (Φ) (for the full (polychromatic) emission spectrum of the radiation source) for NEB in ultrapure water, NEB in presence of *tert*-BuOH and wastewater matrix by UV-A, UV-B and UV-C photolysis

	NEB			NEB + <i>t</i> -BuOH			NEB + wastewater matrix		
	UV-A	UV-B	UV-C	UV-A	UV-B	UV-C	UV-A	UV-B	UV-C
k/s^{-1}	1.3×10^{-5}	4.7×10^{-4}	7.8×10^{-4}	-	5.0×10^{-4}	2.5×10^{-4}	2.8×10^{-5}	4.4×10^{-4}	2.9×10^{-4}
$t_{1/2}/\text{min}$	868	25	15	-	23	46	419	26	40
k'_1/m^2J^{-1}	1.5×10^{-6}	1.6×10^{-4}	2.7×10^{-4}	7×10^{-7}	1.8×10^{-4}	9.7×10^{-5}	9.6×10^{-7}	1.5×10^{-4}	1.2×10^{-4}
Φ_{deg}	-	0.02	0.53	-	0.027	0.19	-	0.023	0.22

(-) No significant degradation

2.5.3 Influence of the of OH-radical in NEB degradation

The degradation of NEB can take place through direct photolysis or indirectly, via reactions with reactive oxygen species (ROS) formed in the primary photochemical reactions [36], e.g. $\cdot\text{OH}$ [37] and singlet oxygen ($^1\Delta_g\text{O}_2$) [38, 39]. The contribution of $\cdot\text{OH}$ on the degradation kinetics of NEB were determined in presence of *tert*-BuOH. Degradation of NEB in the presence of the $\cdot\text{OH}$ scavenger is presented in Figure 2.3.

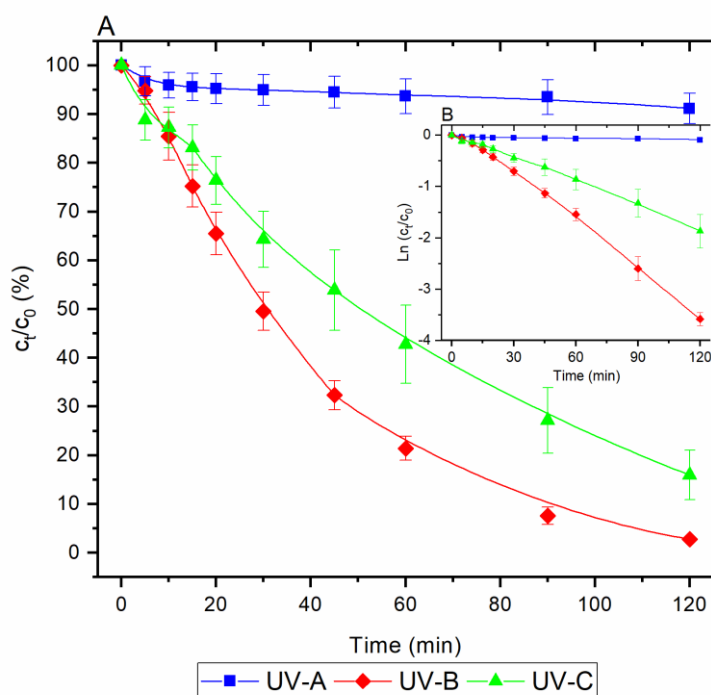


Figure 2.3 (A) NEB degradation in the presence of *tert*-BuOH, inset: (B) linear plots of $\ln(c_t/c_0)$ versus time of NEB degradation in the presence of *tert*-BuOH (Experimental conditions: c_0 (NEB) = $25 \mu\text{mol L}^{-1}$, c_0 (*tert*-BuOH) = 10mmol L^{-1} , volume = 500mL , flow rate = 100mL min^{-1} , pH = 7, $T = 20 \pm 2^\circ\text{C}$).

Comparing Figure 2.2 A and Figure 2.3 A it can be seen that the $\cdot\text{OH}$ scavenger had no significant effect on the NEB elimination in the case of UV-B or UV-A irradiation. However, using the UV-C lamp a significant effect on the NEB degradation was observed. The first order rate constant derived from Figure 2.3 B drops by a factor of approximately 3 Table 2.1. This indicates that $\cdot\text{OH}$ are formed during the photochemical degradation of NEB upon exposure to 254 nm radiation from the UV-C source. Indeed, $\cdot\text{OH}$ was quantified to be $\approx 5 \mu\text{M}$ after complete turnover of NEB. The diagrams of NEB elimination rate versus the $\cdot\text{OH}$ concentration for the different UV lamps are presented in Suppl. 6.4. From these diagrams one can see that the UV-A and UV-B lamps practically produce no $\cdot\text{OH}$ unlike the UV-C lamp. Hence, when the UV-C lamp is used there are probably two mechanisms involved in the degradation of NEB, namely, direct and indirect photooxidation by $\cdot\text{OH}$. Hydroxyl radicals may be formed by the contribution of VUV at 185 nm, since electromagnetic radiation with that wavelength provides sufficient energy to photolyse water [40]. The influence of VUV is only significant for a very small optical path length of few micrometers [40]. However, in this layer H_2O_2 is formed by recombination of $\cdot\text{OH}$, which may diffuse into the bulk solution where it is photolysed to $\cdot\text{OH}$ by 254 nm UV-C radiation.

2.5.4 Influence of the wastewater matrix on the degradation of NEB

The influence of a real wastewater matrix on NEB photodegradation using the three different UV lamps was studied after raising the concentration of NEB in the samples to $25 \mu\text{mol L}^{-1}$. The photodegradation of NEB over time is shown in Suppl. 6.5 A. After 120 min, the percentage of NEB degraded by UV-B and UV-C lamp was $96 \pm 1\%$ and $87 \pm 4\%$, respectively. As expected, UV-A was also not able to degrade NEB in wastewater. The pseudo-first-order rate constant of the photochemical degradation of NEB in the presence of the wastewater matrix is determined by plotting $\ln(c_t/c_0)$ versus time (see Suppl. 6.5 B). The rate constant for the UV-B lamp decreased slightly from $4.7 \times 10^{-4} \text{ s}^{-1}$ to $4.4 \times 10^{-4} \text{ s}^{-1}$ compared to pure water. This decrease can be explained by the slight UV-absorption of the wastewater matrix shown in Suppl. 6.6. For the UV-C lamp the rate constant decreased strongly from $7.8 \times 10^{-4} \text{ s}^{-1}$ to $2.9 \times 10^{-4} \text{ s}^{-1}$. This effect was observed both in the presence of $\cdot\text{OH}$ scavengers and in the presence of the wastewater matrix. The determined half life time for NEB elimination under UV-C radiation was 15 min in pure water, 46 min in pure water with *t*-BuOH, and 40 min in wastewater (Table 1).

The difference in the half life time of NEB elimination can be explained by scavenging of $\cdot\text{OH}$ by the organic matrix in analogy to the experiments in presence of *tert*-BuOH. However, the UV-C absorbance of the wastewater may additionally have reduced the UV-C fluence.

This is somewhat less pronounced for UV-B, since the wastewater does not absorb UV-B so strongly.

The quantum yields for NEB degradation under irradiation with the three different types of UV lamps and all conditions have been calculated and are presented in Table 1. Quantum yields mean the number of NEB molecules transformed (direct and indirect photooxidation) per photon emitted by the radiation source to the surface of the sample (incident light). Since there is no NEB absorption and significant degradation in the UV-A range, no quantum yield could be calculated for the UV-A lamp. The quantum yield for NEB degradation for the UV-B radiation was around 0.02 in all tested matrices. However, under UV-C radiation different quantum yields were determined, i.e., 0.53 in pure water, 0.19 in pure water in the presence of *tert*-BuOH and 0.22 in wastewater, respectively Table 2.1. The *tert*-BuOH has an impact on the quantum yield for the UV-C lamp, unlike for the UV-B lamp. The quantum yield for the degradation of NEB in presence of *tert*-BuOH for the UV-C lamp was 10 times higher than for the UV-B lamp in pure water.

2.5.5 Characterization of the transformation products of NEB formed during photolytic degradation

The transformation products that resulted during the photolytic degradation of NEB were elucidated using high resolution mass spectrometry. Three transformation products could be detected during the photolytic degradation. Structure elucidation was based on the accurate mass measurements. Besides the sum formula, also fragment ions from collision-induced dissociation (CID) experiments, relative mass errors and double bond equivalents (DBEs) were considered. The low relative mass errors obtained in all cases provided a high degree of certainty in defining the molecular composition (Table 2.2).

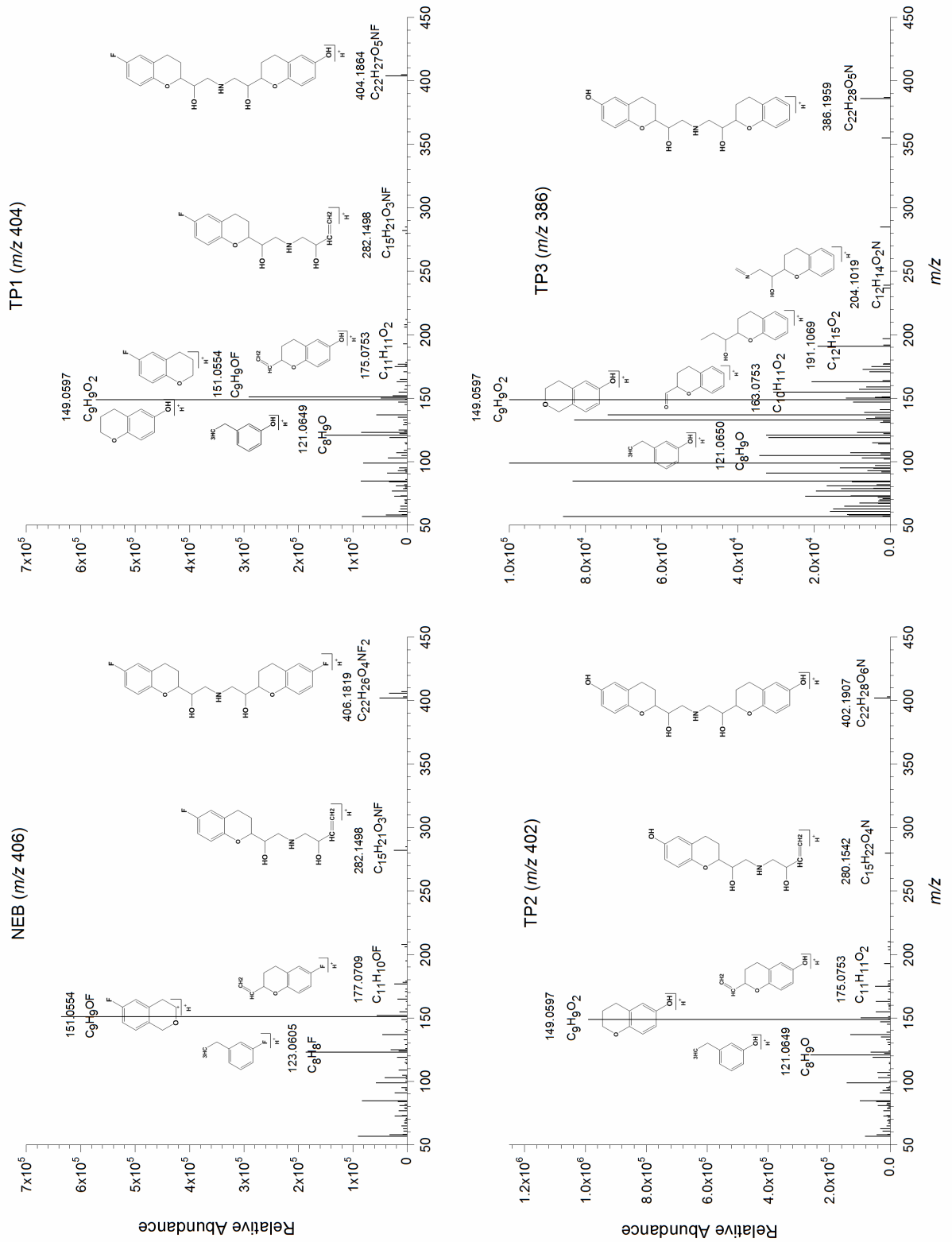
The retention time (R.T) of NEB was 4.32 min and yielded a $[\text{NEB}+\text{H}]^+$ ion with m/z 406.1819 (Figure 2.4). Fragmentation of the $[\text{NEB}+\text{H}]^+$ ion yielded four product ions with m/z 282.1496, 177.0709, 151.0553 and 123.0605. The high abundance peak at m/z 151.0553 represents the ion with the elemental composition $\text{C}_9\text{H}_8\text{OF}$ (6-Fluoro-3,4-dihydro-2H-1-benzopyran ion) and was probably produced through the homolytic cleavage of NEB from both sides. The first transformation product (TP1) of NEB had a retention time of 3.13 min and yielded a $[\text{TP1}+\text{H}]^+$ precursor ion at m/z 404.1863 (Figure 2.4). TP1 and NEB have two similar product ions (m/z 282.1496 and 151.0553) and two additional product ions at m/z 175.0753 and 149.0597 were obtained for TP1. The difference between the two precursor ions resembles the substitution of F with OH at the 6-Fluoro-3,4-dihydro-2H-1-benzopyran moiety. The transformation products TP 2 and TP 3 have a retention time of 2.95 and 2.09

min, respectively, and yielded the [TP2+H]⁺ and [TP3+H]⁺ precursor ions at m/z 402.1907 and m/z 386.1959 (Figure 2.4). The structure of the TP2 and TP3 were also proposed. While the common product ions with NEB at m/z 282.1496 and 151.0553 disappeared, the product ion at m/z 149.0597 appeared. This indicates the substitution of both fluorine atoms by hydroxyl groups.

Table 2.2 Accurate masses for NEB and its transformation products.

<i>Product ID</i>	<i>Theoretical m/z for [M+H]⁺</i>	<i>Measured m/z for [M+H]⁺</i>	<i>Mass deviation (Δppm)</i>	<i>R.T (min)</i>	<i>Sum Formula</i>
NEB	406.1824	406.1819	1.2	4.32	[C ₂₂ H ₂₆ O ₄ NF ₂] ⁺
	282.1500	282.1496	1.4		[C ₁₅ H ₂₁ O ₃ NF] ⁺
	177.0710	177.0709	0.6		[C ₁₁ H ₁₀ OF] ⁺
	151.0554	151.0553	0.4		[C ₉ H ₈ OF] ⁺
	123.0604	123.0605	0.8		[C ₈ H ₈ F] ⁺
TP 1	404.1867	404.1863	1.2	3.13	[C ₂₂ H ₂₇ O ₃ NF] ⁺
	282.1500	282.1498	0.7		[C ₁₅ H ₂₁ O ₃ NF] ⁺
	175.0754	175.0753	0.4		[C ₁₁ H ₁₁ O ₂] ⁺
	151.0554	151.0553	0.5		[C ₉ H ₈ OF] ⁺
	149.0597	149.0597	0.1		[C ₉ H ₉ O ₂] ⁺
	121.0648	121.0649	0.9		[C ₈ H ₉ O] ⁺
TP 2	402.1911	402.1907	1.0	2.09	[C ₂₂ H ₂₈ O ₆ N] ⁺
	280.1543	280.1542	0.5		[C ₁₅ H ₂₂ O ₄ N] ⁺
	175.0754	175.0753	0.4		[C ₁₁ H ₁₁ O ₂] ⁺
	149.0597	149.0596	0.7		[C ₉ H ₉ O ₂] ⁺
	121.0648	121.0649	0.9		[C ₈ H ₉ O] ⁺
TP 3	386.1962	386.1959	0.8	2.95	[C ₂₂ H ₂₈ O ₅ N] ⁺
	204.1019	204.1019	0.1		[C ₁₂ H ₁₄ O ₂ N] ⁺
	191.1069	191.1069	1.5		[C ₁₂ H ₁₅ O ₂] ⁺
	163.0753	163.0753	0.4		[C ₁₀ H ₁₁ O ₂] ⁺
	149.0597	149.0597	0.4		[C ₉ H ₉ O ₂] ⁺
	121.0648	121.0650	1.7		[C ₈ H ₉ O] ⁺

Figure 2.4 High resolution mass spectra of NEB and its transformation products.



2.5.6 Proposed mechanisms for the photolytic degradation of NEB

Figure 2.5 shows that the relative peak areas of the TPs suggest different transformation trends in the presence of UV-B and UV-C radiation although the exact concentrations of the TPs could not be determined as authentic standards were not available. During the UV-B radiation, the peak area of TP 1 increased during the first 30 min interval and then decreased rapidly. Moreover TP 3 increased slightly over the time, while the peak area of TP 2 was steadily increasing throughout the photooxidation period (Figure 2.5 A). On the other hand, the peak areas of TP 1 and TP 2 increased simultaneously during UV-C radiation, but this time only the peak area of TP 1 decreased accompanied with the appearance of TP 3 during the last 60 min interval (Figure 2.5 B). The relative peak areas of TP 1 in UV-B and in UV-C radiation were similar. Conversely, the relative peak area of TP 2 for the UV-B radiation was twice as intense as in UV-C radiation.

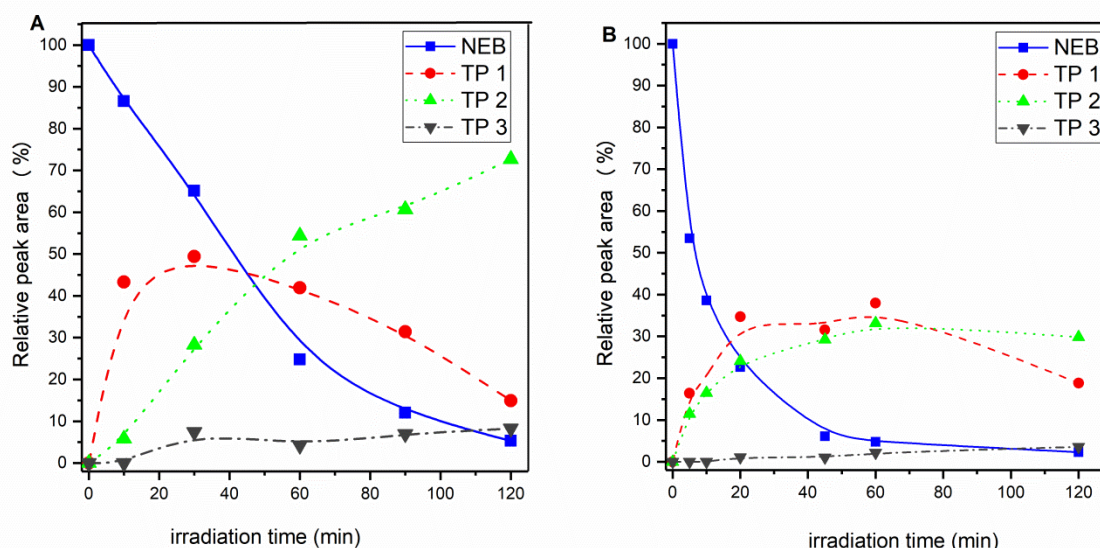


Figure 2.5 Relative peak area of NEB and corresponding transformation products as a function of time during UV-B (A) and UV-C (B) photolysis experiments carried out in pure water ($c_0 = 25 \mu\text{M}$, volume = 500 mL, flow rate = 100 mL min^{-1} , pH = 7, $T = 20 \pm 2 \text{ }^\circ\text{C}$).

The main photoreaction occurring is the photosubstitution of the fluorine atoms of NEB by a hydroxyl group with the formation of the TPs. TP 1 and TP 2 might be formed by defluorination followed by the addition of OH^- to the dihydrobenzopyran, while TP 3 is formed by defluorination of the second fluorine atom. Figure 2.6 shows the increase of fluoride concentration during the degradation of NEB. As can be seen from this diagram the concentration of F^- under UV-B radiation was higher than under UV-C radiation. Principally the transformation from NEB to TP 1 yields 1 mole of F^- per mole NEB degraded and the

transformation of TP 1 to TP 2 or TP 3 yields another mole of F^- . The slope of the linear regression shown in Figure 2.6 indicates a yield of ~ 1 mole fluoride per 1 mole NEB eliminated under conditions of UV-C radiation and ~ 2 moles in the case of UV-B radiation. This indicates that the degradation of NEB follows two different mechanisms for the two different UV treatment procedures, as will be explained below.

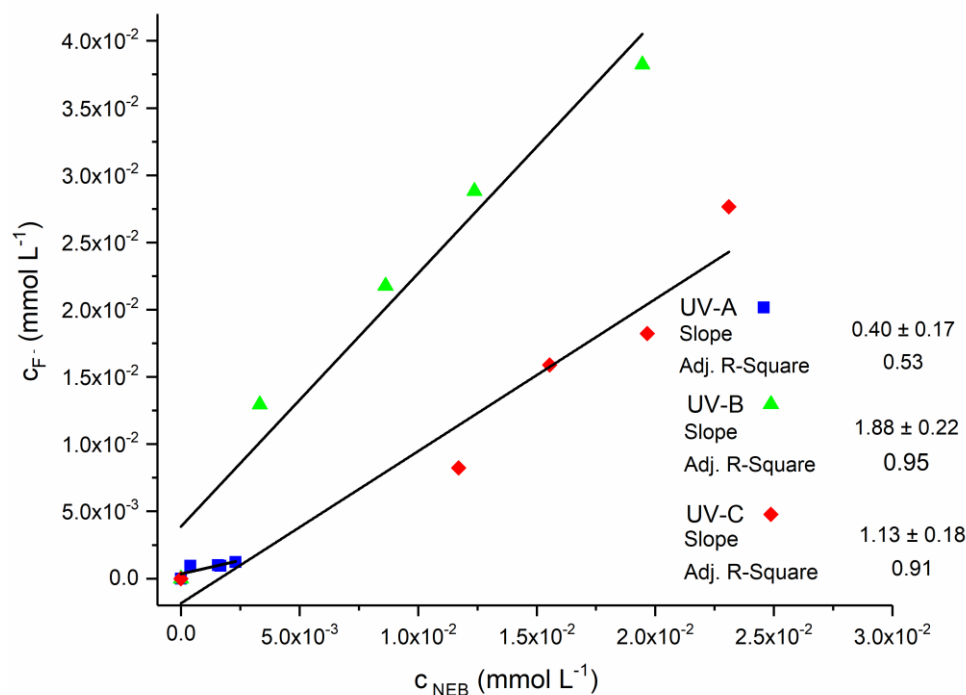
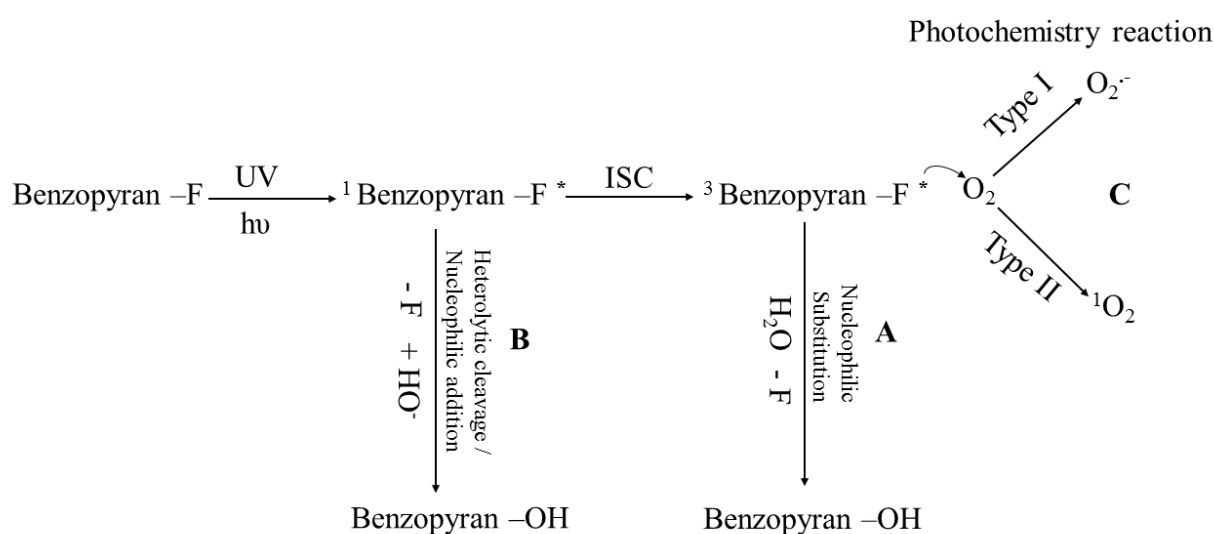


Figure 2.6 Fluoride yield (mmol L^{-1}) versus the NEB degradation (mmol L^{-1}) during the UV-A, UV-B and UV-C radiation: NEB degradation calculated based on LC-MS, F^- yield calculated based on ion chromatography.

In laser flash photolysis studies the quantum yield of defluorination of fluoroquinolones (FQs) in neutral aqueous media have been determined to be in the range of $\Phi_{-F} = 0.001$ to 0.55 [41]. Most of the FQs' photodegradation is predominated by the triplet state through the heterolytic cleavage of fluorine atom or by reaction of the excited state with water in a nucleophilic substitution of the fluoride like in the case of ciprofloxacin (CIP), norfloxacin (NOR) and enoxacin (ENO) ($\Phi_{-F} = 0.007 - 0.13$) [42, 43]. This mechanism is in agreement with our results for NEB ($\Phi_{-F} = 0.02$) in the presence of the UV-B radiation. We could observe electron donating (alkoxy group [44, 45]) and electron withdrawing (fluorine [44, 45]) moieties in the NEB structure. Therefore, the excited triplet state of the fluoro benzopyran ring of NEB reacts with water inducing a nucleophilic substitution of the fluoride (Scheme 2.1 (A)). The second photodegradation mechanism of the fluoroquinolones was reported to be initiated by formation of excited singlet state induced heterolytic cleavage of

the C-F bond with high photodegradation quantum yield in case of lomefloxacin (LOM) in water ($\Phi_{-F} = 0.55$) [41], which is in good agreement with our results for NEB ($\Phi_{-F} = 0.53$) in the presence of the UV-C radiation (Scheme 2.1 (B)). Intersystem crossing (ISC) is an efficient deactivation process from the excited singlet state to a triplet state. The excited triplet state quenching by oxygen may yield reactive oxygen species such as $O_2^{\cdot-}$ (photochemistry type I reaction [46]), or form a singlet oxygen (1O_2) [44] via energy transfer from the excited electron to the oxygen (photochemistry type II reaction [46]) (Scheme 2.1(C)). Other reactive species may be formed upon reactions of $O_2^{\cdot-}$ such as H_2O_2 (product of dismutation) or $\cdot OH$ (product arising from photolysis of H_2O_2) (Suppl. 6.4).



Scheme 2.1 The photodegradation mechanisms of the fluoro benzopyran in the excited state reactivity.

2.6 Conclusions

Upon UV radiation NEB mainly reacted by defluorination and substitution of the fluorine by hydroxyl groups. As the determined TPs are formed by the substitution of the fluorine atom from the benzopyran ring with a hydroxyl group, the biologically active part of the NEB structure is still preserved [25, 27, 47]. Suppl. 6.8 illustrates the biologically active part of the NEB structure in comparison to other β -blockers. This illustrates the importance of coupling the studies on the kinetics of micropollutant degradation with mechanistic studies in order to evaluate if the advanced oxidation process can deactivate the biological effectiveness of the compound and also of its transformation products.

2.7 Acknowledgment

The authors wish to thank Ronald Osmond and Ngoc Dieu Huynh for their laboratory assistance with the photo-degradation experiments, a special thanks to Dr. Andriy Kuklya and Dr. Klaus Kerpen for supporting this study by measuring the UV lamp spectra. Great thanks to Prof. Dr. Oliver J. Schmitz and his group, especially to Dr. Duxin Li for supporting this study and allowing us to use the Exactive Orbitrap MS at Applied Analytical Chemistry (AAC) department at Duisburg Essen University, Essen, Germany.

2.8 References

- [1] S.D. Richardson, S.Y. Kimura, *Water analysis: Emerging contaminants and current issues*, *Anal. Chem.*, 88 (2016) 546-582.
- [2] B. Petrie, R. Barden, B. Kasprzyk-Hordern, *A review on emerging contaminants in wastewaters and the environment: Current knowledge, understudied areas and recommendations for future monitoring*, *Water Res.*, 72 (2015) 3-27.
- [3] R. Moreno-González, S. Rodríguez-Mozaz, M. Gros, D. Barceló, V.M. León, *Seasonal distribution of pharmaceuticals in marine water and sediment from a mediterranean coastal lagoon (SE Spain)*, *Environ. Res.*, 138 (2015) 326-344.
- [4] V. Acuña, D. von Schiller, M.J. García-Galán, S. Rodríguez-Mozaz, L. Corominas, M. Petrovic, M. Poch, D. Barceló, S. Sabater, *Occurrence and in-stream attenuation of wastewater-derived pharmaceuticals in Iberian rivers*, *Sci. Total. Environ.*, 503-504 (2015) 133-141.
- [5] C. Postigo, D. Barceló, *Synthetic organic compounds and their transformation products in groundwater: Occurrence, fate and mitigation*, *Sci. Total. Environ.*, 503-504 (2015) 32-47.
- [6] R. López-Serna, A. Jurado, E. Vázquez-Suñé, J. Carrera, M. Petrović, D. Barceló, *Occurrence of 95 pharmaceuticals and transformation products in urban groundwaters underlying the metropolis of Barcelona, Spain*, *Environ. Pollut.*, 174 (2013) 305-315.
- [7] D.J. Lapworth, N. Baran, M.E. Stuart, R.S. Ward, *Emerging organic contaminants in groundwater: A review of sources, fate and occurrence*, *Environ. Pollut.*, 163 (2012) 287-303.
- [8] C. Postigo, S.D. Richardson, *Transformation of pharmaceuticals during oxidation/disinfection processes in drinking water treatment*, *J. Hazard. Mater.*, 279 (2014) 461-475.

- [9] E. Carmona, V. Andreu, Y. Picó, Occurrence of acidic pharmaceuticals and personal care products in Turia river basin: From waste to drinking water, *Sci. Total. Environ.*, 484 (2014) 53-63.
- [10] W. Xiong, X. Ding, Y. Zhang, Y. Sun, Ecotoxicological effects of a veterinary food additive, copper sulphate, on antioxidant enzymes and mRNA expression in earthworms, *Environ. Toxicol. Pharmacol.*, 37 (2014) 134-140.
- [11] M.S. Diniz, R. Salgado, V.J. Pereira, G. Carvalho, A. Oehmen, M.A. Reis, J.P. Noronha, Ecotoxicity of ketoprofen, diclofenac, atenolol and their photolysis byproducts in zebrafish (*Danio rerio*), *Sci. Total. Environ.*, 505 (2015) 282-289.
- [12] M.D. Overturf, J.C. Anderson, Z. Pandelides, L. Beyger, D.A. Holdway, Pharmaceuticals and personal care products: A critical review of the impacts on fish reproduction, *Crit. Rev. Toxicol.*, 45 (2015) 469-491.
- [13] A.A. Godoy, F. Kummrow, P.A. Pamplin, Occurrence, ecotoxicological effects and risk assessment of antihypertensive pharmaceutical residues in the aquatic environment-A review, *Chemosphere*, 138 (2015) 281-291.
- [14] J. Maszkowska, S. Stolte, J. Kumirska, P. Lukaszewicz, K. Mioduszewska, A. Puckowski, M. Caban, M. Wagil, P. Stepnowski, A. Białk-Bielińska, Beta-blockers in the environment: Part I. Mobility and hydrolysis study, *Sci. Total. Environ.*, 493 (2014) 1112-1121.
- [15] K. Nödler, O. Hillebrand, K. Idzik, M. Strathmann, F. Schipperski, J. Zirlewagen, T. Licha, Occurrence and fate of the angiotensin II receptor antagonist transformation product valsartan acid in the water cycle - A comparative study with selected beta-blockers and the persistent anthropogenic wastewater indicators carbamazepine and acesulfame, *Water Res.*, 47 (2013) 6650-6659.
- [16] S. Haider, S.S. Baqri, Beta-adrenoceptor antagonists reinitiate meiotic maturation in *Clarias batrachus* oocytes, *Comp. Biochem. Physiol., A: Mol. Integr. Physiol.*, 126 (2000) 517-525.
- [17] R. Triebkorn, H. Casper, V. Scheil, J. Schwaiger, Ultrastructural effects of pharmaceuticals (carbamazepine, clofibrac acid, metoprolol, diclofenac) in rainbow trout

(*Oncorhynchus mykiss*) and common carp (*Cyprinus carpio*), *Anal. Bioanal. Chem.*, 387 (2007) 1405-1416.

[18] D.B. Huggett, I.A. Khan, C.M. Foran, D. Schlenk, Determination of beta-adrenergic receptor blocking pharmaceuticals in United States wastewater effluent, *Environ. Pollut.*, 121 (2003) 199-205.

[19] D.B. Huggett, B.W. Brooks, B. Peterson, C.M. Foran, D. Schlenk, Toxicity of select beta adrenergic receptor-blocking pharmaceuticals (B-blockers) on aquatic organisms, *Arch. Environ. Contam. Toxicol.*, 43 (2002) 229-235.

[20] A.Y. Lin, Y.T. Tsai, Occurrence of pharmaceuticals in Taiwan's surface waters: Impact of waste streams from hospitals and pharmaceutical production facilities, *Sci. Total. Environ.*, 407 (2009) 3793-3802.

[21] T.A. Ternes, Occurrence of drugs in German sewage treatment plants and rivers, *Water Res.*, 32 (1998) 3245-3260.

[22] A.C. Alder, C. Schaffner, M. Majewsky, J. Klasmeier, K. Fenner, Fate of beta-blocker human pharmaceuticals in surface water: Comparison of measured and simulated concentrations in the Glatt Valley Watershed, Switzerland, *Water Res.*, 44 (2010) 936-948.

[23] C. Miège, M. Favier, C. Brosse, J.P. Canler, M. Coquery, Occurrence of betablockers in effluents of wastewater treatment plants from the Lyon area (France) and risk assessment for the downstream rivers, *Talanta*, 70 (2006) 739-744.

[24] T.A. Ternes, Analytical methods for the determination of pharmaceuticals in aqueous environmental samples, *Trends Anal. Chem.*, 20 (2001) 419-434.

[25] J.W. Cheng, Nebivolol: A third-generation beta-blocker for hypertension, *Clin. Ther.*, 31 (2009) 447-462.

[26] T. Münzel, T. Gori, Nebivolol: the somewhat-different beta-adrenergic receptor blocker, *J. Am. Coll. Cardiol.*, 54 (2009) 1491-1499.

[27] M. Mangrella, F. Rossi, F. Fici, F. Rossi, Pharmacology of nebivolol, *Pharmacol. Res.*, 38 (1998) 419-431.

- [28] T. Brown, 100 Best-Selling, most prescribed branded drugs through march, Medscape, 2015.
- [29] A.L. Van Nuijs, I. Tarcomnicu, W. Simons, L. Bervoets, R. Blust, P.G. Jorens, H. Neels, A. Covaci, Optimization and validation of a hydrophilic interaction liquid chromatography-tandem mass spectrometry method for the determination of 13 top-prescribed pharmaceuticals in influent wastewater, *Anal. Bioanal. Chem.*, 398 (2010) 2211-2222.
- [30] Chemspider, Nebivolol, <http://www.chemspider.com/Chemical-Structure.64421.html>., 2016, (last accessed, Mar 20, 2017).
- [31] Chemicalize, Nebivolol, <https://chemicalize.com/#/calculation>., 2016, (last accessed, Nov 2, 2016).
- [32] J. Bolton, K. Linden, Standardization of methods for fluence (UV Dose) determination in bench-scale UV experiments, *J. Environ. Eng.*, 129 (2003) 209-215.
- [33] R. Flyunt, A. Leitzke, G. Mark, E. Mvula, E. Reisz, R. Schick, C. von Sonntag, Determination of $\cdot\text{OH}$, O^{2-} , and hydroperoxide yields in ozone reactions in aqueous solution, *J. Phys. Chem. B*, 107 (2003) 7242-7253.
- [34] T. Nash, The colorimetric estimation of formaldehyde by means of the Hantzsch reaction, *Biochem. J.*, 55 (1953) 416-421.
- [35] S. Coutu, L. Rossi, D.A. Barry, N. Chèvre, Methodology to account for uncertainties and tradeoffs in pharmaceutical environmental hazard assessment, *J. Environ. Manage.*, 98 (2012) 183-190.
- [36] P.L. Miller, Y.P. Chin, Indirect photolysis promoted by natural and engineered wetland water constituents: Processes leading to alachlor degradation, *Environ. Sci. Technol.*, 39 (2005) 4454-4462.
- [37] P.P. Vaughan, N.V. Blough, Photochemical formation of hydroxyl radical by constituents of natural waters, *Environ. Sci. Technol.*, 32 (1998) 2947-2953.
- [38] A.L. Boreen, B.L. Edlund, J.B. Cotner, K. McNeill, Indirect photodegradation of dissolved free amino acids: The contribution of singlet oxygen and the differential reactivity of DOM from various sources, *Environ. Sci. Technol.*, 42 (2008) 5492-5498.

- [39] D.E. Latch, K. McNeill, Microheterogeneity of singlet oxygen distributions in irradiated humic acid solutions, *Science*, 311 (2006) 1743-1747.
- [40] C. von Sonntag, Advanced oxidation processes: Mechanistic aspects, *Water Sci. Technol.*, 58 (2008) 1015-1021.
- [41] E. Fasani, F.F. Barberis Negra, M. Mella, S. Monti, A. Albini, Photoinduced C–F bond cleavage in some fluorinated 7-Amino-4-quinolone-3-carboxylic acids, *J. Org. Chem.*, 64 (1999) 5388-5395.
- [42] A. Albini, S. Monti, Photophysics and photochemistry of fluoroquinolones, *Chem. Soc. Rev.*, 32 (2003) 238-250.
- [43] A. Salma, S. Thoroe-Boveleth, T.C. Schmidt, J. Tuerk, Dependence of transformation product formation on pH during photolytic and photocatalytic degradation of ciprofloxacin, *J. Hazard. Mater.*, 313 (2016) 49-59.
- [44] M. De Rosa, Photosensitized singlet oxygen and its applications, *Coord. Chem. Rev.*, 233-234 (2002) 351-371.
- [45] J. Tauber, D. Imbri, T. Opatz, Radical addition to iminium ions and cationic heterocycles, *Molecules*, 19 (2014) 16190-16222.
- [46] G. Cosa, Photodegradation and photosensitization in pharmaceutical products: Assessing drug phototoxicity, *Pure. Appl. Chem.*, 76 (2004) 263-275.
- [47] A. Maffei, C. Vecchione, A. Aretini, R. Poulet, U. Bettarini, M.T. Gentile, G. Cifelli, G. Lembo, Characterization of nitric oxide release by nebivolol and its metabolites, *Am. J. Hypertens.*, 19 (2006) 579-586.

3 pH effects on photolysis and photocatalysis of ciprofloxacin

redrafted from: Alaa Salma , Sven Thoröe-Boveleth , Torsten C. Schmidt, Jochen Tuerk, Journal of Hazardous Materials, 2016, 313, 49-59.

3.1 Abstract

Ciprofloxacin (CIP) is a broad-spectrum antibiotic with five pH dependent species in aqueous medium, which makes its degradation behavior difficult to predict. For the identification of transformation products and prediction of degradation mechanisms, a new experimental concept making use of isotopically labeled compounds together with high resolution mass spectrometry was successfully established. The utilization of deuterated ciprofloxacin (CIP-d8) facilitated the prediction of three different degradation pathways and the corresponding degradation products, four of which were identified for the first time. Moreover, two molecular structures of previously reported transformation products were revised according to the mass spectra and product ion spectra of the deuterated transformation products. Altogether, 18 transformation products have been identified during the photolytic and photocatalytic reactions at different pH values (3, 5, 7 and 9). In this work the influence of pH on both reaction kinetics and degradation mechanism was investigated for direct ultraviolet photolysis (UV-C irradiation) and photocatalysis (TiO₂/UV-C). It could be shown that the removal rates strongly depended on pH with highest removal rates at pH 9. A comparison with those at pH 3 clearly indicated that under acidic conditions ciprofloxacin cannot be easily excited by UV irradiation. We could confirm that the first reaction step for both oxidative treatment processes is mainly defluorination, followed by degradation at the piperazine ring of CIP.

3.2 Keywords

Ciprofloxacin; photolysis; photocatalytic degradation; transformation products.

3.3 Introduction

Antibiotics are one of the most important pharmaceutical groups widely used by humans as well as in veterinary medicine and aquaculture. The worldwide consumption of antibiotics is in the range of 100,000 to 200,000 t yearly [1], from which approximately 10,200 t are used in Europe [2], and nearly 23,000 t in the USA [3].

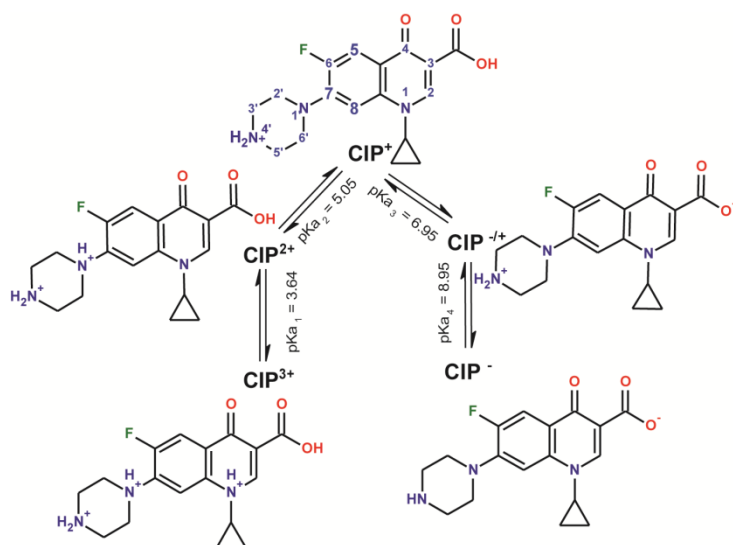
Among the emerging pharmaceuticals are the quinolones, a family of synthetic broad-spectrum antibiotics, which were classified by Ball [4] in three generations. This classification is accredited by the European Centre for Disease Prevention and Control (ECDC), while the American authors mainly classified them in four generations based on Andriole [5]. A surveillance study conducted in 2010 in Europe reported that the consumption of second-generation quinolones was on average three times higher than that of the first- and the third-generation. From the second-generation quinolones, ciprofloxacin (CIP) represented 73% of the total consumption, with 0.39 up to 1.8 daily doses (DD) per 1000 inhabitants [6].

Due to their broad application, the quinolones and their metabolites often end, in their pharmacologically active form, in the environment [7]. Besides sorption to sewage sludge and biological degradation in wastewater treatment, photochemical reactions are relevant after released into the environment [8]. CIP has been detected in hospital wastewaters in concentrations from 3 ng/L to 21 µg/L [9, 10], as well as in wastewater treatment plant (WWTP) effluents [11], in concentrations from 6 ng/L up to several µg/L [10] in secondary treated effluent. Quinolones reaching the environment may lead to development of bacterial resistance that could have toxic effects on fauna and flora with severe impacts on aquatic ecosystems [12]. Thus, reducing the emissions of quinolones into the environment is of strategic importance.

Advanced oxidation processes (AOPs), such as ozonation [13], sonification [14], photolysis [15], and photocatalysis [16] are viable methods for the removal of quinolones. Recently, TiO₂ has been intensively used as a semiconductor photocatalyst to remove fluoroquinolones (FQs) [16-21], including CIP.

CIP has multiple ionisable functional groups, which makes the pattern of acid-base equilibrium quite complex. The carboxylate group at C-3, the N-1' and N-4' amino groups at the piperazine ring, and the N-1 atom in the quinolone ring (Scheme 3.1) are the most significant proton binding sites, leading to pK_a values for CIP of 3.64, 5.05, 6.95 and 8.95 [22]. Scheme 3.1 also illustrates the inter conversion between the species in aqueous medium. The concentration ratio of the different forms depends on the pH value. At neutral pH the largely dominant species is zwitterionic rather than nonionic, while the cationic form and the

anionic form predominate in acidic and in basic solutions, respectively. Thus, the often shown nonionic structure of CIP is rather misleading when looking into reaction reactivities and degradation mechanisms of ciprofloxacin.



Scheme 3.1 Molecular structures and pKa values of the different ciprofloxacin species.

The calculated distribution percentage of the different ciprofloxacin species as a function of the pH [15, 22], is shown in the appendix Suppl. 6.12.

The pH might play an important role for the elimination mechanism of the pharmaceuticals in the environment. With regard to photolysis, the different species might have various photolytic degradation pathways, transformation products, and kinetics of mechanism-based degradation. Therefore, modifying the pH leads to structural changes that could enhance or hamper the CIP degradation by direct photolysis via UV radiation or UV/TiO₂ photocatalysis. The aim of this work was to investigate the influence of pH on the reaction kinetics and the degradation mechanism of ciprofloxacin by direct ultraviolet photolysis and photocatalysis. For structural elucidation of transformation products a new concept using isotopically labeled surrogate compounds was evaluated using high-resolution mass spectrometry. Previous studies observed that the main photoreaction pathway mechanism for ciprofloxacin degradation involves photosubstitution of the fluorine atom by a hydroxyl group via the triplet state of CIP [23] through inter system crossing (ISC) [24]. Only few studies have focused on the investigation of the cleavage at the piperazine ring during photodegradation. Therefore, we used ciprofloxacin-d₈, which is deuterated at the piperazine ring (Suppl. 6.13), for identifying the formed transformation products.

3.4 Material and methods

3.4.1 Materials

Ciprofloxacin (CIP), hydrochloric acid (HCl), nitric acid (HNO₃) and sodium hydroxide (NaOH) were purchased from Fluka (Buchs, Germany). CIP-d8 was obtained from Santa Cruz Biotechnology Inc. (Heidelberg, Germany). HPLC and UPLC/MS grade water and methanol were purchased from Th. Geyer (Renningen, Germany). P-25 titanium dioxide was supplied by Evonik Industries (Hanau, Germany).

3.4.2 Immobilization of TiO₂ on glass plates

0.375 g P-25 titanium dioxide was immobilized as photocatalyst on glass plates according to a previously described procedure [17]. In brief, a glass plate surface was conditioned before TiO₂ suspension deposition as follows. In a first step the glass plate was struck with sand to obtain a rough surface, thus increasing the surface area, followed by washing with water and treatment with NaOH solution in order to increase the number of OH groups. A 7.5 g L⁻¹ TiO₂ (80% anatase and 20% rutile) suspension was prepared in deionized water. The pH of the suspension was adjusted to 3 with diluted HNO₃, followed by sonication. 50 mL of the prepared suspension were carefully poured on the surface of the glass and allowed to dry at room temperature. Afterwards, the plates were heated at 100 °C for an hour, followed by heating for 4 h at 475 °C. The final TiO₂ concentration on the plate was 20.5 g m⁻² and the specific area 48.3 m² g⁻¹, as determined by the Brunauer–Emmett–Teller (BET) method from nitrogen adsorption–desorption isotherms at (-196°C) using an adsorption analyzer from Micromeritics Xiaoxuan Gemini 2375 (Burladingen, Germany).

3.4.3 Degradation experiments

Photolytic and photocatalytic degradation experiments were performed in a home-made 600-mL pyrex reactor equipped with a 3.8 x 48 cm rectangle glass plate (Suppl. 6.14 in the appendix). For every degradation experiment a ciprofloxacin concentration of 60 μmol L⁻¹ was prepared in 500 mL deionized water followed by adjusting the pH using HCl or NaOH solution. The solution was then pumped over the glass plate using a peristaltic pump at a flow rate of 0.5 L min⁻¹. It should be noted that the solution layer over the plate was less than 5 mm in thickness during the experiments. A horizontal UV lamp that emits light at a wavelength of 254 nm (15 W UV-C lamp, F15T8/UV, New NEC Light Ing., Shiga, Japan) was placed close to the glass plate. Before starting the photocatalytic experiments the solution was cycled for 30 min over the coated glass plate in order to achieve adsorption equilibrium. The same procedure was followed for the photolytic experiments without the plate. The irradiation time

was 120 minutes. Samples were collected after 2, 4, 8, 12, 20, 30, 45, 60, 90 and 120 min, and filtered with a 0.45 μm regenerated cellulose acetate syringe filter (Macherey-Nagel, Dueren, Germany) before being analyzed by LC-MS. The degradation experiments were carried out in triplicate for each pH value (3, 5, 7 and 9).

The photon fluence rate for the UV lamp was also determined in triplicate experiment by chemical actinometry using ferrioxalate as an actinometer and was found to be $1.5 \times 10^{-5} \text{ E m}^2 \text{ s}^{-1}$.

3.4.4 CIP-d8 degradation and samples enrichment using solid phase extraction (SPE)

An extra experiment was performed using labeled CIP-d8, with the eight deuterium atoms at the piperazine ring. The same experimental conditions as described previously were applied. A solution of $10 \mu\text{mol L}^{-1}$ of CIP-d8 was photodegraded by photocatalysis at pH 7. In order to identify the transformation products by high-resolution time of flight mass spectrometry, the samples were 10 times concentrated using solid phase extraction (SPE) cartridge with Strata-XL polymeric sorbent (Phenomenex, Aschaffenburg, Germany). The selected 6-mL Strata-XL cartridge with 200 mg sorbent (100 μm particle size) was conditioned with $3 \times 1 \text{ mL}$ methanol and $3 \times 1 \text{ mL}$ deionized water. 10 mL of each sample was loaded onto the SPE cartridge, washed with $3 \times 1 \text{ mL}$ of methanol/deionized water (50/50, v/v) and dried with a gentle stream of nitrogen. Finally, elution was performed twice with 1 mL of acetonitrile and formic acid (98/2, v/v). The extracts were dried under a gentle nitrogen stream and reconstituted with 1 mL of acetonitrile in deionized water (5/95, v/v) for LC-MS/MS analysis. Using the concept of isotopically labeled surrogates like deuterated ciprofloxacin in this study helps in structural elucidation of transformation products. High resolution mass spectrometry is preferred, because of the possibility to calculate the exact sum formula of the new transformation products. Nevertheless also unit resolution mass spectrometers could be used together with isotopically labeled compounds for the description of the reaction mechanism and identification of the preferred reaction site by the mass differences of the detected product ion spectra.

3.4.5 LC-MS/MS analysis

The concentration of CIP was analyzed during the photodegradation process using LC 20 HPLC system (Shimadzu, Duisburg, Germany) coupled by a TurboIonSpray[®] source to a 3200 QTRAP[®] tandem mass spectrometer (AB Sciex, Darmstadt, Germany). The separation was performed on a 150 mm \times 2 mm Synergi 4u Polar RP 80A column (Phenomenex,

Aschaffenburg, Germany) with a water–methanol gradient of 0.1% formic acid in water (v/v mobile phase A) and 0.1% formic acid in methanol (v/v mobile phase B) with a flow rate of 0.3 mL min⁻¹ at 40°C. The gradient program started with 60% organic phase, after 2 minutes it was raised to 100% B, and then kept constant for 30 seconds and afterwards again reduced to 60% B for 30 seconds. The column was re-equilibrated to the initial conditions and stabilized for 5 minutes. The total run time was 8 min. CIP was quantified after positive electrospray ionisation (ESI⁺) in multiple reaction monitoring (MRM) mode. The optimum operating conditions were as follows: the curtain gas (CUR) was set at 15 psi, the nebulizer source gas 1 at 40 psi, and the turbo ion source gas 2 at 80 psi. The declustering potential (DP) and entrance potential (EP) were optimized to 50 V and 6.0 V, respectively. The CIP fragmentation was induced by collisional activated dissociation (CAD) with nitrogen. The collision gas pressure was set at 2.0 psi for MRM quantitation. A collision energy (CE) of 27 eV and a collision cell exit potential (CXP) of 4.0 V were utilized. The Precursor ion (Q1), quantifier, and qualifier ions (Q3) of the HPLC–MS/MS quantification measurements were set at 332.3, 288.4, and 314.3, respectively, with the transition m/z 332 → 288 being used for quantification and m/z 332 → 314 for verification. A dwell time of 150 ms was employed. Data evaluation was done with AnalystTM 1.5 (AB Sciex, Darmstadt, Germany). The calibration was weighted 1/x with a linear regression.

The transformation products (TPs) formed during CIP degradation at different pH values were investigated by a non-target UPLC–MS method. The samples were measured using the Aquity-UPLC-System, which was coupled to a high resolution Q-ToF-MS (SYNAPT-G1, Waters, Eschborn, Germany). The chromatographic separation was performed on a 100 x 2 mm BEH C18 1.7 μm HPLC column (Waters, Eschborn, Germany) at 50 °C. The binary mobile phase consisted of 0.1% formic acid in water and 0.1% formic acid in acetonitrile. The gradient program started with 5% organic phase, within 10 minutes it was raised to 100% and was kept constant for 4 minutes and finally decreased again to 5%. The flow rate was 300 μL min⁻¹.

Samples were introduced into the atmospheric pressure ionization source after LC separation, and ionized by ESI in positive mode. Accurate mass calibration was achieved by the measurement of sodium formate (CHO₂Na, Merck, Darmstadt, Germany) at the start and end of each chromatographic run and a single lock-mass correction was used during analyses, using the [M+H]⁺ ion of leucine enkephalin (Sigma-Aldrich, Schneldorf, Germany) as the lock mass at m/z 556.2771. The scan range was set from m/z 50 to m/z 950. The desolvation and ion source block temperatures were set at 350 °C and 120 °C, respectively. Nitrogen was

used as nebulizer (30 L h^{-1}) as well as desolvation gas (900 L h^{-1}). The optimized voltages for the probe and ion source components were 3 kV for the capillary, 30 V for the sample cone and 3 V for the extractor cone.

Tandem mass spectrometry (MS/MS) experiments were performed using argon in the collision cell at a pressure of 1 bar. Data were collected in centroid mode, and MS^E analysis was performed with two scan functions: 4 eV for the low collision energy scan and a collision energy ramp of 10–30 eV for the high-collision energy scan. MS^E achieved almost simultaneously the acquisition of MS and MS/MS data from a single injection. MassLynx 4.1 and Unifi software (Waters, Eschborn, Germany) were used to evaluate the data provided by the Q-ToF mass spectrometer and finally elucidate the structure of the transformation products. Based on chemical formulas proposed, fragment ions, ring and double bond equivalents (DBEs) and relative mass errors between the theoretical and experimental m/z for product ions were obtained from the accurate m/z values provided by the high resolution of the Q-ToF mass spectrometer.

3.5 Results and discussion

3.5.1 Influence of pH on the degradation of CIP

The degradation kinetics were evaluated at four different pH values (3, 5, 7 and 9) in aqueous solution for two distinct methods: direct ultraviolet photolysis (UV-C irradiation) and photocatalysis ($\text{TiO}_2/\text{UV-C}$).

The kinetics of the degradation process have been determined by measuring the decrease of CIP concentration at different time. The results for both photolytic and photocatalytic degradation are shown in Figure 3.1 and pseudo-first order kinetics were found ($R^2 \geq 0.97$, $n = 3$) with the highest removal rates at pH 9 ($k_{\text{UV and TiO}_2/\text{UV}} = 4.0 \times 10^{-4} \text{ s}^{-1}$). A drop of the pH to 3, resulted in a lower removal rate ($k_{\text{UV}} = 4.0 \times 10^{-5} \text{ s}^{-1}$; $k_{\text{TiO}_2/\text{UV}} = 1.0 \times 10^{-4} \text{ s}^{-1}$). The differences in the degradation rate values are due to the pH-dependent speciation of CIP in the aqueous medium as shown inset in Figure 3.1.

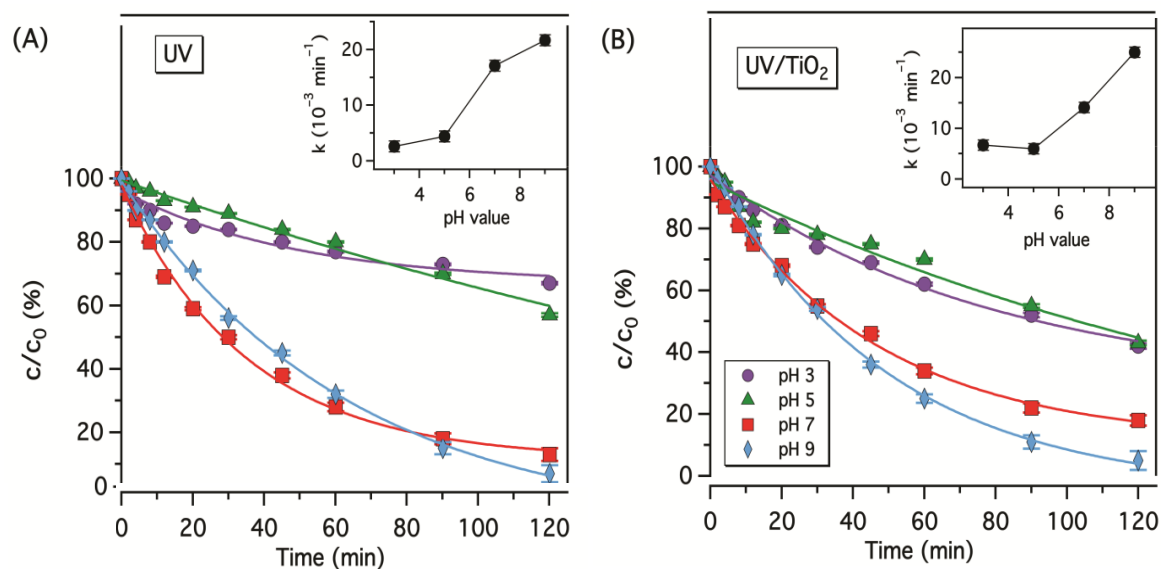


Figure 3.1 Ciprofloxacin elimination as a function of time during photolytic (A) and photocatalytic (B) treatment. Average results of triplicate measurements are shown. Relative standard deviation is indicated by error bars but often smaller than symbol sizes. Inset: effect of pH values on the removal rate constants of photolytic and photocatalytic degradation of 60 μM CIP at 120 min interval.

The degradation rate for each of the photolytic and photocatalytic reaction is the highest at pH 9, which is 10 times higher than the observed reaction constant at pH 3 under the photolytic degradation, and achieved a four times higher k in comparison of the photocatalytic degradation. That might be due to the absorption rate of the different ciprofloxacin species ($\text{CIP}^{1+}/\text{CIP}^{+/-}$, $\text{CIP}^{+/-}/\text{CIP}^{1-}$) under UV-C radiation. Suppl. 6.15. in the appendix shows the changes in the absorption spectra of CIP at different pH values as well as the overlap with the UV-C emission spectrum at 254 nm. Drakopoulos and Ioannou [25] study the excitation and emission spectra of the intrinsic fluorescence of CIP and other fluoroquinolones in aqueous solutions at different pH values. They found that the maximum intensity of fluorescence of CIP is observed in weakly acidic solutions, while in strongly acidic and strongly alkaline solutions there is decreased fluorescence intensity. This behavior might be explained by the pH dependence of the photolysis of CIP. The energy levels of the singlet and triplet state of CIP probably makes the CIP undergo a photo-induced chemical reaction [26]. Many studies on FQs mention that their photo-induced oxidation depends on the photo-generation of FQs in triplet state [23, 27, 28]. The previous studies showed that the transformation products are a result of the CIP defluorination as a direct oxidation. Other TPs are formed by reactive oxygen species like $^1\text{O}_2$, $\text{O}_2^{\bullet-}$ and HO^\bullet . These reactive components were obtained via the energy transfer between excited CIP and the molecular oxygen from the solution. This reaction is called a photodynamic complex II [15, 16], and the reactive oxygen species form as a result of hydrolysis at the piperazine ring [15, 27, 29].

The photolytic degradation rate (CIP^{3+}/CIP^{2+} , CIP^{2+}/CIP^{1+}) after 120 minutes at pH 3 and pH 5 is $33\pm 4\%$ and $43\pm 2\%$, respectively. As mentioned earlier the change in the absorption spectra of CIP with the pH value may have an impact on the photolytic reaction. An improvement of the elimination rates was observed when TiO_2 was used as photocatalyst, with elimination rates of $57\pm 3\%$ at pH 5 and $58\pm 5\%$ at pH 3. This improvement is due to the properties of the TiO_2 catalyst at different pH values and consequently to the different oxidation mechanism for photocatalysis in comparison to photolysis. The TiO_2 surface is positively charged at acidic conditions and negatively charged at basic conditions [18, 30, 31]. Between pH 4 and 8 the overall non-charged TiO_2 species dominates [30]. Thus, in this pH range the CIP species can be adsorbed on the TiO_2 surface due to van der Waals interactions [19]. During all degradation experiments, a decrease in the pH values was observed, except for pH 3. It was also observed that during the photolytic and photocatalytic degradation at acidic conditions most of the TPs are preserving the fluorine atom, while at basic conditions most of the TPs are losing it. The release of hydrogen fluoride during the ciprofloxacin degradation at basic conditions causes a pH drop [32], while the preservation of the fluorine atom on the TPs at pH 3 keeps the pH constant during the degradation process. This fluorine removal is potentially due to the reaction through the CIP^{3*} . This will be explained in detail in paragraph 3.4. The changes of pH values as a function of the degradation time are illustrated in Suppl. 6.16 A,B in the appendix.

3.5.2 Characterization of the transformation products of CIP resulted during photolytic and photocatalytic degradation

The transformation products that resulted during the photolytic and photocatalytic degradation of CIP were investigated in dependence of the pH. An additional experiment with deuterated labeled ciprofloxacin (CIP-d8) was used for the identification of several degradation product structures. Seven observed photolytic transformation products were identified that agree with the transformation products (TPs) identified in previous studies. Table 3.1 shows the theoretical and the measured masses together with calculated sum formula for CIP and its transformation products measured by high-resolution mass spectrometry.

Table 3.1. Accurate masses determined by UPLC-Q-ToF for ciprofloxacin (CIP) and its photodegradation products generated at different pH values (x presented the detected transformation products).

Comp.	R _t (min)	Elemental formula	Difference from CIP	Mass (m/z)		Fragmentation		Error		Matrix pH					Refs.		
				Mass (m/z)		MS/MS	mDa	Ppm	DBE	UV							
				Exp.	Theo.					pH3	pH5	pH7	pH9	pH3		pH5	pH7
CIP	3.11	C ₁₇ H ₁₈ N ₃ O ₃ F	—	332.1411	332.141	314, 288, 268, 274, 245, 231, 205	0.1	0.3	9.5	x	x	x	x	x	x	x	—
TP1	2.54	C ₁₇ H ₁₆ N ₃ O ₄	-(F) + (H, O)	330.1451	330.1454	312, 298, 286, 272, 243, 229	-0.3	-0.9	9.5	x	x	x	x	x	x	x	[15, 20, 27, 33-36]
TP2	2.95	C ₁₇ H ₁₆ N ₃ O ₅	-(F) + (H, 2O)	346.1402	346.1403	328, 300, 287, 244	-0.3	-0.9	9.5	x	x	x	x	x	x	x	[37, 38]
TP3	2.47	C ₁₇ H ₁₇ N ₃ O ₆	-(F, H) + (3O)	360.1196	360.1196	342, 326, 314, 300, 260	0.2	0.6	10.5	x	x	x	x	x	x	x	—
TP4	2.18	C ₁₆ H ₁₇ N ₃ O ₅	-(C, H, F) + (2O)	332.1248	332.1246	314, 298, 288, 274, 260	0.2	0.6	9.5	x	x	x	x	x	x	x	—
TP5	1.63	C ₁₆ H ₁₇ N ₃ O ₆	-(C, H, F) + (3O)	348.1193	348.1196	330, 316, 287, 245, 227	-0.3	-0.9	9.5	x	x	x	x	x	x	x	—
TP6	1.76	C ₁₇ H ₁₆ N ₃ O ₇	-(F) + (H, 4O)	378.1295	378.1301	362, 362, 346, 328, 314, 298, 270	-0.6	-1.6	9.5	x	x	x	x	x	x	x	—
TP7	3.38	C ₁₇ H ₁₇ N ₃ O ₅	-(H, F) + (2O)	344.1249	344.1246	326, 314, 298, 286, 260	0.3	0.9	10.5	x	x	x	x	x	x	x	[36, 39]
TP8	3.63	C ₁₆ H ₁₇ N ₃ O ₄	-(C, H, F) + (O)	316.1294	316.1297	316, 298, 284, 270, 244, 227	-0.3	-0.9	9.5	x	x	x	x	x	x	x	[20, 38]
TP9	2.6	C ₁₈ H ₁₇ N ₃ O ₃	-(2C, H, F)	288.1341	288.1349	270, 256, 227, 213, 199, 186	-0.7	-2.4	8.5	x	x	x	x	x	x	x	[15, 27, 33]
TP10	3.75	C ₁₈ H ₁₅ N ₃ O ₃	-(F, N, 6H, 4C)	245.0919	245.0926	227, 203, 186, 159	-0.7	-2.9	8.5	x	x	x	x	x	x	x	[40]
TP11	2.85	C ₁₇ H ₁₆ N ₃ O ₃ F	-(2H)	330.1251	330.1254	312, 286, 275, 245	-0.3	-0.9	10.5	x	x	x	x	x	x	x	[41]
TP12	3.13	C ₁₇ H ₁₈ N ₃ O ₄ F	-(O)	348.1365	348.136	330, 288, 245, 227	0.5	1.4	9.5	x	x	x	x	x	x	x	[42]
TP13	3.48	C ₁₇ H ₁₆ N ₃ O ₄ F	+(H, 2O)	364.1308	364.1309	346, 332, 318, 288	-0.1	-0.3	9.5	x	x	x	x	x	x	x	[20, 35, 43]
TP14	3.17	C ₁₇ H ₁₆ N ₃ O ₄ F	-(2H) + (O)	346.1201	346.1203	328, 314, 288, 262, 246	-0.2	-0.6	10.5	x	x	x	x	x	x	x	[41, 44, 45]
TP15	3.73	C ₁₇ H ₁₆ N ₃ O ₅ F	-(2H) + (2O)	362.1147	362.1152	344, 316, 298, 277, 258	-0.5	-1.4	10.5	x	x	x	x	x	x	x	[20, 34, 39, 41, 43, 44]
TP16	2.72	C ₁₆ H ₁₆ N ₃ O ₄ F	-(C, 2H) + (O)	334.1212	334.1203	334, 316, 298, 288, 276, 245	0.9	2.7	9.5	x	x	x	x	x	x	x	[20, 34, 38, 39, 41, 43, 46]
TP17	2.8	C ₁₈ H ₁₆ N ₃ O ₃ F	-(2C, 2H)	306.1258	306.1248	288, 274, 245, 213	-0.6	-2	8.5	x	x	x	x	x	x	x	[15, 20, 27, 34, 35, 38, 39, 41, 43, 45-47]
TP18	4.37	C ₁₈ H ₁₁ FN ₃ O ₃	-(4C, 7H, N)	263.0835	263.0832	245, 231, 217, 204	0.3	1.1	8.5	x	x	x	x	x	x	x	[15, 27, 34, 38, 41, 43, 46-48]

3.5.3 Elucidation of transformation products for different ciprofloxacin species

In total eighteen transformation products were detected during the photolytic and photocatalytic degradation reactions at the four investigated pH values (Table 3.1). TP 1, the dominant transformation product, was determined at all studied pH values during both photolytic and photocatalytic processes. We suppose that TP 1 was formed during the photooxidation of CIP, which was induced by the UV radiation. Transformation products TP 3, 5, 11, 12 and 15 were observed only in presence of TiO₂. TP 3 and TP 5 are probably secondary cleavage products. The stepwise cleavage took place at the piperazine ring of TP 1. On the other hand, TP 11, 12 and 15 were formed during further stepwise cleavage at the piperazine ring of ciprofloxacin. At pH 3 seven and eleven TPs were detected during the photolytic and photocatalytic degradation, respectively. It was observed that the transformation products TP 1, TP 11 and TP 17, are formed by a cleavage at the piperazine ring, again.

During the photolytic and photocatalytic degradation at pH 5 eight and ten TPs were detected, respectively. TP 1 was still the dominant transformation product. This was also the case for TP 11 during the photocatalytic treatment. TP 17 and also TP 2 had a significantly smaller intensity in comparison to TP 1. TP 2 was observed at pH ≥ 5 during both photolytic and photocatalytic degradation.

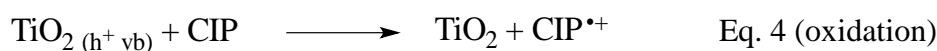
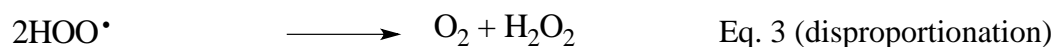
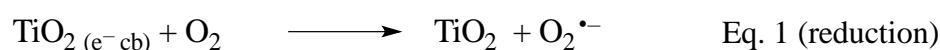
Nine and thirteen TPs were detected at pH 7, while at pH 9 seven and eleven TPs could be analysed during both photolysis and photocatalysis. At pH ≥ 7 , TP 1 and TP 2 were again the dominant transformation products. TP 11 and TP 17 could not be detected at pH 9.

Tps 7, 8, 9 and 10 were observed at pH ≥ 7 during both photolysis and photocatalysis and these transformation products were formed by stepwise cleavage of the piperazine ring of the defluorinated CIP. Elimination of ciprofloxacin and relative intensities of the formed transformation products are shown in dependence of the treatment time in Suppl. 6.17 of the appendix. The use of peak areas for a relative comparison of the distribution of the compounds can only serve as an indication about the underlying concentration distribution. However, it can be used for the identification of the most important compounds, which can be investigated in detail afterwards.

The dominant transformation pathway during the photolysis and photocatalysis above pH 7 was pathway I, while at pH 7 pathway II was preferred. At acidic conditions the degradation follows mainly pathway III.

3.5.4 Proposed mechanisms for the photolytic and photocatalytic degradation of CIP

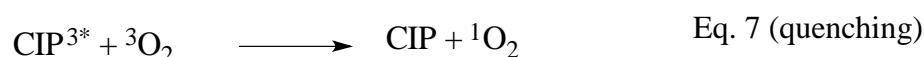
The pattern of the photocatalytic reaction is based on the irradiation of titanium dioxide (TiO_2) particles in presence of dissolved molecular oxygen. The most accepted mechanism of TiO_2 photocatalysis includes redox reactions of adsorbed water and oxygen molecules or of other substrates [49]. The formation of the electron-hole pair ($h^+_{\text{vb}} - e^-_{\text{cb}}$) after excitation is followed by the oxidation of adsorbed water molecules by electron transfer to h^+_{vb} with the formation of hydroxyl radicals and H^+ . The oxygen molecules that are adsorbed at the reductive site of the TiO_2 particle serve as electron acceptors leading to the formation of superoxide radical anions according to Eq. 1 [50]. The superoxide radical anion is a weak base of the conjugated acid HO_2^\bullet in water [51], with a pKa value of 4.8 [52] (see Eq. 2). However, HO_2^\bullet radicals can disproportionate according to Eq. 3 with the formation of molecular oxygen and hydrogen peroxide. Thus, the acid-base equilibrium of Eq. 2 is shifted to HO_2^\bullet and therefore the effective basicity of $\text{O}_2^{\bullet-}$ is significantly increased. This is also confirmed by the low oxidation of CIP in acidic medium. Otherwise, the adsorbed CIP may be oxidized directly by electron transfer at the h^+_{vb} site of the TiO_2 catalyst (see Eq. 4) with formation of radical cations of the substrate. However, adsorption of ciprofloxacin on the surface of TiO_2 is weak due to repulsion between the protonated species of CIP in water and the TiO_2 charged surface.



The photolytic degradation of CIP in presence of molecular oxygen is not based on hydroxyl radical formation but probably takes place through photooxygenation reactions. These photooxygenation reactions are often very complex [53, 54] and depend on the electronic excitation of CIP (Eq. 5). Afterwards, the electronically excited state of CIP may form radicals via single bond homolysis. Carbon centered radicals are efficiently trapped by molecular oxygen to yield peroxy radicals (CIP-O-O^\bullet). These can decompose and finally produce the corresponding oxidation products.

Other mechanisms that have been observed during direct photolysis of CIP include electron transfer to molecular oxygen with formation of a super oxide radical anion and a substrate radical cation (Eq. 6). The radical cations can recombine, rearrange or hydrolyze to the final reaction products.

The electronically excited state of CIP may also be quenched by molecular oxygen with formation of singlet molecular oxygen (Eq. 7) [55].



Oxygen in its singlet excited state is a more reactive species compared to the molecular oxygen in its ground state [55]. This reactivity is due to the high oxidizing potential, which is approximately 1 volt higher than the one of molecular oxygen in its ground state. Consequently, singlet oxygen is significantly more electrophilic [56], reacting rapidly with unsaturated carbon-carbon bonds, neutral nucleophiles such as sulfides [57, 58] and amines [56, 59], as well as with anions, by forming an hydroperoxide as intermediate compound.

We assume that TP 1 ($\text{C}_{17}\text{H}_{20}\text{N}_3\text{O}_4$) and TP 2 ($\text{C}_{17}\text{H}_{20}\text{N}_3\text{O}_5$), which are formed both in CIP photolytic and photocatalytic degradation reactions at pH 5, 7 and 9, are products from the photooxidation reaction through the CIP^{3*} triplet state [28], and the nucleophilic aromatic substitution $\text{S}_\text{N}(\text{Ar})$ reaction [32]. These TPs are formed to a major extent in neutral and basic medium and to a minor extent in acidic medium. Seven of the 18 transformation products observed during the photolytic and photocatalytic degradation reactions have been identified using labelled CIP-d8 (Table 3.2). To the knowledge of the authors, four of the transformation products, namely TP 3 ($\text{C}_{17}\text{H}_{17}\text{N}_3\text{O}_6$), TP 4 ($\text{C}_{16}\text{H}_{17}\text{N}_3\text{O}_5$), TP 5 ($\text{C}_{16}\text{H}_{17}\text{N}_3\text{O}_6$) and TP 6 ($\text{C}_{17}\text{H}_{19}\text{N}_3\text{O}_7$) were identified for the first time. 12 of the other 14 transformation products corroborated previous findings, the other two are newly proposed structures, namely TP 7 ($\text{C}_{17}\text{H}_{17}\text{N}_3\text{O}_5$), (1-cyclopropyl-7-(7,8-dioxa-1,4-diazabicyclo[4.2.0]oct-4-yl)-4-oxo-1,4-dihydroquinoline-3-carboxylic acid) and TP 15 ($\text{C}_{17}\text{H}_{16}\text{N}_3\text{O}_5\text{F}$), (1-cyclopropyl-7-(7,8-dioxa-1,4-diazabicyclo[4.2.0]oct-4-yl)-6-fluoro-4-oxo-1,4-dihydroquinoline-3-carboxylic acid).

Structure of these two compounds has been elucidated using deuterated CIP-d8. The proposed structures of the deuterated transformation products TP_D 7 ($\text{C}_{17}\text{H}_{10}\text{D}_7\text{N}_3\text{O}_5$) and TP_D 15 ($\text{C}_{17}\text{H}_9\text{D}_7\text{N}_3\text{O}_5\text{F}$) were compatible with the corresponding non-deuterated transformation

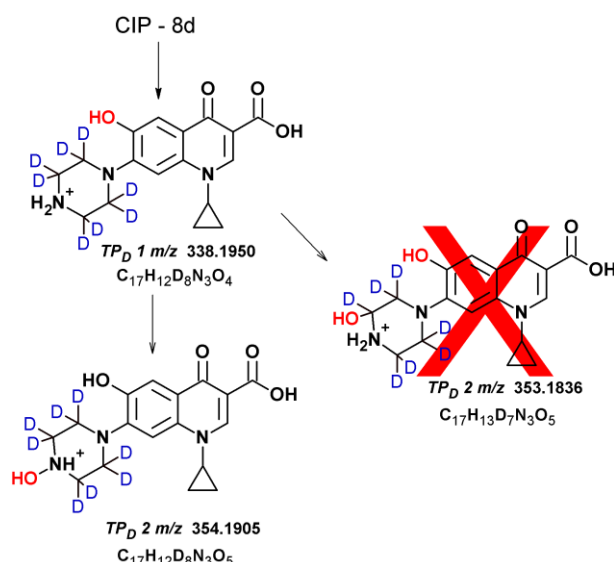
products of CIP. These transformation products have shown the same retention time in the HPLC-MS chromatograms, an equal sum formula, and similar product ion spectra. The fragment pattern spectra of TP 3, TP 7 and TP 15 shows that an O-O peroxide ring is formed between the superoxide radical anion and the piperazine ring. In the next step this ring can be opened and by further oxidation TP_D 8 (C₁₈H₁₁D₆N₃O₄) and TP_D 16 (C₁₆H₁₂D₅N₃O₄F) are formed. The corresponding non-deuterated derivatives are TP 8 (C₁₈H₁₇N₃O₄) and TP 16 (C₁₆H₁₇N₃O₄F), respectively. Additionally, the use of CIP-d8 facilitated the identification of three competing pathways for the CIP photodegradation.

Pathway I: The main photoreaction occurring is photosubstitution of the fluorine atom of CIP by the hydroxyl radical with the formation of TP 1 (C₁₇H₁₉N₃O₄). The proposed structure for TP 1 was already reported previously [15, 27, 33, 39]. The corresponding deuterated derivative is TP_D 1 (C₁₇H₁₂D₈N₃O₄), which showed the same retention time as TP 1 in the HPLC-MS chromatograms. The fragment pattern obtained for TP1, [M+H]⁺ *m/z* 330.1454, was compatible with the one obtained for TP_D 1 (Suppl. 6.18, MS² spectrum of TP_D 1).

In the next step, TP 2 is formed from TP 1 by addition of HO⁻. Several authors proposed that the most reasonable sites at which the addition of a hydroxyl radical could occur are positions C8, C5 and C2, respectively, at the quinolone ring [34, 39, 60]. This could not be corroborated in our study. In contrast, the fragment pattern of the corresponding deuterated derivative TP_D 2 (C₁₇H₁₂D₈N₃O₅) (Suppl. 6.18, MS² spectrum of TP_D 2), indicates that the addition of HO⁻ is taking place at the secondary aliphatic amine groups (N-4') at the piperazine ring as mentioned in Scheme 3.2. Ferdig, et al. [42] have investigated the transformation products of ciprofloxacin and six other fluoroquinolones in aqueous solutions under sunlight irradiation for 6 days. In their study it was assumed that either substitution of the fluorine atom for a hydroxyl group or subjected to the amine groups (N-4') at the piperazine ring takes place. However, they were more inclined to the second assumption because of the stepwise cleavage that took place at the piperazine ring for other detected transformation products. Using the isotopically labeled ciprofloxacin we could clearly distinguished between the exchange of fluorine by an hydroxyl group in the first step following by the addition of HO⁻ to the piperazine ring in a second reaction.

Table 3.2. Accurate masses determined by UPLC-Q-ToF for deuterated Ciprofloxacin (CIP-d8) and its photodegradation products (TPD) generated at pH 7.

Compound	Rt (min)	Elemental formula	Difference from CIP	Mass (m/z)		Error		
				Exp.	Theo.	DBE	ppm	mDa
CIP_d	3.15	—	—	340.19	340.191	9.5	1.8	-0.6
TP_d 1	2.51	C ₁₇ H ₁₁ D ₈ N ₃ O ₄	-(F), +(H, O)	338.193	338.196	9.5	-6.5	-2.2
TP_d 2	2.95	C ₁₇ H ₁₁ D ₈ N ₃ O ₅	-(F) +(H, 2O)	345.191	354.191	9.5	2	0.7
TP_d 7	3.4	C ₁₇ H ₁₀ D ₇ N ₃ O ₅	-(D, F) +(2O)	351.169	351.168	10.5	-0.9	-0.3
TP_d 8	3.6	C ₁₆ H ₁₁ D ₆ N ₃ O ₄	-(C, 2D, F) +(H, O)	322.168	322.167	9.5	0.3	0.1
TP_d 15	3.7	C ₁₇ H ₉ D ₇ N ₃ O ₅ F	-(2D) +(2O)	369.158	369.159	9.5	0.3	-0.3
TP_d 16	2.7	C ₁₆ H ₁₁ D ₅ N ₃ O ₄ F	-(C, 3D) +(H, O)	339.116	339.152	9.5	0.3	0.1
TP_d 18	4.37	C ₁₃ H ₁₁ N ₂ O ₃ F	-(4C, 8D, N) +(H)	263.083	263.083	8.5	-0.4	-0.1

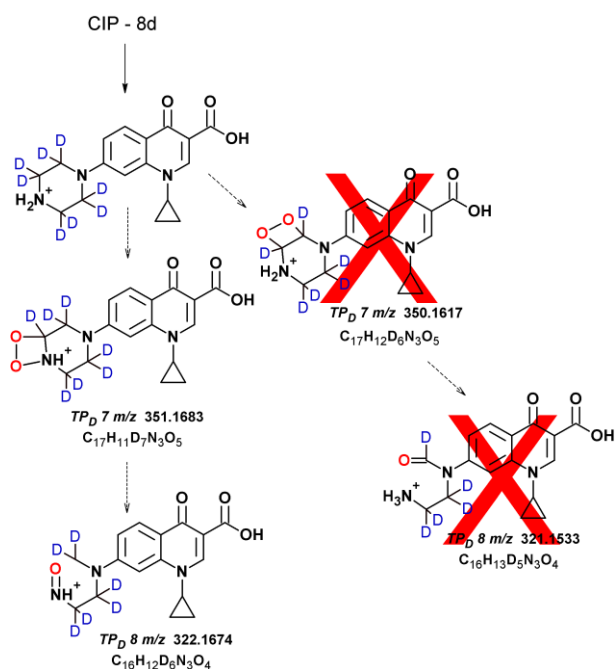


Scheme 3.2 Photocatalysis of CIP-d8 for structural elucidation of transformation product $TP_D 2$ as surrogate of TP 2 (1-cyclopropyl-6-hydroxy-7-(4-hydroxypiperazin-1-yl)-4-oxo-1,4-dihydroquinoline-3-carboxylic acid).

At $pH \geq 7$, TP 3 is further transformed to TP 4 ($C_{16}H_{18}N_3O_5$) and TP 5 ($C_{16}H_{18}N_3O_6$) ($C_{17}H_{18}N_3O_6$) under photocatalytic oxidation and to TP 6 ($C_{17}H_{20}N_3O_7$) under photolytic oxidation. We hypothesize that the transformation at the piperazine ring occurs via addition of oxygen with the formation of a peroxy-piperazine ring (1,2 dioxetanes), followed by the loss of a CO group and opening of the piperazine ring which produces a nitrous moiety in TP 4, a keton-derivative, and a carboxylic group in TP 5. We assume that hydroperoxide forms as an intermediate compound, induced by a dioxetane via cycloaddition of singlet oxygen at the piperazine ring.

Pathway II: The reaction occurs with CIP molecular fragmentation at the C-F bond in the excited state or by water addition, followed by fluoride loss. This could be attributed to the deprotonation of the amino substituent that can increase the electron donating ability. So we note that reaction takes place at the piperazine ring. One of the identified transformation products formed following this pathway is TP 7 ($C_{17}H_{17}N_3O_5$), as defluorination photodegradation product of CIP, with the corresponding deuterated derivative $TP_D 7$ ($C_{17}H_{11}D_7N_3O_5$). The fragment patterns are also illustrated in supplementary material (Suppl. 6.18, MS^2 spectrum of $TP_D 7$). The further irradiation of TP 7 ($C_{17}H_{17}N_3O_5$) led to loss of a CO group and opening of the piperazine ring forming TP 8 ($C_{16}H_{18}N_3O_4$) and the corresponding deuterated derivative $TP_D 8$ ($C_{16}H_{11}D_6N_3O_4$) Scheme 3.3 shows structures of the transformation products of TP_{D7} and TP_{D8} . TP 8 ($C_{16}H_{18}N_3O_4$) is further transformed to TP 9 ($C_{15}H_{17}N_3O_3$), which was previously identified by Turiel, et al. [40], as the main

photolytic degradation product of CIP at pH 7. TP 10 ($C_{13}H_{13}N_2O_3$) is the final transformation product of CIP following this pathway under neutral conditions.



Scheme 3.3 Structural elucidation of transformation products of TP_D 7 and TP_D 8 as surrogates for TP 7 and TP 8, respectively.

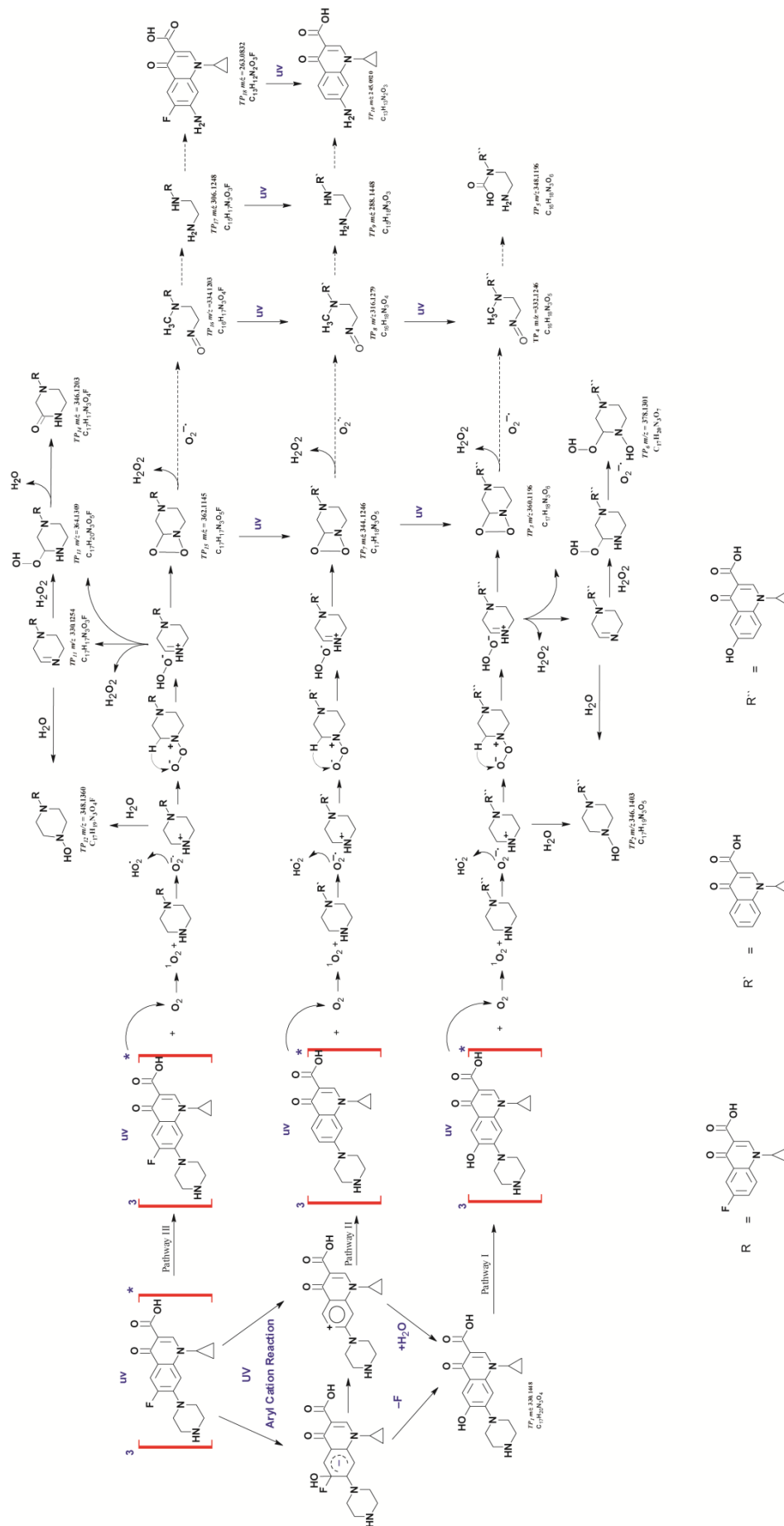
Pathway III occurred especially at neutral and acidic pH in presence of TiO_2 at the piperazine ring with preservation of the fluorine atom. TP 11 ($C_{17}H_{16}N_3O_3F$) under photocatalytic oxidation is further degraded to TP 12 ($C_{17}H_{18}N_3O_4F$), which has been previously suggested by Ferdig, et al. [42]. The addition of HO^- is done on the amine group as mentioned in pathway I. TP 13 ($C_{17}H_{19}N_3O_5F$) is further degraded from TP 11 ($C_{17}H_{16}N_3O_3F$) under photocatalytic oxidation; TP 14 ($C_{17}H_{16}N_3O_4F$), a ketone derivative, is formed from TP 13 without any cleavage on the piperazine ring. This structure has been suggested by Sturini, et al. [61] who have investigated the degradation of CIP in untreated river water under solar light as well as under the same conditions in the presence of suspended TiO_2 . TP 16 ($C_{16}H_{16}N_3O_4F$) is formed from TP 15 ($C_{17}H_{16}N_3O_5F$) via piperazine ring cleavage and CO group loss. The corresponding deuterated derivative is TP_D 16 ($C_{16}H_{11}D_5N_3O_4F$). TP 16 ($C_{16}H_{16}N_3O_4F$) is further degraded to TP 17 ($C_{15}H_{16}N_3O_3F$) and TP 18 ($C_{13}H_{12}N_2O_3F$). Previously, TP 18 ($C_{13}H_{12}N_2O_3F$) was isolated and identified by NMR as final degradation product of CIP at low pH [47, 48]. We were also able to identify TP_D 18 (Suppl. 6.18, MS^2 spectrum of TP_D 18) as end product of the CIP-d8 photodegradation at pH 7. Using the concept of deuterated surrogate compounds, we could clearly show that the interaction takes place at the piperazine ring of CIP via quenching the electron of the triplet state by oxygen, leading to the formation of singlet oxygen (1O_2) and the superoxide anion (O_2^-).

Scheme 3.4 illustrates these pathways correspond to some extent to the ones proposed in previous studies carried out on photolytic degradation of fluoroquinolones [23, 27-29, 32, 61]. (i) Photosubstitution of the fluorine atom by an hydroxyl group is expected to be a quite common result in neutral and moderately basic solutions; or (ii) defluorination which occurs in neutral solutions; (iii) Fluorine conservation under strongly acidic conditions. Moreover, in the latter case, the excited state of the FQs causes electron or hydrogen transfer from the electron-rich moiety present, namely the amine groups subsequent to oxidative degradation of the piperazine ring. In the photocatalytic process induced by combined UV-A or sunlight with TiO_2 , a sizeable fraction of incoming light is absorbed by the titania particles and therefore the photosubstitution of the fluorine is in competition with the TiO_2 . The interaction with the adsorbed FQs would tend to direct photo-hole (h^+) oxidation and hydroxyl radical addition on the sites exhibiting the highest electron density [51, 55]. A combination of TiO_2 as photocatalyst and UV-C irradiation as photon source enhanced both the photolysis and the photocatalysis mechanism for the degradation of CIP due to the higher photon energy produced by UV-C in comparison with UV-A or sunlight.

3.6 Conclusions

The pseudo-first order reaction kinetics were dependent on the different dissociation species of ciprofloxacin. The highest removal rate was observed at pH 9. Structure elucidation and identification of transformation products could be carried out by the use of isotopically labeled surrogate compounds by both unit and high resolution mass spectrometry. Three degradation pathways and the corresponding degradation products were identified. To the knowledge of the authors, four transformation products have been detected for the first time, two more were newly proposed structures supported by results using deuterated ciprofloxacin. We could confirm that the first step in both photolytic and photocatalytic degradation is mainly defluorination, followed by degradation at the piperazine ring of ciprofloxacin.

Scheme 3.4 Three competing pathways for CIP photodegradation, the dominant transformation pathway during the photolysis and photolysis above pH 7 was pathway I, while at pH 7 pathway II was the preferred transformation pathway. At acidic conditions the degradation follows mainly pathway III. TP structures are presented as protonated species $[M+H]^+$; m/z represent the mass of the protonated species.



3.7 Acknowledgment

Laboratory assistance and cooperation of Dima Chehade and the support of Dr. Kai Lehnberg for starting this cooperation are gratefully acknowledged. Special thanks to Prof. Dr. Wolfgang Dott for supporting this study and allowing us to use the SYNAPT LC-MS at Institute for Hygiene and Environmental Medicine in Aachen, Germany. We are grateful to Dr. Jens Jacobsen for providing us with the Unifi software by Waters, which was used to analyze the MS data.

3.8 References

- [1] R. Wise, Antimicrobial resistance: priorities for action, *J. Antimicrob. Chemother.*, 49 (2002) 585-586.
- [2] K. Kümmerer, Antibiotics and Animals, *Pharmaceuticals in the Environment*, Springer Berlin, 2008, pp. 75-93.
- [3] C.M. Benbrook, Antibiotic drug use in U.S. aquaculture., *The northwest science and environmental policy center Sandpoint, Idaho, USA.*, 2002, pp. 22.
- [4] P. Ball, Quinolone generations: natural history or natural selection?, *J. Antimicrob. Chemother.*, 46 Suppl T1 (2000) 17-24.
- [5] V.T. Andriole, The future of the quinolones, *Drugs*, 58 Suppl 2 (1999) 1-5.
- [6] N. Adriaenssens, S. Coenen, A.C. Kroes, A. Versporten, V. Vankerckhoven, A. Muller, H.S. Blix, H. Goossens, E.P. Group, European surveillance of antimicrobial consumption (ESAC): Systemic antiviral use in Europe, *J. Antimicrob. Chemother.*, 66 (2011) 1897-1905.
- [7] A.J. Watkinson, E.J. Murby, S.D. Costanzo, Removal of antibiotics in conventional and advanced wastewater treatment: Implications for environmental discharge and wastewater recycling, *Water Res.*, 41 (2007) 4164-4176.
- [8] S. Babic', M. Periša, I. Škoric', Photolytic degradation of norfloxacin, enrofloxacin and ciprofloxacin in various aqueous media, *Chemosphere*, 91 (2013) 1635-1642.
- [9] A. Hartmann, A.C. Alder, T. Koller, R.M. Widmer, Identification of fluoroquinolone antibiotics as the main source of umuC genotoxicity in native hospital wastewater, *Environ. Toxicol. Chem.*, 17 (1998) 377-382.

- [10] X. Van Doorslaer, J. Dewulf, H. Van Langenhove, K. Demeestere, Fluoroquinolone antibiotics: An emerging class of environmental micropollutants, *Sci. Total. Environ.*, 500-501 (2014) 250-269.
- [11] N. Le-Minh, S.J. Khan, J.E. Drewes, R.M. Stuetz, Fate of antibiotics during municipal water recycling treatment processes, *Water Res.*, 44 (2010) 4295-4323.
- [12] I. Ebert, J. Bachmann, U. Kühnen, A. Küster, C. Kussatz, D. Maletzki, C. Schlüter, Toxicity of the fluoroquinolone antibiotics enrofloxacin and ciprofloxacin to photoautotrophic aquatic organisms, *Environ. Toxicol. Chem.*, 30 (2011) 2786-2792.
- [13] T.G. Vasconcelos, K. Kümmerer, D.M. Henriques, A.F. Martins, Ciprofloxacin in hospital effluent: degradation by ozone and photoprocesses, *J. Hazard. Mater.*, 169 (2009) 1154-1158.
- [14] E. De Bel, J. Dewulf, B.D. Witte, H. Van Langenhove, C. Janssen, Influence of pH on the sonolysis of ciprofloxacin: Biodegradability, ecotoxicity and antibiotic activity of its degradation products, *Chemosphere*, 77 (2009) 291-295.
- [15] X. Wei, J. Chen, Q. Xie, S. Zhang, L. Ge, X. Qiao, Distinct photolytic mechanisms and products for different dissociation species of ciprofloxacin, *Environ. Sci. Technol.*, 47 (2013) 4284-4290.
- [16] X. Van Doorslaer, K. Demeestere, P.M. Heynderickx, H. Van Langenhove, J. Dewulf, UV-A and UV-C induced photolytic and photocatalytic degradation of aqueous ciprofloxacin and moxifloxacin: Reaction kinetics and role of adsorption, *Appl. Catal. B*, 101 (2011) 540-547.
- [17] N. Daneshvar, D. Salari, A. Niaei, M.H. Rasoulifard, A.R. Khataee, Immobilization of TiO₂ nanopowder on glass beads for the photocatalytic decolorization of an azo dye C.I. Direct Red 23, *J. Environ. Sci. Health. A Tox. Hazard. Subst. Environ. Eng.*, 40 (2005) 1605-1617.
- [18] E.S. Elmolla, M. Chaudhuri, Photocatalytic degradation of amoxicillin, ampicillin and cloxacillin antibiotics in aqueous solution using UV/TiO₂ and UV/H₂O₂/TiO₂ photocatalysis, *Desalination*, 252 (2010) 46-52.

- [19] K. Demeestere, J. Dewulf, H. Van Langenhove, B. Sercu, Gas–solid adsorption of selected volatile organic compounds on titanium dioxide Degussa P25, *Chem. Eng. Sci.*, 58 (2003) 2255-2267.
- [20] T. Paul, M.C. Dodd, T.J. Strathmann, Photolytic and photocatalytic decomposition of aqueous ciprofloxacin: transformation products and residual antibacterial activity, *Water Res.*, 44 (2010) 3121-3132.
- [21] T. Paul, P.L. Miller, T.J. Strathmann, Visible-light-Mediated TiO₂ photocatalysis of fluoroquinolone antibacterial agents, *Environ. Sci. Technol.*, 41 (2007) 4720-4727.
- [22] Z. Qiang, C. Adams, Potentiometric determination of acid dissociation constants (pK_a) for human and veterinary antibiotics, *Water Res.*, 38 (2004) 2874-2890.
- [23] A. Albini, S. Monti, Photophysics and photochemistry of fluoroquinolones, *Chem. Soc. Rev.*, 32 (2003) 238-250.
- [24] G. Cosa, Photodegradation and photosensitization in pharmaceutical products: Assessing drug phototoxicity, *Pure. Appl. Chem.*, 76 (2004) 263-275.
- [25] A.I. Drakopoulos, P.C. Ioannou, Spectrofluorimetric study of the acid–base equilibria and complexation behavior of the fluoroquinolone antibiotics ofloxacin, norfloxacin, ciprofloxacin and pefloxacin in aqueous solution, *Anal. Chim. Acta*, 354 (1997) 197-204.
- [26] P. Bilski, L.J. Martinez, E.B. Koker, C.F. Chignell, Photosensitization by norfloxacin is a function of pH, *Photochem. Photobiol.*, 64 (1996) 496-500.
- [27] M. Mella, E. Fasani, A. Albini, Photochemistry of 1-Cyclopropyl-6-fluoro-1,4-dihydro-4-oxo-7-(piperazin-1-yl)quinoline-3-carboxylic Acid (=Ciprofloxacin) in aqueous solutions, *Helv. Chim. Acta*, 84 (2001) 2508-2519.
- [28] S. Monti, S. Sortino, E. Fasani, A. Albini, Multifaceted photoreactivity of 6-fluoro-7-aminoquinolones from the lowest excited states in aqueous media: a study by nanosecond and picosecond spectroscopic techniques, *Chem. Eur. J.*, 7 (2001) 2185-2196.
- [29] E. Fasani, M. Rampi, A. Albini, Photochemistry of some fluoroquinolones: effect of pH and chloride ion, *J. Chem. Soc., Perkin Trans 2*, (1999) 1901-1907.

[30] C. Kormann, D.W. Bahnemann, M.R. Hoffmann, Photolysis of chloroform and other organic molecules in aqueous titanium dioxide suspensions, *Environ. Sci. Technol.*, 25 (1991) 494-500.

[31] R. Vargas, O. Núñez, Hydrogen bond interactions at the TiO₂ surface: Their contribution to the pH dependent photo-catalytic degradation of p-nitrophenol, *J. Mol. Catal. A Chem.*, 300 (2009) 65-71.

[32] E. Fasani, F.F. Barberis Negra, M. Mella, S. Monti, A. Albini, Photoinduced C–F bond cleavage in some fluorinated 7-Amino-4-quinolone-3-carboxylic acids, *J. Org. Chem.*, 64 (1999) 5388-5395.

[33] J.A. Perini, B.F. Silva, R.F. Nogueira, Zero-valent iron mediated degradation of ciprofloxacin - Assessment of adsorption, operational parameters and degradation products, *Chemosphere*, 117 (2014) 345-352.

[34] Y. Ji, C. Ferronato, A. Salvador, X. Yang, J.M. Chovelon, Degradation of ciprofloxacin and sulfamethoxazole by ferrous-activated persulfate: Implications for remediation of groundwater contaminated by antibiotics, *Sci. Total. Environ.*, 472 (2014) 800-808.

[35] Z. Zhou, J.Q. Jiang, Reaction kinetics and oxidation products formation in the degradation of ciprofloxacin and ibuprofen by ferrate(VI), *Chemosphere*, 119 (2015) S95-100.

[36] Y. Lester, D. Avisar, I. Gozlan, H. Mamane, Removal of pharmaceuticals using combination of UV/H₂O₂/O₃ advanced oxidation process, *Water Sci. Technol.*, 64 (2011) 2230-2238.

[37] T. Haddad, E. Baginska, K. Kümmerer, Transformation products of antibiotic and cytostatic drugs in the aquatic cycle that result from effluent treatment and abiotic/biotic reactions in the environment: An increasing challenge calling for higher emphasis on measures at the beginning of the pipe, *Water Res.*, 72 (2015) 75-126.

[38] A.S. Maia, A.R. Ribeiro, C.L. Amorim, J.C. Barreiro, Q.B. Cass, P.M. Castro, M.E. Tiritan, Degradation of fluoroquinolone antibiotics and identification of metabolites/transformation products by liquid chromatography-tandem mass spectrometry, *J. Chromatogr. A*, 1333 (2014) 87-98.

- [39] T. Haddad, K. Kümmerer, Characterization of photo-transformation products of the antibiotic drug Ciprofloxacin with liquid chromatography-tandem mass spectrometry in combination with accurate mass determination using an LTQ-Orbitrap, *Chemosphere*, 115 (2014) 40-46.
- [40] E. Turiel, G. Bordin, A.R. Rodriguez, Study of the evolution and degradation products of ciprofloxacin and oxolinic acid in river water samples by HPLC-UV/MS/MS-MS, *J. Environ. Manage.*, 7 (2005) 189-195.
- [41] L. Hu, A.M. Stemig, K.H. Wammer, T.J. Strathmann, Oxidation of antibiotics during water treatment with potassium permanganate: Reaction pathways and deactivation, *Environ. Sci. Technol.*, 45 (2011) 3635-3642.
- [42] M. Ferdig, A. Kaleta, W. Buchberger, Improved liquid chromatographic determination of nine currently used (fluoro)quinolones with fluorescence and mass spectrometric detection for environmental samples, *J. Sep. Sci.*, 28 (2005) 1448-1456.
- [43] C. Liu, V. Nanaboina, G. Korshin, Spectroscopic study of the degradation of antibiotics and the generation of representative EfOM oxidation products in ozonated wastewater, *Chemosphere*, 86 (2012) 774-782.
- [44] B. De Witte, J. De wulf, K. Demeestere, H. Van Langenhove, Ozonation and advanced oxidation by the peroxone process of ciprofloxacin in water, *J. Hazard. Mater.*, 161 (2009) 701-708.
- [45] M. Yahya, N. Oturan, K. El Kacemi, M. El Karbane, C.T. Aravindakumar, M.A. Oturan, Oxidative degradation study on antimicrobial agent ciprofloxacin by electro-Fenton process: kinetics and oxidation products, *Chemosphere*, 117 (2014) 447-454.
- [46] B. De Witte, J. De wulf, K. Demeestere, V. Van De Vyvere, P. De Wispelaere, H. Van Langenhove, Ozonation of ciprofloxacin in water: HRMS identification of reaction products and pathways, *Environ. Sci. Technol.*, 42 (2008) 4889-4895.
- [47] K. Tornainen, C.P. Askolin, J. Mattinen, Isolation and structure elucidation of an intermediate in the photodegradation of ciprofloxacin, *J. Pharm. Biomed. Anal.*, 16 (1997) 439-445.

- [48] K. Torniainen, J. Mattinen, C.P. Askolin, S. Tammilehto, Structure elucidation of a photodegradation product of ciprofloxacin, *J. Pharm. Biomed. Anal.*, 15 (1997) 887-894.
- [49] M.R. Hoffmann, S.T. Martin, W. Choi, D.W. Bahnemann, Environmental applications of semiconductor photocatalysis, *Chem. Rev.*, 95 (1995) 69-96.
- [50] N. Getoff, Purification of drinking water by irradiation. A review, *J. Chem. Sci.*, 105 (1993) 373.
- [51] E. Oliveros, P. Suardi-Murasecco, T. Aminian-Saghafi, A.M. Braun, H.-J. Hansen, 1H-Phenalen-1-one: Photophysical properties and singlet-oxygen production, *Helv. Chim. Acta*, 74 (1991) 79-90.
- [52] B.H.J. Bielski, D.E. Cabelli, R.L. Arudi, A.B. Ross, Reactivity of $\text{HO}_2/\text{O}^{-2}$ radicals in aqueous solution, *J. Phys. Chem. Ref. Data*, 14 (1985) 1041-1100.
- [53] M. Elbouamri, J.P. Gorrichon, A.M. Braun, E. Oliveros, The reactivity of Citronellol and alpha- Thujene with singlet oxygen - Rate constants of chemical - Reaction and physical quenching, *Photochem. Photobiol.*, 54 (1991) 619-623.
- [54] R.G. Zepp, Factors affecting the photochemical treatment of hazardous waste, *Environ. Sci. Technol.*, 22 (1988) 256-257.
- [55] M. De Rosa, Photosensitized singlet oxygen and its applications, *Coord. Chem. Rev.*, 233-234 (2002) 351-371.
- [56] E.L. Clennan, A. Pace, Advances in singlet oxygen chemistry, *Tetrahedron*, 61 (2005) 6665-6691.
- [57] E.L. Clennan, M.-F. Chen, A. Greer, F. Jensen, Experimental and computational evidence for the formation of iminopersulfonic acids, *J. Org. Chem.*, 63 (1998) 3397-3402.
- [58] A. Greer, M.-F. Chen, F. Jensen, E.L. Clennan, Experimental and ab initio computational evidence for new peroxidic intermediates (iminopersulfonic acids). Substituent effects in the photooxidations of sulfenic acid derivatives, *J. Am. Chem. Soc.*, 119 (1997) 4380-4387.
- [59] G. Chen, M. Li, X. Liu, Fluoroquinolone antibacterial agent contaminants in soil/groundwater: A literature review of sources, fate, and occurrence, *Water, Air, Soil Pollut.*, 226 (2015) 11.

[60] T. An, H. Yang, G. Li, W. Song, W.J. Cooper, X. Nie, Kinetics and mechanism of advanced oxidation processes (AOPs) in degradation of ciprofloxacin in water, *Appl. Catal. B*, 94 (2010) 288-294.

[61] M. Sturini, A. Speltini, F. Maraschi, A. Profumo, L. Pretali, E.A. Irastorza, E. Fasani, A. Albini, Photolytic and photocatalytic degradation of fluoroquinolones in untreated river water under natural sunlight, *Appl. Catal. B*, 119-120 (2012) 32-39.

4 Evaluation of UV irradiation effects on the photolytic degradation of micropollutants in water

4.1 Abstract

Pharmaceuticals are micropollutants of emerging concern that have been detected in the aquatic environment and in some cases in drinking water at nanogram per liter levels. Photolysis is often used as an effective disinfection step for drinking water and wastewater. Recently, direct ultraviolet (UV) photolysis has been widely reported as a method for the removal of organic micropollutants. The first aim of this study was monitoring the concentrations of diclofenac, metoprolol, carbamazepine, sulfamethoxazole and benzotriazole in the effluent of a wastewater treatment plant over a period of 4 months. While the second aim was to investigate the removal of the five micropollutants from water by direct UV photolysis, using three different UV sources, namely UV-A, UV-B and UV-C. The degradation rates of the pharmaceuticals were determined. Diclofenac shows moderate degradation under UV-A radiation, while carbamazepine, sulfamethoxazole, benzotriazole and metoprolol were hardly degraded by this wavelength range. UV-B and UV-C showed a good yield on the degradation of the investigated pharmaceuticals. The photodegradation rate constants of metoprolol and carbamazepine increased in presence of WWTP effluent matrix under UV-B and UV-C irradiation in comparison to experiments performed in deionized water. This promotion is probably due to the presence of photosensitizer compounds in the WWTP effluent matrix. In contrast, diclofenac and sulfamethoxazole showed decreased in the photodegradation rate constants, which might be due to the physical or chemical quenching of the photochemical degradation intermediates. The WWTP effluent matrix also posed non-negligible influences on benzotriazole photodegradation process. Overall, direct photolysis was demonstrated to be relevant for micropollutant abatement from the aquatic environmental. However, it is essential to further understand how this process is affected by the UV sources, micropollutant structures and matrix composition.

4.2 Keywords

Advanced oxidation processes, photolysis, quantum yield, pharmaceuticals

4.3 Introduction

The evolution and increase of chemical analysis techniques' sensitivity [1] made possible the measurement of micropollutants at very low concentrations, in the range of ng L^{-1} to $\mu\text{g L}^{-1}$, in wastewater [2], surface water [3], groundwater [4-6], and even drinking water [7]. Micropollutants (pharmaceuticals, personal-care products, corrosion inhibitors, pesticides, etc.) are being detected continuously around the world in wastewater effluents, water bodies, and water supplies [2, 7, 8]. Several prescription drugs such as diclofenac, carbamazepine, sulfamethoxazole and others have been found in the aquatic environment [9]. Therefore, pharmaceuticals, as an important part of micropollutants, are raising concerns due to the possible negative effects that they might have on the ecosystem and their potential to reach drinking water [10]. Pharmaceuticals are released to the environment by various routes, including human excretion, direct waste disposal to sewage, and from veterinary application. Monitoring efforts are being conducted by the European Union (EU) in the aquatic environment on several pharmaceuticals and hormones to evaluate and support possible future regulations. Recently, the EU (Commission Implementing Decision EU 2015/495 of March 2015) added the natural hormone E1 and the antibiotic erythromycin to their watch list, which already included diclofenac and two other hormones, namely EE2 and E2. 156 micropollutants were analyzed in effluents from 90 European wastewater treatment plants (WWTPs). Among them diclofenac, carbamazepine, and some antibiotics showed the highest median concentration levels [11]. Diclofenac has been also found to occur nearly ubiquitous in water bodies and was even detected in German groundwater in concentrations up to several $\mu\text{g L}^{-1}$ [12], as well as in groundwater in Spain [13]. Diclofenac has been identified as a pharmaceutical affecting the wildlife [14]. Bradley, et al. [15] investigated the fate and transport of 110 pharmaceuticals from wastewater effluents to shallow groundwater. About 43 - 55% of the target pharmaceuticals were detected in surface waters and 6 - 16% were detected in groundwater. Carbamazepine and sulfamethoxazole were detected at concentrations $> 0.02 \mu\text{g L}^{-1}$. Metoprolol has been frequently identified in aquatic environments due to its low sorption affinity on activated sludge [16]. Maszkowska, et al. [17] indicated in their study a high hydrolytic stability of metoprolol with an estimated half-life of more than one year. Other studies showed that metoprolol can reach concentrations of up to $0.35 \mu\text{g L}^{-1}$ in groundwater [5] and up to $0.038 \mu\text{g L}^{-1}$ in drinking water [18]. Benzotriazole is a heterocyclic compound used as corrosion inhibitor. It is considered one of the most detected micropollutants in the aquatic environment [2]. It was detected in different European river waters in the range of $0.5 - 8.0 \mu\text{g L}^{-1}$ [19], as well as in groundwater at a

maximum concentration of $1 \mu\text{g L}^{-1}$ [6]. Diclofenac, carbamazepine, sulfamethoxazole, metoprolol and benzotriazole have been considered as emerging contaminants in the EU due to the fact that they have often been detected in the aquatic environment [19]. Bergmann, et al. [20] classified them as high priority micropollutants in the environment due to their potential effect in the environment depending on their ecotoxicity, environmental concentrations and quantities consumed.

In recent years, advanced oxidation processes (AOPs) have been developed to fill up the gap in the existing water treatment methods, which are not sufficiently efficient to remove micropollutants from wastewater [21, 22]. Photodegradation of micropollutants was studied using different light sources including UV light [23], solar simulation [24] and natural sunlight [25] for a variety of water matrices including pure water [26], fresh water (from rivers and lakes) [27] and wastewater [28]. The effectiveness of photodegradation depends on the integrative effects of photon flux, the structure of the molecule and water-matrix composition [24]. For example, Baeza and Knappe [29] found that the water matrix (ultrapure water, lake water, wastewater treatment plant effluent) has an effect on photodegradation of diclofenac and sulfonamides (sulfamethoxazole, sulfamethazine, sulfadiazine) under the UV - C irradiation. The pseudo first-order kinetic rate constants of the direct and indirect photolysis of carbamazepine and diclofenac depended on their initial concentrations (at mg/L levels) [30]. Salma, et al. [31] reported that the photodegradation mechanism of neбиволol varied with the UV source.

In this study, selected micropollutants, namely diclofenac, metoprolol, carbamazepine, sulfamethoxazole and benzotriazole, in the effluent of the wastewater treatment plant at Duisburg-Hochfeld have been monitored over a period of 4 months, and their photodegradation in the water and WWTP effluent was investigated. To that end, the systematic investigation of photolysis under different UV lamps, namely UV-C (254 nm), UV-B (312 nm) and UV-A (365 nm) in the elimination of the above mentioned micropollutants from water and wastewater was studied in a bench-scale reactor.

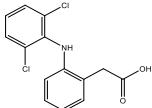
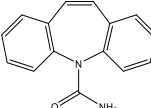
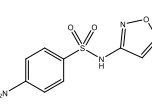
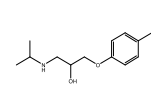
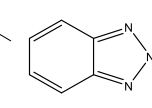
4.4 Experimental section

4.4.1 Reagents and materials

Water for LC-MS, acetonitrile and methanol were received from Th. Geyer GmbH & Co. KG (Renningen, Germany). Diclofenac, metoprolol, carbamazepine, sulfamethoxazole and benzotriazole have been purchased from Sigma-Aldrich (Taufkirchen, Germany) (see Table 4.1).

The UV absorption spectra of the investigated compounds are shown in Figure 4.1.

Table 4.1 Physical and chemical properties of the studied micropollutants [32].

	Diclofenac	Carbamazepine	Sulfamethoxazole	Metoprolol	Benzotriazole
Molecular weight (g mol ⁻¹)	296.2	236.2	253.2	267.3	119.1
Solubility in water (mg L ⁻¹)	2.37	17.66	3942	4777	5957
pKa	4	15.96	1.97/ 6.16	9.67/ 14.09	0.60/ 8.63
Molecular sum formular	C ₁₄ H ₁₁ Cl ₂ NO ₂	C ₁₅ H ₁₂ N ₂ O	C ₁₀ H ₁₁ N ₃ O ₃ S	C ₁₅ H ₂₅ NO ₃	C ₆ H ₅ N ₃
Molecular Structures					

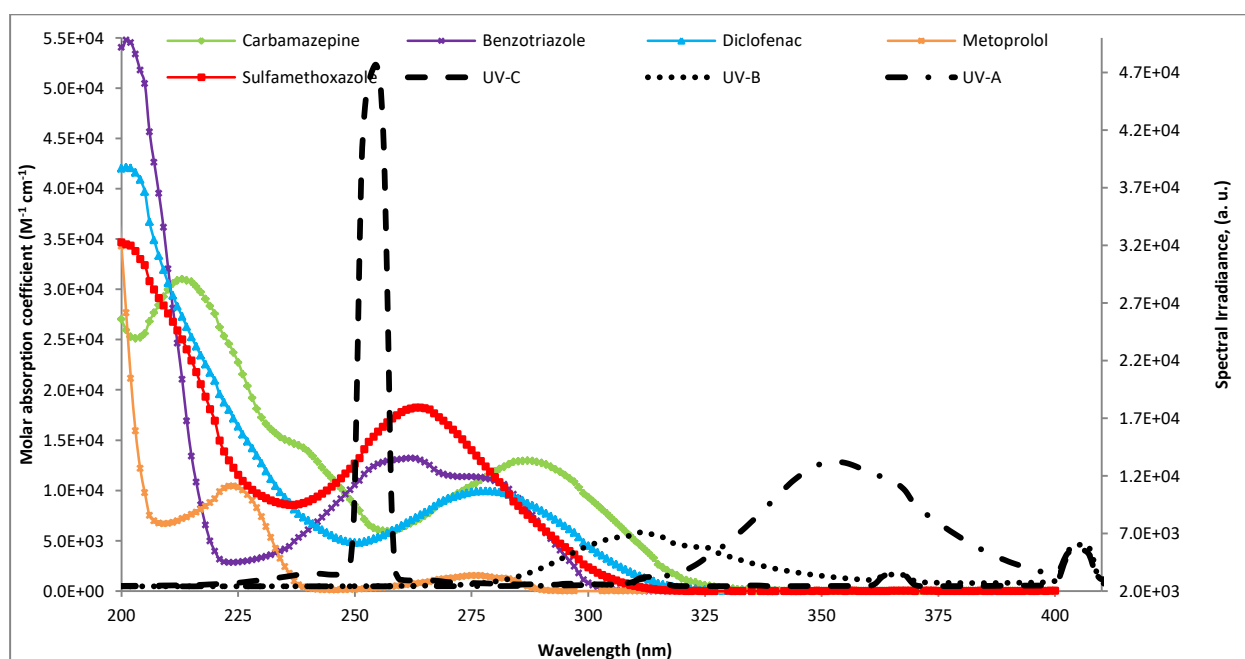


Figure 4.1 Absorption spectra of the investigated compounds (1 mg L⁻¹, pH = 7) and emission spectra of the UV-lamps used in this study.

4.4.2 Sample preparation

24 h composite samples on different days of the week were collected from the effluent of WWTP Duisburg-Hochfeld (92,000 population equivalent, PE). Also information on the weather condition (wet /dry) was gathered. The collected samples were filtered with 0.45 µm regenerated cellulose syringe filters (Chromafil RC-45/15MS, Machery-Nagel, Düren, Germany), and measured with LC-MS/MS.

4.4.3 HPLC-MS/MS analysis

HPLC-MS/MS analysis were performed with an Agilent 1100 series HPLC system consisting of an Agilent 1260 Infinity Quaternary LC communication bus module, 1100 LC- vacuum

degasser, Agilent 1100 series binary pump, a CTC Pal HTS auto sampler (CTC Analytics, Zwingen, Schweiz), and column oven (Hotdog, Prolab Instruments GmbH, Reinach, Switzerland) coupled to a QTRAP 6500 system (AB SCIEX Deutschland GmbH, Darmstadt, Germany). Data analysis was conducted with the Analyst™ software 1.6.2 (AB Sciex, Darmstadt, Germany). The chromatographic separation was performed on a C18 Chromolith® Fast Gradient RP 18e endcapped monolithic HPLC silica column (50×2 mm, Merck KGaA, Darmstadt, Germany) at 40 °C. The eluents, water (A) and methanol (B), contained each 0.1% formic acid, the pH was between 2.2 and 2.8 and no buffer was added. The eluents were applied for the chromatographic separation of 50 µL sample aliquots at a flow rate of 0.5 mL min⁻¹. The gradient program started with 1% B organic phase and increased to 99% B within 5 min, then was kept constant for 3 min and afterwards the gradient decreased to 1% B in 10 seconds. After 11 min, the column was rinsed and re-equilibrated. All analyses were carried out in the MRM mode with the most intense transitions as listed in Table 4.2. A second MRM transition verifying the compound is additionally indicated as well as compound-specific instrumental parameters. Preceding experiments revealed the optimized settings for curtain gas (40 psi), ion source temperature (550 °C), ion source gases (55 and 60 psi), positive electrospray ionization (5,500 V), and collision cell exit potential (4 V) and these were kept constant for all compounds. Calibration was performed in the working range of 10 – 1000 ng L⁻¹, with a good linearity ($r^2 > 0.99$) and an accuracy between 80 and 120%.

Table 4.2 Optimized MRM conditions for the HPLC/MS/MS analysis.

Compound	RT [min]	Quantification transition <i>m/z</i>	Verification transition <i>m/z</i>	Declustering potential DP [V]	Collision energy CE [eV]
Diclofenac	8.2	296 → 214	296 → 215	80	50
Metoprolol	3.2	268 → 133	268 → 103	102	35
Carbamazepine	5.7	237 → 194	237 → 193	126	28
Sulfamethoxazole	2.8	254 → 156	254 → 92	85	23
1 <i>H</i> -Benzotriazole	2.1	120 → 65	120 → 92	51	31

4.4.4 Ferrioxalate actinometry

Ferrioxalate actinometry was conducted according to Bolton and Linden (2003) to determine the fluence rate of the UV lamps. UV-A gave polychromatic radiation with the highest E_{avg} (1.95 mW cm^{-2}), followed by UV-B, also with polychromatic radiation (1.67 mW cm^{-2}), while UV-C produced monochromatic radiation (0.64 mW cm^{-2}). Detailed information about the experimental procedure, as well as the calculated values of the light intensity (I) (Einstein/s) and energy flux (E_{avg}) (W cm^{-2}) of the UV lamps can be found in the Ferrioxalate actinometry section in the supplementary material 6.2.

4.4.5 Photodegradation experiments

The experiments were carried out in a 2-L glass photoreactor (see Figure 4.2) provided by IBL Umwelt- und Biotechnik GmbH (Heidelberg, Deutschland). 1 mg L^{-1} pharmaceutical solutions (diclofenac, carbamazepine, sulfamethoxazole, benzotriazole and metoprolol) were prepared in millipore grade water. The experiments were evaluated in triplicate, one hour for each experiment. 1 mL sample was collected in HPLC vials during the experiments at an interval time of 0, 5, 10, 15, 20, 30, 45 and 60 minutes. Three types of 15 W UV lamps were used during the experiments: (1) a UV-A lamp, mainly emitting in the wavelength range 315 to 400 nm, main emission band at 365 nm with an average fluence rate (E_{avg}) of 1.95 mW cm^{-2} (Vilber Lourmat, Eberhardzell, Germany), (2) a UV-B lamp mainly, emitting in the wavelength range 280 to 360 nm, main emission band at 312 nm and an E_{avg} of 1.67 mW cm^{-2} (Vilber Lourmat, Eberhardzell, Germany) and (3) a low pressure UV lamp (New NEC Light Ing., Shiga, Japan) that mainly emits in the UV-C range (254 nm) with an E_{avg} of 0.64 mW cm^{-2} . The emission spectra of the UV lamps are shown in Figure 4.1. The lamp was introduced into the reactor and kept separated from the irradiated solution using a quartz glass tube. The reactor was connected to a cooling system RM6 Thermostat (Lauda-Königshofen, Germany) by a peristaltic pump Multifix constant MC 1000 FEC, Alfred Schwinherr KG (Schwäbisch-Gmünd, Germany), which fed continuously the thermostat with an irradiate solution at a flow rate of 100 mL min^{-1} to maintain the temperature of the system at $20 \pm 1 \text{ }^{\circ}\text{C}$ for constant reaction conditions. The solution was continuously mixed with a magnetic stirrer (Heidolph MR 1000, Schwabach, Germany) at 300 rpm. Before starting each new experiment, the whole experimental setup was cleaned twice by running pure water into the reactor for 10 minutes in order to remove any contaminant left from the previous experiment. Also the UV lamp was pre-heated by running it for 15 minutes before each new experiment.

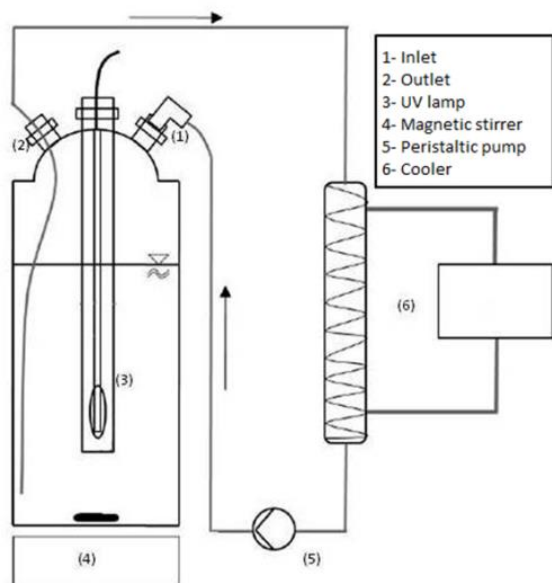


Figure 4.2 Scheme of the experimental set-up, namely of the UV photooxidation reactor.

4.4.6 Kinetic experiments

The photodegradability of the micropollutants was individually investigated under three different UV sources that cover UV-A, UV-B and UV-C emission range (see Figure 4.1). The reaction kinetic during micropollutant degradation by UV photolysis was modeled using the following equation:

$$\ln \frac{[c]_0}{[c]_t} = k_1 t \quad (\text{Eq.1})$$

Where k_1 [s^{-1}] is the time-based pseudo first-order rate constant for the direct photolysis of each compound; it can be obtained from the slope of a plot of $\ln ([c]_0/[c]_t)$ vs. reaction time for the direct photolysis. If $\ln ([c]_0/[c]_t)$ is plotted versus the UV dose [J cm^{-2}], one can obtain the corresponding direct photolysis fluence-based rate constant k'_1 [$\text{cm}^2 \text{J}^{-1}$] (Bolton and Stefan, 2002).

The quantum yield is a fundamental parameter that quantifies the photon efficiency of a photochemical reaction. According to Bolton and Stefan [33], the quantum yield Φ_c depends on the wavelength and can be determined from the fluence-based first-order rate constant:

$$\Phi_c = \frac{k'_1 \times 10 \times U_\lambda}{\varepsilon_c \ln(10)} \quad (\text{Eq.2})$$

Where U_λ is the energy of one mole of photons at wavelength λ in J Einstein^{-1} and ϵ_c is the molar absorption coefficient in $\text{M}^{-1}\text{cm}^{-1}$.

The UV dose required to degrade 90% of the micropollutants H'_{90} (mJ m^{-2}) through direct photolysis under UV-A, UV-B and UV-C irradiation was calculated using equation 3 as described by Bolton and Linden [34].

$$H'_{90} = \frac{10 \times U_\lambda}{\epsilon_c \times \Phi_c} \quad (\text{Eq.3})$$

4.5 Results and discussions

4.5.1 Occurrence of the micropollutants in the wastewater treatment plant effluent

The occurrence and fate of micropollutants in WWTP effluents has been recognized as one of the emerging issues in environmental chemistry [35]. Loos, et al. [19] identified 156 micropollutants in 90 European WWTPs. 125 of the micropollutants (80% of the target micropollutants) in European wastewater effluents were determined at concentrations ranging from ng L^{-1} to mg L^{-1} . Figure 4.3 presents as black boxplots the concentration range in which the investigated micropollutants were detected in the effluent of the wastewater treatment plant Duisburg-Hochfeld over a period of 4 months. The bars illustrate the variation in the substances' concentrations that can be due to the sampling on different days of the week and at different weather conditions (wet / dry). The grey boxplots present the data determined in other studies for the same type of substances [18, 19, 22, 36-61].

$3.1 \mu\text{g L}^{-1}$ and $3.0 \mu\text{g L}^{-1}$ represent the determined median concentration of diclofenac and metoprolol (see boxplots). These values corroborate the ones determined in a previous study performed in WWTPs in Germany [35, 36, 46]. Other countries reported lower concentrations [19, 37, 45, 62]. Carbamazepine and sulfamethoxazole were determined in median concentrations of $1.3 \mu\text{g L}^{-1}$ and $0.19 \mu\text{g L}^{-1}$. These values are similar to the ones observed in several other studies [19, 37, 45, 49, 50, 54, 62].

The determined median concentration of benzotriazole was $4.6 \mu\text{g L}^{-1}$, making it one of the most abundant emerging contaminants in the environment. In this study the WWTP effluents had a benzotriazole maximum concentration of $8.1 \mu\text{g L}^{-1}$ (see boxplots). The median concentration of benzotriazole in our WWTP effluent samples was lower than the ones proposed in other studies [58, 59, 61]. The high occurrence of benzotriazole in WWTPs is probably due to the wide use of this substance as a corrosion inhibitor (e.g., in engine coolants, antifreeze liquids, aircraft deicers, metal processing) and for silver protection in dishwashing detergents. Benzotriazoles also used in plastics, automobile parts, building

materials, paint, skin creams, and shampoos [63], which is believed to represent a major route for the contamination of the environment [55-57].

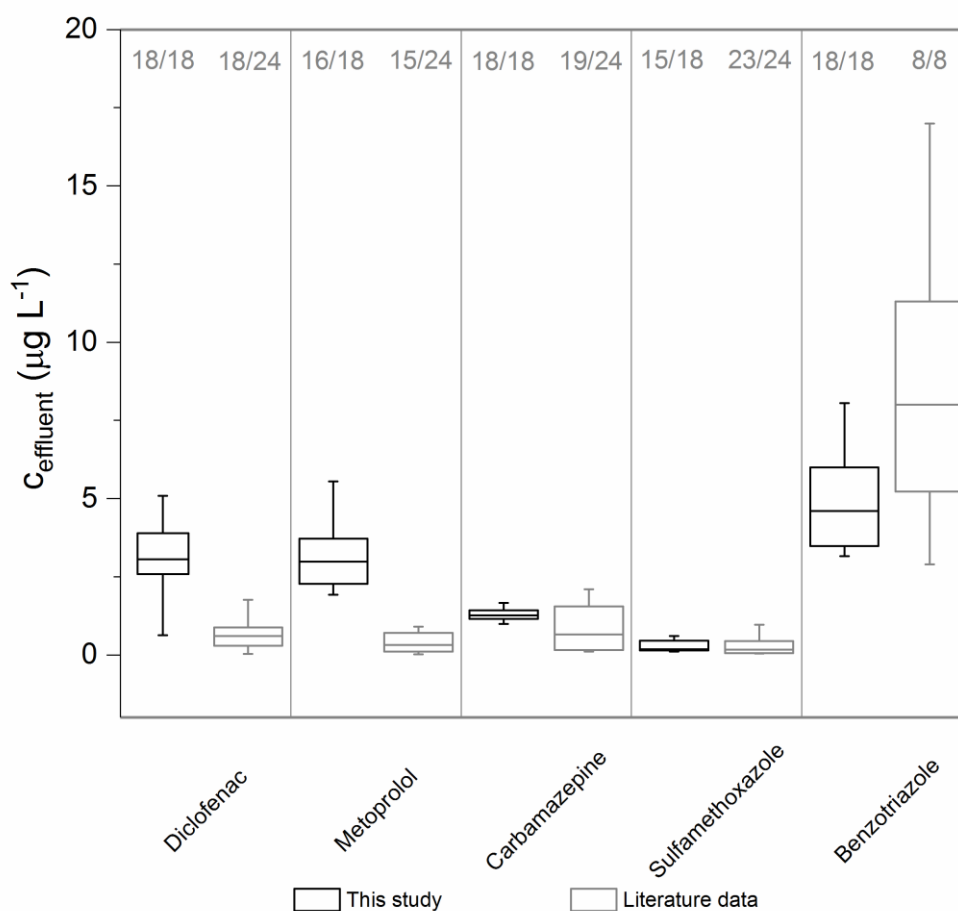


Figure 4.3 Boxplots (black) of the concentration of diclofenac, metoprolol, carbamazepine, sulfamethoxazole and benzotriazole in the studied effluent wastewater treatment plant at different days over a period of 4 months, compared to the values determined in previous studies (grey) in effluent wastewater treatment plants from Germany, Spain, Sweden, Switzerland, Italy, China, France, Taiwan, Canada, and USA [18, 19, 22, 36-61]. Data above each box denote the number of positive results and the number of studies considered (which are influenced by the limit of detection in the specific studies).

4.5.2 Photolysis of the micropollutants

Pseudo first-order degradation was observed for all investigated micropollutants under direct UV photolysis. The UV directs photolysis pseudo first-order rate constants k [s^{-1}], as well as the quantum yields Φ_c for the investigated compounds are given in Table 4.3

Diclofenac shows moderate degradation in the UV-A range, while carbamazepine, sulfamethoxazole, benzotriazole and metoprolol were hardly degraded by the UV-A irradiation. Under UV-B irradiation, diclofenac and sulfamethoxazole show fast photolytic

degradation. In comparison benzotriazole and carbamazepine were removed less than 10% and the photolytic degradation was negligible in the case of metoprolol. It is obvious that the UV-C lamp is very effective in the direct photodegradation of diclofenac and sulfamethoxazole, since they have the highest direct photolysis rate constants among all investigated micropollutants.

In the wastewater matrix the photolytic degradation of carbamazepine, benzotriazole and metoprolol seems to improve, probably due to the presence of photosensitizer compounds, which play an important role in natural photochemical degradation [64]. On the other hand, a decrease in the photolytic degradation of sulfamethoxazole and diclofenac was observed. According to von Sonntag [65] the photochemical degradation mechanisms can be divided into direct and indirect photolysis. In the case of direct photolysis, the absorption of radiation by the pollutants leads to photodegradation. While in the case of indirect photolysis various reactive intermediate oxidants such as singlet oxygen ($^1\text{O}_2$), hydroxyl radical ($\cdot\text{OH}$) and peroxy radicals ($\cdot\text{OOH}$) form as a result of phototransformation of photosensitizer compounds [64]. In this study we found that carbamazepine, benzotriazole and metoprolol can be eliminated by indirect photodegradation. More than 30% of carbamazepine, benzotriazole and metoprolol were removed under UV-B and UV-C irradiation.

The quantum yields for micropollutants degradation under irradiation with the three different types of UV lamps and all conditions have been calculated and are presented in Table 4.3. Quantum yields mean the number of molecules transformed (direct and indirect photooxidation) per photon absorbed, which is emitted by the radiation source to the surface of the sample (incident light). Many researchers have reported a very fast removal of diclofenac upon UV irradiation. Shu, et al. [30] reported that the quantum yield for diclofenac achieved by MP-UV (1 kW) was 0.035, while Wols and Hofman-Caris [66] found a quantum yield of 0.29 by LP-UV (120 W output UV-C 38 W). In our study a quantum yield of 0.01 and 0.007 were found for diclofenac under the UV-B (2.9 W) and UV-C (2.6 W) irradiation, respectively. Sulfamethoxazole also exhibits good degradability by direct photolysis under UV-B and UV-C irradiation. Quantum yields of 0.011 and 0.0037 were obtained in the case of sulfamethoxazole under the UV-B (2.9 W) and UV-C (2.6 W) irradiation, respectively. Benzotriazole shows a significant degradation by direct photolysis only under the UV-C irradiation, with quantum yields of 0.00026 and 0.00024 under the UV-B (2.9 W) and UV-C (2.6 W) irradiation, respectively. For carbamazepine quantum yields of 0.0011 and 0.00007 were achieved under the UV-B (2.9 W) and UV-C (2.6 W) irradiation, respectively. These values are comparable with the ones determined in previous research [30, 67]. Metoprolol

exhibited low quantum yields under the UV-B (2.9 W) and UV-C (2.6 W) irradiation. This is probably due to the fact that metoprolol absorbs at 225 nm, which is outside the range of the UV-B (2.9 W) and UV-C (2.6 W) lamps. The quantum yield is wavelength-dependent, so the disparity between the values determined in our study and the ones determined by other researchers is due to the distribution of the micropollutants absorption in the UV spectrum range, which is overlapping in different proportions with emitted spectrum range of the UV lamps. On the other hand, Carlson, et al. [68] have reported that the quantum yield for both 4-Nonylphenol and 4-tert-octylphenol are dependent on their initial concentration, which is decreasing as the concentration increases. Hessler, et al. [69] also reported similar trends; the quantum yields for photolysis of atrazine and metazachlor at 253.7 nm are a function of concentration. According to these previous research results we suppose that the quantum yields of the studied micropollutants are also dependent on their initial concentration.

Table 4.3 Kinetic data determined during the micropollutants' degradation experiments in the bench scale reactor under UV-A, UV-B and UV-C irradiation in deionized water and WWTP effluent (k = reaction constant, $t_{1/2}$ = half-life, repetition $n=3$, the standard deviations are given for the rate constants and the correlation coefficients of the plots are given in the brackets).

UV-A		Deionized water				WWTP effluent		
Substance	k [s^{-1}] / 10^{-5}	$t_{1/2}$ [min]	Quantum yield (Φ_c) / 10^{-4}	Removal % after 60 min	H'_{90} ($mJ\ m^{-2}$)	k [s^{-1}] / 10^{-5}	$t_{1/2}$ [min]	Removal % after 60 min
Diclofenac	15 ± 1.2 (0.96)	79	5.40	45	$2.4E+06$	37 ± 1.8 (0.96)	32	29
Metoprolol	0.41 ± 0.06 (0.94)	2800	0.76	2	$9.0E+07$	53 ± 2.3 (0.96)	22	36
Carbamazepine	0.95 ± 0.03 (0.93)	1200	0.15	4	$4.3E+06$	26 ± 2.1 (0.95)	45	38
Sulfamethoxazole	0.93 ± 0.04 (0.92)	1200	0.32	4	$4.0E+07$	11 ± 1.5 (0.98)	110	21
Benzotriazole	1.3 ± 0.3 (0.92)	860	0.78	5	$2.6E+07$	14 ± 1.3 (0.95)	82	24
UV-B		Deionized water				WWTP effluent		
Substance	k [s^{-1}] / 10^{-5}	$t_{1/2}$ [min]	Quantum yield (Φ_c) / 10^{-4}	Removal % after 60 min	H'_{90} ($mJ\ m^{-2}$)	k [s^{-1}] / 10^{-5}	$t_{1/2}$ [min]	Removal % after 60 min
Diclofenac	97 ± 4.1 (0.98)	12	100	97	$1.0E+05$	23 ± 1.8 (0.93)	51	36
Metoprolol	0.74 ± 0.07 (0.91)	1600	0.34	3	$1.5E+07$	4.5 ± 0.2 (0.91)	250	40
Carbamazepine	2.8 ± 0.05 (0.95)	420	1.10	10	$3.5E+06$	1400 ± 23 (0.88)	0.8	99
Sulfamethoxazole	81 ± 3.6 (0.98)	14	110	96	$1.2E+05$	7.1 ± 0.4 (0.93)	160	35
Benzotriazole	1.6 ± 0.2 (0.97)	710	2.6	6	$6.0E+06$	66 ± 2.2 (0.96)	17	35

Substance	Deionized water					WWTP effluent		
	$k [s^{-1}] / 10^5$	$t_{1/2} [min]$	Quantum yield (Φ_c) / 10^{-4}	Removal % after 60 min	$H'_{90} (mJ m^{-2})$	$k [s^{-1}] / 10^{-5}$	$t_{1/2} [min]$	Removal % after 60 min
Diclofenac	120 ± 3.3 (1.00)	9	71	99	$3.8E+04$	36 ± 4.0 (0.82)	32	34
Metoprolol	1.4 ± 0.03 (0.89)	840	16	5	$3.5E+06$	69 ± 5.2 (0.81)	17	62
Carbamazepine	1.8 ± 0.09 (0.79)	640	0.73	8	$2.5E+06$	83 ± 4.8 (0.93)	14	95
Sulfamethoxazole	170 ± 3.5 (0.96)	7	37	99	$2.5E+04$	10 ± 1.2 (0.84)	110	34
Benzotriazole	9.7 ± 0.2 (0.97)	120	2.4	31	$4.7E+05$	11 ± 0.7 (0.90)	100	33

The UV dose required to degrade 90% of the micropollutants H'_{90} through direct photolysis under UV-A, UV-B and UV-C irradiation are present in Table 4.3.

The UV dose required to reduce 90% of sulfamethoxazole and diclofenac concentrations in water by one order of magnitude is in the range of $1.0 \times 10^4 - 1.0 \times 10^5 \text{ mJ cm}^{-2}$. In comparison, Bolton and Stefan [33] and Carlson, et al. [68] reported that the UV-C fluence required to remove 90% of N-nitrosodimethylamine and sulfamethoxazole from water are approximately 1000 and 780 mJ cm^{-2} , respectively. These results are consistent somewhat with our results, since the start concentrations of N-nitrosodimethylamine and sulfamethoxazole ($10 \sim 100 \mu\text{g L}^{-1}$) are about 10 to 100 factor lower than the micropollutant concentrations used in our study, namely $1000 \mu\text{g L}^{-1}$.

The present investigation proves the effectiveness of direct photolysis in the degradation of diclofenac and sulfamethoxazole. On the other hand, direct photolysis has less effect on carbamazepine and benzotriazole degradation, and negligible effect on metoprolol degradation.

4.6 Acknowledgement

The authors wish to thank Dr. Andriy Kuklya and Dr. Klaus Kerpen for supporting this study by measuring the UV lamps spectra.

4.7 References

- [1] S.D. Richardson, S.Y. Kimura, Water analysis: Emerging contaminants and current issues, *Anal. Chem.*, 88 (2016) 546-582.
- [2] B. Petrie, R. Barden, B. Kasprzyk-Hordern, A review on emerging contaminants in wastewaters and the environment: Current knowledge, understudied areas and recommendations for future monitoring, *Water Res.*, 72 (2015) 3-27.

- [3] R. Moreno-González, S. Rodríguez-Mozaz, M. Gros, D. Barceló, V.M. León, Seasonal distribution of pharmaceuticals in marine water and sediment from a mediterranean coastal lagoon (SE Spain), *Environ. Res.*, 138 (2015) 326-344.
- [4] C. Postigo, D. Barceló, Synthetic organic compounds and their transformation products in groundwater: Occurrence, fate and mitigation, *Sci. Total. Environ.*, 503-504 (2015) 32-47.
- [5] R. López-Serna, A. Jurado, E. Vázquez-Suñé, J. Carrera, M. Petrović, D. Barceló, Occurrence of 95 pharmaceuticals and transformation products in urban groundwaters underlying the metropolis of Barcelona, Spain, *Environ. Pollut.*, 174 (2013) 305-315.
- [6] D.J. Lapworth, N. Baran, M.E. Stuart, R.S. Ward, Emerging organic contaminants in groundwater: A review of sources, fate and occurrence, *Environ. Pollut.*, 163 (2012) 287-303.
- [7] C. Postigo, S.D. Richardson, Transformation of pharmaceuticals during oxidation/disinfection processes in drinking water treatment, *J. Hazard. Mater.*, 279 (2014) 461-475.
- [8] V. Acuña, D. von Schiller, M.J. García-Galán, S. Rodríguez-Mozaz, L. Corominas, M. Petrović, M. Poch, D. Barceló, S. Sabater, Occurrence and in-stream attenuation of wastewater-derived pharmaceuticals in Iberian rivers, *Sci. Total. Environ.*, 503-504 (2015) 133-141.
- [9] K. Kümmerer, The presence of pharmaceuticals in the environment due to human use-present knowledge and future challenges, *J. Environ. Manage.*, 90 (2009) 2354-2366.
- [10] E. Carmona, V. Andreu, Y. Picó, Occurrence of acidic pharmaceuticals and personal care products in Turia river basin: From waste to drinking water, *Sci. Total. Environ.*, 484 (2014) 53-63.
- [11] R. Loos, R. Carvalho, A.D. C., S. Comero, G. Locoro, S. Tavazzi, B. Paracchini, M. Ghiani, T. Lettieri, L. Blaha, B. Jarosova, S. Voorspoels, K. Servaes, P. Haglund, J. Fick, R.H. Lindberg, D. Schwesig, B.M. Gawlik, EU-wide monitoring survey on emerging polar organic contaminants in wastewater treatment plant effluents, *Water Res.*, 47 (2013) 6475-6487.

- [12] F. Sacher, F.T. Lange, H.J. Brauch, I. Blankenhorn, Pharmaceuticals in groundwaters analytical methods and results of a monitoring program in Baden-Württemberg, Germany, *J. Chromatogr. A*, 938 (2001) 199-210.
- [13] A. Jurado, E. Vázquez-Suñé, J. Carrera, M. López de Alda, E. Pujades, D. Barceló, Emerging organic contaminants in groundwater in Spain: a review of sources, recent occurrence and fate in a European context, *Sci. Total. Environ.*, 440 (2012) 82-94.
- [14] J.L. Oaks, M. Gilbert, M.Z. Virani, R.T. Watson, C.U. Meteyer, B.A. Rideout, H.L. Shivaprasad, S. Ahmed, M.J. Iqbal Chaudhry, M. Arshad, S. Mahmood, A. Ali, A. Ahmed Khan, Diclofenac residues as the cause of vulture population decline in Pakistan, *Nature*, 427 (2004) 630-633.
- [15] P.M. Bradley, L.B. Barber, J.W. Duris, W.T. Foreman, E.T. Furlong, L.E. Hubbard, K.J. Hutchinson, S.H. Keefe, D.W. Kolpin, Riverbank filtration potential of pharmaceuticals in a wastewater-impacted stream, *Environ. Pollut.*, 193 (2014) 173-180.
- [16] M. Barbieri, T. Licha, K. Nödler, J. Carrera, C. Ayora, X. Sanchez-Vila, Fate of beta-blockers in aquifer material under nitrate reducing conditions: Batch experiments, *Chemosphere*, 89 (2012) 1272-1277.
- [17] J. Maszkowska, S. Stolte, J. Kumirska, P. Lukaszewicz, K. Mioduszevska, A. Puckowski, M. Caban, M. Wagil, P. Stepnowski, A. Białk-Bielińska, Beta-blockers in the environment: Part I. Mobility and hydrolysis study, *Sci. Total. Environ.*, 493 (2014) 1112-1121.
- [18] R. López-Serna, S. Perez, A. Ginebreda, M. Petrovic, D. Barceló, Fully automated determination of 74 pharmaceuticals in environmental and waste waters by online solid phase extraction-liquid chromatography-electrospray-tandem mass spectrometry, *Talanta*, 83 (2010) 410-424.
- [19] R. Loos, B.M. Gawlik, G. Locoro, E. Rimaviciute, S. Contini, G. Bidoglio, EU-wide survey of polar organic persistent pollutants in European river waters, *Environ. Pollut.*, 157 (2009) 561-568.
- [20] A. Bergmann, R. Fohrmann, F.A. Weber, Zusammenstellung von Monitoringdaten zu Umweltkonzentrationen von Arzneimitteln, Umweltbundesamt, Germany, 2011, pp. 108.

- [21] U. Hubner, U. von Gunten, M. Jekel, Evaluation of the persistence of transformation products from ozonation of trace organic compounds - A critical review, *Water Res.*, 68 (2015) 150-170.
- [22] R. Rosal, A. Rodríguez, J.A. Perdígón Melón, A. Petre, E. García-Calvo, M.J. Gomez, A. Agüera, A.R. Fernández-Alba, Occurrence of emerging pollutants in urban wastewater and their removal through biological treatment followed by ozonation, *Water Res.*, 44 (2010) 578-588.
- [23] V.J. Pereira, K.G. Linden, H.S. Weinberg, Evaluation of UV irradiation for photolytic and oxidative degradation of pharmaceutical compounds in water, *Water Res.*, 41 (2007) 4413-4423.
- [24] S.R. Batchu, V.R. Panditi, K.E. O'Shea, P.R. Gardinali, Photodegradation of antibiotics under simulated solar radiation: Implications for their environmental fate, *Sci. Total. Environ.*, 470-471 (2014) 299-310.
- [25] V. Romero, F. Méndez-Arriaga, P. Marco, J. Giménez, S. Esplugas, Comparing the photocatalytic oxidation of metoprolol in a solarbox and a solar pilot plant reactor, *Chem. Eng. J.*, 254 (2014) 17-29.
- [26] S. Canonica, L. Meunier, U. von Gunten, Phototransformation of selected pharmaceuticals during UV treatment of drinking water, *Water Res.*, 42 (2008) 121-128.
- [27] M. Sturini, A. Speltini, F. Maraschi, L. Pretali, A. Profumo, E. Fasani, A. Albini, R. Migliavacca, E. Nucleo, Photodegradation of fluoroquinolones in surface water and antimicrobial activity of the photoproducts, *Water Res.*, 46 (2012) 5575-5582.
- [28] M.M. Dong, R. Trenholm, F.L. Rosario-Ortiz, Photochemical degradation of atenolol, carbamazepine, meprobamate, phenytoin and primidone in wastewater effluents, *J. Hazard. Mater.*, 282 (2015) 216-223.
- [29] C. Baeza, D.R. Knappe, Transformation kinetics of biochemically active compounds in low-pressure UV photolysis and UV/H₂O₂ advanced oxidation processes, *Water Res.*, 45 (2011) 4531-4543.

- [30] Z. Shu, J.R. Bolton, M. Belosevic, M.G. El Din, Photodegradation of emerging micropollutants using the medium-pressure UV/H₂O₂ advanced oxidation process, *Water Res.*, 47 (2013) 2881-2889.
- [31] A. Salma, H.V. Lutze, T.C. Schmidt, J. Tuerk, Photolytic degradation of the beta-blocker nebivolol in aqueous solution, *Water Res.*, 116 (2017) 211-219.
- [32] Chemspider, Molecular Structures, <http://www.chemspider.com/Chemical-Structure.64421.html>, 2017, (last accessed, Mar 20, 2017).
- [33] J.R. Bolton, M.I. Stefan, Fundamental photochemical approach to the concepts of fluence (UV dose) and electrical energy efficiency in photochemical degradation reactions, *Res. Chem. Intermed.*, 28 (2002) 857-870.
- [34] J. Bolton, K. Linden, Standardization of methods for fluence (UV Dose) determination in bench-scale UV experiments, *J. Environ. Eng.*, 129 (2003) 209-215.
- [35] T. Heberer, Occurrence, fate, and removal of pharmaceutical residues in the aquatic environment: a review of recent research data, *Toxicol. Lett.*, 131 (2002) 5-17.
- [36] M.J. Hilton, K.V. Thomas, Determination of selected human pharmaceutical compounds in effluent and surface water samples by high-performance liquid chromatography-electrospray tandem mass spectrometry, *J. Chromatogr. A*, 1015 (2003) 129-141.
- [37] D. Bendz, N.A. Paxéus, T.R. Ginn, F.J. Loge, Occurrence and fate of pharmaceutically active compounds in the environment, a case study: Höje River in Sweden, *J. Hazard. Mater.*, 122 (2005) 195-204.
- [38] T.A. Ternes, Analytical methods for the determination of pharmaceuticals in aqueous environmental samples, *Trends Anal. Chem.*, 20 (2001) 419-434.
- [39] M. Gros, M. Petrović, D. Barceló, Tracing pharmaceutical residues of different therapeutic classes in environmental waters by using liquid chromatography/quadrupole-linear ion trap mass spectrometry and automated library searching, *Anal. Chem.*, 81 (2009) 898-912.
- [40] A.Y. Lin, T.H. Yu, S.K. Lateef, Removal of pharmaceuticals in secondary wastewater treatment processes in Taiwan, *J. Hazard. Mater.*, 167 (2009) 1163-1169.

- [41] J. Radjenovic', M. Petrovic', D. Barceló, Fate and distribution of pharmaceuticals in wastewater and sewage sludge of the conventional activated sludge (CAS) and advanced membrane bioreactor (MBR) treatment, *Water Res.*, 43 (2009) 831-841.
- [42] T. Deblonde, C. Cossu-Leguille, P. Hartemann, Emerging pollutants in wastewater: a review of the literature, *Int. J. Hyg. Environ. Health.*, 214 (2011) 442-448.
- [43] W.J. Sim, J.W. Lee, E.S. Lee, S.K. Shin, S.R. Hwang, J.E. Oh, Occurrence and distribution of pharmaceuticals in wastewater from households, livestock farms, hospitals and pharmaceutical manufactures, *Chemosphere*, 82 (2011) 179-186.
- [44] E. Gracia-Lor, J.V. Sancho, R. Serrano, F. Hernández, Occurrence and removal of pharmaceuticals in wastewater treatment plants at the Spanish Mediterranean area of Valencia, *Chemosphere*, 87 (2012) 453-462.
- [45] Y. Luo, W. Guo, H.H. Ngo, L.D. Nghiem, F.I. Hai, J. Zhang, S. Liang, X.C. Wang, A review on the occurrence of micropollutants in the aquatic environment and their fate and removal during wastewater treatment, *Sci. Total. Environ.*, 473-474 (2014) 619-641.
- [46] T.A. Ternes, Occurrence of drugs in German sewage treatment plants and rivers, *Water Res.*, 32 (1998) 3245-3260.
- [47] P.A. Lara-Martín, E. González-Mazo, M. Petrovic, D. Barceló, B.J. Brownawell, Occurrence, distribution and partitioning of nonionic surfactants and pharmaceuticals in the urbanized Long Island Sound Estuary (NY), *Mar. Pollut. Bull.*, 85 (2014) 710-719.
- [48] K.D. Brown, J. Kulis, B. Thomson, T.H. Chapman, D.B. Mawhinney, Occurrence of antibiotics in hospital, residential, and dairy effluent, municipal wastewater, and the Rio Grande in New Mexico, *Sci. Total. Environ.*, 366 (2006) 772-783.
- [49] M. Al Aukidy, P. Verlicchi, A. Jelic, M. Petrovic, D. Barcelò, Monitoring release of pharmaceutical compounds: Occurrence and environmental risk assessment of two WWTP effluents and their receiving bodies in the Po Valley, Italy, *Sci. Total. Environ.*, 438 (2012) 15-25.
- [50] T.H. Fang, F.H. Nan, T.S. Chin, H.M. Feng, The occurrence and distribution of pharmaceutical compounds in the effluents of a major sewage treatment plant in Northern Taiwan and the receiving coastal waters, *Mar. Pollut. Bull.*, 64 (2012) 1435-1444.

- [51] A. Wick, G. Fink, A. Joss, H. Siegrist, T.A. Ternes, Fate of beta blockers and psychoactive drugs in conventional wastewater treatment, *Water Res.*, 43 (2009) 1060-1074.
- [52] K. Nödler, O. Hillebrand, K. Idzik, M. Strathmann, F. Schiperski, J. Zirlewagen, T. Licha, Occurrence and fate of the angiotensin II receptor antagonist transformation product valsartan acid in the water cycle - A comparative study with selected beta-blockers and the persistent anthropogenic wastewater indicators carbamazepine and acesulfame, *Water Res.*, 47 (2013) 6650-6659.
- [53] C. Miège, M. Favier, C. Brosse, J.P. Canler, M. Coquery, Occurrence of betablockers in effluents of wastewater treatment plants from the Lyon area (France) and risk assessment for the downstream rivers, *Talanta*, 70 (2006) 739-744.
- [54] S. Rodriguez-Mozaz, S. Chamorro, E. Marti, B. Huerta, M. Gros, A. Sanchez-Melsio, C.M. Borrego, D. Barceló, J.L. Balcázar, Occurrence of antibiotics and antibiotic resistance genes in hospital and urban wastewaters and their impact on the receiving river, *Water Res.*, 69 (2015) 234-242.
- [55] Y.S. Liu, G.G. Ying, A. Shareef, R.S. Kookana, Occurrence and removal of benzotriazoles and ultraviolet filters in a municipal wastewater treatment plant, *Environ. Pollut.*, 165 (2012) 225-232.
- [56] W. Giger, C. Schaffner, H.P.E. Kohler, Benzotriazole and tolyltriazole as aquatic contaminants. 1. Input and occurrence in rivers and lakes, *Environ. Sci. Technol.*, 40 (2006) 7186-7192.
- [57] D. Voutsas, P. Hartmann, C. Schaffner, W. Giger, Benzotriazoles, alkylphenols and bisphenol A in municipal wastewaters and in the Glatt river, Switzerland, *Environ. Sci. Pollut. Res. Int.*, 13 (2006) 333-341.
- [58] S. Weiss, T. Reemtsma, Determination of benzotriazole corrosion inhibitors from aqueous environmental samples by liquid chromatography-electrospray ionization-tandem mass spectrometry, *Anal. Chem.*, 77 (2005) 7415-7420.
- [59] T. Reemtsma, U. Miehe, U. Duennbier, M. Jekel, Polar pollutants in municipal wastewater and the water cycle: Occurrence and removal of benzotriazoles, *Water Res.*, 44 (2010) 596-604.

- [60] T. Reemtsma, S. Weiss, J. Mueller, M. Petrovic, S. González, D. Barcelo, F. Ventura, T.P. Knepper, Polar pollutants entry into the water cycle by municipal wastewater: A european perspective, *Environ. Sci. Technol.*, 40 (2006) 5451-5458.
- [61] J.A. van Leerdam, A.C. Hogenboom, M.M.E. van der Kooi, P. de Voogt, Determination of polar 1H-benzotriazoles and benzothiazoles in water by solid-phase extraction and liquid chromatography LTQ FT Orbitrap mass spectrometry, *Int. J. Mass Spectrom.*, 282 (2009) 99-107.
- [62] A.Y. Lin, Y.T. Tsai, Occurrence of pharmaceuticals in Taiwan's surface waters: Impact of waste streams from hospitals and pharmaceutical production facilities, *Sci. Total. Environ.*, 407 (2009) 3793-3802.
- [63] M.D. Alotaibi, A.J. McKinley, B.M. Patterson, A.Y. Reeder, Benzotriazoles in the aquatic environment: A review of their occurrence, toxicity, degradation and analysis, *Water, Air, Soil Pollut.*, 226 (2015) 226.
- [64] E. Lee, H.K. Shon, J. Cho, Role of wetland organic matters as photosensitizer for degradation of micropollutants and metabolites, *J. Hazard. Mater.*, 276 (2014) 1-9.
- [65] C. von Sonntag, Advanced oxidation processes: Mechanistic aspects, *Water Sci. Technol.*, 58 (2008) 1015-1021.
- [66] B.A. Wols, C.H.M. Hofman-Caris, Review of photochemical reaction constants of organic micropollutants required for UV advanced oxidation processes in water, *Water Res.*, 46 (2012) 2815-2827.
- [67] B.A. Wols, C.H. Hofman-Caris, D.J. Harmsen, E.F. Beerendonk, Degradation of 40 selected pharmaceuticals by UV/H₂O₂, *Water Res.*, 47 (2013) 5876-5888.
- [68] J.C. Carlson, M.I. Stefan, J.M. Parnis, C.D. Metcalfe, Direct UV photolysis of selected pharmaceuticals, personal care products and endocrine disruptors in aqueous solution, *Water Res.*, 84 (2015) 350-361.
- [69] D.P. Hessler, V. Gorenflo, F.H. Frimmel, Degradation of aqueous atrazine and metazachlor solutions by UV and UV/H₂O₂ — Influence of pH and herbicide concentration, *Acta Hydrochim. Hydrobiol.*, 21 (1993) 209-214.

5 General conclusions and outlook

The photodegradation process of several micropollutants under different conditions and in different matrices was investigated in this thesis, including reaction kinetics and mechanisms. The analytical method developed for these studies, based on liquid chromatography coupled to tandem mass spectrometry (LC-MS/MS), to measure the selected compounds in wastewater treatment plants, and to follow their photolytic degradation rates proved to be very efficient to investigate the degradation of the studied micropollutants.

The study showed that the photodegradation of the studied micropollutants obeyed pseudo-first-order reaction kinetics and that the photodegradation process can be influenced by the choice of the UV source (here UV-A, UV-B and UV-C), the matrix (here pure water, pure water in the presence of $\cdot\text{OH}$ scavenger and in wastewater) in which the process takes place, as well as the matrix's pH. New knowledge was gained regarding the combination of the photodegradation process with the matrix effect. These results show that different UV sources as well as the matrix conditions have a high impact on the result of the photodegradation. This confirmed some of the knowledge already reported in literature for other processes and compounds [1-4]. However, the role of UV sources is worthwhile as reported here. Therefore, by knowing the fluence rate of the photoreactor and the degradation rate of the micropollutants, practitioners can easily design an efficient photolysis system that will achieve an acceptable level of trace micropollutant degradation. It is necessary to emphasize the fact that the absorbance spectrum of the micropollutant affects the choice of the most effective UV radiation source for its degradation. This is the one for which the emission spectrum shows the maximal overlapping with the absorbance spectrum of the micropollutant. Additionally, the UV lamps should have a sufficient photon flux and appropriate geometry for successful photoreactor design. The mechanisms of the photochemical degradation of the micropollutants can be mainly divided into direct and indirect photolysis. The principle of direct photolysis is the direct light absorption by the specific compound. In the case of indirect photolysis, photosensitizers play an important role in the phototransformation of the micropollutants, which takes place via reactions with reactive oxygen species (ROS), e.g. $\cdot\text{OH}$ [5] and singlet oxygen ($^1\text{O}_2$), [6, 7] formed in the primary photochemical reactions [8]. Also the matrix can play a dual role of sensitizer and quencher for the reactive species, which is important for the elimination mechanism of micropollutants in the environment. The co-existence of other constituents, as the ones present in wastewater treatment plants effluents (WWTPs), may influence the elimination of the micropollutants, since water constituents such

as the dissolved organic matter (DOM) and the bicarbonate ion (HCO_3^-) may scavenge the reactive oxygen species ($\cdot\text{OH}$, $^1\text{O}_2$). With regard to photolysis, the different species of micropollutant might have various photolytic degradation pathways, transformation products and reaction kinetics. Therefore, modifying the pH leads to structural changes that could enhance or hamper the photolytic reactions.

In this study the degradation by direct photolysis of the micropollutants was successful at lab scale; the effectiveness of the method should be tested also at pilot scale.

It is important to underline the fact that knowledge on the TPs is still very limited in general and especially when it comes to assessment and prediction of their formation during the photodegradation. Two different types of high resolution mass spectrometer were used to identify the TPs of the photodegradation for each of CIP and NEB. The LC-QTOF-MS was applied to identify the CIP transformation products. While the LC-Orbitrap-MS was used to identify the NEB transformation products. Both techniques have particularly shown excellent detection and identification capabilities for TPs in various matrices based on high resolution accurate mass measurement of precursor and product ions.

Even though HR-MS, like the LC-QTOF-MS which provides high mass resolution accuracy can provide exact masses and mass fragments that lead to the identification of TPs, it is not sufficient to confirm chemical structures. High purity and isolated analytical standards are needed for confirmation either by MS or other analytical methods like NMR, raman or infrared spectroscopy. In the case where no analytical standards are available and only MS spectra are obtained, the TPs are “tentative identified”. Therefore, the degradation study of CIP proved the effectiveness of using deuterated compounds, in this case deuterated ciprofloxacin, in identifying the transformation product structures.

During the degradation study of NEB it was observed that the biologically active part of the NEB's structure is still preserved in its transformation products. This illustrates the importance of coupling the studies on the kinetics of micropollutant degradation with mechanistic studies in order to evaluate if the advanced oxidation process can deactivate the biological effectiveness of the compound and also of its transformation products.

This research has led to many questions in need of further investigation. In order to fill this gap, future photooxidation studies should focus on ecotoxicity assessment and genotoxic effects of micropollutants and their transformation products especially on higher organisms such as plankton and fish.

A cost-benefit analysis of photolysis and photocatalysis should be carried out and results compared with other AOPs [9, 10]. The use of light-emitting diodes (LEDs) as radiation

source should be studied, possibly emerging as a new technology with lower energy consumption, longer lifetime, and cheaper than fluorescent lamp sources [11, 12].

5.1 References

- [1] X. Van Doorslaer, K. Demeestere, P.M. Heynderickx, H. Van Langenhove, J. Dewulf, UV-A and UV-C induced photolytic and photocatalytic degradation of aqueous ciprofloxacin and moxifloxacin: Reaction kinetics and role of adsorption, *Appl. Catal. B*, 101 (2011) 540-547.
- [2] B.A. Wols, C.H.M. Hofman-Caris, Review of photochemical reaction constants of organic micropollutants required for UV advanced oxidation processes in water, *Water Res.*, 46 (2012) 2815-2827.
- [3] Y. Lester, I. Ferrer, E.M. Thurman, K.G. Linden, Demonstrating sucralose as a monitor of full-scale UV/AOP treatment of trace organic compounds, *J. Hazard. Mater.*, 280 (2014) 104-110.
- [4] Y. Lester, H. Mamane, D. Avisar, Enhanced removal of micropollutants from groundwater, using pH modification coupled with photolysis, *Water, Air, Soil Pollut.*, 223 (2012) 1639-1647.
- [5] P.P. Vaughan, N.V. Blough, Photochemical formation of hydroxyl radical by constituents of natural waters, *Environ. Sci. Technol.*, 32 (1998) 2947-2953.
- [6] A.L. Boreen, W.A. Arnold, K. McNeill, Photodegradation of pharmaceuticals in the aquatic environment: A review, *Aquat. Sci.*, 65 (2003) 320-341.
- [7] D.E. Latch, K. McNeill, Microheterogeneity of singlet oxygen distributions in irradiated humic acid solutions, *Science*, 311 (2006) 1743-1747.
- [8] P.L. Miller, Y.P. Chin, Indirect photolysis promoted by natural and engineered wetland water constituents: Processes leading to alachlor degradation, *Environ. Sci. Technol.*, 39 (2005) 4454-4462.
- [9] R.J. Braham, A.T. Harris, Review of major design and scale-up considerations for solar photocatalytic reactors, *Ind. Eng. Chem. Res.*, 48 (2009) 8890-8905.

[10] A. Durán, J.M. Monteagudo, I. San Martín, Photocatalytic treatment of an industrial effluent using artificial and solar UV radiation: an operational cost study on a pilot plant scale, *J. Environ. Manage.*, 98 (2012) 1-4.

[11] W.K. Jo, R.J. Tayade, New generation energy-efficient light source for photocatalysis: LEDs for environmental applications, *Ind. Eng. Chem. Res.*, 53 (2014) 2073-2084.

[12] M. Izadifard, G. Achari, C. Langford, Application of photocatalysts and led light sources in drinking water treatment, *Catalysts*, 3 (2013) 726.

6 Appendix

6.1 Supplementary material of chapter 2

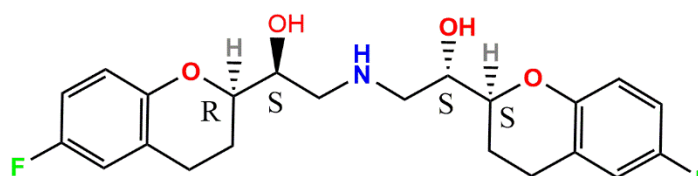
Suppl. 6.1 Physical and chemical properties of nebivolol.

Molecular weight (g mol⁻¹) 405.4

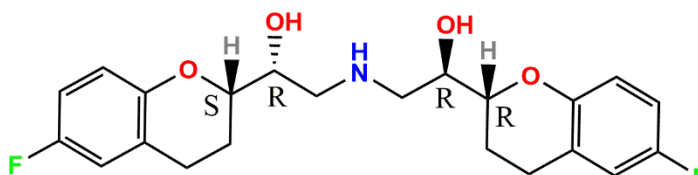
Solubility in water (mg L⁻¹) 83.99

pKa 8.65

Chemical structure of [S3R]-
nebivolol and [R3S]-nebivolol.



L (-) - Nebivolol



D (+) - Nebivolol

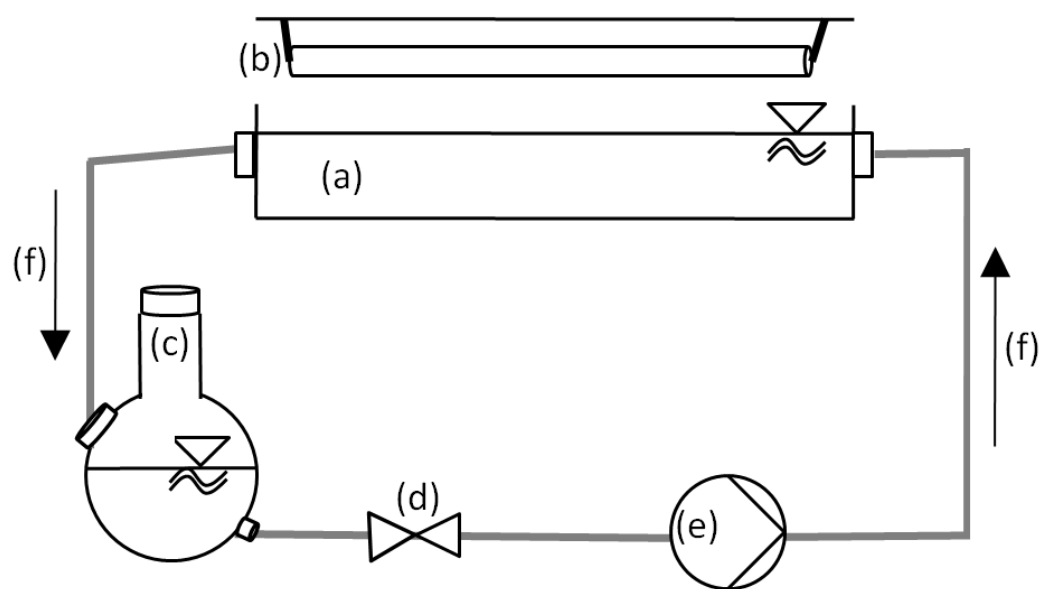
Sum formula

C₂₂H₂₅F₂NO₄

Degradation kinetics

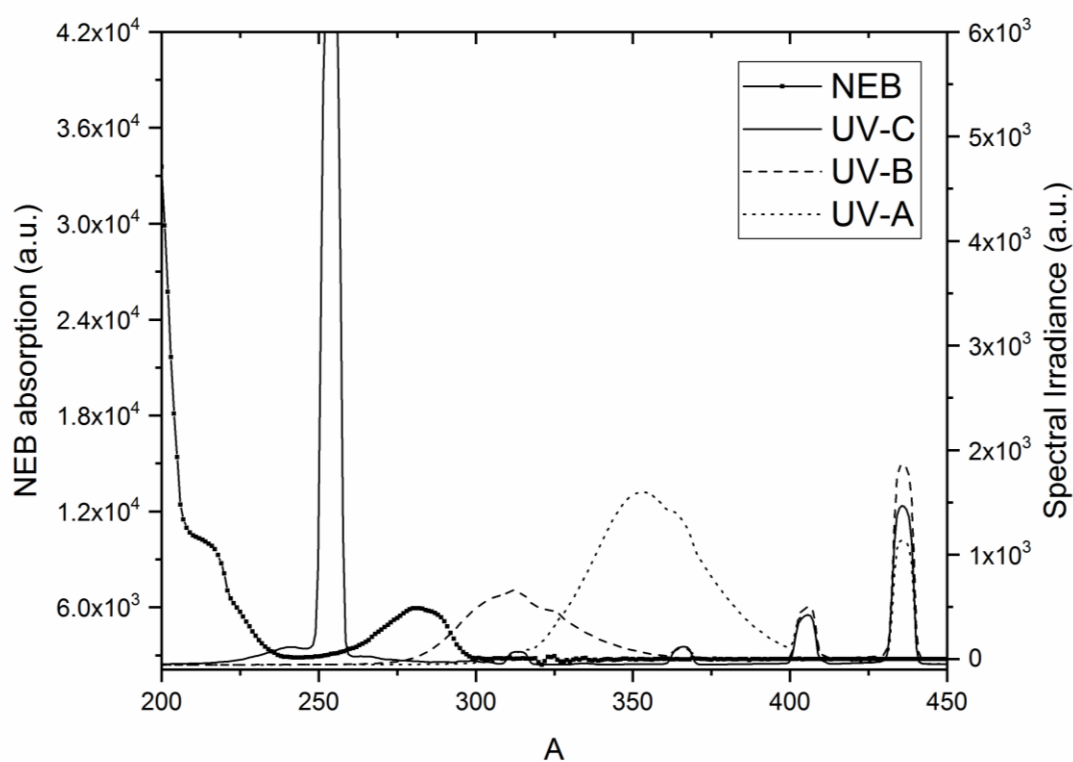
Influence of the UV source on the photodegradation of NEB

Suppl. 6.2 Experimental set up of the lab scale plant: (a) pyrex reactor, (b) UV sources, (c) reservoir, (d) sampling point, (e) peristaltic pump, (f) flow direction (dimensions are not to scale).



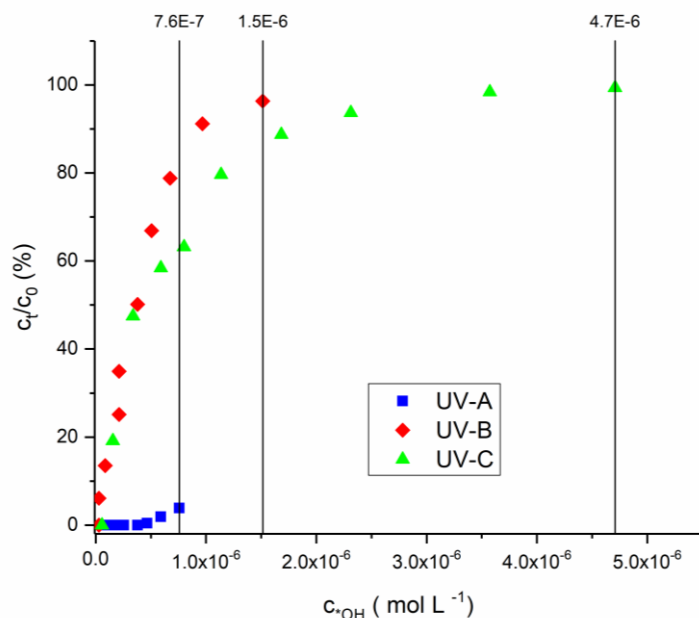
Suppl. 6.3 shows the overlap between Nebivolol's absorption and the three UV lamps' emission spectra, namely a 15 W medium-pressure mercury lamp emitting light at 315–400 nm (UV-A range), a 15 W medium-pressure mercury lamp emitting light at 280–360 nm (UV-B range) and a 15 W low-pressure mercury lamp emitting light at 254 nm (UV-C range). NEB absorbs light between 243 nm and 302 nm with the highest absorbance at 281 nm. In contrast to the UV-B and UV-C lamp, there is no overlap between the emission spectrum of the UV-A lamp and the absorption spectrum of NEB.

Suppl. 6.3 Absorption spectrum of nebivolol (primary Y-axis) overlaid with the normalized emission spectra of the three investigated UV lamps.

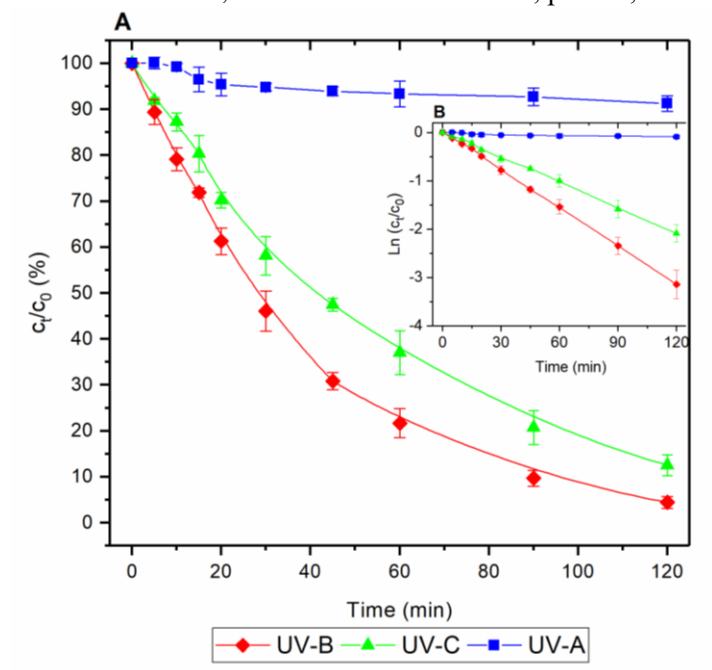


Influence of the OH radical scavenger on the degradation of NEB

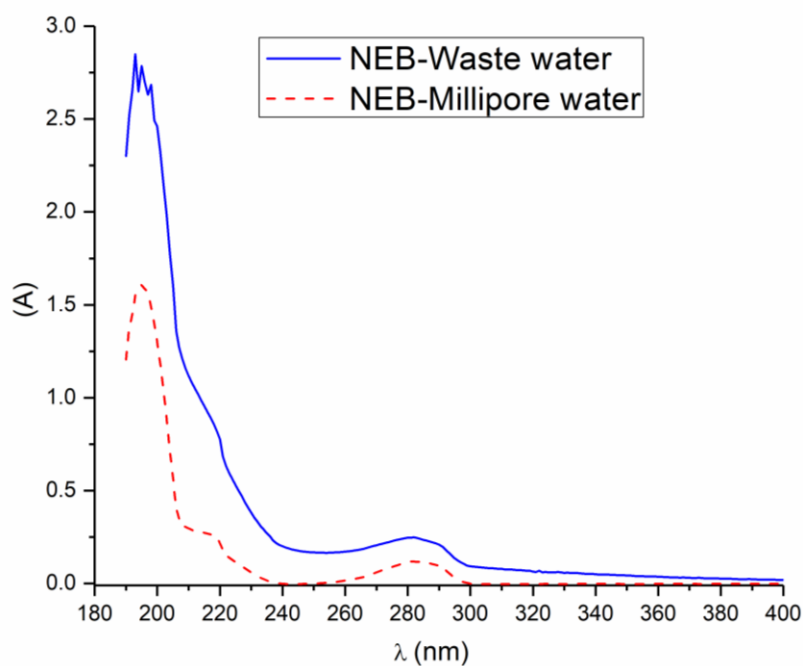
Suppl. 6.4 Plot of the elimination rate of Nebivolol versus the OH radical products during the UV irradiation.



Suppl. 6.5 (A) Nebivolol degradation, inset: (B) Linear plots of $\ln(c/c_0)$ versus time of nebivolol degradation in the presence of the wastewater matrix, (Experimental conditions: $c_0 = 25 \mu\text{mol L}^{-1}$, volume = 500 mL, flow rate = 100 mL min^{-1} , pH = 7, $T = 20 \pm 2 \text{ }^\circ\text{C}$).



Suppl. 6.6 UV absorption spectrum of nebivolol in Milipore water and in wastewater (Experimental conditions: c_0 (NEB) = $25 \mu\text{mol L}^{-1}$, pH = 7, $T = 20 \pm 2 \text{ }^\circ\text{C}$).



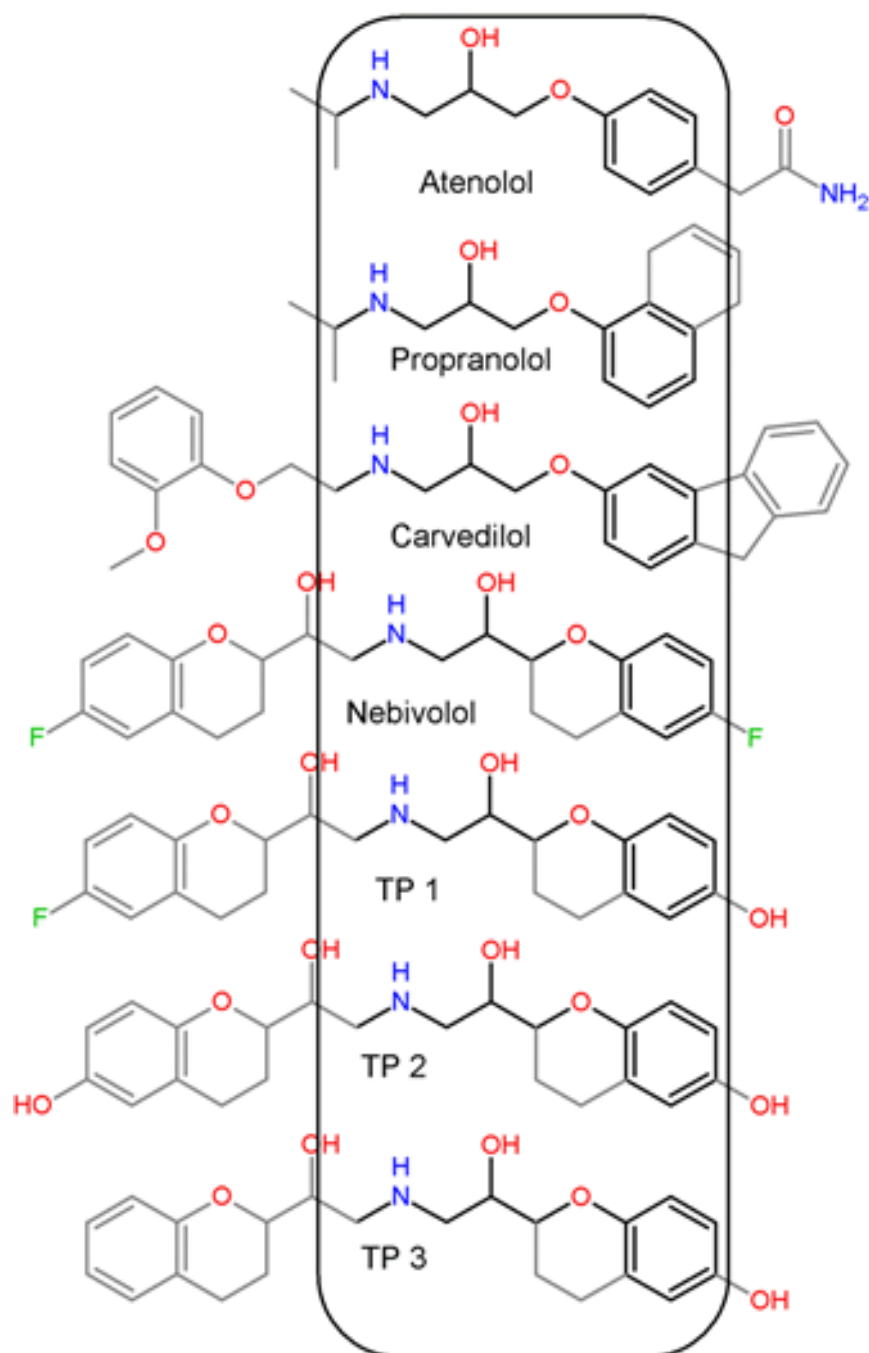
Kinetic experiments

Suppl. 6.7 Summary of kinetic parameters of neбиволол degradation.

UV	k (s ⁻¹)			Half life (min)			Elimination % after 2 h		
	NEB	NEB + t-BuOH	NEB in WWTP matrix	NEB	NEB + t-BuOH	NEB in WWTP matrix	NEB	NEB + t-BuOH	NEB in water matrix
UV-A	1.3 x10 ⁻⁵	-	2.8 x10 ⁻⁵	868	-	419	13	9	27
UV-B	4.7 x10 ⁻⁴	5.0 x10 ⁻⁴	4.4 x10 ⁻⁴	25	23	26	96	97	96
UV-C	7.8 x10 ⁻⁴	2.5 x10 ⁻⁴	2.9 x10 ⁻⁴	15	46	40	99	84	87

Note: “-“ = no degradation

Suppl. 6.8 Chemical structures of NEB and its transformation products in comparison with other β -blockers. The active moieties responsible for the biological activity are highlighted.



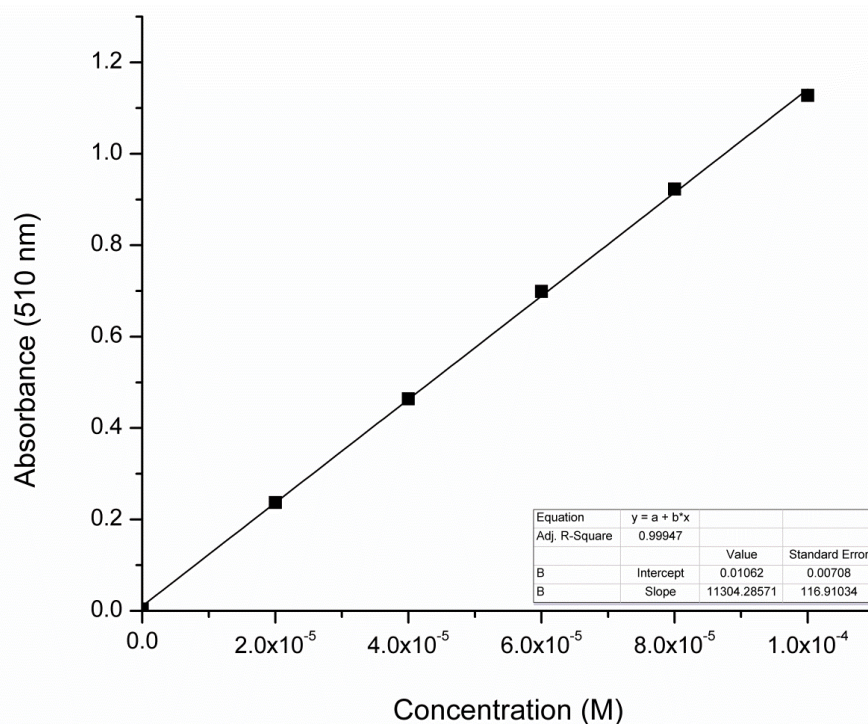
Ferrioxalate actinometry

The UV dose was calculated as the volume averaged irradiance multiplied by the exposure time. Since, in a collimated beam, irradiance and fluence rate are the same, these measurements also allowed the determination of the fluence rates.

30 mM ferrioxalate solution is prepared by dissolving 14.737 g of $K_3Fe(C_2O_4)_3$ and 2.745 mL H_2SO_4 in pure water in a 1-L volumetric flask. H_2SO_4 is added to prevent the oxidation of Fe(II) to Fe(III) by reacting with the water (Hydrolysis) and oxygen present.

The concentration of Fe(II) formed during the irradiation is measured based on standard actinometric ferrioxalate solution. Based on the standard curve created from the standard solution (Suppl. 6.9), the Fe(II) concentrations of the actual samples are calculated from the absorbance values measured at 510 nm (1,10-phenanthroline, $\epsilon = 10910 \text{ dm}^3 \text{ mol}^{-1} \text{ cm}^{-1}$).

Suppl. 6.9 Standard curve for ferrioxalate actinometry.



The molar absorption coefficient of the $Fe(C_2O_4)_3^{3-}$ ion at the detection wavelength can be determined by the slope of the standard curve, being $\epsilon = 1.14 \times 10^4 \text{ (M}^{-1} \text{cm}^{-1})$.

The number of photon produced per time is calculated by the slope of Fe(II) concentration and the studied time. They were $7.2 \times 10^{-5} \text{ mol min}^{-1}$, $5.4 \times 10^{-5} \text{ mol min}^{-1}$, and $2.1 \times 10^{-5} \text{ mol min}^{-1}$ under irradiation with UV-A, UV-B, and UV-C, respectively. Additionally, the light intensity of the UV lamps was calculated based on equation (3), from the photon formed (I) ($\text{Einstein s}^{-1} \text{ m}^{-2}$) and the energy flux (E_{avg}) (W m^{-2})

$$I = \frac{\Delta n}{10^{-3} \Phi A_t t} \quad (\text{Eq. 1})$$

I	Light intensity	Einstein s ⁻¹ m ⁻²
Δn	Ferrous iron photo-generated	mol
Φ	Quantum yield for ferrioxalate (0.006 M)	Φ _λ = 1.20 at 254 nm Φ _λ = 1.23 at 312 nm Φ _λ = 1.26 at 365 nm
A _t	Irradiated area	m ²
t	Irradiation time	s

$$\Delta n = 10^{-3} \frac{V_1 V_3}{V_2} C_t \quad (\text{Eq. 2})$$

V ₁	Irradiated volume	mL
V ₂	Volume taken from the irradiated samples	mL
V ₃	Volume after dilution for concentration determination	mL
c _t	Concentration of ferrous iron after dilution	M

$$E_{\text{avg}} = \sum_{\lambda} I \cdot U_{\lambda} \quad (\text{Eq. 3})$$

E _{avg}	Average photon irradiance	W m ⁻²
I	Light intensity	Einstein s ⁻¹ m ⁻²
U _λ	Energy carried by 1 mol of photons of wavelength λ	J Einstein ⁻¹

Suppl. 6.10 Results of the actinometry experiment.

Parameter	UV-A	UV-B	UV-C
Einstein s ⁻¹	10.1 x 10 ⁻⁷	7.9 x 10 ⁻⁷	2.8 x 10 ⁻⁷
λ (nm)	315 - 400	270 - 360	254
E _{avg} (J.m ⁻² .min ⁻¹)	766	172	155

For monochromatic radiation the photolytic degradation rate of the compound can be expressed with the following formula:

$$\ln \left(\frac{C_0}{C_t} \right) = \frac{\Phi_C E_p'(\text{avg}) \varepsilon_C \ln(10)}{1000} t \quad (\text{Eq. 4})$$

And for polychromatic radiation, it is:

$$\ln\left(\frac{c_0}{c_t}\right) = \sum_{\lambda} \frac{\Phi_c^{\lambda} E_p'(avg) \varepsilon_c^{\lambda} \ln(10)}{1000} t \quad (\text{Eq. 4})'$$

c_0	Initial concentration	M
c_t	Final concentration	M
Φ_c	Quantum yield	
ε_c	Molar absorption coefficient	$\text{M}^{-1}\text{cm}^{-1}$
$E_p'(avg)$	Average photon irradiance	
t	time	s

$$\varepsilon_c = \frac{1}{d} \frac{A}{c} \quad (\text{Eq. 5})$$

ε_c	Molar absorption coefficient	$\text{M}^{-1}\text{cm}^{-1}$
A	Absorbance at certain wavelength	
c_t	Compound concentration	M
d	path length	cm

Fluence H' is one expression to substitute two parameters of the equation and to integrate fluence based rate expression for direct photolysis of one compound at one irradiation wavelength. E_{avg} is another expression to express the average irradiance with the following relation:

$$E'_{avg} = E_p'(avg) U_{\lambda} \quad (\text{Eq. 6})$$

For polychromatic radiation:

$$E'_{avg} = \sum_{\lambda} E_p'(avg) U_{\lambda} \quad (\text{Eq. 6})'$$

$$H' = E_p'(avg) U_{\lambda} t \quad (\text{Eq. 7})$$

For polychromatic radiation

$$H' = \sum_{\lambda} E_p'(avg) U_{\lambda} t \quad (\text{Eq. 7})'$$

E'_{avg}	Average photon irradiance	W m^{-2}
U_{λ}	Energy carried by 1 mol of photons of wavelength λ	J Einstein^{-1}
H'		J m^{-2}

The E'_{avg} is the average photon irradiance and can be determined from the chemical actinometry with addition correction factors of Water Factor (WF) and Divergence Factor (DF).

$$WF = \frac{1-10^{-al}}{al \ln(10)} \quad (\text{Eq. 8})$$

$$DF = \frac{L}{L+l} \quad (\text{Eq. 9})$$

WF	Water factor	
a	Absorption coefficient of the solution	m^{-1}
	at the wavelength of irradiation	
l	Path length	m
DF	Divergence factor	
L	Distance from the top of solution in	m
	irradiation dish to the light source	

From eq. 4, eq.6, and eq.7 the following integrated formula is formed:

$$\ln\left(\frac{C_0}{C_t}\right) = \frac{\Phi_C \varepsilon_C \ln(10)}{1000 U_\lambda} H' \quad (\text{Eq. 10})$$

For polychromatic radiation:

$$\ln\left(\frac{C_0}{C_t}\right) = \sum_{\lambda} \frac{\Phi_C^\lambda \varepsilon_C^\lambda \ln(10)}{1000 U_\lambda} H' \quad (\text{Eq. 10})'$$

The final formula for the fluence based first order rate constant k'_1 is:

$$k'_1 = \frac{\Phi_C \varepsilon_C \ln(10)}{1000 U_\lambda} \quad (\text{Eq. 11})$$

For polychromatic radiation:

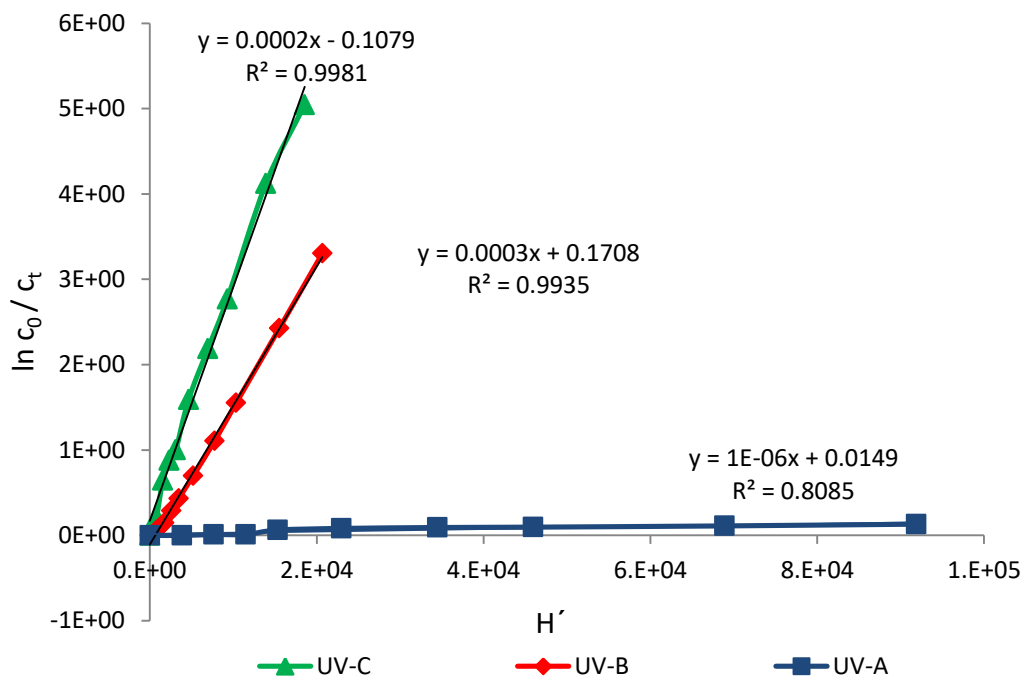
$$k'_1 = \sum_{\lambda} \frac{\Phi_C^\lambda \varepsilon_C^\lambda \ln(10)}{1000 U_\lambda} \quad (\text{Eq. 11})'$$

The fluence-based first-order rate constant k'_1 for the investigated compounds can be determined from the photochemical kinetic experiment. k'_1 ($\text{m}^2 \text{J}^{-1}$) is calculated from the plot of $\ln(C_0/C_t)$ versus H' .

Thus, the quantum yield Φ_C at various wavelengths can be determined from the degradation specific compound experiments. After the compound-specific photochemical parameters Φ_C and ε_C are known, the fluence based rate constants at given wavelength can be further estimated.

The H' values are calculated from multiplication of average photon irradiance (energy flux value) and time elapsed. The k'_1 determined from the plot H' vs. $\ln(c_0/c_t)$ are shown in Suppl. 6.11.

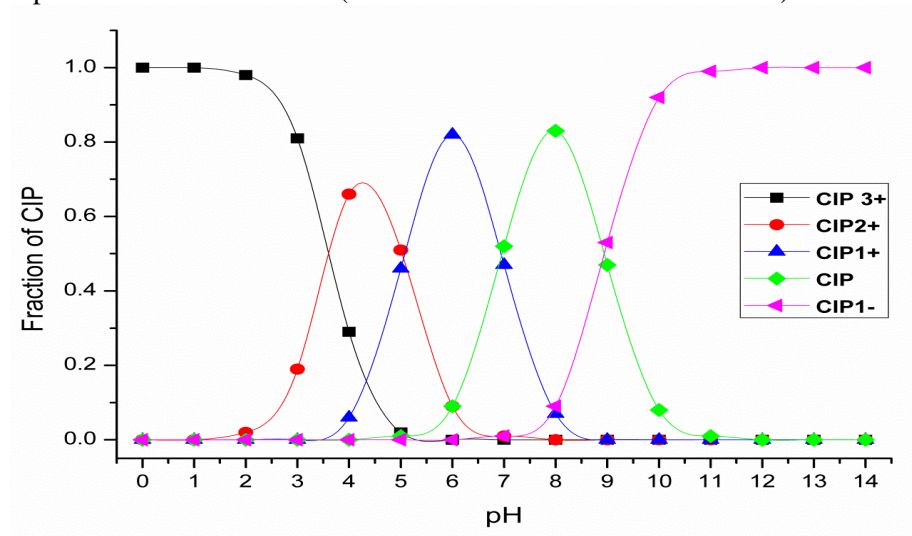
Suppl. 6.11 k'_1 determination from H' and $\ln(c_0/c_t)$ plot.



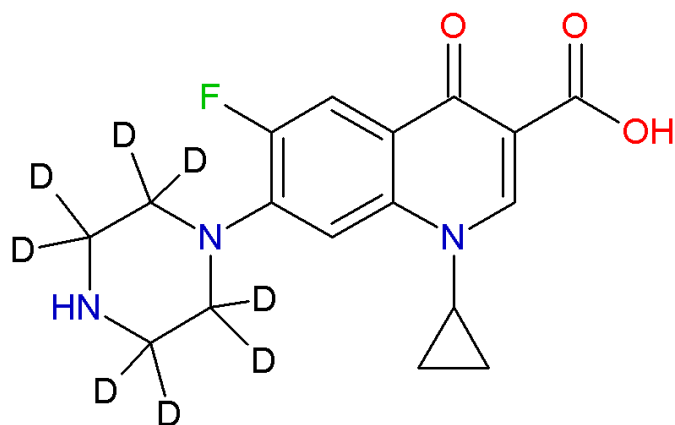
After k'_1 values have been calculated, the quantum yield of nebigolol under all conditions could be determined. Table 2.1 shows the experimental fluence based rate constants of nebigolol direct photolysis under irradiation with three different types of UV lamps. Since there is no absorption and degradation of nebigolol in UV-A range, no quantum yield could be calculated for UV-A.

6.2 Supplementary material of chapter 3

Suppl. 6.12 Distribution of the ciprofloxacin (CIP) species at different pH values based on the pK_as reported in the literature 15 (the structures are shown in scheme 1).



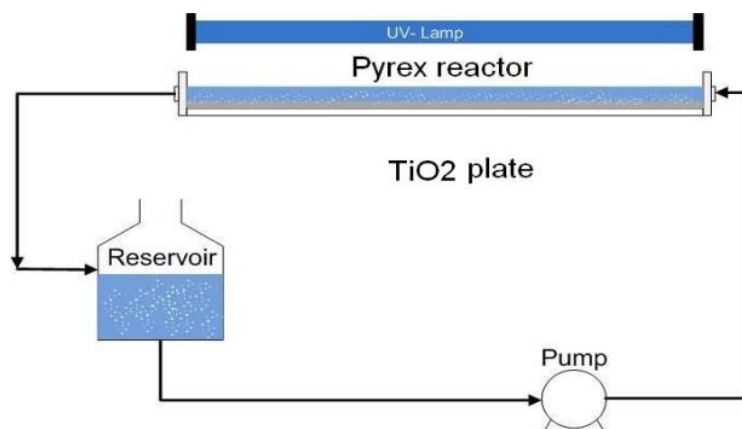
Suppl. 6.13 Structural formula of (CIP-d8), emphasizing the 8-deuterium atoms at the piperazine ring.



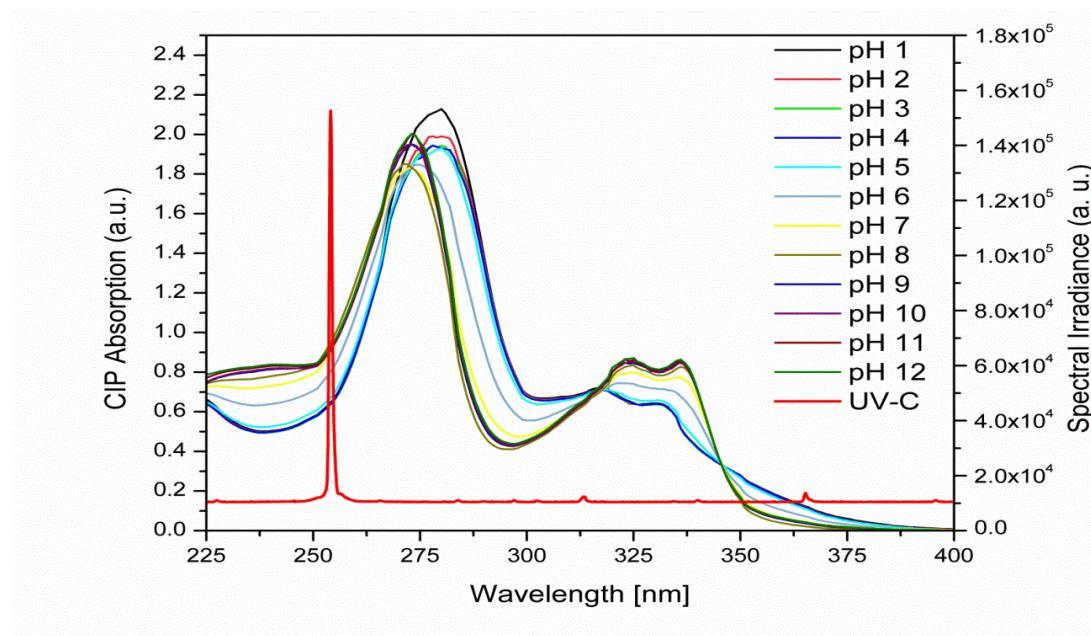
CIP - d8

Exact Mass (Da) 339.1834

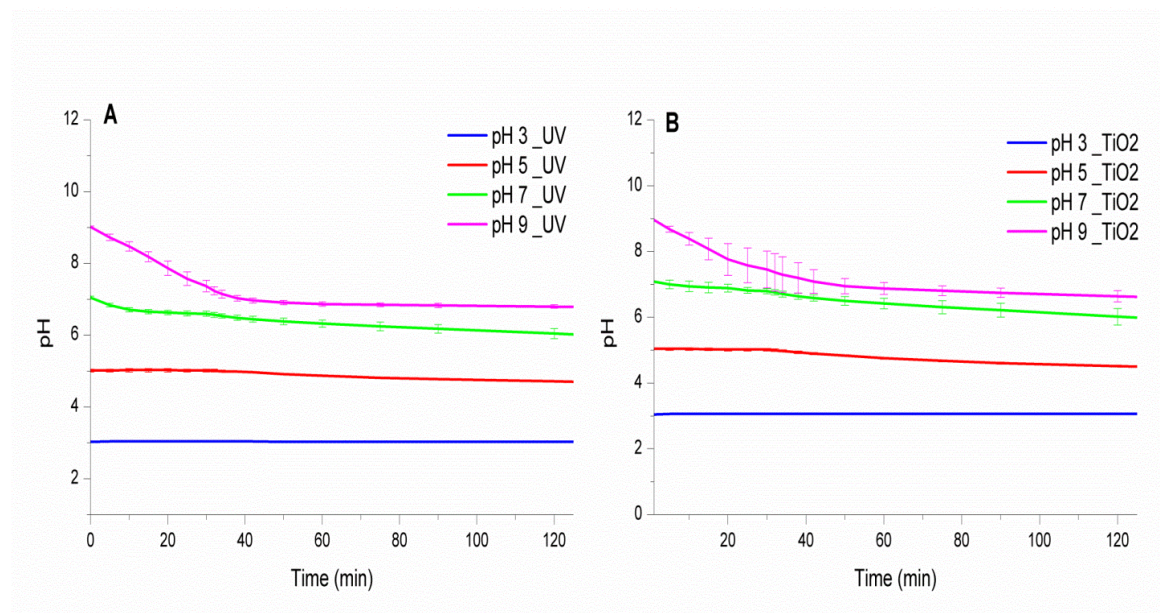
Suppl. 6.14. Experimental set-up.



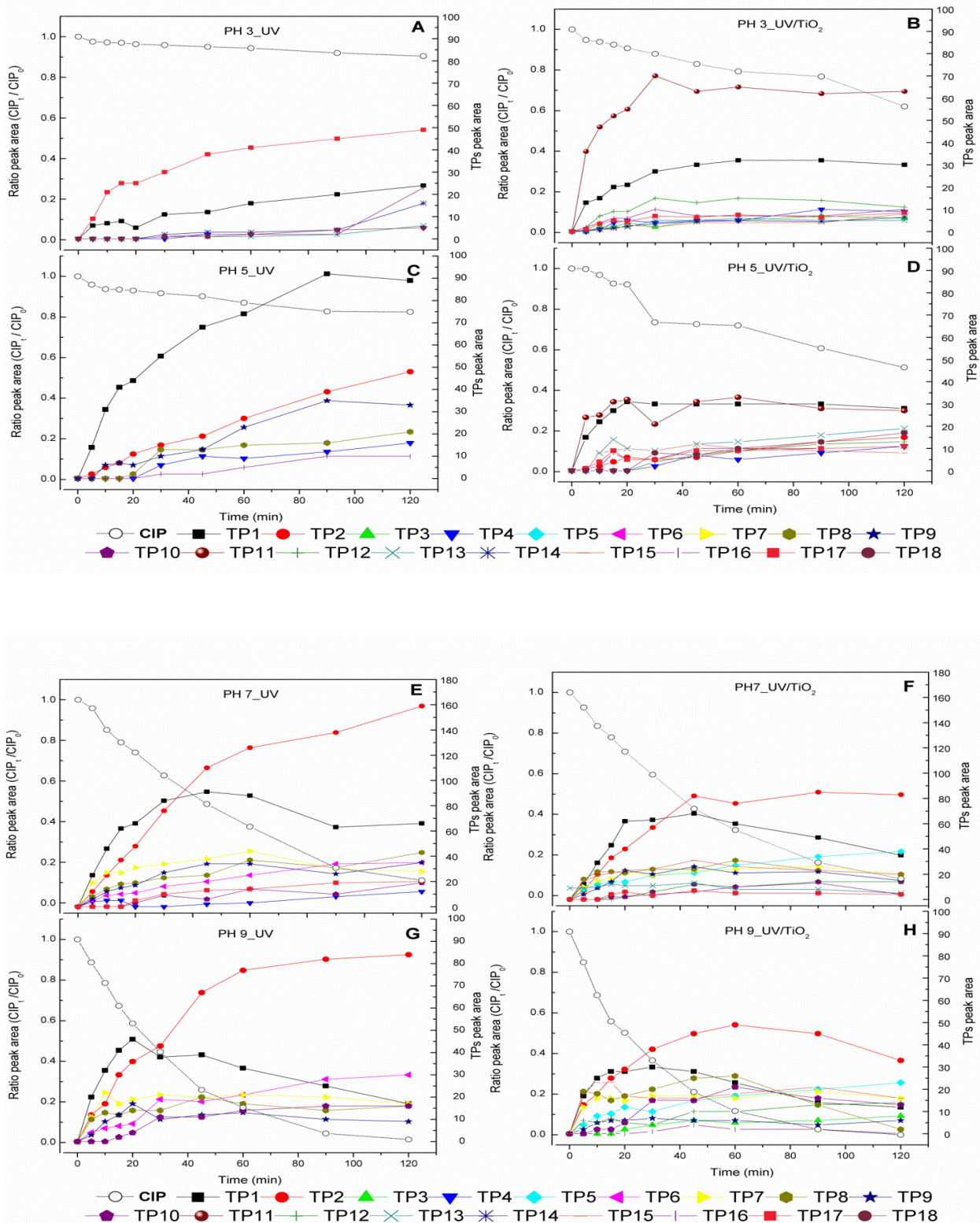
Suppl. 6.15. Spectra of the UV-C Lamp and the absorption spectra of a 60 μM ciprofloxacin unbuffered aqueous solution at different pH values.



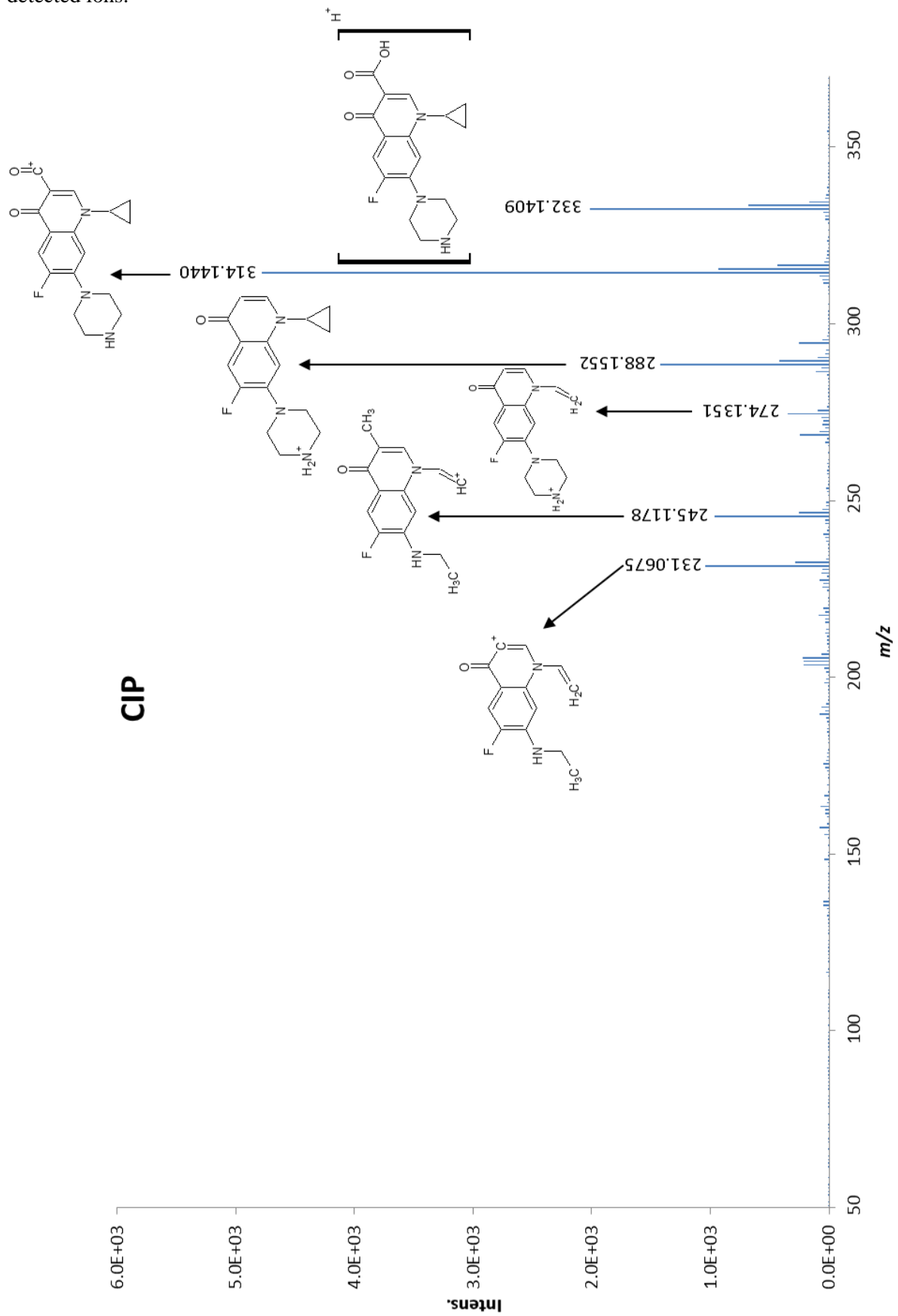
Suppl. 6.16. The change of pH values during the photolytic (A) and photocatalytic (B) degradation of ciprofloxacin.

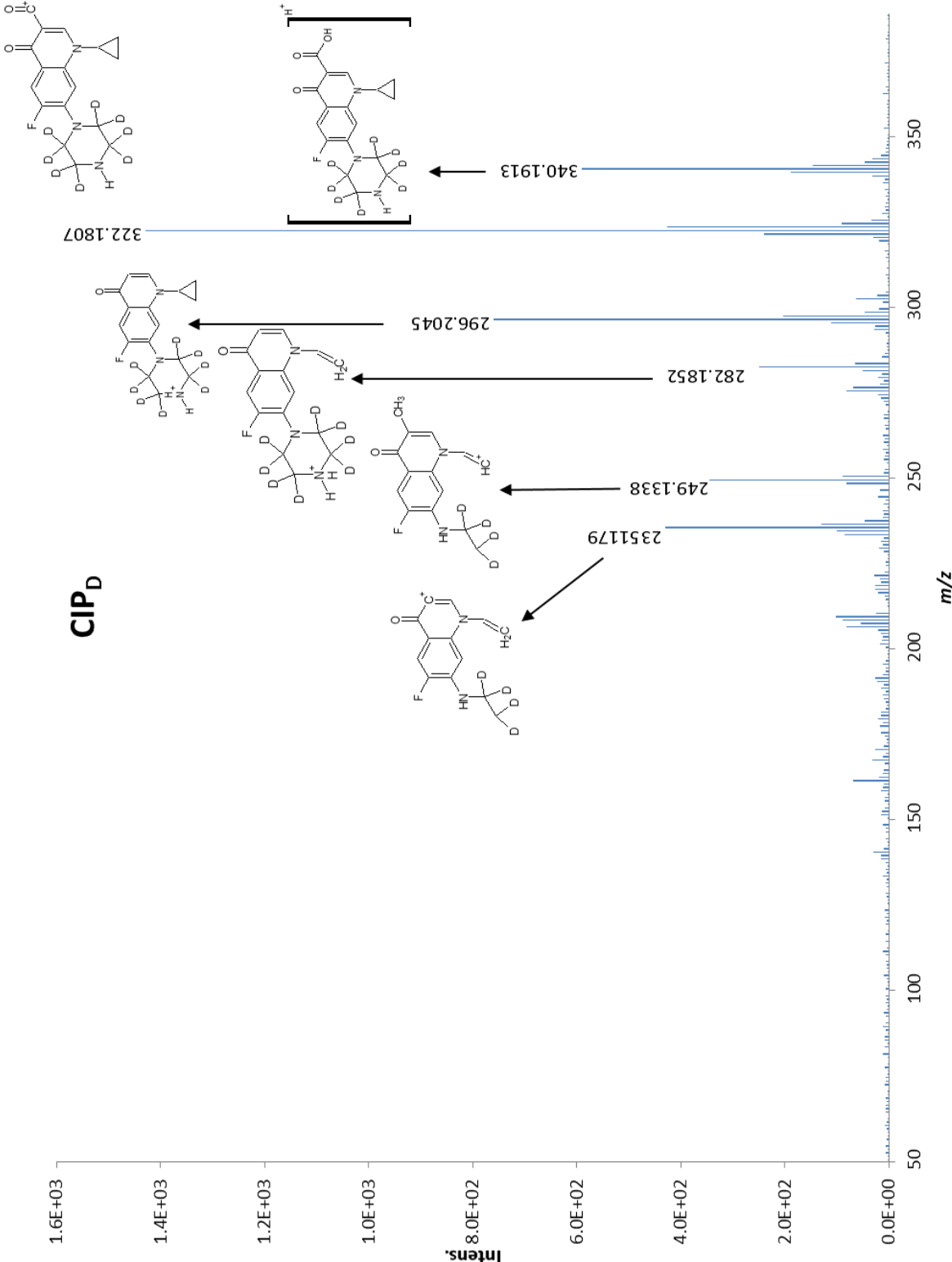


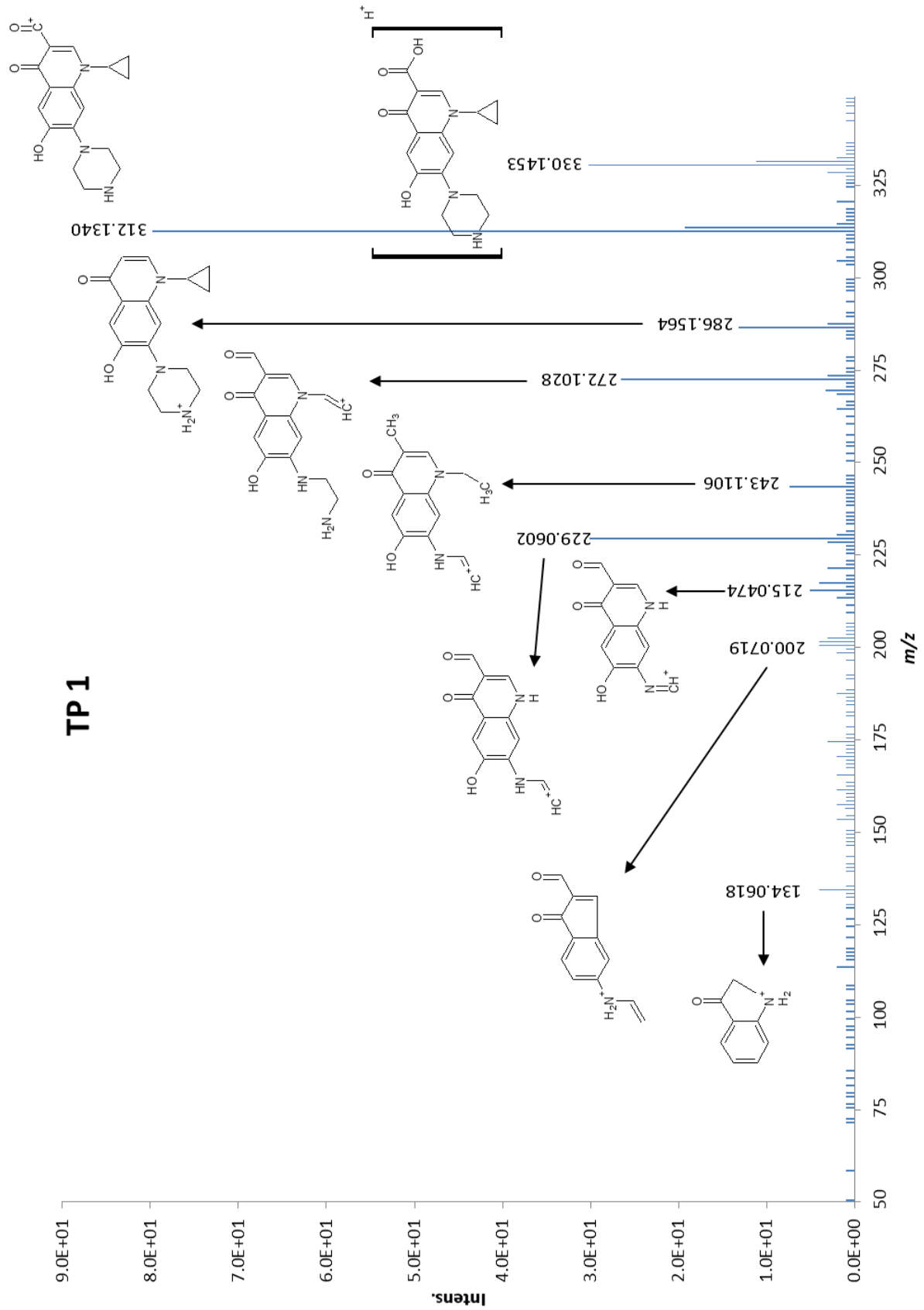
Suppl. 6.17. Photolysis and photocatalysis transformation products of CIP plotted as a function of the irradiation time monitored by LC-MS at pH 3, 5, 7 and 9.

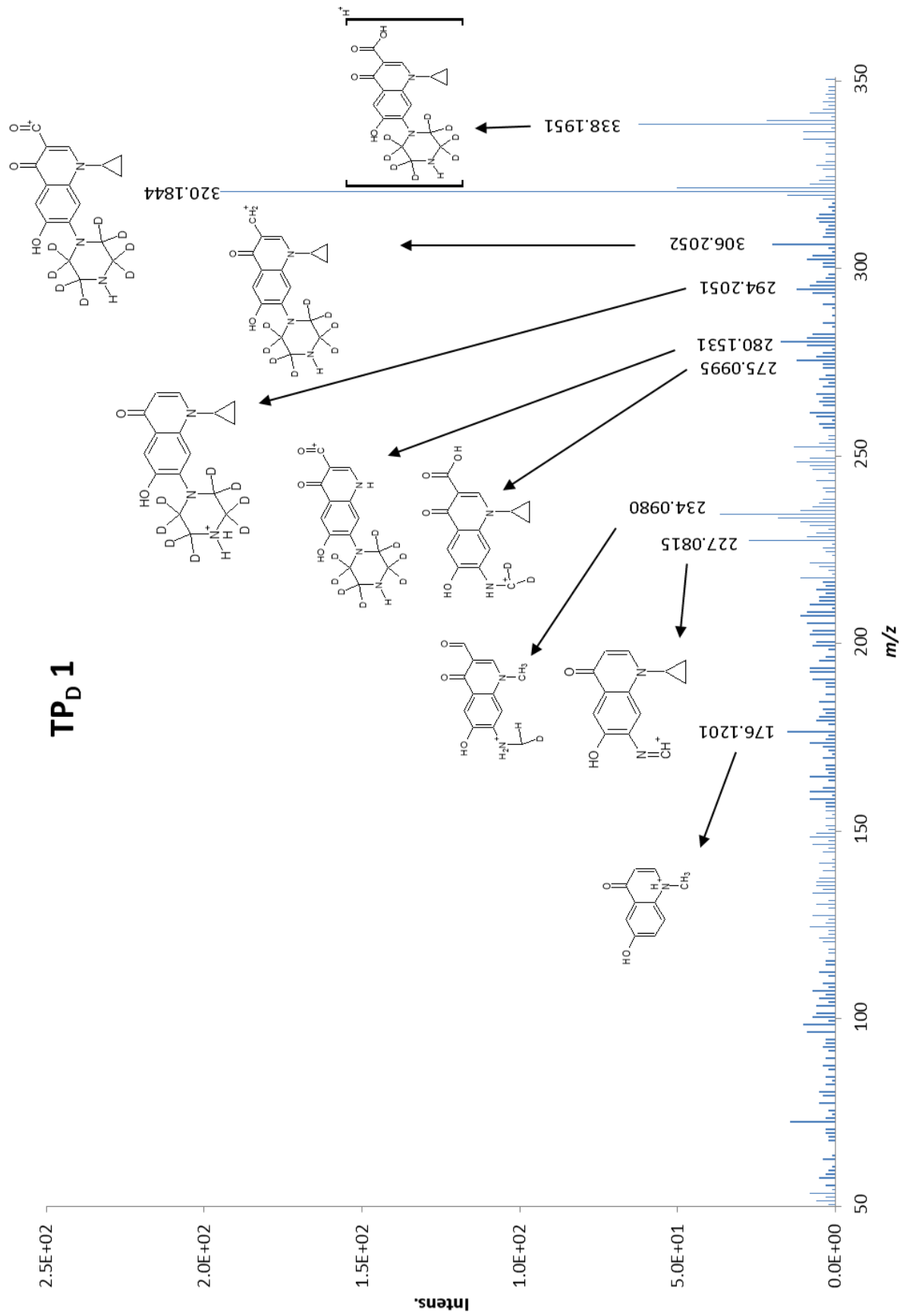


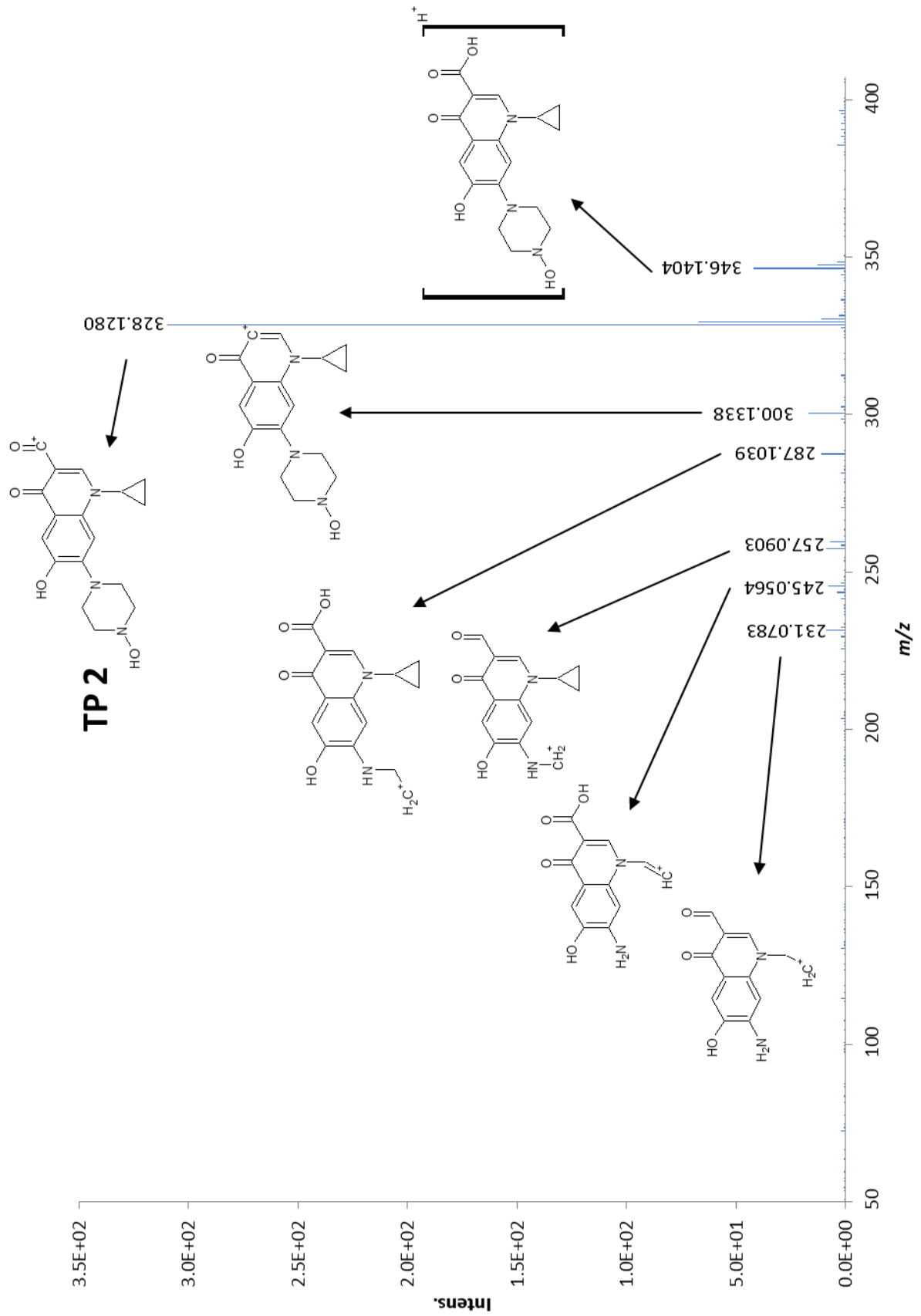
Suppl. 6.18. MS2 spectrum of CIP and its transformation products, proposed fragment structure of detected ions.

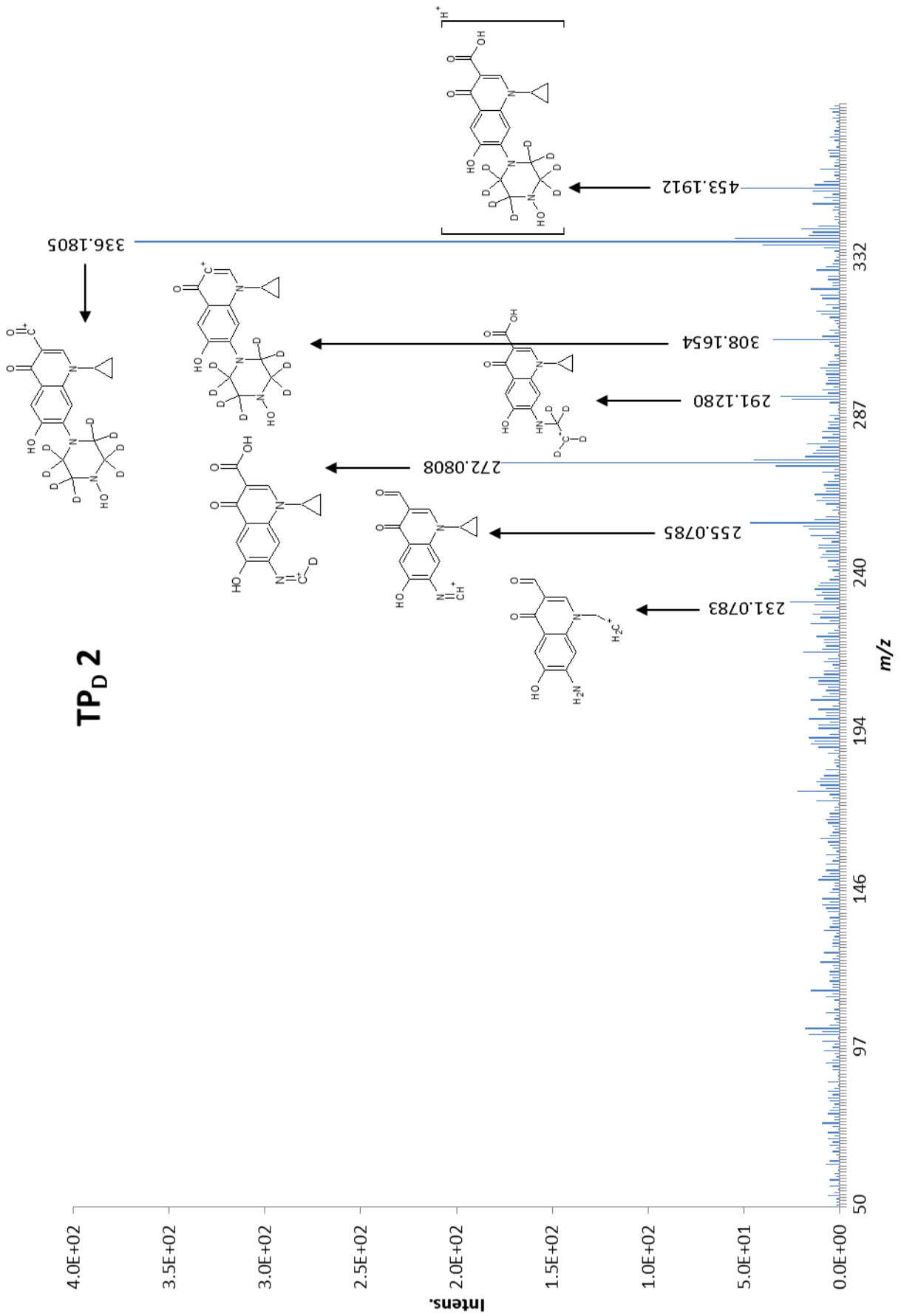


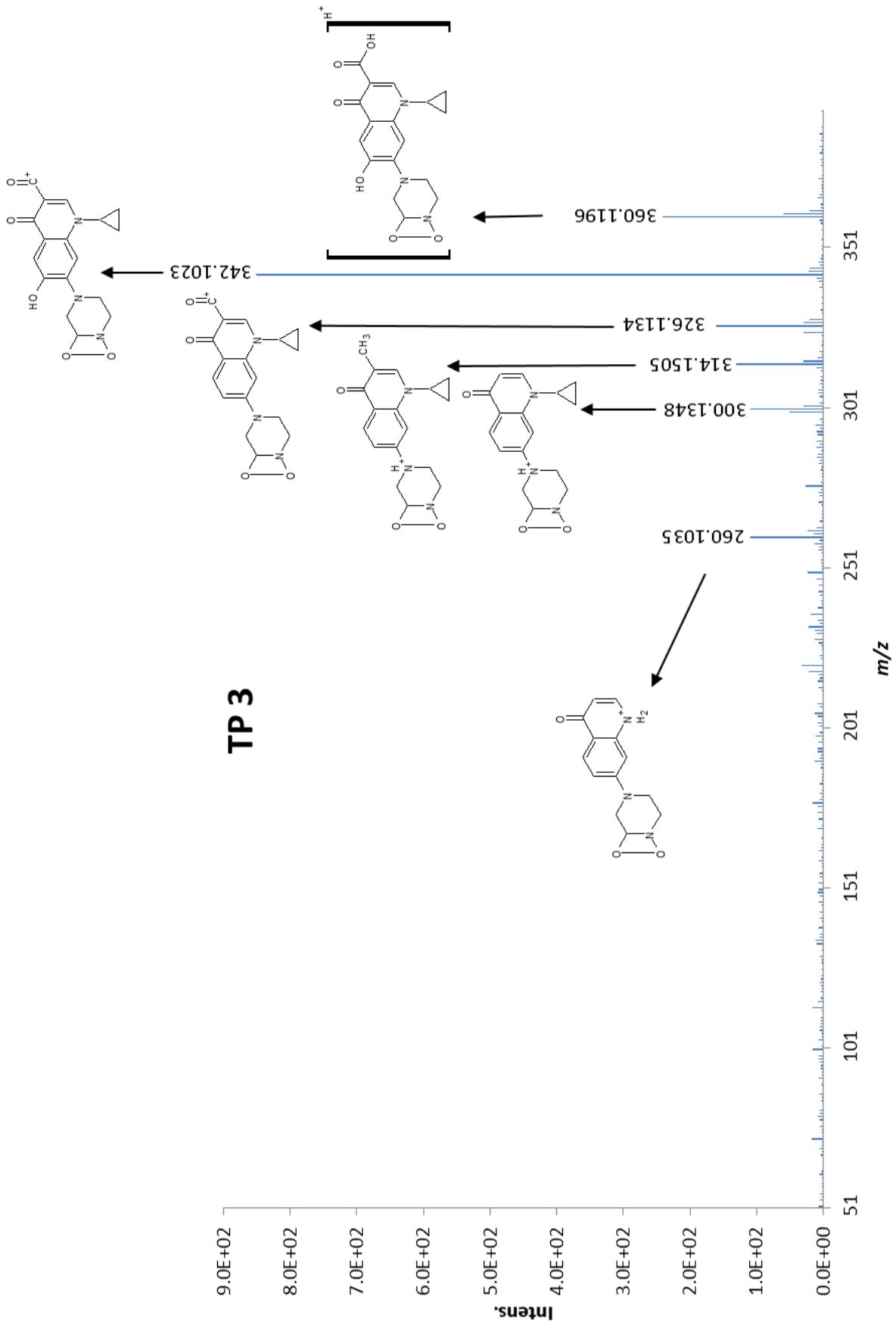


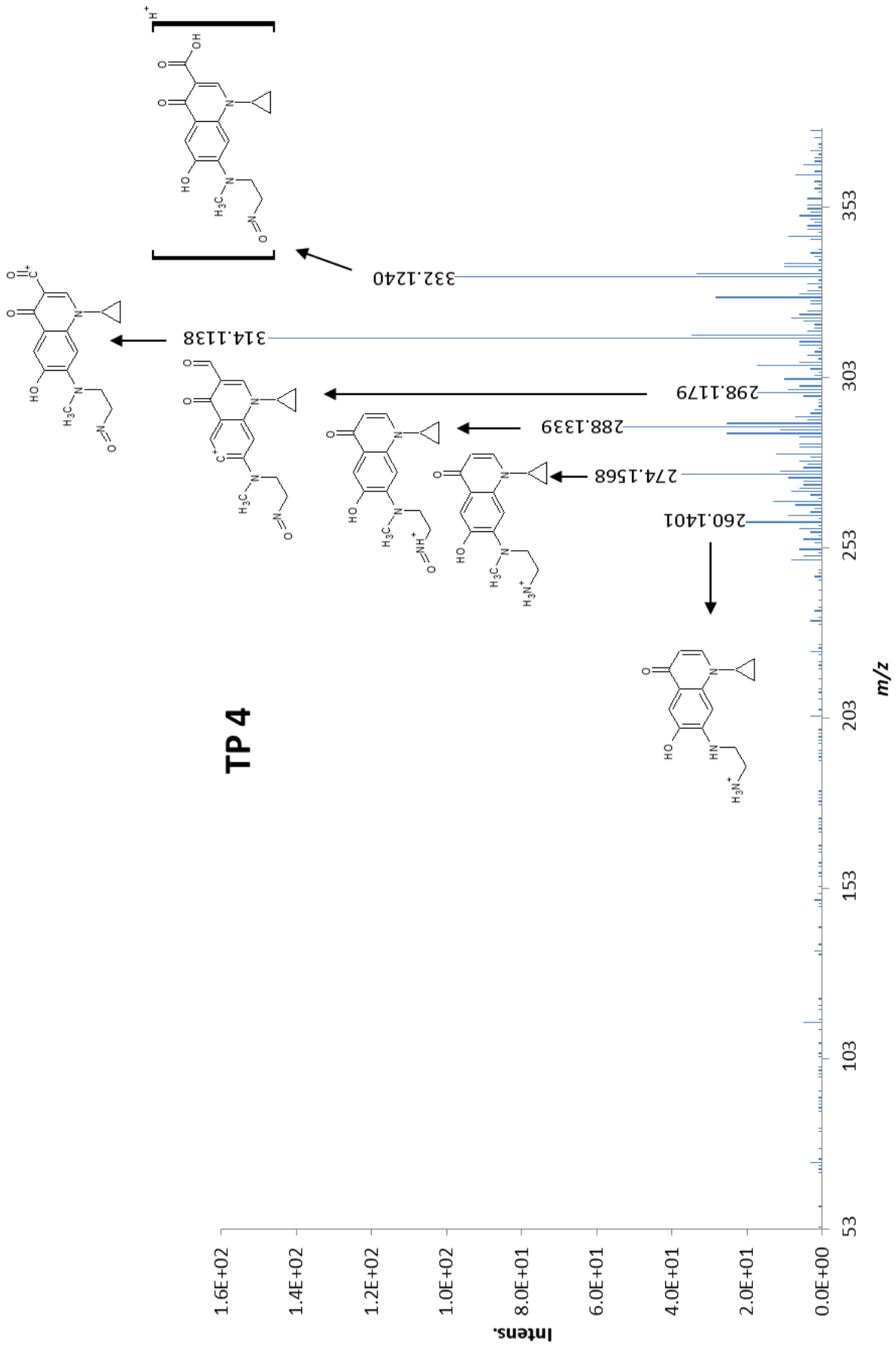


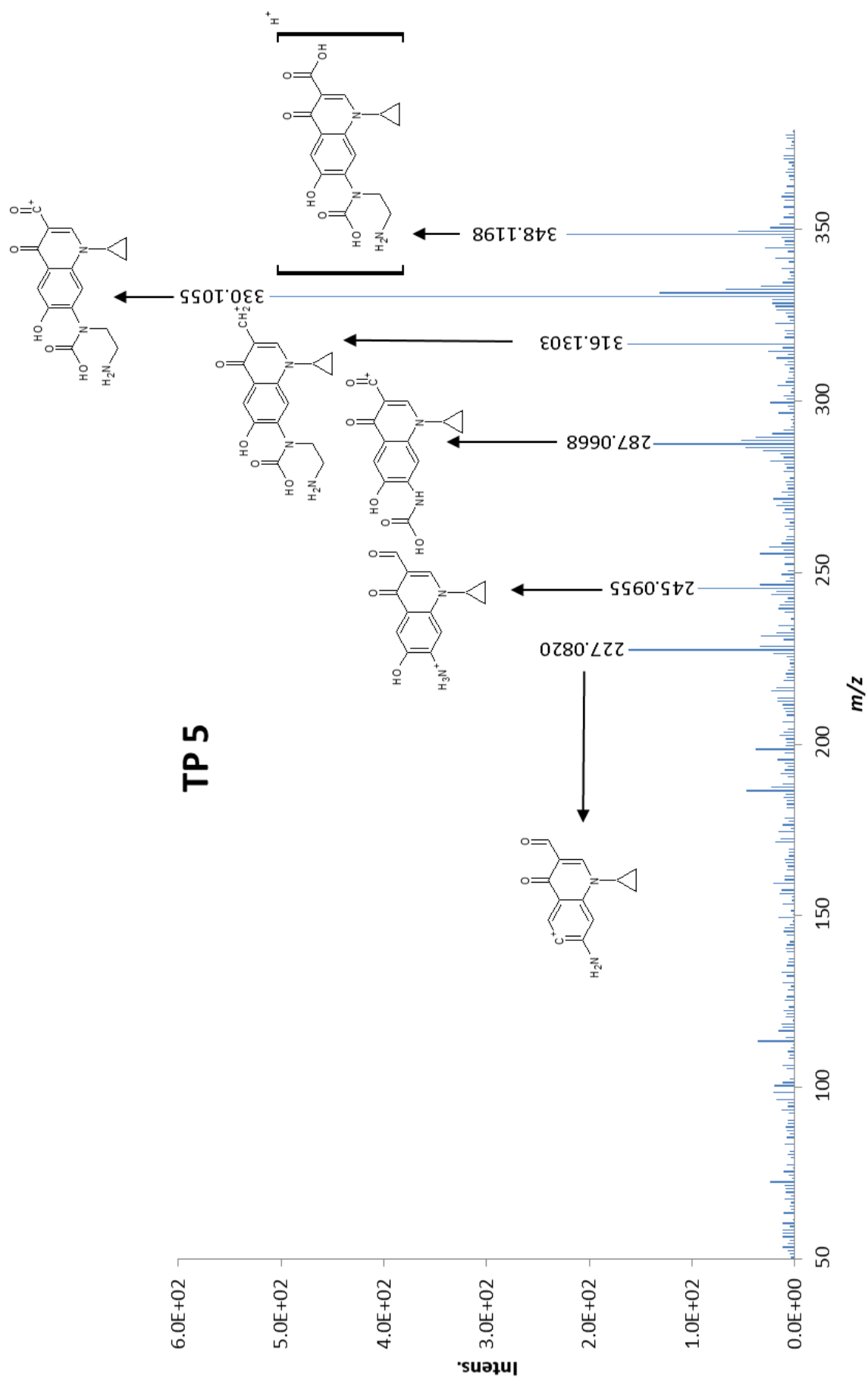


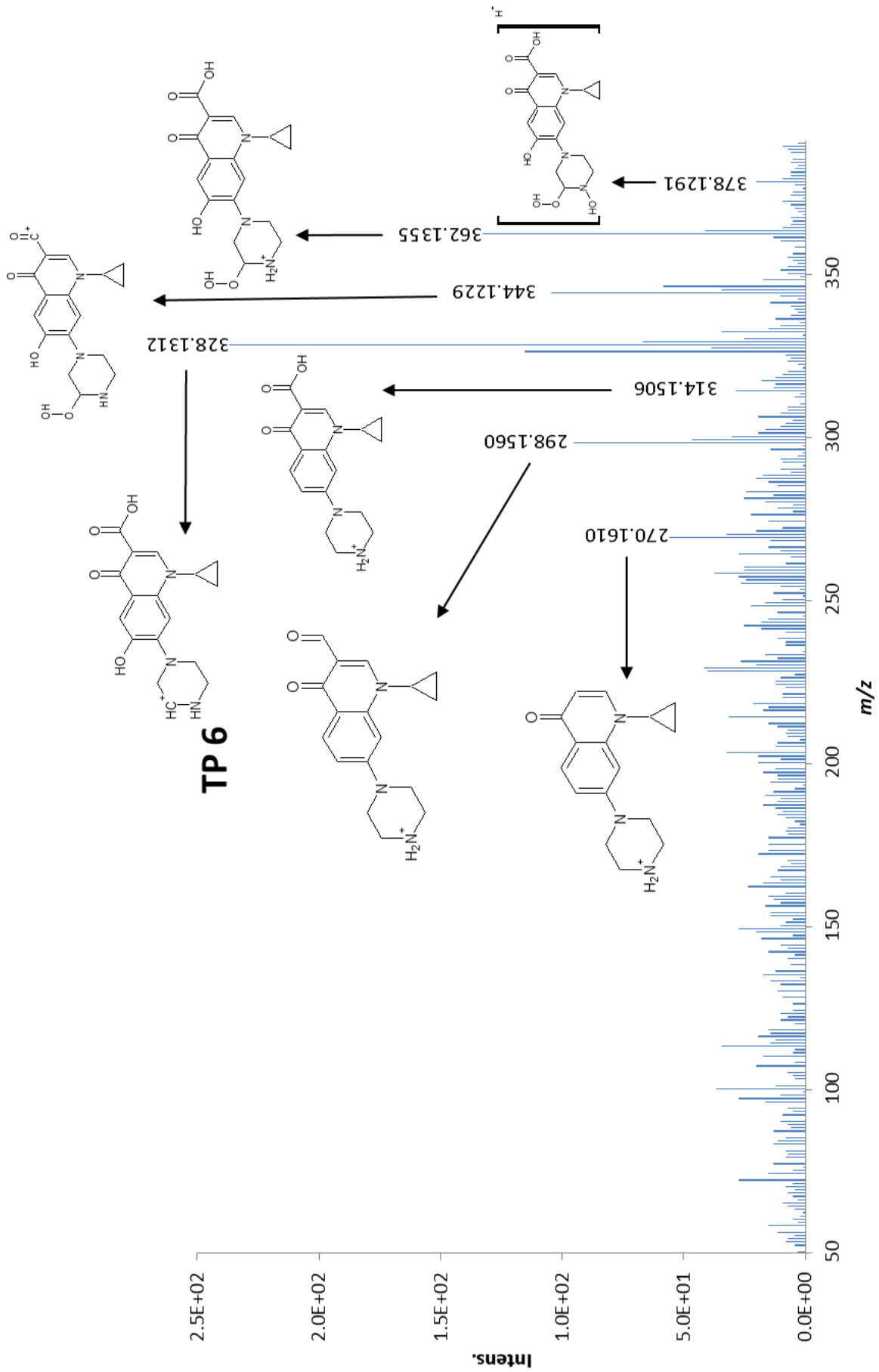


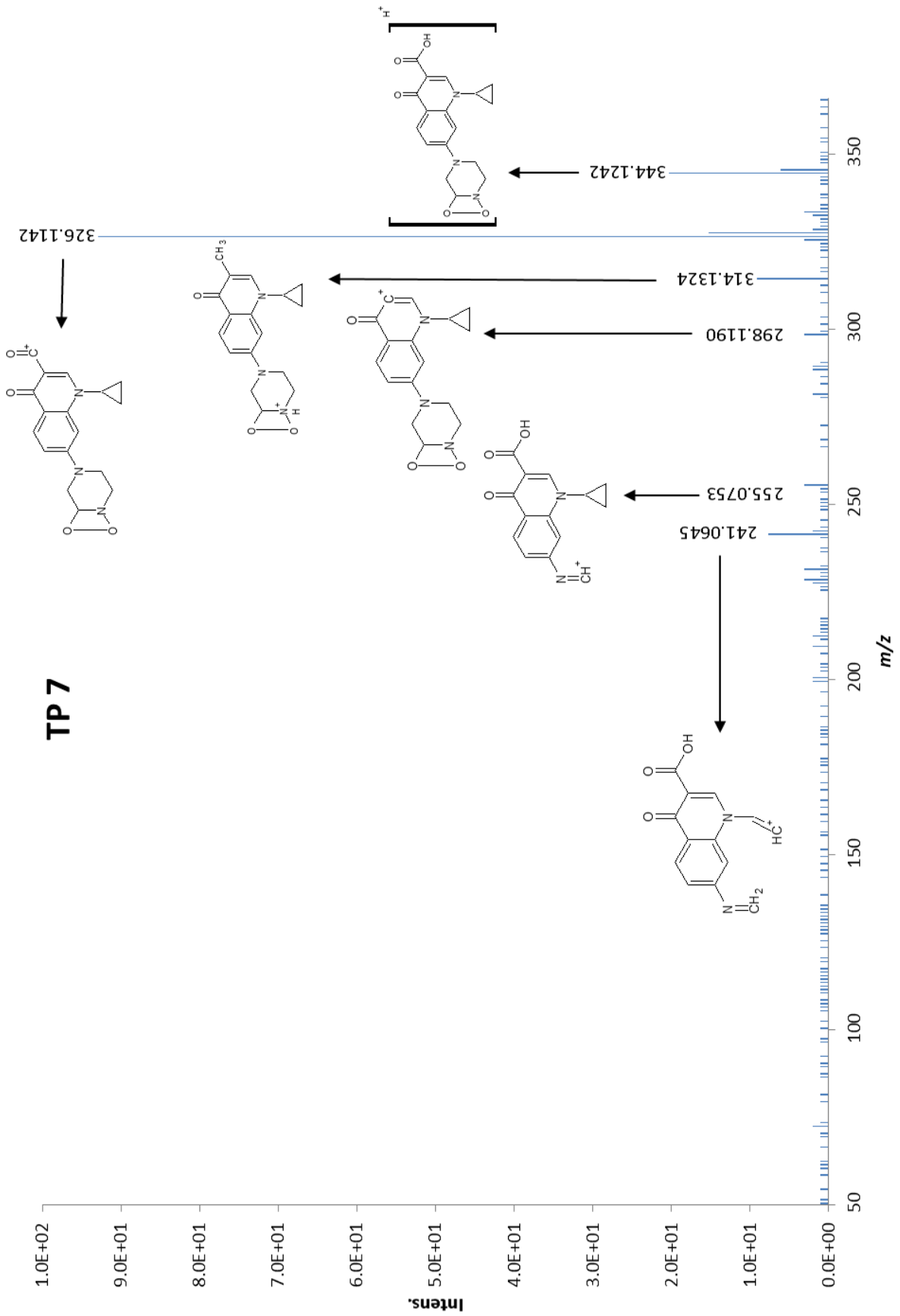


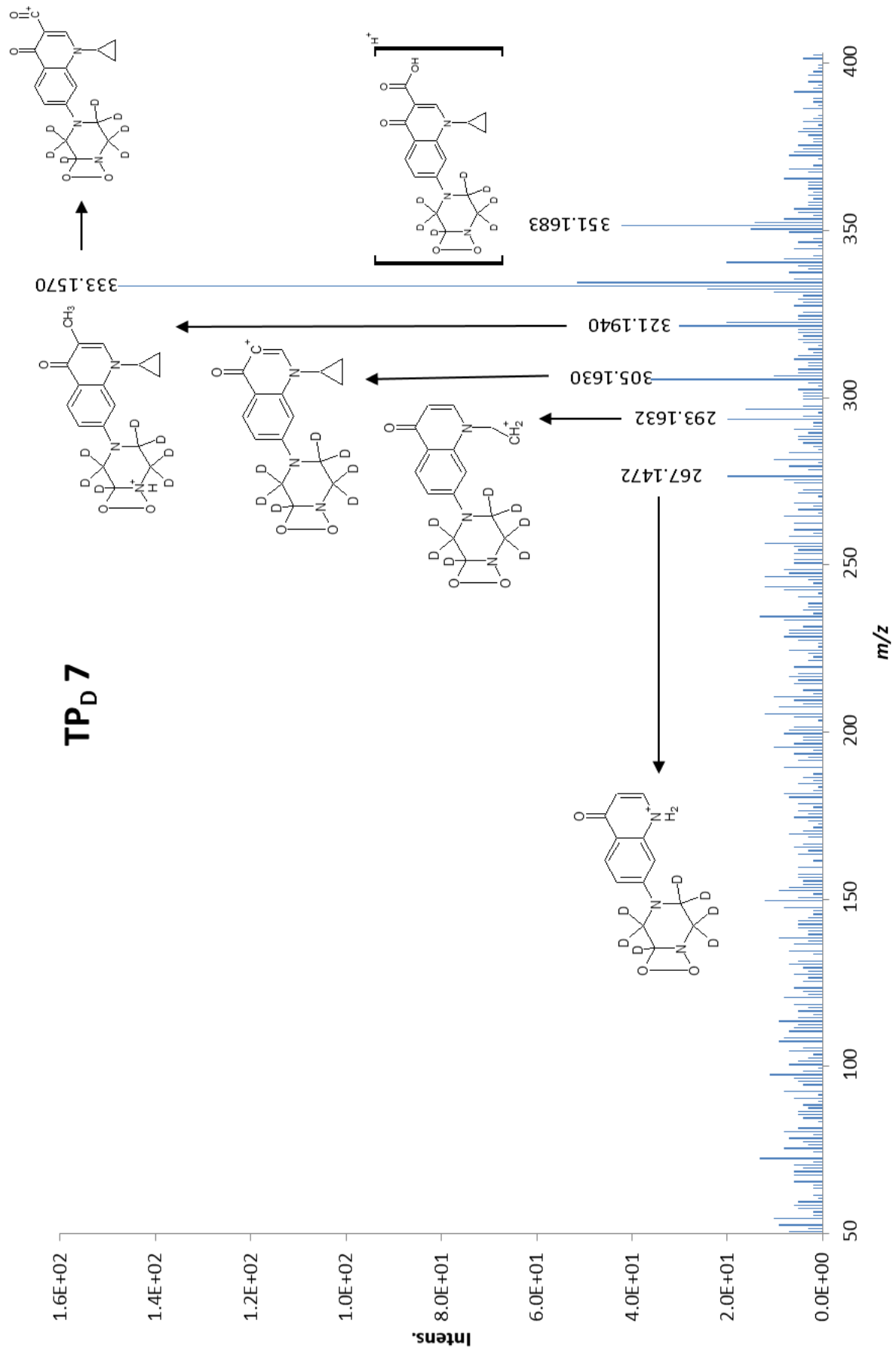


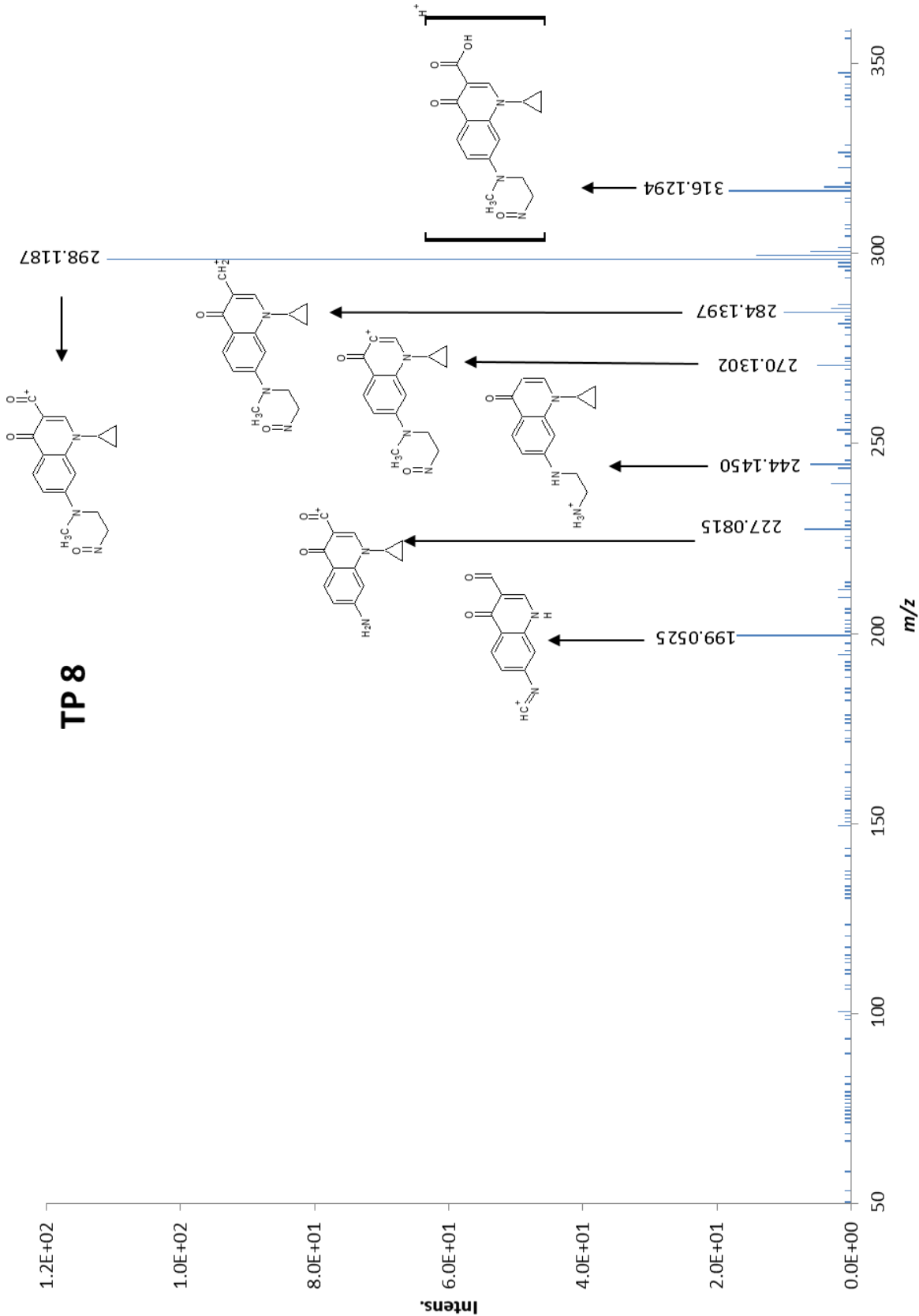


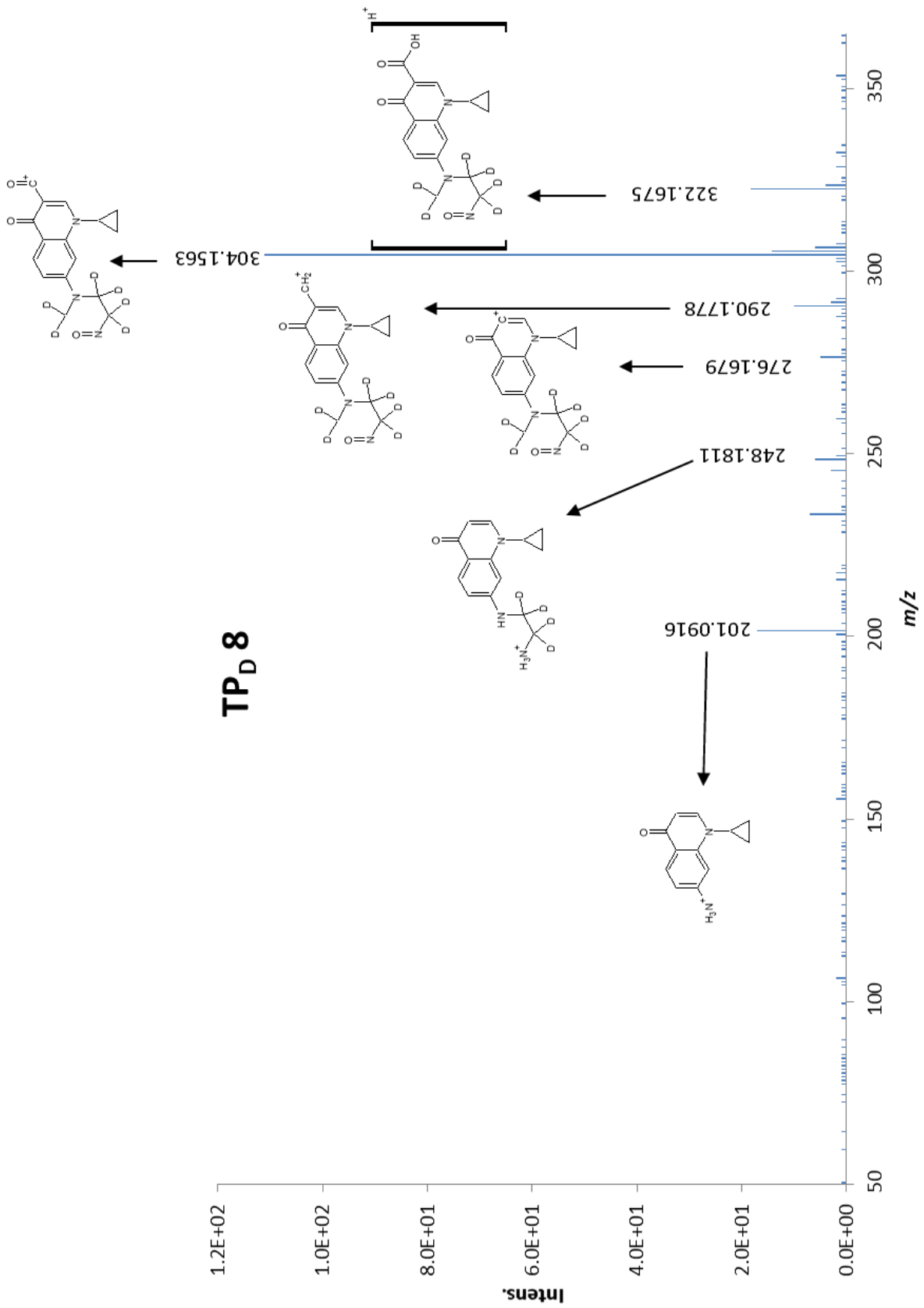


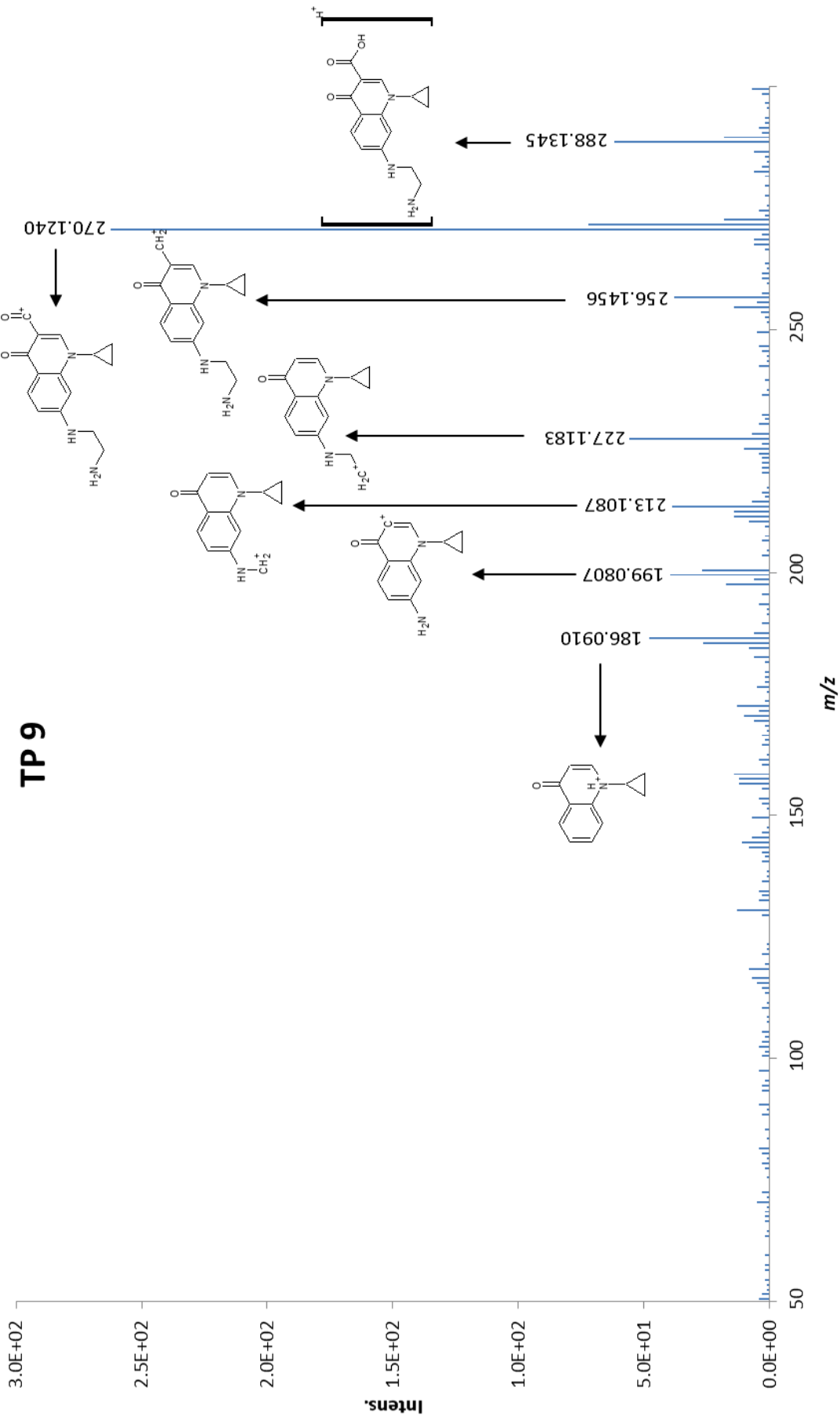


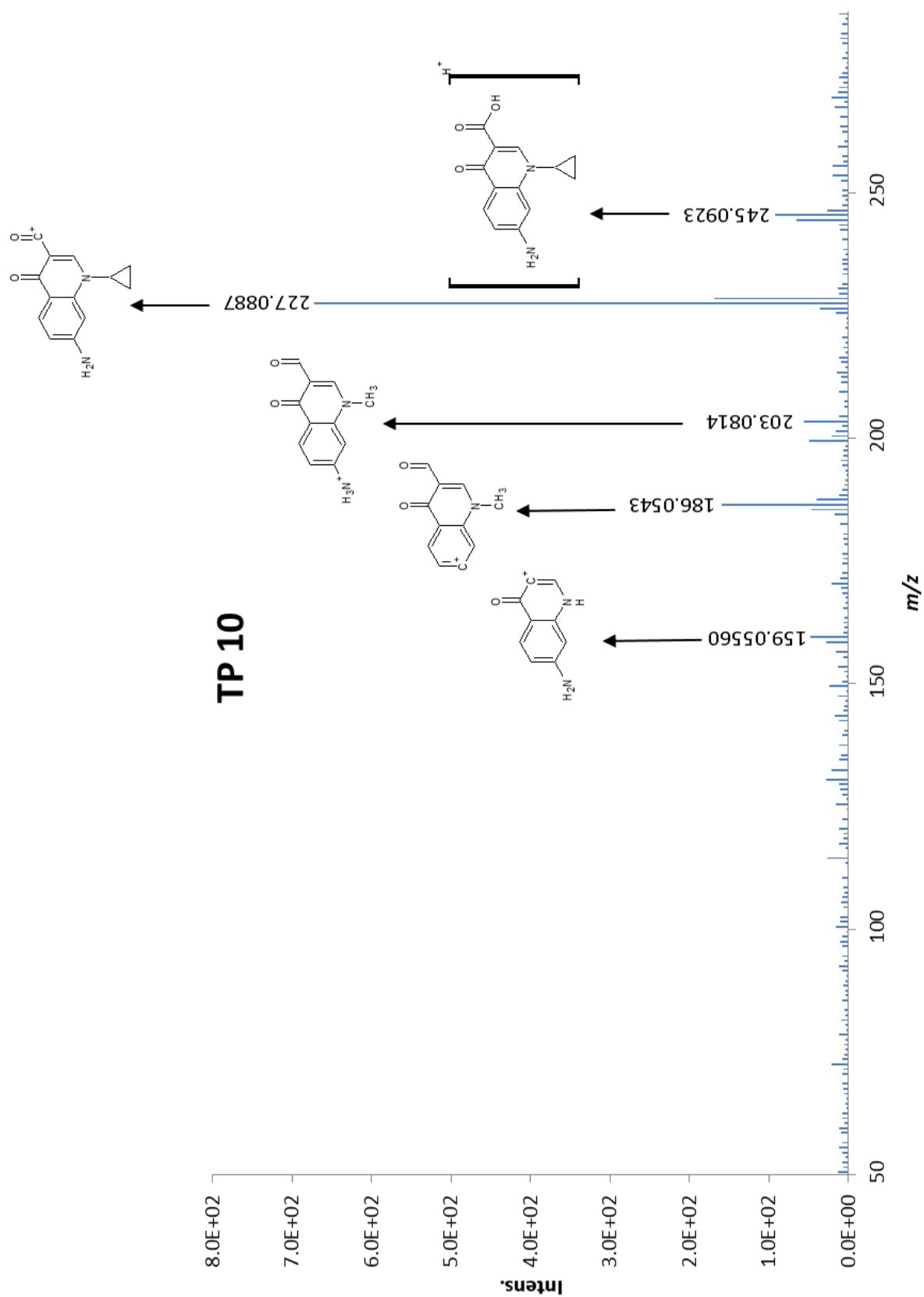


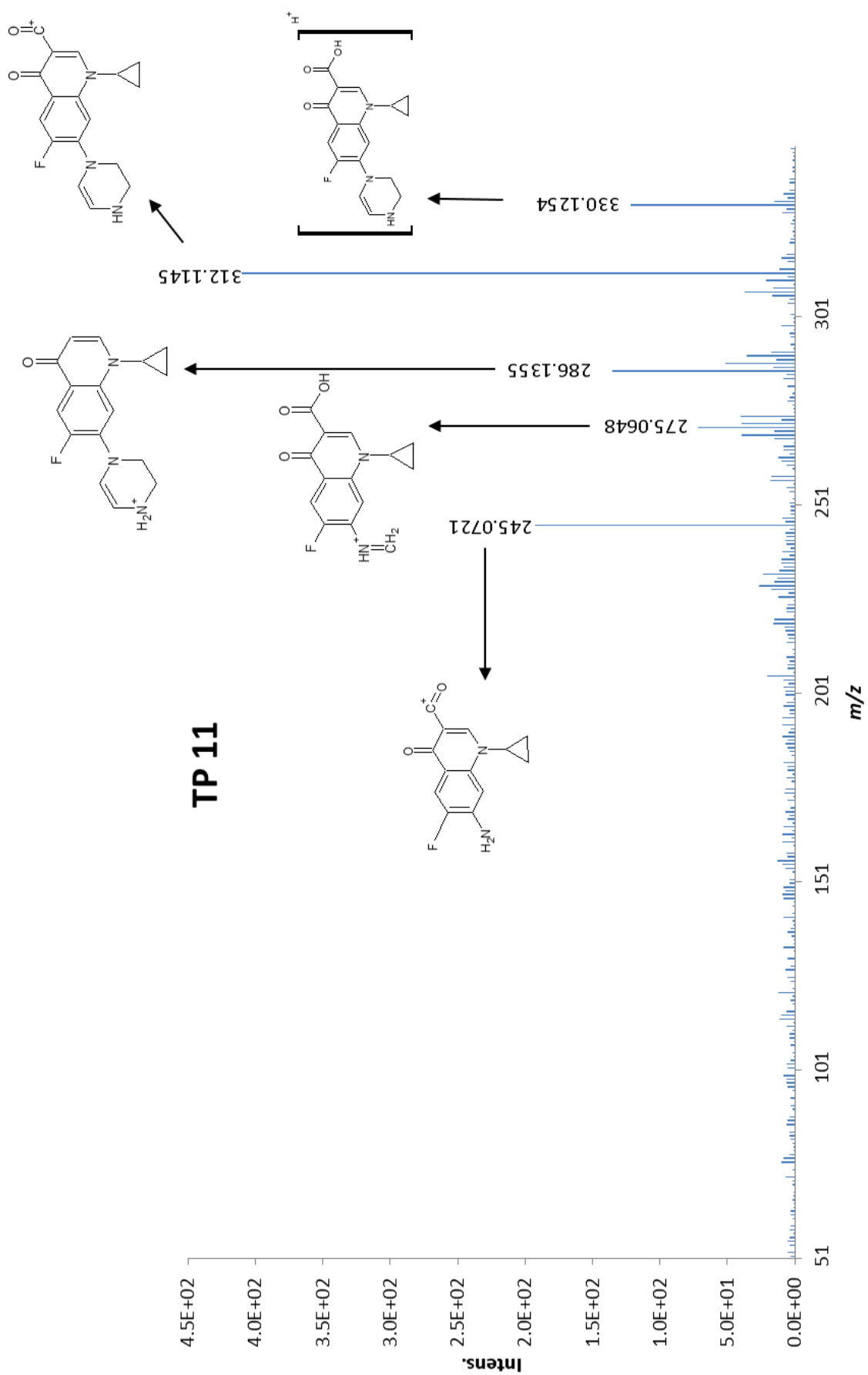


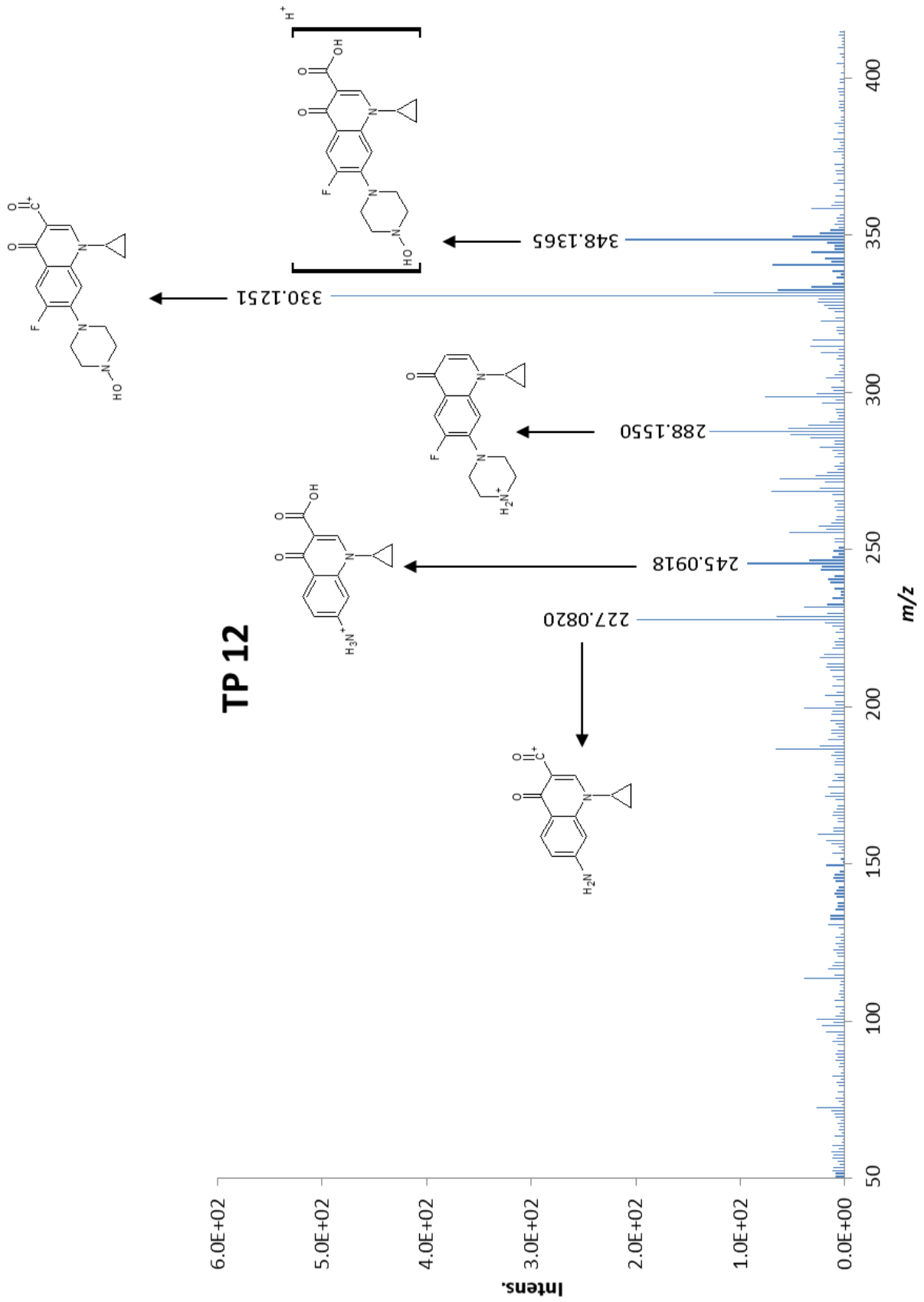


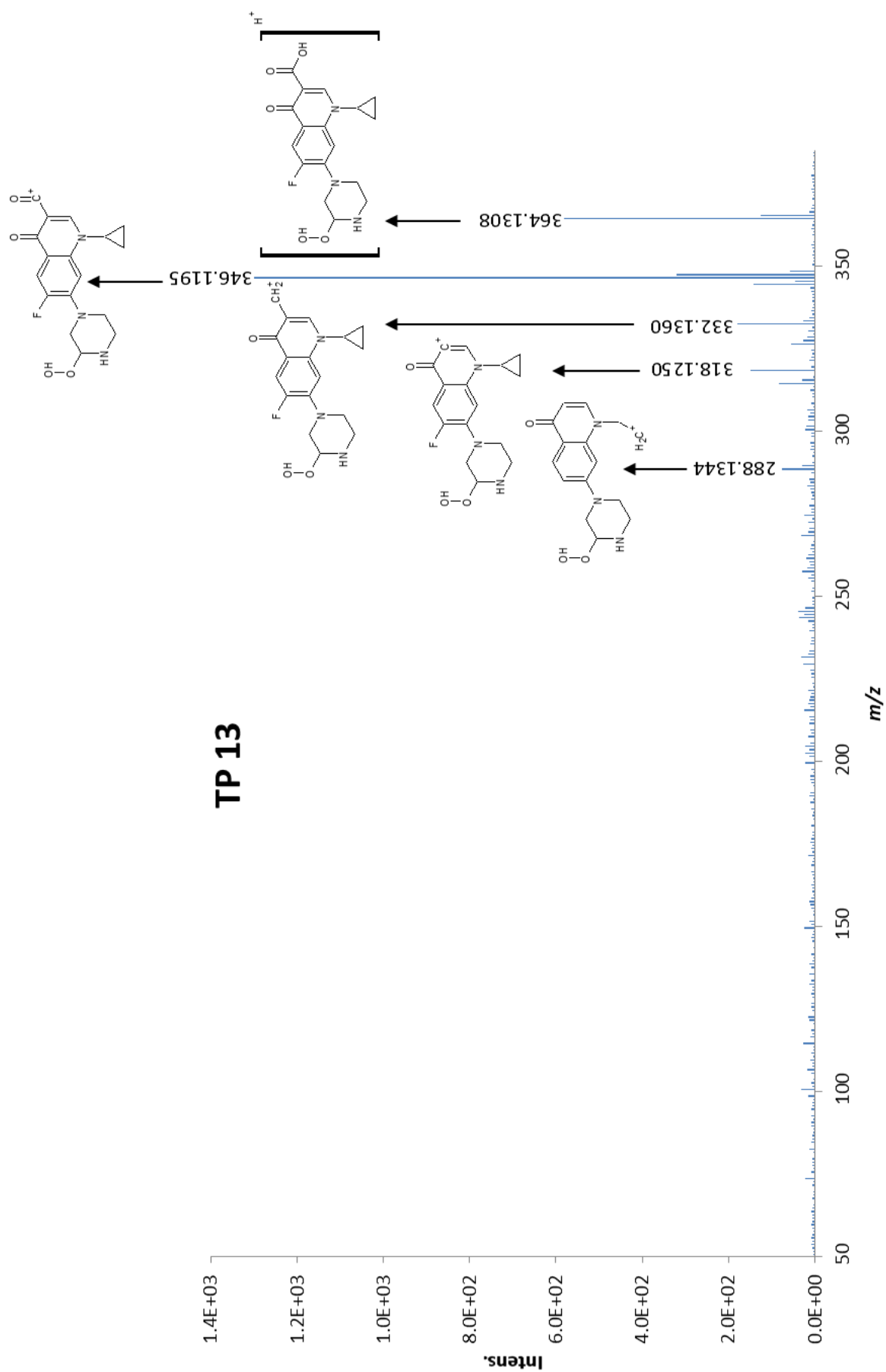


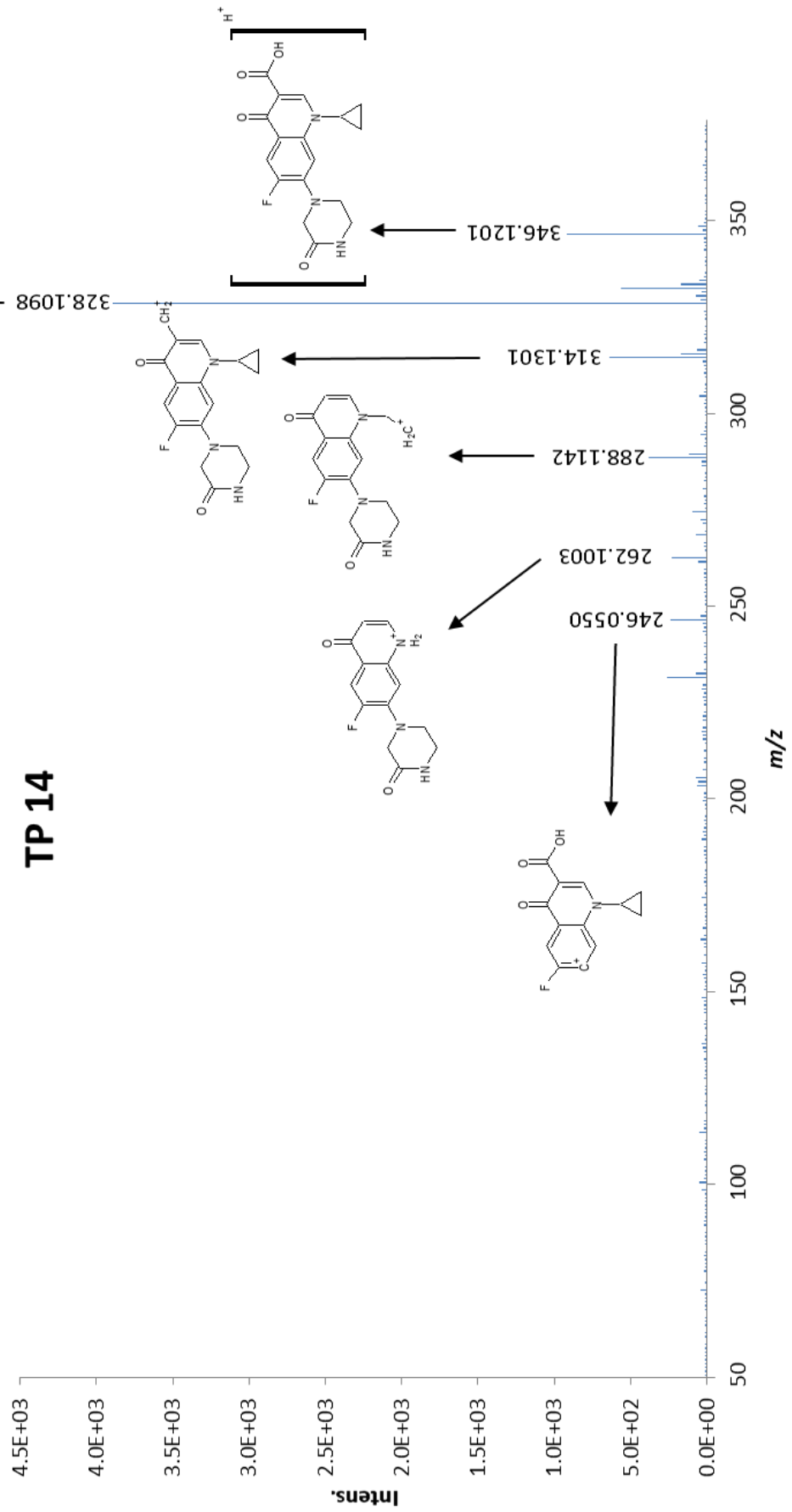


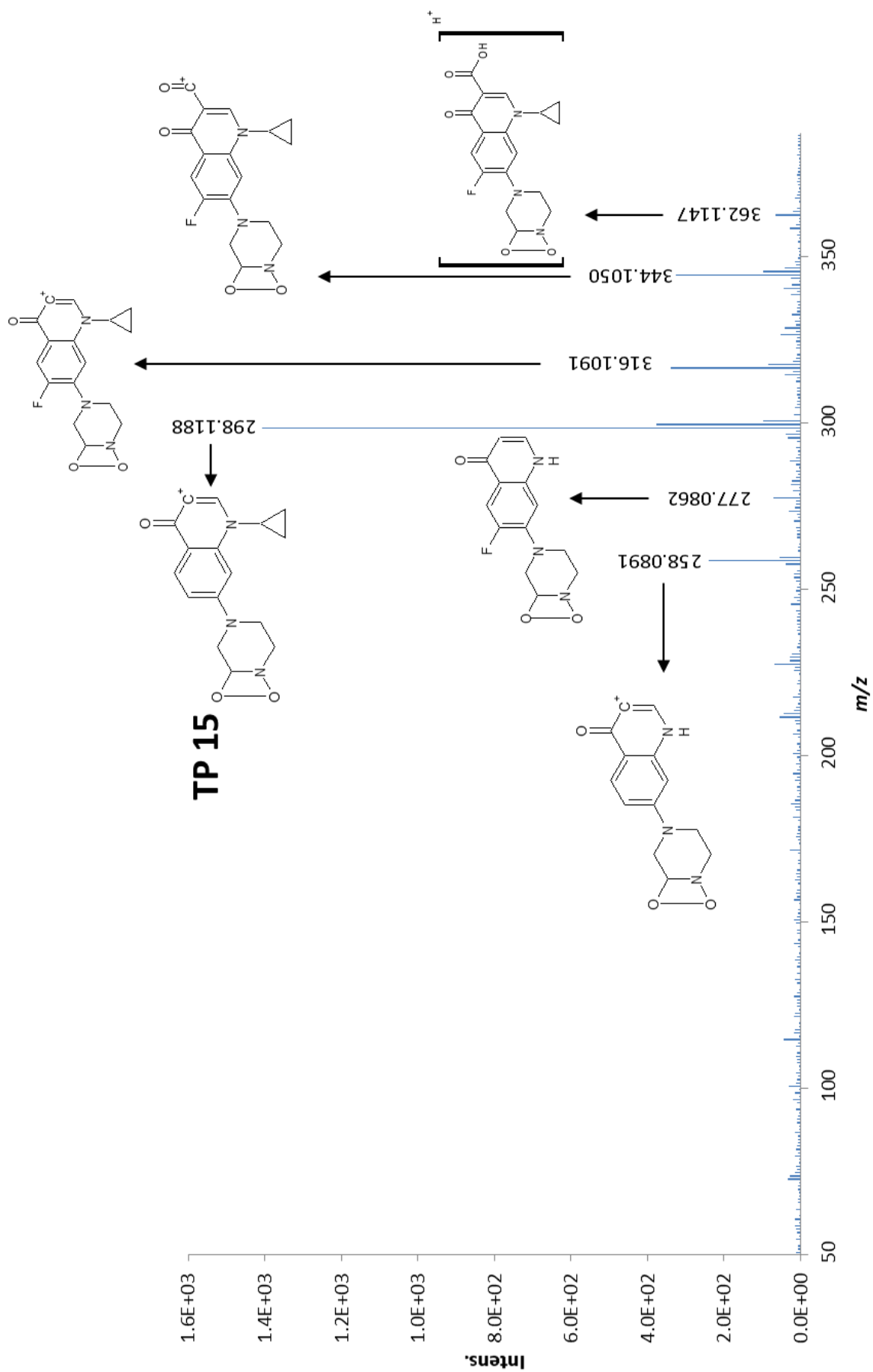


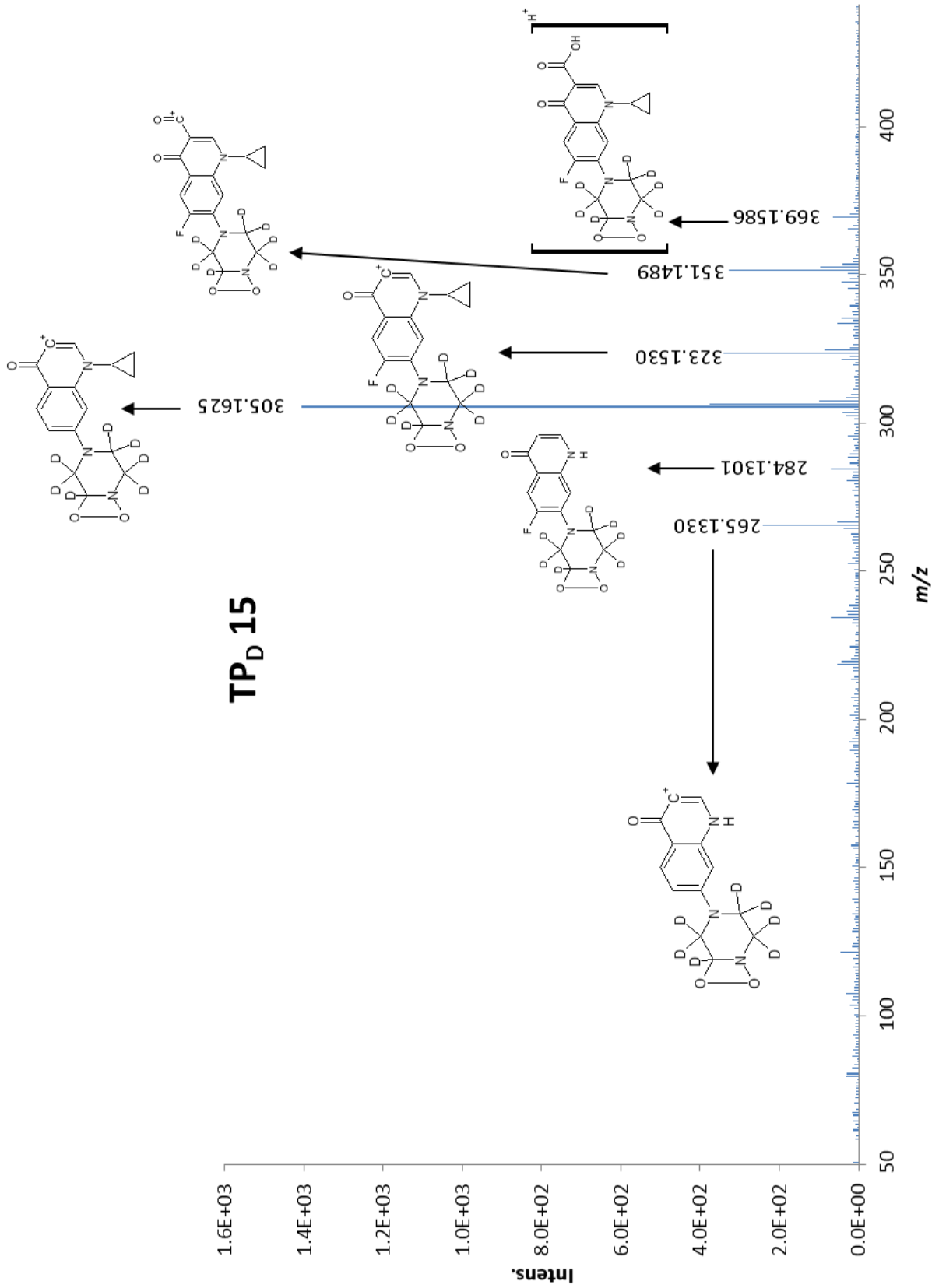


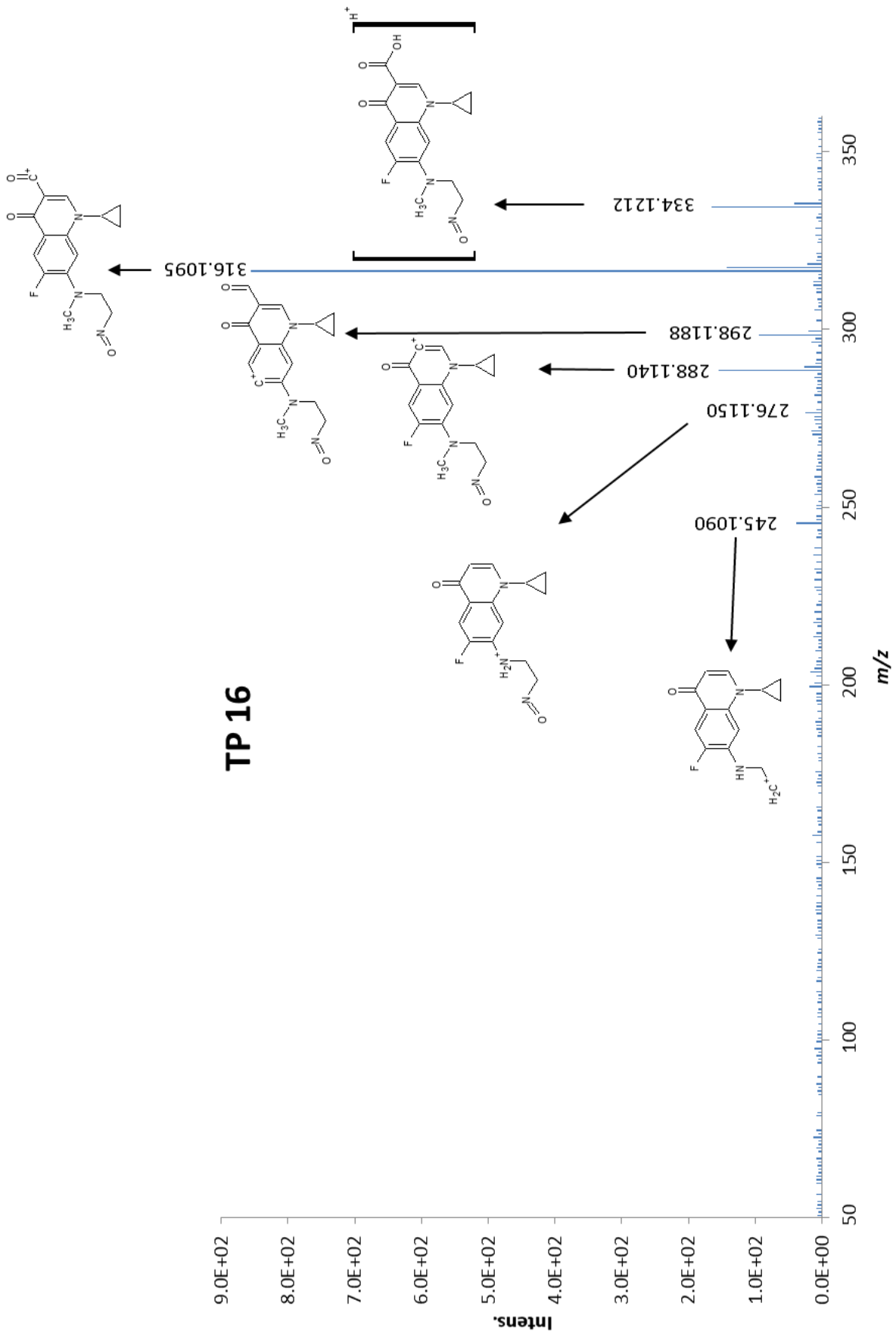


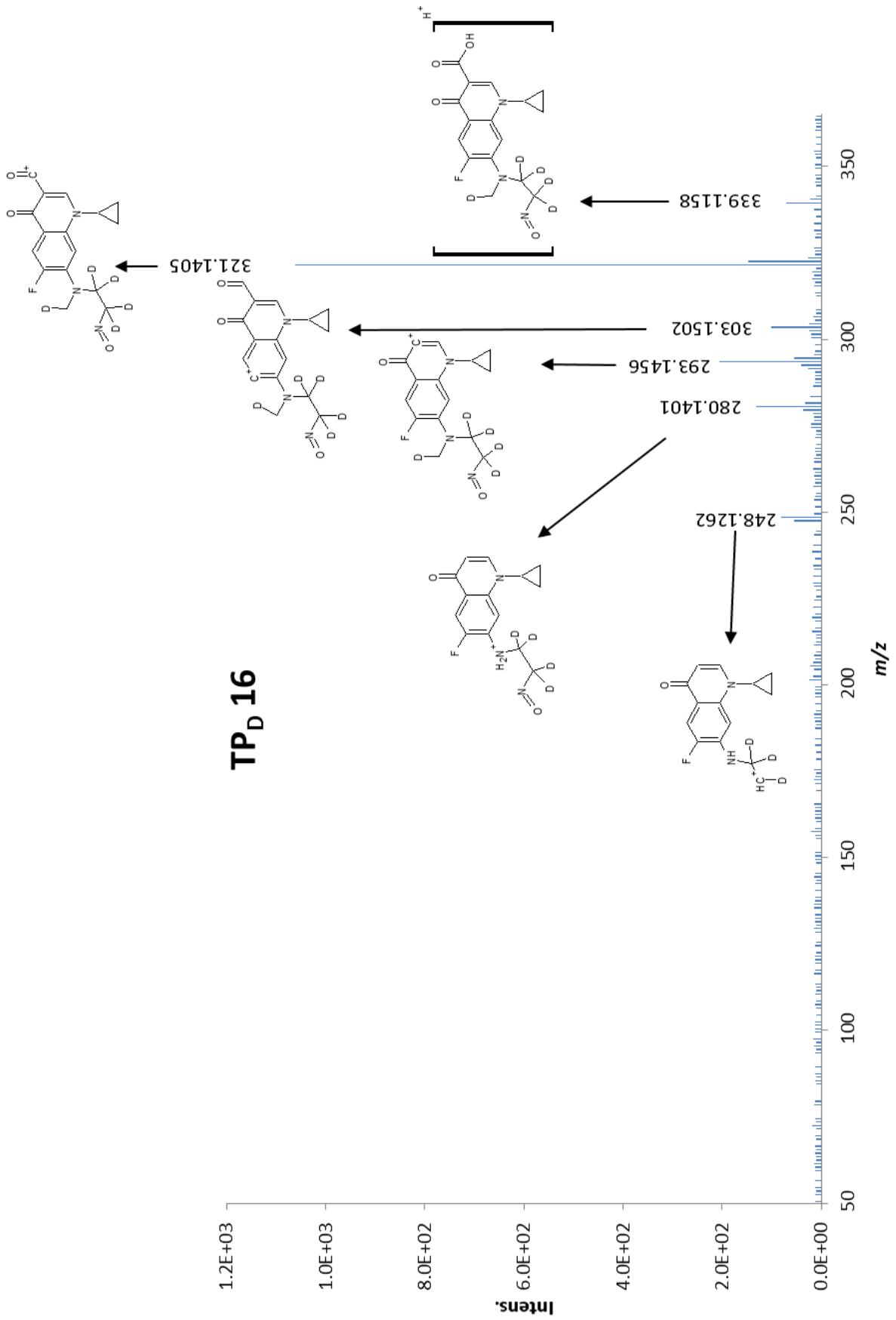


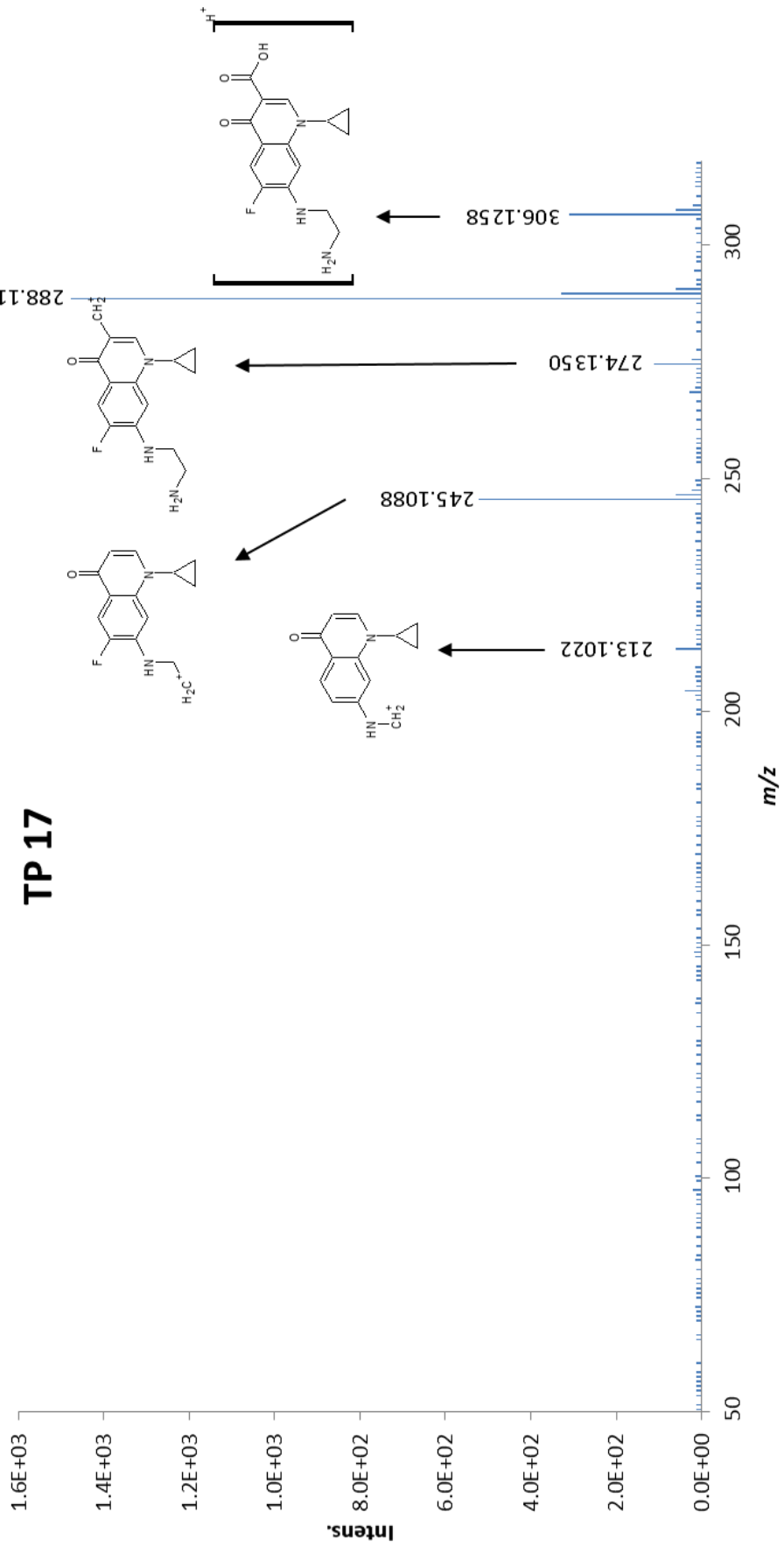


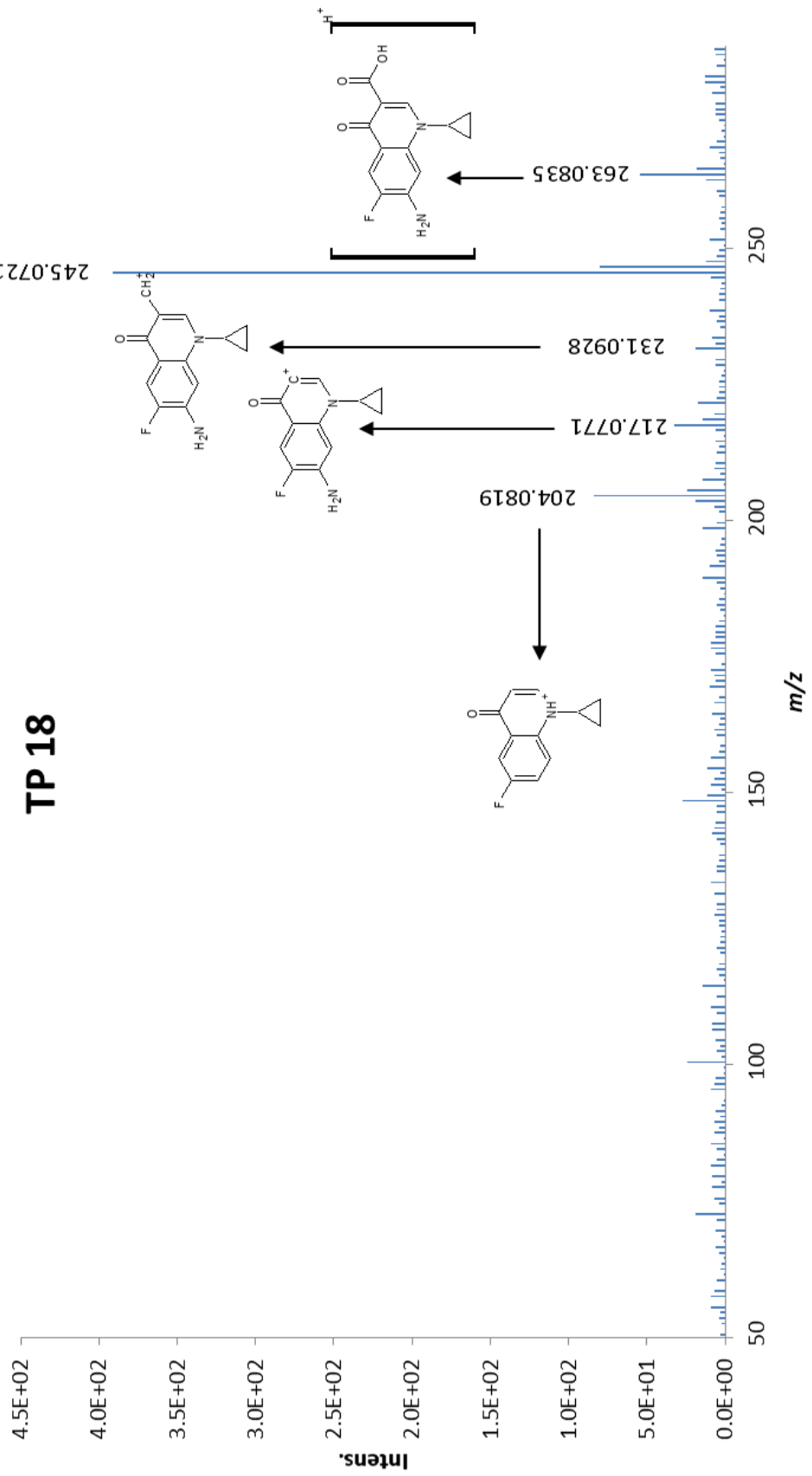


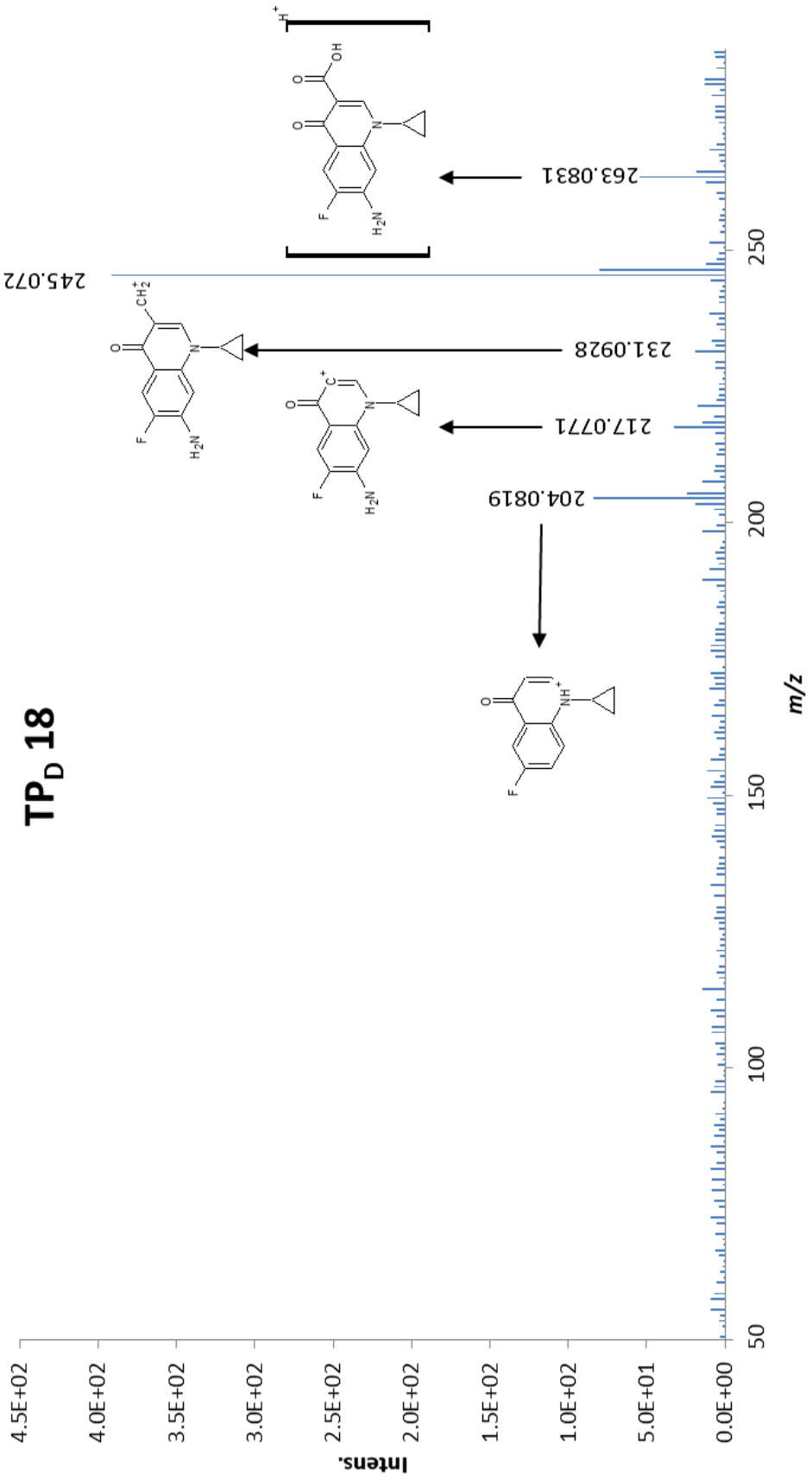












6.3 List of abbreviations

$\cdot\text{OH}$	Hydroxyl radical
$^{\circ}\text{C}$	degree Celsius
$\cdot\text{OOH}$	peroxy radicals
$^1\text{O}_2$	singlet molecular oxygen
$^3\text{O}_2$	triplet molecular oxygen
A_I	Irradiated area
Apr.	April
Aug.	August
AOPs	Advanced oxidation processes
a-Ox	auxiliary oxidant
APPI	atmospheric pressure photon ionization
A_{λ}	Absorbance at wavelength λ
BDE	Bond dissociation energy
BOD	Biochemical oxygen demand
C	Speed of light
c_0	Initial concentration
C_{18}	Octadecyl carbon chain, $\text{C}_{18}\text{H}_{37}$ alkyl group
$\text{C}_5\text{H}_8\text{O}_2$	Acetylacetone
CB	conduction band
CE	collision energy
CEP	collision cell entrance potential
CH_3COOH	acetic acid
CH_3COONa	Sodium acetate
CID	collision-induced dissociation
CIP	Ciprofloxacin
cm	Centimetre
c_t	Final concentration
CXP	collision cell exit potential
D	Deuterium
Da	Dalton
DAN	Danofloxacin
DBEs	double bond equivalents
DD	daily doses
DIF	Difloxacin
DOC	Dissolved organic carbon
DOM	Dissolved organic matter
DP	Declustering potential
Dr. rer. nat.	Doctor rerum naturalium
E	Energy flux
E2	17 β -Estradiol
E_{avg}	Average photon irradiance
E_{bg}	Band gap energy
ECDC	European Centre for Disease Prevention and Control
EE2	17 α -Ethinylestradiol
EI	Electron impact ionization
ENO	Enoxacin
ENR	Enrofloxacin

EP	Entrance potential
EPI	Enhanced product ion scan
EQS	Environmental quality standards
ESI	Electrospray ionization
ESI	Electrospray ionisation
et al.	et alii or et aliae
eV	Electron volt
F ⁻	Fluoride
F ₂	Fluorine
Feb.	Februar
FeSO ₄ ·7 H ₂ O	Ferrous sulfate
FLE	Fleroxacin
FLU	Flumequine
FQs	Fluoroquinolones
FT-ICR	Fourier transform ion cyclotron resonance
FT-IR-MS	Fourier transform infrared mass spectrometer
g	Gram
GC	Gas chromatography
GC-MS	Gas chromatography-mass spectrometry
GmbH	Gesellschaft mit beschränkter Haftung
GmbH & Co.KG	Gesellschaft mit beschränkter Haftung & Compagnie Kommanditgesellschaft
H	Planck constant
H ⁺	UV dose
h ⁺	Positive hole
H ₂ O	Water
H ₂ SO ₄	Sulfuric acid
HCl	Hydrochloric acid
HF	Hydrofluoric acid
HNO ₃	Nitric acid
HO ₂ [•]	Perhydroxyl radical
HO ₂ ⁻	Hydrogen peroxide anion
HPLC	High performance liquid chromatography
HRMS	High resolution mass spectrometry
I	Light intensity
ISC	Inter system crossing
IT	Ion trap
IUTA	Institut für Energie- und Umwelttechnik e.V. (Institute of Energy and Environmental Technology)
Jun.	Juni
Jul.	Juli
K	Reaction constant
K ₃ Fe(C ₂ O ₄) ₃ ·3H ₂ O	Potassium ferric oxalate trihydrate
kg	Kilogram
L	Litre
LC	liquid chromatography
LC-MS	liquid chromatography - mass spectrometry
LEV	Levofloxacin
Ln	Natural logarithm
LOD	Limit of detection
log	Logarithm

LOM	Lomefloxacin
LOQ	Limit of quantification
LTQ Orbitrap	Linear ion trap/orbitrap
M	Mol
M*	Electronically excited molecule
m/z	Mass-to-charge ratio
$M^{+\bullet}$	Radical cation
Mar.	März
MAR	Marbofloxacin
mg	Milligram
min	Minute
mL	Millilitre
mm	Millimeter
M-O-O [•]	Peroxy radicals
MOX	Moxifloxacin
MRM	Multiple reaction monitoring
MS	Mass spectrometry
N	Number of measurements
n.d.	not determined
Na ₂ CO ₃	Sodium carbonate
NaOH	Sodium hydroxide
NEB	Nebivolol
Ng	Nanogramme
ng	Nanogram
NH ₄ C ₂ H ₃ O ₂	Ammonium acetate
Nm	nanometer
NOR	Norfloxacin
O ₂	Oxygen
O ₂ ⁻	Superoxide
O ₂ ^{•-}	Superoxide radical anions
O ₃	Ozone
OFL	Ofloxacin
pCBA	4-Chlorobenzoic acid
PE	Population equivalent
PEF	Pefloxacin
pH	pH value
pKa	Acid dissociation constant
ppm	Parts per million
Prof.	Professor
psi	Pound-force per square inch
Q1	Precursor ion (quadrupole 1 of a triple quadrupole mass spectrometer)
Q3	Qualifier ions (quadrupole 3 of a triple quadrupole mass spectrometer)
QC	Quality control
QIT	Quadrupole ion trap
QqQ	Triple quadrupole (mass spectrometer)
QTOF	Quadrupole TOF (mass spectrometer)
QTRAP	Hybrid mass spectrometer, where the third quadrupole could be used as quadrupole or linear ion trap
R.T.	Retention time
Redox	Oxidation-reduction
S/N	Signal-to-noise

SAR	Sarafloxacin
SD	Standard deviation
SPE	Solid phase extraction
SQ	Single quadrupole (mass spectrometer)
Suppl.	Supplementary material
t	Ton
$t_{1/2}$	Half life times
tert-BuOH	Tertiary butanol
TiO ₂	Titanium dioxide
TOF	Time-of-flight
TOS	Tosufloxacin
TPs	Transformation products
TQ	Triple quadrupole (mass spectrometer)
TRO	Trovafloxacin
TSS	Total suspended solids
UHPLC	Ultra high performance liquid chromatography
US	Ultrasound
USA	United States of America
UV	Ultraviolet
UV/TiO ₂	Photo excitation of titanium dioxide
UV-A	Ultraviolet emitting in the wavelength range 315 to 400 nm
UV-B	Ultraviolet emitting in the wavelength range 280 to 360 nm
UV-C	Ultraviolet emitting in the wavelength range 200 to 280 nm
$U\lambda$	Energy of one mole of photons at wavelength λ
V	Volume
V	Volt
v/v	Volume to volume ratio
VB	Valence band
VIS	Visible
vol	Volume
VUV	Vacuum ultraviolet
W	Watt
WF	Water factor
WFD	Water Framework Directive
WWTP	Wastewater treatment plant
B	Beta
ϵ_c	Molar absorption coefficient
Λ	Wave length
μL	Microlitre
μm	Micrometer
Φ	Quantum yield

6.4 List of figures

Figure 1.1	Fate and transport of pharmaceuticals in the environment.....	2
Figure 1.2	Chemical structure of β -blockers. The active moieties responsible for the biological activity are highlighted with bold line, based on [44].	6
Figure 1.3	4-quinolone skeleton of fluoroquinolones.....	8
Figure 1.4	Level of hydrophilicity and hydrophobicity of pharmaceutical compounds, based on [84].	11
Figure 1.5	Example for the calculation of mass resolution, $m = 1000$ and $\Delta m = 0.208$, so the 10 % valley definition gives a resolution of $1000 / 0.208 = 4,800$	12
Figure 1.6	Comparison of systematic workflows of environmental samples analysis (i) quantitative target analysis with reference standards, (ii) suspect screening without reference standards, and (iii) non-target screening of unknowns in environmental samples. Reproduced from Krauss, et al. [82].	14
Figure 1.7	Flow diagram of a conventional wastewater treatment plant (figure taken from Riffat [94]).	15
Figure 1.8	Schematic illustration of the photophysical and photochemical processes of the semiconductor particle TiO_2 , modified according to [102].	19
Figure 1.9	Visualization of the different chapters' contribution to the overall goal of the thesis.....	21
Figure 2.1	NEB concentrations in influents and effluents of 12 German WWTPs presented as box-and-whisker plots (median, 25 % quartile, 75 % quartile, maximum and minimum).	40
Figure 2.2	Elimination of NEB (A), inset: reaction kinetic plot (B) for the three UV sources (Experimental conditions $c_0(\text{NEB}) = 25 \mu\text{mol L}^{-1}$, volume = 500 mL, flow rate = 100 mL min^{-1} , pH = 7, $T = 20 \pm 2^\circ\text{C}$).	41
Figure 2.3	(A) NEB degradation in the presence of <i>tert</i> -BuOH, inset: (B) linear plots of $\ln(c_t/c_0)$ versus time of NEB degradation in the presence of <i>tert</i> -BuOH (Experimental conditions: $c_0(\text{NEB}) = 25 \mu\text{mol L}^{-1}$, $c_0(\text{tert-BuOH}) = 10 \text{ mmol L}^{-1}$, volume = 500 mL, flow rate = 100 mL min^{-1} , pH = 7, $T = 20 \pm 2^\circ\text{C}$).....	42
Figure 2.4	High resolution mass spectra of NEB and its transformation products.....	46

Figure 2.5	Relative peak area of NEB and corresponding transformation products as a function of time during UV-B (A) and UV-C (B) photolysis experiments carried out in pure water ($c_0 = 25 \mu\text{M}$, volume = 500 mL, flow rate = 100 mL min^{-1} , pH = 7, $T = 20 \pm 2 \text{ }^\circ\text{C}$).	47
Figure 2.6	Fluoride yield (mmol L^{-1}) versus the NEB degradation (mmol L^{-1}) during the UV-A, UV-B and UV-C radiation: NEB degradation calculated based on LC-MS, F_{yield} calculated based on ion chromatography.....	48
Figure 3.1	Ciprofloxacin elimination as a function of time during photolytic (A) and photocatalytic (B) treatment. Average results of triplicate measurements are shown. Relative standard deviation is indicated by error bars but often smaller than symbol sizes. Inset: effect of pH values on the removal rate constants of photolytic and photocatalytic degradation of 60 μM CIP at 120 min interval.	62
Figure 4.1	Absorption spectra of the investigated compounds (1 mg L^{-1} , pH = 7) and emission spectra of the UV-lamps used in this study.....	84
Figure 4.2	Scheme of the experimental set-up, namely of the UV photooxidation reactor.	87
Figure 4.3	Boxplots (black) of the concentration of diclofenac, metoprolol, carbamazepine, sulfamethoxazole and benzotriazole in the studied effluent wastewater treatment plant at different days over a period of 4 months, compared to the values determined in previous studies (grey) in effluent wastewater treatment plants from Germany, Spain, Sweden, Switzerland, Italy, China, France, Taiwan, Canada, and USA [18, 19, 22, 36-61]. Data above each box denote the number of positive results and the number of studies considered (which are influenced by the limit of detection in the specific studies).....	89

6.5 List of tables

Table 1.1	β -blockers concentrations in different aqueous matrices. The aqueous matrices were categorized: +++ for $c_{\max} > 1000 \text{ ng L}^{-1}$; ++ for $c_{\max} 100\text{-}1000 \text{ ng L}^{-1}$; + for $c_{\max} < 100 \text{ ng L}^{-1}$; n.d. if no data were available. 7
Table 1.2	Structural formulae of fluoroquinolones. 8
Table 1.3	FQs concentrations in different aqueous matrices. The aqueous matrices were categorized: +++ for $c_{\max} > 1,000 \text{ ng L}^{-1}$; ++ for $c_{\max} 100 - 1,000 \text{ ng L}^{-1}$; + for $c_{\max} < 100 \text{ ng L}^{-1}$. n.d. if no data were available. 10
Table 1.4	The redox potential of a number of chemical systems used for water treatment. 17
Table 1.5	List of typical photochemical systems 17
Table 2.1	Pseudo-first order rate constants (time-based and fluence-based), half life time and quantum yields (Φ) (for the full (polychromatic) emission spectrum of the radiation source) for NEB in ultrapure water, NEB in presence of <i>tert</i> -BuOH and wastewater matrix by UV-A, UV-B and UV-C photolysis 42
Table 2.2	Accurate masses for NEB and its transformation products. 45
Table 3.1.	Accurate masses determined by UPLC-Q-ToF for ciprofloxacin (CIP) and its photodegradation products generated at different pH values (x presented the detected transformation products). 64
Table 3.2.	Accurate masses determined by UPLC-Q-ToF for deuterated Ciprofloxacin (CIP-d8) and its photodegradation products (TPD) generated at pH 7. 69
Table 4.1	Physical and chemical properties of the studied micropollutants [32]. 84
Table 4.2	Optimized MRM conditions for the HPLC/MS/MS analysis. 85
Table 4.3	Kinetic data determined during the micropollutants' degradation experiments in the bench scale reactor under UV-A, UV-B and UV-C irradiation in deionized water and WWTP effluent (k = reaction constant, $t_{1/2}$ = half-life, repetition $n = 3$, the standard deviations are given for the rate constants and the correlation coefficients of the plots are given in the brackets). 91

6.6 List of supplementary figures and tables

Suppl. 6.1	Physical and chemical properties of nebivolol.....	104
Suppl. 6.2	Experimental set up of the lab scale plant: (a) pyrex reactor, (b) UV sources, (c) reservoir, (d) sampling point, (e) peristaltic pump, (f) flow direction (dimensions are not to scale).....	105
Suppl. 6.3	Absorption spectrum of nebivolol (primary Y-axis) overlaid with the normalized emission spectra of the three investigated UV lamps.....	106
Suppl. 6.4	Plot of the elimination rate of Nebivolol versus the OH radical products during the UV irradiation.	107
Suppl. 6.5	(A) Nebivolol degradation, inset: (B) Linear plots of $\ln(c/c_0)$ versus time of nebivolol degradation in the presence of the wastewater matrix, (Experimental conditions: $c_0 = 25 \mu\text{mol L}^{-1}$, volume = 500 mL, flow rate = 100 mL min^{-1} , pH = 7, $T = 20 \pm 2 \text{ }^\circ\text{C}$).	107
Suppl. 6.6	UV absorption spectrum of nebivolol in Milipore water and in wastewater (Experimental conditions: c_0 (NEB) = $25 \mu\text{mol L}^{-1}$, pH = 7, $T = 20 \pm 2 \text{ }^\circ\text{C}$).	107
Suppl. 6.7	Summary of kinetic parameters of nebivolol degradation.	108
Suppl. 6.8	Chemical structures of NEB and its and transformation products in comparison with other β -blockers. The active moieties responsible for the biological activity are highlighted.....	109
Suppl. 6.9	Standard curve for ferrioxalate actinometry.....	110
Suppl. 6.10	Results of the actinometry experiment.....	111
Suppl. 6.11	k'_1 determination from H' and $\ln(c_0/c_t)$ plot.....	114
Suppl. 6.12	Distribution of the ciprofloxacin (CIP) species at different pH values based on the pKas reported in the literature 15 (the structures are shown in scheme 1).	115
Suppl. 6.13	Structural formula of (CIP-d8), emphasizing the 8-deuterium atoms at the piperazine ring.....	115
Suppl. 6.14.	Experimental set-up.	115
Suppl. 6.15.	Spectra of the UV-C Lamp and the absorption spectra of a $60 \mu\text{M}$ ciprofloxacin unbuffered aqueous solution at different pH values.	116

Suppl. 6.16.	The change of pH values during the photolytic (A) and photocatalytic (B) degradation of ciprofloxacin.	116
Suppl. 6.17.	Photolysis and photocatalysis transformation products of CIP plotted as a function of the irradiation time monitored by LC- MS at pH 3, 5, 7 and 9...	117
Suppl. 6.18.	MS2 spectrum of CIP and its transformation products, proposed fragment structure of detected ions.....	118

6.7 List of publications

Salma, A., Thoröe-Boveleth, S., Schmidt, T.C. and Tuerk, J. 2017. Photolytic degradation of the β -blocker nebivolol in aqueous solution. *Water Research* 116, 211-219.

Salma, A., Thoröe-Boveleth, S., Schmidt, T.C. and Tuerk, J. 2016. Dependence of transformation product formation on pH during photolytic and photocatalytic degradation of ciprofloxacin. *Journal of Hazardous Materials* 313, 49-59.

Oral presentations and posters

02. - 04. Mai. 2016 A. Salma, H. Lutze, T. C. Schmidt and J. Tuerk, Poster presentation Photolytic degradation of the β -blocker nebivolol in aqueous solution, Wasser, Die Wasserchemische Gesellschaft - Fachgruppe in der GDCh, Bamberg, Deutschland.
31. Aug. - 04. Sep. 2014 A. Salma, H. Lutze, T. C. Schmidt and J. Tuerk, Oral presentation (Comparative study of different UV types (UV-C, UV-B, and UV-A) induced photolysis of a new β - blocker (nebivolol) in aquatic solution), 5th EuCheMS Chemistry Congress, WOW Istanbul Convention Center, Istanbul, Türkei
26. - 28. Mai. 2014 A. Salma, S. Thoröe-Boveleth, T. C. Schmidt and J. Tuerk, Poster presentation (Elucidation of the effect of pH on the photolytic and photocatalytic degradation of ciprofloxacin), Wasser, Die Wasserchemische Gesellschaft - Fachgruppe in der GDCh, Haltern am See, Deutschland.
08. - 09. Oct. 2013 C. vom Eyser, A. Salma, A. Börgers, S. Thoröe-Boveleth, J. Tuerk, Oral presentation (Elimination of pharmaceuticals and investigation of transformation products during oxidative water treatment), MS Technology Days, Waters User Meeting, Stuttgart and Berlin
25. - 28. Jun. 2013 A. Salma, S. Thoröe-Boveleth, T. C. Schmidt and J. Tuerk. Poster presentation (Effect of pH on the photolysis and photocatalytic degradation of ciprofloxacin (kinetic and mechanism)), ICCE 14th EuCheMS International Conference on Chemistry and the Environment, 25 – 28 June 2013, Barcelona, Spain, The Best Poster Award.

06. - 08. Mai. 2012

A. Salma, S. Thoröe-Boveleth, T. C. Schmidt and J. Tuerk. Poster presentation (Investigation of ciprofloxacin transformation products during TiO_2/UV treatment), 6th IWA Specialist Conference Oxidation Technologies for Water and Wastew Treatment. 06-08 May 2012, Goslar, Deutschland.

6.8 Lebenslauf

Der Lebenslauf ist in der Online-Version aus Gründen des Datenschutzes nicht enthalten.

6.9 Erklärung

Hiermit versichere ich, dass ich die vorliegende Arbeit mit dem Titel

„Advanced oxidation of micropollutants in water by photolytic and photocatalytic processes”

selbst verfasst und keine außer den angegebenen Hilfsmitteln und Quellen benutzt habe, und dass die Arbeit in dieser oder ähnlicher Form noch bei keiner anderen Universität eingereicht wurde.

Essen, im Juli 2017

Alaa Salma

6.10 Acknowledgements

My greatest appreciation belongs to Prof. Dr. Torsten C. Schmidt for his excellent support. I thank him for the helpful discussions, his commitment, his patience and the chances he had given to me.

A big thank also to Dr. Jochen Türk, who took care of me during my work at IUTA, who has been a constant source of encouragement and wise advice.

Many thanks to Prof. Dr. Kristof Demeestere for the willingness to examine this work and for all his efforts.

Thanks also to Dr. Holger Lutze and Dr. Thorsten Teutenberg for the long discussions and the valuable hints that supported this work.

The presented work was made possible and supported by IUTA's projects.

Moreover, I highly appreciate my colleagues Andrea Börgers, Georg Reinders, Helmut Gräwe, Oliver Gassner, Linda Gehrman, Fabian Itzel, Claudia von Eyser, Christiane Balden, Terence Hetzel, Juri Leonhardt, Martin Kläßen, and Tjorben Posch for professional discussions and a pleasant working environment.

As a representative of all my friends, my infinite thanks goes to Ana Maria. Thank you for proofreading this work and for the emotional support.

Mum, Dad and Helen – Thank you for your patience.